

176

THE DEVELOPMENT OF A ROAD PROFILE MEASURING DEVICE  
WITH REFERENCE TO ENDURANCE TESTING  
OF MOTOR VEHICLES

by

J.F.Koehler

A thesis submitted in fulfillment of the requirements for the  
degree of Master of Science in Engineering.

Department of Mechanical Engineering

University of Cape Town

March 1990

The copyright of this thesis vests in the author. No quotation from it or information derived from it is to be published without full acknowledgement of the source. The thesis is to be used for private study or non-commercial research purposes only.

Published by the University of Cape Town (UCT) in terms of the non-exclusive license granted to UCT by the author.

## DECLARATION

This is to certify that the results and work presented in this thesis are essentially my own, and that no part of it has been submitted for a degree at any other university.

.....  
J.F.Koehler

March 1990

### ABSTRACT

This project describes the development of a device to measure the profile of a road. The data describing the roads characteristics are used to compare the qualities of the test tracks at present used by Volkswagen SA (Pty) Ltd for endurance testing of their products, and the Synthetic Road used on their new hydraulic road simulator.

The comparison shows that the simulator does not apply the same peak loads encountered on the road. It has far higher average values over the frequency range tested. It is therefore a more severe test of the body fatigue strength than the test roads.

The thesis first reviews the different methods of vehicle endurance testing. It describes the development of the measuring device, as well as the data processing. Finally a comparison is made between road testing techniques and the use of an hydraulic road simulator.

ACKNOWLEDGEMENTS

The author wishes to thank the following for their assistance in this project.

Professor K.F.Bennett for his supervision and keen appraisal.

Dr A.Yates for useful assistance and guidance.

Dr N.Morrison for his advice.

Mr R.Main and Mr N.Box of VW.

Messieurs M.Batho, A.Warburton and H.Tomlinson,

J.Mayer and S.Schrire for technical assistance.

CONTENTS

	<u>Page</u>
ABSTRACT	i
ACKNOWLEDGEMENTS	ii
TABLE OF CONTENTS	iii
LIST OF FIGURES	vi
SYMBOLS AND NOMENCLATURE	vii
1. INTRODUCTION	
1.1 Background	1
1.2 Volkswagen's Road Simulator	2
1.3 Thesis Objectives	3
2. LITERATURE SURVEY	
2.1 Introduction	4
2.2 The objective of endurance testing	4
2.3 Endurance test methods	4
2.4 The influence of the test technique and objectives on the method of measuring the road profile	8
2.5 Methods of data measurement	9
2.6 Correlation of the methods	14
2.7 Methods of analysing and using the data	14
2.8 Indirect methods of measuring the road profile	19
3. SOLUTION DEVELOPMENT	21
3.1 Definition of problem	21
3.2 Requirements	21
3.3 Constraints	22

3.4	Criteria	22
3.5	Solution specification	22
3.6	Concept formation	23
4.	MEASURING PROCEDURE AND EXPERIMENTAL APPARATUS	
4.1	The measuring procedure.	33
4.2	Digital Sampling as related to this particular test device	40
4.3	Design of the anti-aliasing filter	42
5.	EXPERIMENTAL RESULTS	
5.1	The integration procedure	44
5.2	Calibration on the shaker	45
5.3	Calibration on the drum	46
5.4	Testing on the road	47
5.5	The measurements made at VW/Uitenhage	51
6.	DISCUSSION OF THE RESULTS AND CONCLUSIONS	
6.1	Discussion of the shaker results	52
6.2	Conclusions from the shaker results	53
6.3	Discussion of the drum test results	54
6.4	Discussion of the road test results	54
6.5	Comparison with the Synthetic Road of the VW test tracks	55
6.6	Conclusions about the road measuring procedure	56
6.7	Conclusions from the measurements made at VW	58
6.8	Recommendations	58

## REFERENCES AND BIBLIOGRAPHY

60

## APPENDICES

- A. The Statistics of Random Processes
- B. Fourier Analysis
- C. Digital Sampling and Filtering
- D. Development of the Measuring Equipment
- E. Development of the Fifth Wheel
- F. Design of a Mechanical Accelerometer
- G. Data Sampling Program
- H. Spectral Analysis Program
- I. Test Results



<u>LIST OF FIGURES</u>	<u>Page</u>
Figure 2.1 Methods of providing force inputs to the car body	7
Figure 2.2 Rod and Level used for surveying of the profile	9
Figure 2.3 Measuring Beam and Wheel	11
Figure 2.4 Potentiometer and accelerometer mounted on car	12
Figure 2.5 Restricted Peak Value Measuring Method	17
Figure 2.6 Peak Value Measuring Method	17
Figure 2.7 Range Count	18
Figure 2.8 Time in Band Count	18
Figure 3.1 Spectrum of the synthetic road	29
Figure 3.2 Coherence between the tracks of the synthetic road	31
Figure 4.1 Schematic drawing of the mounted fifth wheel	34
Figure 4.2 Graphs of displacement, velocity and acceleration for a mathematically ideal bump	35
Figure 4.3 The distance in which the wheel is accelerated to the top of an obstruction	36
Figure 4.4 The response of the car and the wheel to a step in the road profile	38
Figure 4.5 Combination of the signals from the LVDT and the accelerometer to give the profile	39
Figure 6.1 Comparative table of spectral values	55

GLOSSARY

$a_0$	Constant term in the Fourier Series
$a_n$	Coefficients of the cosine terms in the Fourier Series
$A, A_{\max}$	(Maximum) amplitude of a sinusoid
$b_n$	Coefficients of the sine terms in the Fourier Series
$C$	Capacitance in Farads (F)
$C_n$	Complex coefficients of the complex Fourier Series
$D$	The differential operator
$f_0$	Fundamental Frequency
$f_{3dB}$	The frequency at which the output is 3dB less than the input
$f_{\text{samp}}$	The sampling frequency
$f_{\max}$	The highest frequency of interest
$G$	Gain value
$H$	Feedback Value
$k$	variable, integer step in the Fourier Series coefficients
$m$	Distance in metres
$\bar{m}$	Mean value of a sample
$M$	Mass (kg)
$n$	variable, integer step in the Fourier Series coefficients
$n$	The order of an electrical filter
$N$	Force in Newtons
$N$	The number of samples
$r$	the number of the sample
$R$	Resistance in Ohms ( $\Omega$ )
$t, t$	Time in seconds
$T$	Period in seconds
$V, V_{\text{in}}$	Voltage
$x$	A variable, usually horizontal displacement
$x_0$	A fixed value of $x$
$x_r$	terms in a discrete series
$X_k$	Complex coefficient of the complex Fourier series
$y$	Displacement usually orthogonal to $x$ (m)
$\dot{y}$	Velocity, the first derivative of displacement (m/s)
$\ddot{y}$	Acceleration, the second derivative of displacement (m/s <sup>2</sup> )
$z$	Vertical displacement, orthogonal to $x$ and $y$

$A(\omega)$	Component of the Fourier transform of $x(t)$
$B(\omega)$	Component of the Fourier transform of $x(t)$
$d()/dt$	Denotes differentiation with respect to time
$p()$	Probability function for a variable
$R_x(t)$	Autocorrelation function of $x(t)$
$\langle x \rangle$	Mean value of $x$
$S_x(\omega)$	Mean square spectral density of $\omega$

$\Delta$	The step between samples
$\theta$	Angle in radians
$\lambda$	Wavelength (m)
$\pi$	$= 22/7$
$\rho, \rho_{xy}$	Correlation coefficient
$\sigma, \sigma_x, \sigma_y$	Standard deviation
$\Sigma$	Summation
$\tau$	A variable used for Autocorrelation
$\omega$	Angular Frequency ( $\text{rad.s}^{-1}$ )

## NOMENCLATURE

### Accelerometer

A device which produces a voltage directly proportional to the acceleration applied to it.

### Aliasing

The distortion of a digitally sampled signal due to the presence of frequencies higher than half the sampling frequency.

### Analog to Digital (A/D), Digital to Analogue (D/A) conversion

The process of converting a continuous analogue waveform into a series of numbers representing discrete points along the waveform. The inverse process (D to A) reconverts the numbers into an analogue waveform.

### Anti-Aliasing Filter

A low-pass electrical filter. For digital sampling it is necessary to pass the signal to be sampled through a filter whose cut-off frequency is less than or equal to half the sampling frequency. This prevents aliasing effects.

### Bias Error

The error in reproducing a digitally sampled signal due to too low a sampling frequency. Sampling must be done at more than twice the highest frequency it is desired to detect to avoid bias error.

### Convolution

A mathematical term. It is the transform of a mathematical operation in one domain into a different mathematical operation in another domain. For example, integration in the time domain can be transformed to multiplication in the frequency domain.

### FFT or Fast Fourier Transform

A routine for calculating the coefficients of a discrete Fourier series representing a periodic waveform. The IFFT or inverse transform can be used to reconstruct the waveform from the coefficients

### High-pass, low-pass Filters

Filters which respectively attenuate low and high frequencies in any signal that is passed through them.

### LVDT

Linearly Variable Differential Transducer. A device for producing a voltage directly proportional to displacement.

### Mass Dominated Region

That part of the frequency range of a dynamic system where the response is determined by the mass of the system. It usually occurs at high frequencies where the inertia of the mass is significant.

### MIRA

Motor Industry Research Association. A British organisation which consults and engages in the Motor Vehicle Research. Amongst its assets are several different kinds of permanent test roads.

### Nyquist's sampling frequency

The minimum sampling frequency necessary when sampling data to detect its frequency content. Sampling must be done at two and a half times the frequency of the highest frequency present in order to detect it.

### PSD, PSA

The Power Spectral Density is the spectrum created by performing a Fourier analysis on data. The process is also called Power Spectral Analysis.

### PC

A personal computer or microcomputer. One of the smallest types of computer in general use. Equipped with a random memory and floppy disk drives for storage of data in non-volatile form.

### Sampling, Oversampling

The process of recording the value of a signal at discrete intervals. According to Nyquist's theorem there is a minimum sampling frequency necessary for acceptable reproduction of the signal. If the signal is sampled at a frequency higher than this frequency, it is said to be oversampled.

### Spring Stiffness Dominated Region

That part of the frequency range of a dynamic system where the response is determined by the stiffness of the spring. It occurs at low frequencies where the inertia of the mass is not significant.

### Synthetic Road

A random road profile stored on tape representing the Volkswagen AG accelerated proving ground (EHRA) in Germany. It has been modified for simulator testing by increasing the frequency of occurrence of the undulations, and reducing their peak values.

### Time Domain

The domain in which time is the independent variable.

## 1. INTRODUCTION

### 1.1 Background

Testing of vehicles is a crucial part of the development process before marketing. The testing should allow any defects in the design to be noted and rectified before the vehicle is sold.

An important factor in vehicle evaluation is endurance testing on the road (Andrew [1], Butkunas [12]). This is done by driving vehicles over suitable sections of road or specially constructed test tracks. The test track is chosen to be representative of the worst conditions likely to be encountered, so that any defects may speedily be detected.

However, driving on test tracks is time consuming, and is subject to uncertainties such as driver performance, weather conditions and natural changes in the condition of the roads (Smith [66]).

Laboratory testing has the following advantages over track testing, provided that the objectives are defined, and any limitations are accounted for:-

- i) Conditions can be held constant and testing can be carried out continuously.
- ii) In repetitive endurance testing, human concentration is no longer a variable influence.
- iii) The total testing time is reduced as the testing is not delayed by the failure of unrelated components.

There are many different approaches to endurance testing described in the literature. The method of testing influences the type of data collected on the road surface, and the way the data is used.

The loadings encountered on a vehicle driving over various surfaces occur in three ways :

- 1) loading applied vertically at the tyre contact patch due to changes in the road profile.
- 2) loading due to the inertia of the body. This occurs during braking, acceleration and cornering.
- 3) loading through excitation of natural resonances in the vehicle, as a result of the above two loadings.

The loadings are partly absorbed by the suspension, but also cause vertical, bending and torsional forces to act on the car body. The effect of these forces is to cause fatigue damage to the components, and in exceptional cases may cause immediate failure.

### 1.2 Volkswagen's road simulator

VW has recently installed a Schenk Hydropuls roads simulator in its test plant at Uitenhage. This applies vertical loads to the vehicle under test. It has four hydraulic actuators, each of which is positioned under a wheel of the test vehicle. The motion of the hydraulic actuators is controlled by a magnetic tape with one channel for each actuator. The data currently used is based on test tracks in Germany.



The rig is thus capable of supplying the type of loadings encountered when travelling steadily in a straight line. As well as testing the fatigue strength of the suspension and body, VW wish to test the resistance of the body to torsional loading. Just as important is to test the effectiveness of the dust seals under these body deformations.

Torsional loading occurs due to unevenness in the road surface as a result of differences in the height of the wheel tracks on each side of the vehicle, or unevenness in the same track along the vehicle length. Generally the most uneven roads are those with low-quality surfaces, such as dirt roads. This surface creates conditions where resistance to dust entry is most necessary.

### 1.3 Thesis objectives

The objective of this project is to develop, construct and test a device to measure the profile of a road surface. The device is employed to measure the dirt tracks around the VW plant at Uitenhage used for endurance testing of its vehicles.

The data describing the test tracks may then be compared with that of the synthetic road from Germany used for the simulation. If the difference is significant, a new random profile could be generated to simulate the local roads.

## 2. LITERATURE SURVEY

### 2.1 Introduction

A survey of the literature on endurance testing reveals many different aspects of the subject. The following topics are the main divisions in endurance testing.

- 1) The objectives of the testing.
- 2) The test methods used.
- 3) The method of data gathering, analysis and use of the results.

### 2.2 The objective of endurance testing

The objective of endurance testing is to see how the vehicle under test withstands the loads that will be applied to it in service conditions over its expected life-time. The testing determines fatigue resistance and durability (McConnel [44], Nolan [48], Shinkle [63], Wenstrup [72], White [73]).

### 2.3 Endurance test methods

#### 2.3.1 Test Roads

The simplest method of endurance testing is to drive sample vehicles over sections of road similar to those encountered in service until failure of components occurs (Smith [66]).

However, this method is wasteful of time and resources. It involves driving the vehicle to and from the test track. Roads may also contain stretches which do little damage to the car between more severe stretches. The road is subject to variability due to usage by others. Unnecessary testing of all components occurs, and failure of non-essential or unimportant components can delay testing. The broken-down vehicle must then be returned to workshops for repair. Other road users and animals also present a hazard on the roads.

### 2.3.2 Direct Copy Test Tracks

A permanent copy of the test track is made in concrete or similar, and used. The ordinary test track is subject to great variability, since local conditions and usage will alter it. The drivers concentration and technique will also vary. This puts uncertainty in the results thus obtained. For instance, the relative fatigue damage results obtained by Smith varied by as much as 40 times in one year (Smith [66]).

The advantage of testing on a permanent copy of the test track is that all the forces that occur under real conditions do occur and consistently, even though the testers may not be able to identify them all. The original test track must be measured in order to duplicate it.

### 2.3.3 Artificial Accelerated Test Tracks

A refinement is to construct an artificial road for accelerated testing (Bobbert [11], Craggs [17], Fogg [29], Flanagan [30], McConnel [44], Singh [65], Smith [66], Stockley [67], White [73]). This eliminates the disadvantages of using a test road.

The properties of the road are fixed, and it is situated conveniently near to the test centre. No time is lost driving to the test track, or in recovering failed vehicles.

The track itself is designed so that the most severe conditions are encountered more often than usual, and non-damaging conditions are not present. This achieves accelerated testing of the vehicle, but without exaggerated loadings being applied. The MIRA Belgian pave is a well known example of this (Fogg [29]).

### 2.3.4 Laboratory testing

Testing in the laboratory follows logically as a method of testing vehicle endurance. It eliminates the problems of driver fatigue, vehicle support in case of breakdowns and repeatability of the experiment. When testing in the laboratory one must decide what factors must be modelled, and the minimum accuracy needed to achieve valid results. It does not supply all conditions encountered on the road.

The two methods commonly used are:

- 1) A rotating drum or steel belt on which obstructions are placed (Ashley [2], Engels [27]).

Another common method of testing is to have the vehicle spindle-coupled, where the actuators are mounted to the axle shafts. As well as applying vertical loads, transverse and longitudinal loads may also be applied. For this to be done an opposing force must be applied at the complimentary mounting points. The system then becomes semi-inertial rather than fully inertial, since part of the vehicle is restrained.

The vehicle body may itself be fully restrained, and loads applied to the suspension. This of course tests only the suspension and its mounting points, not the whole body.

#### 2.4 The influence of the test technique and objectives on the method of measuring the road profile

The method of testing the vehicle determines the data required for the test. For input through the wheels the profile of the road surface is necessary, or a function of it (Betz [9]).

The motion of some part of the suspension may be recorded, and the input at the wheel from the actuator modified until the same motion is reproduced (Betz [9], Jacoby [40]). This can lead to difficulties if the transfer function of all the components is not known or is difficult to estimate accurately enough. The results thus obtained are specific to that particular model of vehicle under the same loading conditions.

If input at the wheel stub axles is the method employed, the above method may be useful. If the road profile is used, then compensation must be made for the tyre transfer function.

The range of wavelengths which must be measured is dependant on the road speeds that it is wished to simulate. Frequencies much above 40 Hz will be absorbed by the tyre (VW [70]).

## 2.5 Methods of Data Measurement

For the type of simulator installed by VW, the actual road profile is best suited as a controlling function. Measuring methods described in the literature are listed below.

### 2.5.1 Survey Methods

The simplest method conceptually is by surveying with rod and level. A vertical rod is moved across the surface to be measured. Its change in height relative to a sight line is recorded against its position along the ground.

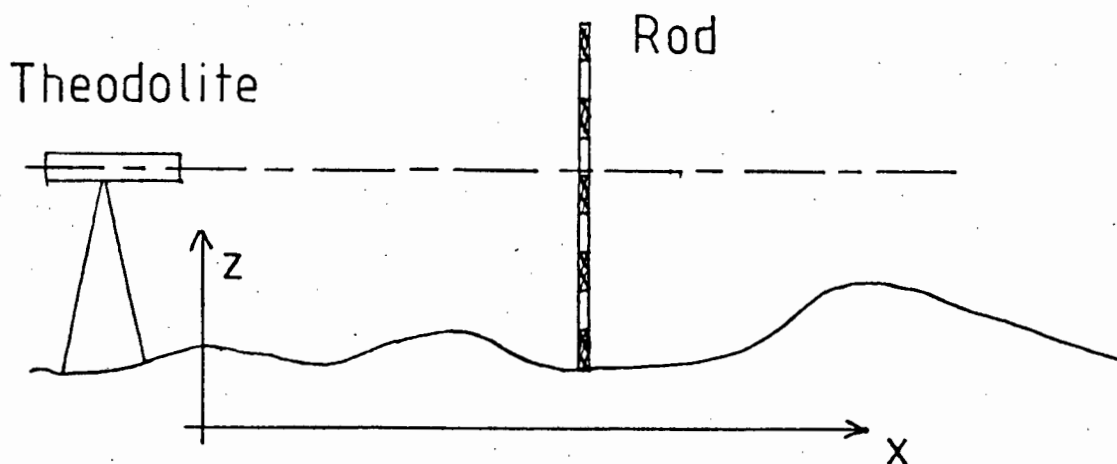


Figure 2.2 Rod and level used for surveying of profile

The method is accurate, but slow. For the resolution required the measuring rate would be 100m per day. The data points must still be entered into a computer for analysis.

Aerial survey was also investigated (Ruether [58]). It is not used for such high vertical resolution ( <1cm ). The vertical resolution is measured in metres rather than in centimetres.

Aerial survey is very expensive, and needs trained operators and special equipment not easily available. The time for processing the data is also long. It would not be much faster than the rod and level method, and more expensive.

#### 2.5.2 Geodetic Beam and Wheel

An improvement in convenience on this method is to use a geodetic beam with a measuring wheel running along it (Bobbert [11]). The beam is placed horizontally over the road, and the movement of the wheel relative to the beam is measured as it rolls over the road. The maximum wavelength it can measure is limited by the length of the beam. This can be extended if the beam can be moved and repositioned in the same line as before.

The beam would not be convenient to set up for extended measurements of the profile.

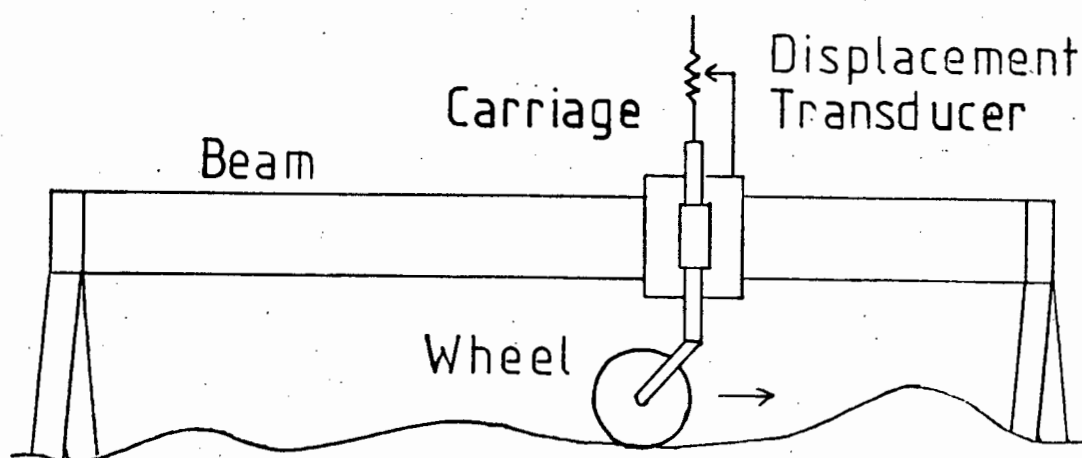


Figure 2.3. Measuring Beam and Wheel

### 2.5.3 Car and Measuring wheel

A much improved method is to tow a wheel over the road surface and measure its displacement. The displacement of the measuring wheel relative to the vehicle is measured by a potentiometer. The vertical accelerations of the vehicle are measured by an accelerometer. When this signal is integrated twice it gives the absolute displacement of the vehicle. Added to the signal of the potentiometer, the absolute profile of the road is obtained. The recorded data thus gives the road profile (Betz [9]).

This method can be used to measure over long sections of the road surface. Disadvantages are that it is dependent on the accelerometers low frequency response when measuring long wavelengths. Extraneous vibrations of the car body will also influence the accelerometer signal.



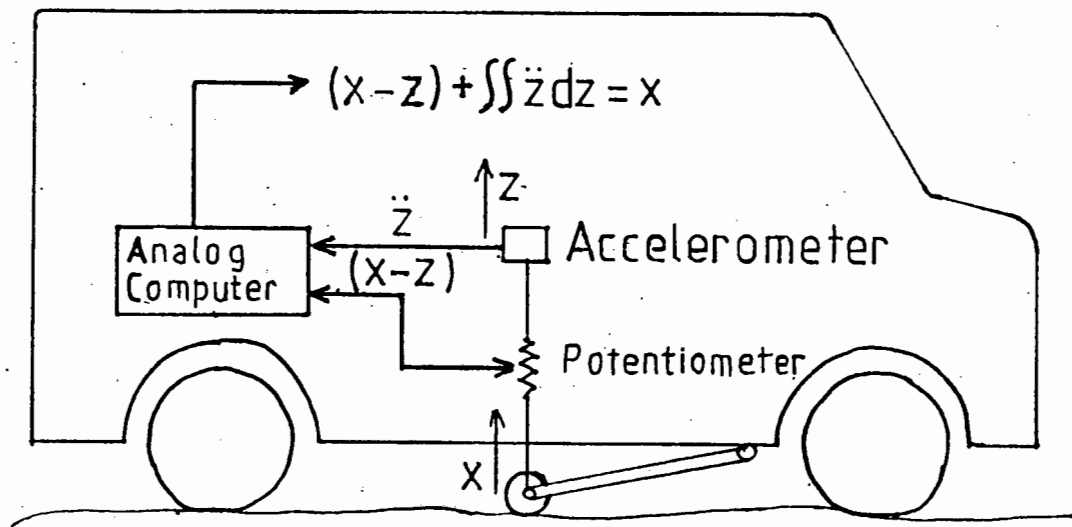


Figure 2.4 Potentiometer and Accelerometer mounted on car

#### 2.5.4 Accelerometer only

A similar method is described by Vogel and Bosch [71]. A very stiff wheel is held on the road by a strong spring. Only an accelerometer is used to measure the accelerations of the wheel, which is converted to give the road profile.

This measuring technique was used to measure roads in Germany. High measuring speeds of 80 km/h were used, and the results were employed to compare various type of smooth paved surfaces. This is not suitable for rough surfaces.

#### 2.5.5 Gyroscopic slope measurement

In the Chloe profilometer design a wheelset is towed over the road surface (described in Shear, [62]). The slope of the wheelset is measured using a gyroscope and used to calculate the road profile.

The profilometer is independent of time, but requires an expensive and delicate gyroscope.

#### 2.5.6 Pendular slope measurement

A French design (described by Shear, [62]) uses a pendular mass on a towed carriage. The slope of the road is determined from the change in angular position of the mass relative to the towing vehicle. Neither its frequency response nor its suitability for measuring rough surfaces is described.

#### 2.5.7 Non-contacting sensors

The final development of this technique is to use non-contacting sensors. This allows very accurate measurements of the the road profile, and also allows high measuring speeds. Systems using lasers are described by Chaka [15], and by Jacobs [39] who uses a gyroscopic datum. The laser is shone onto the road surface. The deflection of the reflected beam is measured and allows the distance from the transmitter to the road surface to be calculated.

Sonic transducers using the same principle are also a possibility. They have been used to read the road surface and control the firmness of the car's suspension in experimental applications (Schefter [59]). In all cases the signals are stored on magnetic tape for later processing.

These methods are improvements on the previous methods, since the measuring speed is not constrained by the ability of the sensor to follow the road surface.

However, the non-contacting sensors still require accelerometer or gyroscopic data. Furthermore the equipment is very expensive, and may be susceptible to dust interference and ingress.

## 2.6 Correlation of the methods

Since all the methods are designed to measure the road profile, one would expect good correlation between them. A survey of the correlation between the methods has not been found.

The different methods are used to measure different regions in the wavelength domain. One could only compare them where their working regions overlap. One would expect rod-and-level surveying to provide the yardstick against which to compare the other methods.

## 2.7 Methods of analysing and using the data

### 2.7.1 Direct replay without analysis

Once the data is in the required form, it must be put into a format compatible with the simulator control system. The simplest method of using the data is to drive the test actuators from the road profile signal stored on the tape (Betz [9]). No analysis of the data, apart from checking its accuracy, is necessary, since it simply reproduces the profile.

### 2.7.2 Gaussian analysis

If it is desired to determine the properties of the road an analysis is necessary. It will then be possible to see what features of the road are predominant, and which cause the most damage. It is easy to calculate the mean value for the data. But since the process is random this does not indicate much about the data. It is necessary to be able to describe the data more fully.

If the data is assumed to be Gaussian, a probability distribution can be used to describe its behaviour ( Bobbert [11], Stockley [67]). It may be necessary to simplify the data depending on how much there is of it.

Accuracy is reduced for ease of manipulation. With one channel of data the simplification is hardly necessary (Andrew [1]). Andrew also thinks that random vibration is best dealt with on a time basis and stress history on a distance basis. He only considers the central 99% of the data, ignoring the extremes.

Methods of measuring the characteristics of the data are given below.

#### 2.7.2.1 Peak Value Measurement

Maxima and minima in the data are recorded over the sample. They may be of two types, local or those that cross the axis. Using the local minima detects harmonics of the signal. Detecting peaks after they cross the axis emphasizes the fundamental. See figures 2.5, 2.6, pg.17.

#### 2.7.2.2 Range Count Measurement

This method measures the intervals between successive local maxima and minima. See figure 2.7, pg.18.

#### 2.7.2.3 Level Crossing

The vertical axis is divided into levels. Each time that the signal passes through a level the event is recorded. Andrew [1] finds it more convenient to calculate level crossings per unit time or distance. This gives an indication of changes in the road surface or other input.

#### 2.7.2.4 Amplitude Probability Distribution

This measures the time between levels that the signal spends. See figure 2.8 pg.18. (A review of the statistics of random processes is given in Appendix A.)

#### 2.7.2.5 Power Spectral Density

If one wants to include frequency in the analysis, then Power Spectral Analysis is suitable. It indicates the strength of the harmonics of the function. These harmonics are the coefficients of the Fourier series describing the data. See Appendix B for more detail.

All of the above methods are suitable for describing the data. Power Spectral Density is the only one which describes the data in terms of the wavelengths present in the profile, and can be intuitively related to the road profile. It is also the method used by VW in describing their synthetic street.

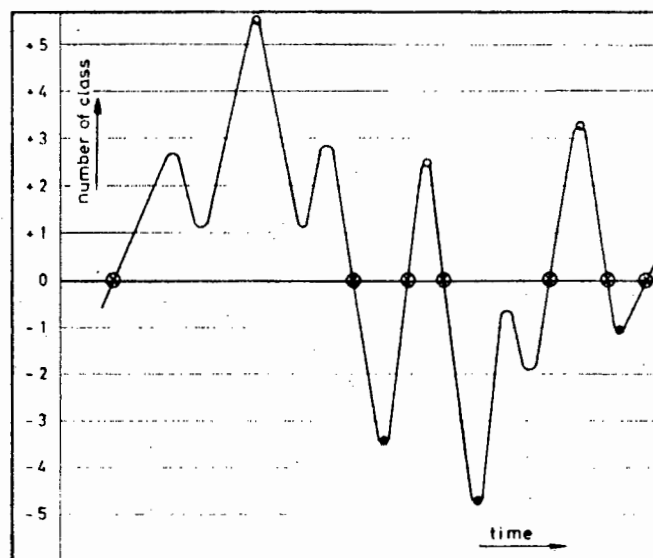


Figure 2.5 Scheme of restricted peak value method.

Only the maxima or minima after zero crossings are recorded. (After Bobbert [11])

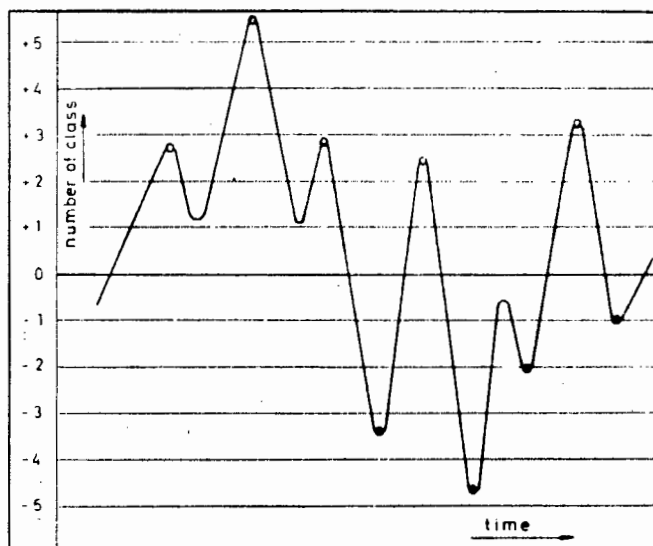


Figure 2.6 Scheme of peak value method. Each maximum and minimum is recorded.

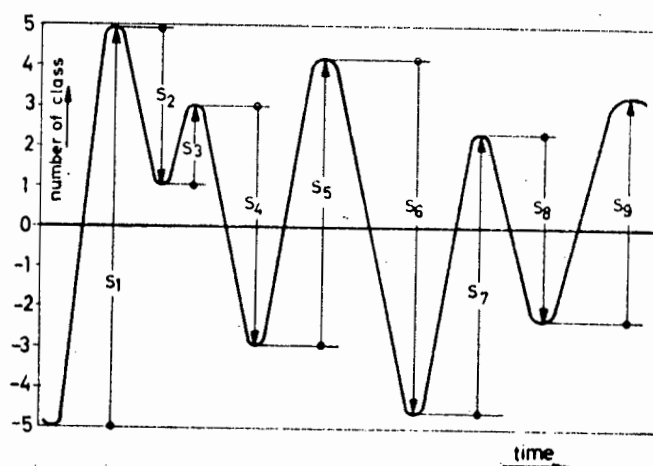


Figure 2.7 Scheme of range counting method. The ranges between maxima and minima are measured and classified.

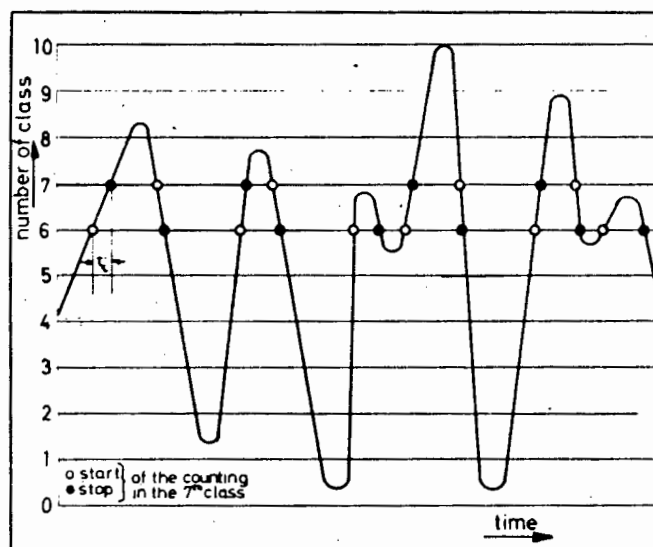


Figure 2.8 Scheme of time in band method. The procedure is shown for the seventh class. Each time the vibration enters the band, one count is made.

## 2.8 Indirect methods of Measuring the road profile

### 2.8.1 Forces in the suspension

The original suggestion for measuring the road was to measure the forces input at the wheels. This could be done by using load cells at the suspension mountings. Lotus have used this device in the control system for their active suspension (Baker [3], Dominy [25]).

### 2.8.2 Strain cycle counting

An indirect method is to strain gauge components. The output from the strain gauges can be analysed using counters and level crossing as well as spectral analysis. The strains induced give an indication of the road quality, but are more useful for comparison between roads than for direct reproduction of the road (Smith [66]).

### 2.8.3 Road Roughness integrators

Further quantitative methods listed in Shear's thesis [62] of road classification are the BPR Roughometer and the TRRL Bump Integrator. These measure the movement of a wheel relative to a heavy trailer towed behind the measuring vehicle. The displacement is integrated mechanically to give roughness units against distance.

Also described in Shear's thesis are the PCA-Portland Cement Road Meter, Mays Meter and Naasra Meter. These and the CSIR-Photologger measure the movement of the rear axle relative to the car body by means of transducers.



The Naasra meter converts the movement of the axle into rotation of a shaft, but the data is also in roughness units per unit distance. These meters measure the movement of the rear axle relative to the car. All of these indirect methods give a qualitative indication of the road roughness, but no profile.

### 3. TEST METHODS

#### 3.1 Definition of the problem

##### 3.1.1 Problem Statement

Determine and use the optimum data for local conditions to drive VW's Hydropuls road simulator.

3.1.2 This can be further expanded as follows:

- a) Determine the best form of data to drive the Hydropuls.
- b) Design equipment to measure, store and use the data.
- c) Compare the quality of the test tracks at present used with that of the synthetic street from Germany. Depending on the results, decide whether or not the synthetic street needs modification.

#### 3.2 Requirements

- i) The data must be in a form which can be used by the Hydropuls control system.
- ii) The data must simulate the stresses encountered in service.
- iii) The measurements must either allow recall of the true road profile, or allow the derivation of its statistical properties to be made. From these a random profile can be generated.

### 3.3 Constraints

i) The project must not require a large investment in new equipment.

### 3.4 Criteria

- i) The data should be applicable to all vehicle types.
- ii) The data should allow editing to speed up testing.
- iii) The measuring equipment should be a self-contained unit, which can be attached to an unmodified car, when it is required to measure the road profile.

### 3.5 Solution specification

The development of the solution is described after the specification, outlined below.

3.5.1 The choice of control function for the Hydropuls is the road profile. This is used in the form of a voltage signal on magnetic tape, proportional to the amplitude of the undulations in the road.

3.5.2 The road profile data is measured by means of a wheel towed behind a test car. The wheel is instrumented to give signals which are combined to give the profile of the road. The signals are stored on magnetic tape. They are transferred to computer for manipulation to generate the road profile.

3.5.3 The road profile data is analysed using Fourier Transform techniques to give the average spectrum of amplitude against wavelength over the range from 12 m to 0.3 m. The equivalent frequency is dependant on the speed of the vehicle, since the wavelengths of the components are fixed.

In the case of the synthetic road, the speed for which the data is given is 15.5 m/s (= 55 km/h). The frequency range is 0.2 to 50 Hz (See Figure 3.1). The amplitude vs. wavelength spectrum measured on VWSA's test tracks is to be compared to the one available for the synthetic street. If there is a significant difference, either a new synthetic street can be generated or the measured road profile can be used.

### 3.6 Concept formation

#### 3.6.1 The choice of control function.

The original proposal from VW was to set up a test vehicle to measure the force input at all four wheels. This data was to be used to control the Hydropuls.

After initial research had been done it became apparent that this was not the best method. The data so gained would be unique to the test vehicle. The forces at the wheels would be different for any other vehicle.

The literature survey showed that the use of a signal which controlled the motion via a transfer function was complex and could lead to instability (Betz [9]).

In the method first considered, the force at the suspension mounting was the control signal. The springing and damping of the suspension and tyres was the transfer function for the input signal from the road to the mounting. Tyres are certainly non-linear (Overton [50]) which presents difficulty in accurate modelling, and the springs and dampers may also be non-linear.

The motion of the actuator would have to be adapted to compensate for the transfer function, to produce the correct forces at the mounting.

Other possibilities such as measuring the suspension movement relative to the body were considered, but offered no improvement as a simulator control function over measuring the forces acting at the wheels.

For practical consideration and from the evaluation of the literature surveyed, the road profile was chosen as a controlling function. This was because:

- 1) It was independent of the vehicle.
- 2) It could be adjusted to simulate any speed.
- 3) The data for the synthetic road was given as a spectrum of amplitude versus wavelength. The only way to compare the two roads was to have the spectrum for the test tracks. Statistically, spectra were an acceptable way of defining the road (Newland [47], Robson [52, 53]), and comparison of the roads could be made on this basis.

### 3.6.2 The measuring method

The object of the measurement is to create a signal that corresponds to the profile of the road. This signal is analysed, for comparison with the synthetic street.

The ideal method of measuring the road is to traverse the measuring equipment over it at a constant height. The undulations of the road are given relative to the datum. One way of achieving this is to use the geodetic beam as described in the literature survey (Bobbert [11]).

When a continuous record over a large distance is needed this is not practical, and a measuring vehicle must be used. The vehicle becomes the datum against which the measurements are made. Some means of compensation must be developed for its motion.

For the method chosen, a "fifth-wheel" , of the type normally used to measure the road speed of a car, is attached to the car. It consists of a bicycle wheel and trailing arm with a universal-joint connecting it to a frame for attaching it to a car. A Linearly Variable Differential Transducer (LVDT) is fixed to the mounting frame so that it measures the vertical displacement of the trailing arm and hence the tyre relative to the frame and car.

An accelerometer is also fixed to the frame, adjacent to the LVDT. This provides a signal which when integrated twice gives the displacement of the mounting point relative to an absolute datum.

By adding the LVDT and double-integrated accelerometer signals, the movement of the test car is eliminated. The resultant signal is that of the road profile relative to the accelerometers 'absolute' datum.

The system has a low frequency cut-off imposed by the accelerometer's poor response at very low frequencies, i.e.  $< 1.5$  Hz. Due to the low frequency cut-off of the system, the datum is not absolute but follows the general trend of the road. This is not a disadvantage, since the simulator cannot duplicate the ascent of a mountain pass, say. Such low frequencies (below 0.2 Hz at 15 m/s) have little effect on the vehicle structure, since the wavelength is much longer than the wheelbase of the car.

The tyre acts as a high frequency filter, since any wavelength shorter than the tyre contact patch and of small enough amplitude will be absorbed by the tyre (VW [70]). Large amplitude, high frequency undulations will however force the tyre to move. The tyre will, just as on a car, only be sensitive to positive undulations shorter than the contact patch. Negative undulations shorter than the contact patch will be bridged by the tyre.

A further discussion of the combination of accelerometer and LVDT signals is given in Appendix D.

Some method of relating the signals generated (amplitude) to the distance travelled (wavelength) must be made. If the vehicle is driven at a steady speed, the signal can be related to wavelength as a function of time. The difficulty of driving with acceptable error at the low speeds envisaged is so great that this was not considered feasible. The data is therefore related to the distance travelled by sampling on a pulse generated every time the wheel rotates through an angle of  $30^\circ$ .

A metal disc, with slots milled into its periphery, is bolted to the wheel hub. The slots break the light beam of a photo-sensitive diode, which generates a square voltage pulse. Since the slots are at a fixed interval from each other, the distance travelled between each pulse is known. If each pulse is used to trigger a sample of the LVDT and accelerometer signals, then they are sampled on a constant, distance related basis. See Appendix C for a discussion of Digital Sampling.

This assumes that the wheel does not slip, and that the compression of the tyre remains constant.

Once the data has been captured by driving over the road surface and recording the signal, it is passed through anti-aliasing filters and "down-loaded" through an Analogue to Digital conversion card into a micro-computer.



With the data stored in the computer, a FFT program is run on the data to produce a spectrum of amplitude against wavelength.

The signals are processed in the computer to give the profile. This could be output again through the D/A converters if required. In this case the spectra of the true profile are calculated and used for comparison with that of the synthetic road.

### 3.6.3 Requirements for the analysis

In order to compare the two road profiles, a spectrum of amplitude against wavelength is necessary for both surfaces. That for the synthetic road is published in VW Technical Report HD 4004 [70], and is given below.

It tabulates the values of the spectral components of the synthetic road used to reproduce the Ehra accelerated proving ground in Germany. The frequency components of the road profile for a road speed of 55 km/h are given. This allows the equivalent wavelengths to be calculated. Although the local test tracks will be measured at a lower speed (25km/h), the wavelengths are independent of speed, and can be compared.

The Spectral Components are the coefficients of the Fourier Series (see Appendix B) which describes the waveform, which is the road profile in this case. By describing the profile in a series of frequency components, the significant frequency ranges can easily be identified.

For accelerated testing it is possible to ignore the unimportant components, and concentrate on those likely to cause the most damage.

To produce damage on the simulator equivalent to that caused by driving over the test track, it is necessary to identify which components cause the significant damage. Their frequency of occurrence is increased, and their amplitude decreased (VW [70]).

The data has been passed through three filters (see Appendix C) to attenuate both ends of the frequency range. The filters are as follows:

- High-pass filter, 8th order at 1.2 Hz
- Low-pass filter, 1st order at 24 Hz
- Low-pass filter, 8th order at 28 Hz

Frequency (Hz) at 55 kph (15 m/s)	Wavelength (m)	Order of the Harmonic	Power Spectral Density (mm <sup>2</sup> /Hz)
0.20	76	1	0.04
1.00	15.2	5	6.00
2.00	7.6	10	37.00
2.20	6.9	11	46.00
2.40	6.3	12	49.00
2.50	6.1	12.5	50.00
3.00	5.1	15	37.00
10.00	1.52	50	2.50
20.00	0.76	100	0.50
25.00	0.61	125	0.170
27.00	0.56	136	0.130
30.00	0.50	152	0.030
50.00	0.31	245	< 0.001

Figure 3.1 Spectrum of the Synthetic Road

The power spectral density is given in the standard units of  $\text{mm}^2/\text{Hz}$ . Analogous to these units is the expression for the power dissipated in a resistance by an alternating current. The power is proportional to the square of the mean current. The total area under the spectrum is equal to the total power dissipated.

The spectrum of the road can be interpreted as indicating the frequency ranges where the motor vehicle suspension will have to absorb the most energy.

The data shows that the highest amplitudes occur in the range of wavelengths from 15 metres to 5 metres. This is thus the area where the suspension and body are tested most severely.

The very long wavelengths have been severely filtered, since they would be difficult to reproduce on the simulator.

Similarly the high frequencies have also been filtered, although their amplitudes start to drop off before the filtering starts. The presence of the very high frequencies would tax the simulator performance, and be unnecessary.

For the simulator test program, the collective occurrence of each frequency is raised by 50%, and the maximum amplitudes lowered by 20%.

The test is run for 180 hours, equivalent to 10 000 km at 55 kph. Approximately 90% of the damage caused by driving over the test track for the same distance is reproduced.

The correlation between the left and the right hand wheel tracks for the synthetic street is as follows (VW [70])

Frequency (Hz) at 55 kph (15 m/s)	Wavelength (m)	Coherence between tracks
0.00	>76.0	0.40
0.40	37.5	0.60
1.00	15.00	0.80
2.00	7.5	0.65
4.00	3.75	0.40
10.00	1.5	0.10
30.00	0.5	< 0.01

Figure 3.2 Coherence between the tracks of the synthetic road

The coherence or correlation between the amplitudes of the wavelengths of the left and right tracks is greatest at 15m, and falls off on either side of this value. The very high frequencies have little coherence.

When a random road profile is generated from the spectrum, separate profiles will be generated for each track. The coherence between them should be similar to the coherence given above.

Interestingly, it may also be possible to use the same signal for both tracks, with a phase difference between them.

Alternatively the same signal could be simultaneously played from opposite ends for each track. As long as the coherence is correct, it will give the required results.

#### 4. MEASURING PROCEDURE AND EXPERIMENTAL APPARATUS

##### 4.1 The measuring procedure

The fifth wheel is mounted onto the back of the test car as shown in Figure 4.1. The LVDT and Accelerometer are mounted on it to record the wheel and frame movements. The signals are stored on a digital four-channel tape recorder, capable of recording from 0 Hz to 10 kHz.

The signal from the pulse generator on the wheel, which is related to distance covered, is also stored on tape. This is used later to trigger sampling of the two other signals. The AC voltage for the equipment is supplied by an inverter run from the car's 12V electrical system. The tape recorder is provided with voice recording facilities. The different sections are noted by voice over on the tape. Calibration of the equipment is described in Appendix D.

As well as long trends in the profile, the accelerometer measures accelerations at the start and end of bumps. (By long trends is meant any slope in the average value of the data. A line fitted to the average value of the data, would not lie parallel to the axis. This is due to very low wavelengths, with periods significant compared to that of the sample.)

If the accelerometer is directly coupled to the wheel it will undergo four different accelerations traversing one bump, assuming ideal behaviour of the wheel and the bump. The first two occur at the start of the bump, and the last two at its end.

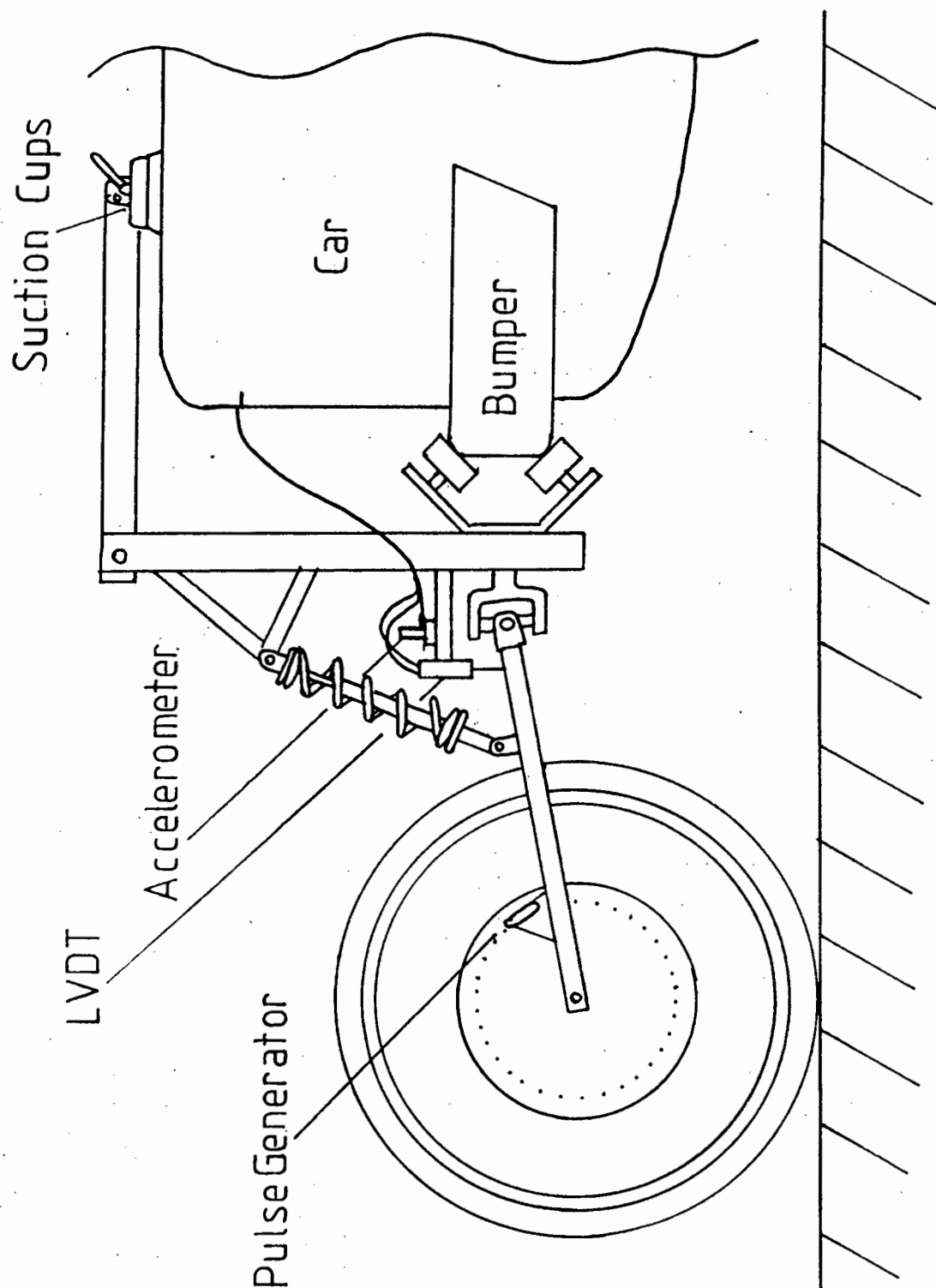


Figure 4.1 Schematic drawing of the mounted fifth wheel.  
(not to scale)

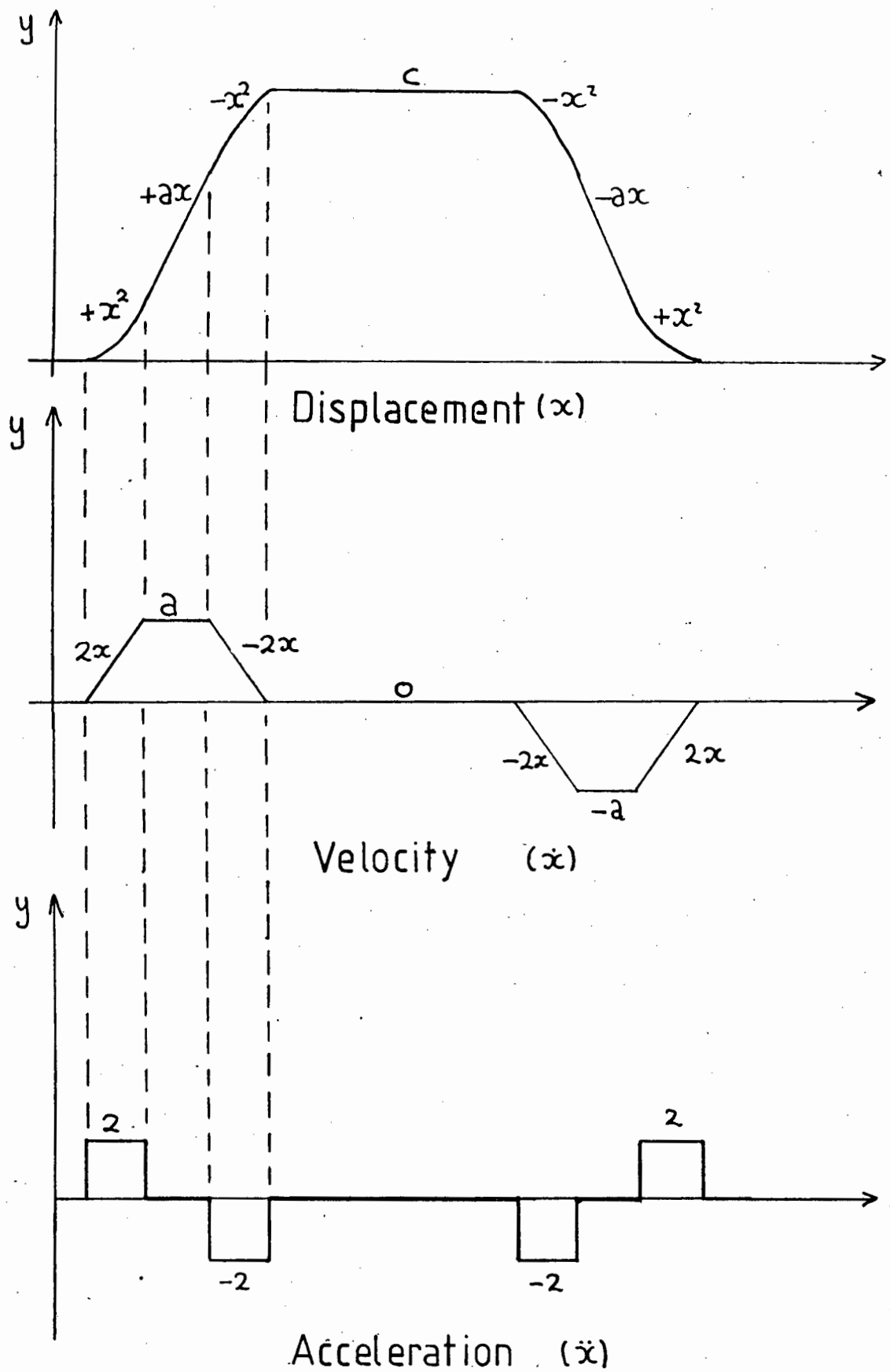


Figure 4.2 Graphs of displacement, velocity and acceleration for a mathematically ideal bump.



Figure 4.2 shows the relationship between displacement, velocity and acceleration. If the bump is abrupt in starting, then each pair of accelerations occurs in a distance of roughly 0.05 m, for a wheel radius of 0.31 m and a bump height of 0.01 m. Each acceleration will occur in 0.025 m if they are evenly spaced. In Figure 4.3, which shows how the parameters are measured,  $X$  is the distance from the centre of the contact patch to the step and  $Y$  is the height of the step.

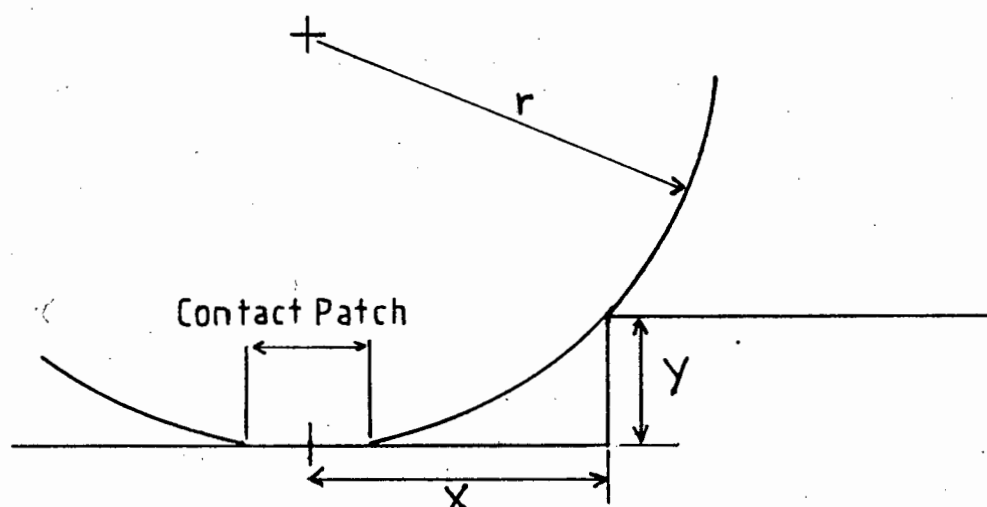


Figure 4.3 The distance in which the wheel is accelerated to the top of an obstruction.

The wheel smooths the shape of the obstruction. When rolling along a smooth surface it only has one point of contact. On encountering an obstruction with a radius on the wheel's side smaller than that of the wheel, as in Figure 4.3, the number of points of contact increases to two. The wheel can only move along these points, and moves from the one to the other without touching the surface in between the points. If the bump has a smooth shape such as shown in Figure 4.2, the wheel only has one point of contact at all times and no distortion of the measured shape occurs.

If no point on the surface has a radius less than that of the wheel, then its shape is reproduced accurately. The amount of smoothing is determined by the wheel radius and the radii of the undulations of the surface.

The wheel acts as a low-pass filter (see Appendix C). As the wheel radius increases, it starts to filter from lower frequencies. When it encounters a square obstruction it smooths its profile. In the same way, a low-pass filter would remove the high frequencies of a square wave, smoothing its shape.

Figure 4.4 shows the response of the car and the wheel to a step in the road profile. The wheel encounters the step at a time  $t$  after the car, determined by its distance from the car and the car's speed. It also shows how the wheel smooths the profile of the bump.

Figure 4.5 shows how the addition of the twice integrated signal from the accelerometer and that from the LVDT combine to give the profile as seen by the fifth wheel.

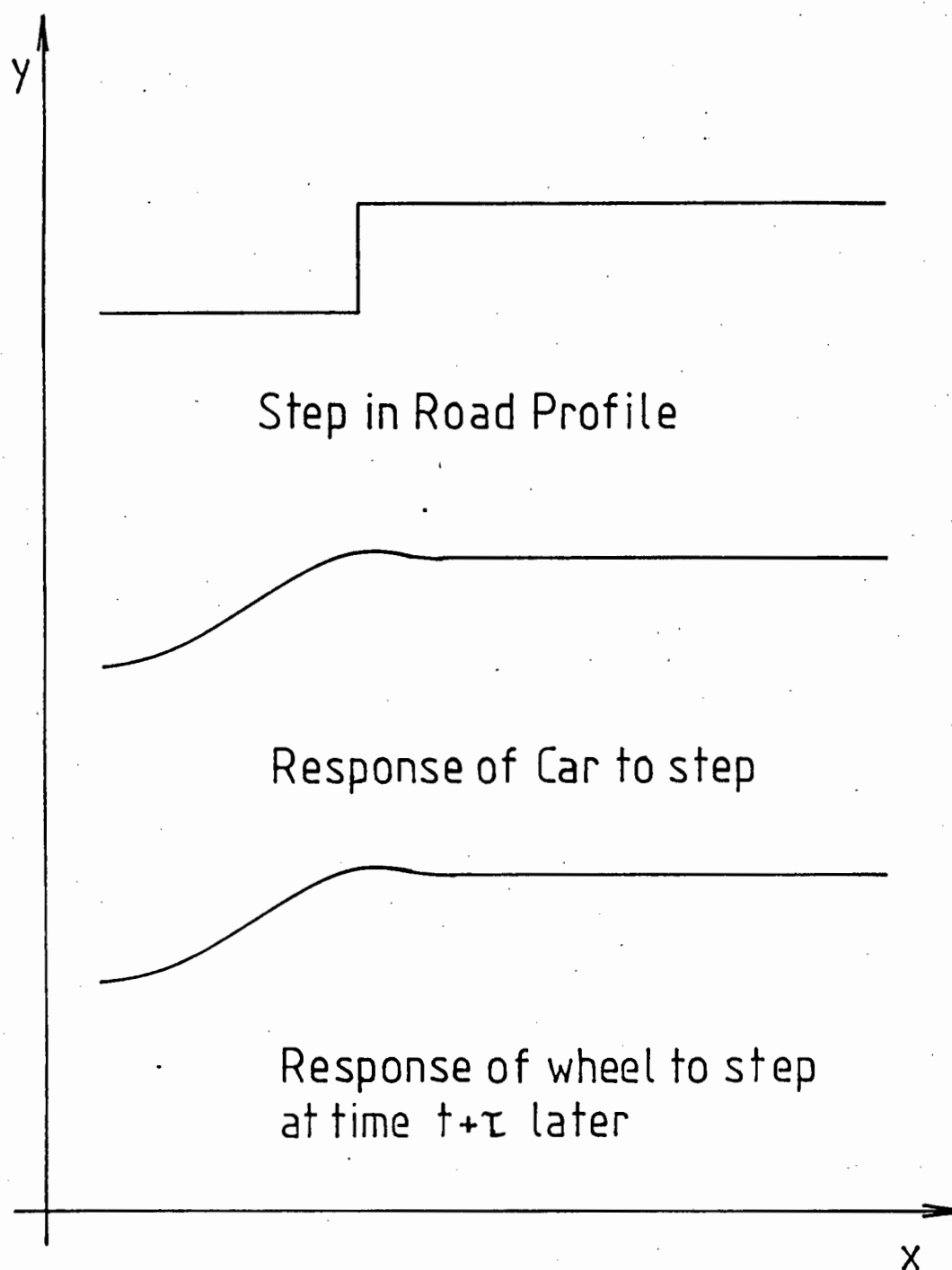


Figure 4.4 The response of the car and the wheel to a step in the road profile.

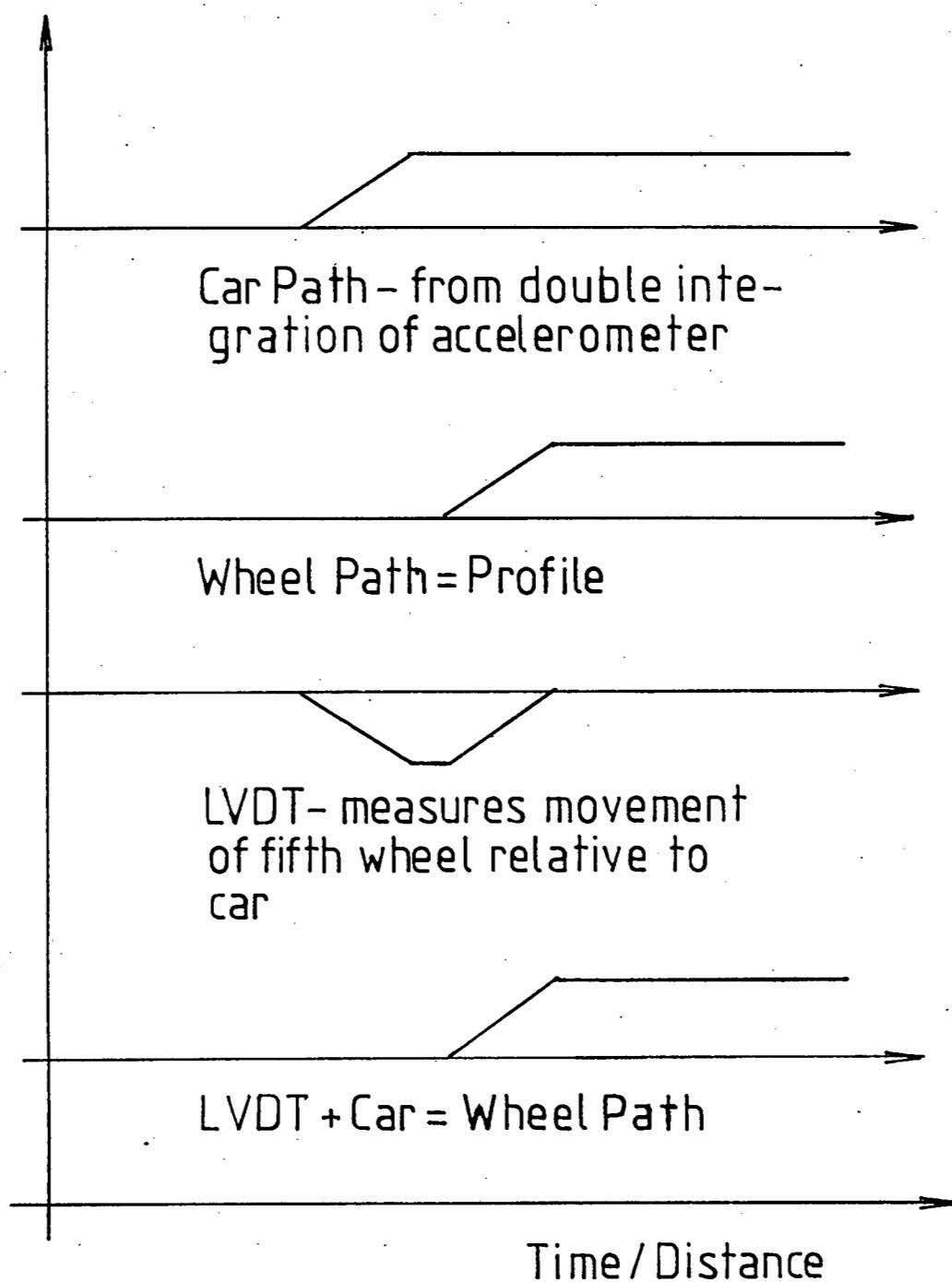


Figure 4.5 Combination of the signals from the accelerometer and the LVDT to give the profile.

#### 4.2 DIGITAL SAMPLING AS RELATED TO THIS PARTICULAR TEST DEVICE

The spectral analysis is performed over a set of readings equivalent to the longest waveform of interest. When sampling with respect to distance, the number of data points for one wave-length is easily calculated since the distance between sampling points is known. Sampling based on distance covered rather than time elapsed also eliminates errors due to easily occurring speed fluctuations. Digital Sampling is described in Appendix C.

The number of pulses generated per unit distance determines the shortest wavelength which can be measured.

The bicycle wheel diameter is 0.67m, taking into account the compression of the tyre. The perimeter is thus 2.1m. There are 120 Pulses per revolution, which gives a distance of 0.0175 m between pulses.

Using Nyquist's sampling theorem (Hamming [31]) the shortest wavelength which can be detected is twice this, viz. 0.035 m. It is eight times less than the required minimum of 0.3 m.

Although the sampling is done on a distance basis, the accelerometer operates in the time domain. Low speeds will benefit the LVDT and the accuracy with which the wheel follows the road. They will reduce the length of the longest wavelengths which the accelerometer will measure.

The accelerometer has a lower frequency limit to its measuring range. The longest wavelength it can measure is determined by that wavelength's equivalent frequency. This in turn is dependant on the vehicle speed.

One must travel faster in order to measure longer wavelengths with the accelerometer. The final speed is thus a compromise between the LVDT's and the accelerometer's requirements.

#### 4.2.1 The Measuring Speed

Initially, using a motorcycle wheel the measuring speed had been chosen to be 6km/h. This was done after observing up to what speed the motorcycle wheel accurately followed the drum profile on a test stand.

After determining the low frequency response of the accelerometer during calibration (down to 1Hz), it was realized that it would not measure the amplitude of wavelengths greater than 1.5m at 6km/h accurately enough. The speed was increased to 10km/h, where the wheel could still follow the profile, although with some distortion, and the accelerometer could measure longer wavelengths up to 3m.

This was still not long enough and the speed was increased to 25km/h. The wheel assembly now passed from the spring stiffness dominated region into the mass dominated region. The frame movement did not distort the signal significantly, and the wheel still detected the bump. However the motorcycle tyre's mass and inherent damping and springing superimposed themselves strongly on the signal.

The motorcycle wheel was replaced with a bicycle wheel with lower mass, less springing and damping and less compliance. This distorted the measurement four times less, using for comparison the accelerometer trace when mounted at the axle.

A discussion of the fifth wheel development is given in Appendix E.

#### 4.3 Design of the anti-aliasing filter.

These are low-pass filters (Appendix C) used to prevent aliasing of the sampled data. They do this by filtering frequencies in the input data higher than half the sampling frequency. They may also be set to filter at lower frequencies.

Although sampling is done in the wavelength domain, the filters operate in the time domain, and the filter calculations are made in the time domain. This means that the wheel speed should be kept steady (within 15%, or between 21 and 28km/h) so that the cut-off frequency of the filters acts at the correct point. If the car goes too quickly, the highest frequency data will be filtered out. If it goes too slowly, aliasing error may occur. The filter cut-off frequency can be set lower than the Nyquist frequency, since the data is being over-sampled. This allows a margin for error in the sampling speed.

The measuring equipment is constrained to operate steadily in the time domain by the accelerometer and the filter requirements.

The calculation of the sampling frequency is as follows:

Wheel circumference = 2.095 m

Wheel velocity = 7 m/s

Pulses per revolution = 120

Pulses per second = 400

Therefore the sampling frequency is 400 Hz

The anti-alias filter must therefore be set at less than  $1/2$  this, i.e.  $f_{\text{cutoff}} < 200$  Hz. According to the sampling theorem, only frequencies less than  $1/2$  the sampling frequency can be detected, so no information is lost if  $f_{\text{cutoff}} = 200$  Hz.

The shortest wavelength to be measured is 0.3m. It has an equivalent frequency of 17 Hz at this speed. If the filter frequency is set at about four times this value or 60 Hz, then a margin is left for fluctuations in the road speed.

To avoid large bias error (see Appendix C), one should sample at at least six times the highest frequency that one wishes to observe. For good accuracy with linear interpolation between points, sampling at ten times the highest frequency gives adequate results. The shortest wavelength of 0.3m is sampled 17 times over its length, which will reproduce it accurately.



## 5. EXPERIMENTAL RESULTS AND DISCUSSION

The results of measurements made in the laboratory and on the road are described below. Descriptions of the intermediate results and graphs of all the results are given in Appendix I. The results are as follows:

- 1) Testing of the integration routine.
- 2) Comparison of the accelerometer measured displacement against the LVDT measurement.
- 3) Testing of the fifth wheel on a rotating drum with and without an obstruction on its surface.
- 4) Tests on various types of road surface.

### 5.1 The integration procedure

Retrieving the accelerometer displacement by double integration is vital to the method of measurement. The first tests verify that integration of a signal's spectrum in the frequency domain is accurate.

#### 5.1.1 The standard waveforms used to test the routine

The integration procedure is tested on many different waveforms. The four shown in Appendix I are a sine wave, a sine wave with noise superimposed, a square wave and an ideal acceleration curve. Integration in the frequency domain is shown to work.

The presence of noise superimposed on the sine wave of example I-2, introduces frequencies below the frequency of the sine wave, as well as higher frequencies. Integration proportionately increases the strength of these low frequencies, which distort the signal.

However they can be removed from the spectrum, since they are below the frequency range of interest. When they are removed, the integral of the sine wave is recovered.

## 5.2 Calibration on the shaker

The same data that was used to calibrate the accelerometer acceleration output, is used to check the accuracy with which it is converted to displacement. The accelerometer displacement signal is subtracted from the LVDT signal, and the resultant signal indicates how closely they agree. Perfect agreement will result in complete cancellation.

At 10 Hz with a peak to peak displacement of 3mm, the LVDT displacement measurement and the integrated accelerometer signal are within 10% of each other.

At 2Hz the accelerometer signal still measures the displacement, although much noise is superimposed on its output.

At 0.5Hz the acceleration levels with such a small displacement are too low to measure accurately, and are heavily obscured by higher frequency vibrations. Nevertheless, the correct shape for the displacement is measured, although the amplitude is nearly two times too large. A high precision low frequency shaker is necessary for accurate assessment of the accelerometer's low frequency, low amplitude behaviour.

The design of a mechanical accelerometer, which gives insight into the requirements, is found in Appendix F.

### 5.3 Calibration on the drum

Tests on a rotating drum are made at a peripheral speed of 7m/s, the speed at which measurements will be made on the road. The fifth wheel is attached to the stand in the same way it would be to a car. The measurements made on the drum are run through the program. It is expected that the resultant measured displacement will mainly be due to the LVDT, since the frame is fixed. The results obtained over several samples show this to be true.

The drum thus does not test the accelerometer's ability to compensate for movement of the LVDT. It does indicate what errors can be expected from the accelerometer due to drift and vibration.

#### 5.3.1 A smooth drum surface

The LVDT body and accelerometer are subjected to high frequency, small amplitude vibrations due to the motion of the wheel. The accelerometer measures an insignificant displacement. The LVDT measures the vibration of the wheel as it rolls over the smooth surface, which is excited by the 1mm runout of the drum.

The very low frequencies of small amplitude are also exaggerated by the integration. They have to be removed in order to regain the profile.

### 5.3.2 The drum surface with a 0.3m long bump on it

(Figure I-8) The height of the bump is 10mm. The LVDT indicates that the wheel follows the bump, and then bounces on leaving it and dropping to the drum surface before striking the bump again. The spectrum shows the period of the drum at 1.5m and its harmonics, and the bump at 0.3m. The bump is coincident with the fifth harmonic of the drum's rotation.

The accelerometer shows a strong vibration at each occurrence of the bump. Its spectrum shows the same peaks as the LVDT, but the amplitudes are reversed. Its integrated spectrum shows the peaks still present, but they are overshadowed by the amplified low frequencies.

The summation of the displacements is dominated by the low frequencies of the accelerometer. If they are removed, then the displacement trace and spectrum is much the same as just from the LVDT measurement, as it should be.

## 5.4 Testing on the road

Once the accuracy of the measuring procedure has been determined in the laboratory, the process is applied to signals measured on the road.

The displacements encountered on the road are much larger than those simulated in the laboratory. The forces generated by wavelengths of similar period but larger amplitude are greater, and easier for the accelerometer to measure.

Wavelengths longer than 14m and shorter than 0.3m are set to zero. Longer wavelengths are too long to be measured with the accelerometer, and shorter ones are not required for the simulation.

#### 5.4.1 Measurement on a level tarred surface. (Figure I-9)

The LVDT shows the surface to be uneven. The surface seems level but uneven with one large excursion at 30m. It must be remembered that the x-axis units are metres and the y-axis units are millimetres, so that the amplitude of the undulations appears exaggerated.

The accelerometer shows a similar pattern to the LVDT. On integration it measures small displacements of up to 6mm, except at 30m, where it shows a displacement of opposite sign to the LVDT and 25mm amplitude. The final profile shows the road to be very smooth, with its maximum excursion still at 30m, but amplitude now 14mm.

The spectral components are all small ( $< 1.5\text{mm}^2/\text{Hz}$ ), with the largest at the lowest frequencies.

#### 5.4.2 Measurement of a speed bump (Figure I-10)

The sample is made over 36m. It shows the measurement of a speed bump of 3.7m length and 0.12m height. Judged by eye, the bump has a radius of curvature of about 6m, but is not constant. The road on either side of the bump is a level but uneven tarred surface.

a) The LVDT

This shows the movement of the fifth wheel relative to the car. The irregularities in the road are accentuated and distorted by movement of the car in response to the road.

When the front wheels of the car encounter the bump, the front starts to rise. The car pivots about the contact patch of the rear wheel. Relative to a line from the front to the back of the car, it seems that the fifth wheel has risen. This explains the first positive displacement shown.

As the car straddles the bump, the back wheel is still on the road surface, and is now lowered relative to the car. This is indicated as the negative reading. As the car leaves the bump, the fifth wheel passes over it, and indicates a positive displacement. At the end of the sample, it is on the level road again.

The LVDT spectrum shows very strong low frequency content, but also a separate group of peaks around 3m, the wavelength of the bump. At the points of large displacement as measured by the LVDT, the accelerometer shows similar trends.

It must be remembered that the two instruments are now not measuring the same displacement. The LVDT measures the displacement of the wheel relative to the car, and the accelerometer the displacement of the LVDT body and car relative to an absolute datum.

#### b) The Accelerometer

The acceleration trace is difficult to read, due to the high frequency content. The acceleration spectrum shows strong content at all wavelengths. As expected, integration decreases the amplitudes of all frequencies greater than  $2 \pi$ , but proportionately emphasizes the low frequencies.

The sum of the two signals quite clearly shows the presence of the bump. The effect of the car's front wheels passing over the bump first is still evident. It has a similar wavelength to the bump, and approximately one third of its amplitude. The resulting spectrum has strong low frequency content. Peaks at the wavelength of the bump are also apparent. They are masked by the lowest frequencies.

#### 5.4.3 Measurement on a dirt track (Figure I-11)

Addition of the accelerometer displacement signal to the profile measured by the fifth wheel cancels out the movement of the car, and gives a realistic profile.

The spectrum shows that the large amplitudes occur at the low wavelengths.

The programs used for data sampling and processing are contained in Appendices G and H.

### 5.5 The measurements made at VW/Uitenhage

An hour of recordings was made on two of the test roads used by VW at their plant. The one road is the Steytlerville road, and the other the Van Staden's pass road.

The Steytlerville road is a dirt road, about three hundred and fifty kilometres long. It consists of a mixture of level but rough surfaces, steep dips and rises, washaways and washboard or corrugation. Many small stones are present in the surface, and provide a continuous high frequency input. It is above the frequency range that is measured, but is always noticeable.

Van Staden's pass is a few kilometres long. The surface is hard, and smooth over short wavelengths less than one metre. Longer wavelengths are present, and cause torsional loadings, due to their unevenness across the road. Also, since there are many corners, it imposes high inertial forces on the vehicles driven over it at the test speeds.

The spectra for each road are plotted in Appendix I, figures I-12 and I-13. For both sets of samples the average, maximum and minimum values are shown.

Very little frequency content is apparent above wavelengths of 1m. The maximum values occur at the lowest wavelengths.



## 6. DISCUSSION OF THE RESULTS AND CONCLUSIONS

### 6.1 Discussion of the shaker results

1) The presence of high frequencies introduces low frequency content into the profile's spectrum as discussed in 5.2. That the low frequencies are further amplified by integration is mathematically correct. However the result of this amplification distorts the data. The highest frequency to be detected after integration should be higher than the fundamental frequency. Four times the record or fundamental frequency gives adequate discrimination.

2) Reduction of the low frequencies is necessary to see the presence of the higher frequencies in the signal.

3) As shown in the literature, windowing the data at the start and end is necessary. It does distort the data in those regions, especially on reconstitution after integration.

4) The accelerometer is easily distorted at low frequencies. A small error in acceleration amplitude is amplified on converting to displacement. Small amplitude high frequencies mask the signal when measuring the lowest frequencies.

5) When the very lowest frequencies are measured (close to the fundamental frequency of the sample), then they are all important and cannot be deleted.

## 6.2 Conclusions from the shaker results.

Using an accelerometer to measure displacement is feasible, with limitations:

1) The lowest frequency to be measured should be greater than four times the fundamental frequency of the sample. Setting the low frequencies to zero extracts the higher frequencies, but is not accurate since there is a small high frequency content in the original displacement trace. As long as this limitation is kept in mind, and only wavelengths above this limit are considered, no error is introduced.

2) When the acceleration is measured at frequencies of 2Hz in real time, the accelerometer output voltage is very low, and is distorted by small amplitude, high frequency accelerations. When the accelerometer is measuring at 0.5Hz, the output is very low, and not accurate to within a millimetre as with the frequencies greater than 2Hz. The accelerometer should only be used to measure large amplitudes (cm) at frequencies  $< 2\text{Hz}$ .

The accelerometer measures higher frequencies than the LVDT does. These are above the range to be measured on the road, and are filtered.

3) When the LVDT and the accelerometer displacement signals are added, the high frequencies are not cancelled completely. Their presence is not significant, since they are above the frequency range to be measured. Their amplitudes are also small ( $< 20\%$  of the shaker displacement).

4) High frequencies which are not necessary for the analysis should be filtered from the raw signal, so as not to produce distortion later.

5) The accelerometer is an acceleration force measuring device. When the frequency and the amplitude become small, the force is also small, and is difficult to measure. Increasing either the frequency or the displacement or both will increase the force and allow it to be measured.

In contrast to the piezoelectric accelerometer which is limited in its low frequency response by charge leakage, the piezoresistive is only limited by its minimum force sensitivity.

### 6.3 Discussion of the drum test results

This test does not test the use of the accelerometer to compensate for movement of the LVDT body. It does show that the accelerometer displacement reading is subject to low frequency errors at these very low acceleration levels. It shows that the LVDT measures the profile, with small distortions due to the dynamic behaviour of the system.

### 6.4 Discussion of the road test results

The signal resultant from summing the accelerometer and LVDT outputs reproduces the road profile. An error is introduced by rotation of the car's body as it passes over a large, long bump.

It was found during testing that in order to compare spectra easily, they must be calculated over the same sample length with the same number of data points. The spectrum indicates the power at each frequency component. The power is equal to the area under the curve. As the interval between components decreases, the area under the curve will be divided between the new components. The height of the spectrum will also be changed at those points.

Spectra calculated by taking a different sample length or number of data points will show peaks around the same frequencies, but of different amplitudes. Without recalculation, only a qualitative comparison can be made.

#### 6.5 Comparison with the Synthetic Road of the VW test tracks

Figure 6.1 is a table comparing the spectrum of the synthetic road with the average values of the two test tracks measured.

Wavelength (m)	Power Spectral Density (mm <sup>2</sup> /Hz)		
	Synthetic Road	Steytlerville Average	Van Staden's Average
76.0	0.04	0.00	0.00
15.2	6.00	0.00	0.00
7.6	37.00	2.59	0.03
6.9	46.00	2.69	0.06
6.3	49.00	0.06	0.23
6.1	50.00	0.39	0.16
5.1	37.00	2.25	0.03
1.52	2.50	0.006	0.004
0.76	0.50	0.001	0.010
0.61	0.170	0.002	< 0.001
0.56	0.130	< 0.001	< 0.001
0.50	0.030	0.008	< 0.001
0.31	< 0.001	0.008	0.003

Figure 6.1 Comparative table of spectral values

Although the values are significantly smaller than those of the synthetic road, plotting them like this is misleading. If the data describing the synthetic road is smooth, then it is reasonable to assume that any spectral value is representative of the values near to it. In the case of the test roads, the spectrum is uneven, and each value is unique.

1) From the single wheel path measurement taken, van Staden's pass seems very much less taxing than the Steytlerville road. The average spectral values are approximately one hundred times less.

2) The average values of the Steytlerville road are about 20 times less than those of the synthetic road. The maximum values of the Steytlerville road are up to 50 times higher.

3) The wavelengths less than one metre are much larger than those on either of the two test roads.

#### 6.6 Conclusions about the road measuring procedure

A device has been developed which allows the road profile to be recorded and analysed.

The use of a Fourier transform program enables integration of the accelerometer signal to be performed. It also allows the filtering of low frequency components in the signal longer than those required. Finally it allows the resultant road profile to be described as a function of its frequency content.

The part of the road spectra with the largest amplitudes is located at the lowest wavelengths. Wavelengths shorter than 1m are not prominent.

The equipment is limited in its performance by conflicting requirements.

These are:

1) The fifth wheel follows the road most accurately when towed slowly over it. (This does not eliminate distortion of the signal due to the relative movement of the car body). As the measuring speed rises, dynamic effects of the tyre and the fifth wheel assembly distort the data.

2) The accelerometer becomes less accurate at frequencies less than 2Hz. This requires that the measuring speed be high in order to measure long wavelengths.

3) The assembly is required to be attachable to an unmodified vehicle. This means that it cannot be rigidly fixed to the vehicle, nor that it can be mounted in the optimum position near the centre of the vehicle where the pitching effect is the least. The resultant play in the mounting, especially over rough roads will distort the signal. The accelerometer can only compensate for movement of the LVDT in the vertical axis it is mounted in.

Bearing these restrictions in mind, the equipment reproduces the surface well. It allows the characteristics of the surface to be determined.

### 6.7 Conclusions from the measurements made at VW

- 1) The Synthetic road seems to be, on average, a more severe test of the motor vehicle endurance strength than either of the two test tracks.
- 2) The Steytlerville road applies extremely high peak values, which test static strength rather than fatigue strength.
- 3) The van Staden's pass does not seem particularly severe from inspection of its spectrum, but is known to provide severe torsional and inertial loading. An examination of the cross-correlation between the left and right hand wheel paths would show this.
- 4) The simulator can be used to test for fatigue strength of the body, since it is continuously more severe than either test road.
- 5) Vw will get more useful data, more quickly by using the Hydropuls.

### 6.8 Recommendations

#### 6.8.1 Recommendations for the Measuring Device

- 1) To improve the accuracy of measurement, a more permanent mounting would have to be made. This will probably be more specific to one measuring vehicle.

2) The accelerometer and LVDT casing should be mounted on an inertial mass inside the device, to cushion the accelerometer from high frequency shocks which are not significant, but will distort its signal.

3) The development of an electrical integrator should be pursued. This will save having to run the integration on the computer, since the signal will indicate displacement before it is even stored on the tape. It will also improve the accuracy of the measurement, since the higher frequencies will be filtered out.

4) Some method of eliminating the very low frequency content of the wave should be developed, or finding the causes in the original signal and removing them before integration.

5) The device should be tested over surfaces whose profiles and spectra are known, for comparison and determination of its performance compared to other such devices.

#### 6.8.1 Recommendations for evaluating the simulator

1) To compare the effects of the simulator and the test roads, cars of similar specification should be run on both. Correlation of damage and the time taken can then be made.

2) Vehicles should also be instrumented for strain and torsion, to compare the maximum and average values produced by the different tests.



## BIBLIOGRAPHY

Books used for reading and reference are listed in alphabetical order. The reference number is given in front of each entry.

[1] Andrew S., Macaulay M.A.,

Analysis of stresses in service for the specification of endurance tests, Proc IMechE Vol 182 Pt 3B, pp 5-14, London, 1967-1968

[2] Ashley C., Mills B.,

The laboratory investigation of vehicle vibration, Proc IMechE Vol 182 Pt 3B, pp 23-31, London, 1967-1968

[3] Baker A.,

Lotus' active suspension, Automotive Engineer, Vol 9 No.1, pp 56-57, London, February/March 1984

[4] Barson C.W., James D.H., Morcombe A.W.

Some aspects of tyre and vehicle vibration testing, Proc IMechE Vol 182 Pt 3B, pp 32-42, London, 1967-1968,

[5] Barson C.W., Gough V.E., Hutchinson J.C., James D.H.,

Tyre and vehicle vibration, Proc IMechE , Vol 179 Pt 2A No 7, pp 213-229, London, 1964-1965

[6] Barson C.W., Dodd A.M.,

Vibrational characteristics of tyres, C94/71, from Vibration and Noise in Motor Vehicles, Proc IMechE, pp 1-12, London, 1971

[7] Barson C.W., Walker J.C.,

Analysis technique for vehicle shake, C132/84, from Vehicle Noise and Vibration, Proc IMechE, pp 47-54, London, 1984

[8] Bastow D.,

Car suspension and handling, Pentech Press, London, 1980

[9] Betz E.R.,

Studying structure dynamics with the Cadillac road simulator, Society of Automotive Engineers, SAE 690101, Warrendale, Pa., 1969

[10] Blackman R.B., Tukey J.W.,

The Measurement of Power Spectra, Dover Publications Inc., New York, 1958

[11] Bobbert G.

Evaluation of vibration design data by statistical means, from Advances in Automobile Engineering (Part III), pp 59-74, Ed. G.H.Tidbury, Pergamon Press, Oxford, 1964

[12] Butkunas, A.,

Random vibration analysis and vehicle developments, Society of Automotive Engineers, SAE 690109, Warrendale, Pa., 1969

[13] Butkunas A.A.,

Random vibration analysis and vehicle shake, C111/71 from  
Noise and Vibration in Motor Vehicles, Proc IMechE, pp 161-170,  
London, 1971

[14] Cain B.S.,

Vibration of Rail and Road Vehicles, Pitman Publishing Co., New  
York, 1940

[15] Chaka R.J.,

The design and development of a highway speed road profilometer,  
Society of Automotive Engineers, SAE 780064, Warrendale, Pa.,  
1978

[16] Cox H.L.,

The riding qualities of wheeled vehicles, Instn Mech Engrs, Proc  
of the Automobile Division, No. 10, pp 265-274, London, 1955-  
1956

[17] Craggs A.,

The assessment of pave'test track loads using random vibration  
analysis, from Advances in Automobile Engineering (Part III),  
pp 31-52, Ed. G.H.Tidbury, Pergamon Press, Oxford, 1964

[18] Crolla D.A., Dale A.K.,

Off-road vehicle vibration, C131/84, from Vehicle Noise and  
Vibration, Proc IMechE, pp 55-64, London 1984

[19] Dahlberg, T.,

Ride comfort and road-holding of a 2-DOF vehicle travelling on a randomly profiled road, Journal of Sound and Vibration (1978)  
Vol 58(2), pp 179-187

[20] Davisson J.A.,

Designer describes how tyres react to applied forces, SAE Journal, New York, April 1970, Volume 78, Number 4, pp 50-53,

[21] Dodds, C.J.,

The laboratory simulation of vehicle service stress, Journal of Engineering for Industry, pp 391-398, New York, May 1974

[22] Dodds, C.J., Robson, J.D.,

The response of vehicle components to random road-surface undulations, FISITA congress, Brussels, 1970

[23] Dodds, C.J., Robson, J.D.,

Techniques for the laboratory testing of Vehicles and components, Journal Auto. Eng., Vol 3, pp 17-19 (1972)

[24] Dodds, C.J., Robson, J.D.,

The description of road surface roughness, Journal of Sound and Vibration (1973), Vol 31(2), pp 175-183

[32] Harms T.,

The application of a Dobbie-McInnes Indicator to record the transient vibration of vehicle suspension model,

(B.Sc. Thesis) UCT, 1981

[33] den Hartog J.P.,

Mechanical Vibrations, 2nd edition,

McGraw-Hill, New York and London, 1940

[34] Hodkin R.K.,

Hydraulic vibrators in automobile testing with special reference to the Rootes suspension parameter rig, Proc IMechE Vol 182

Pt 3B, pp 54-62, London, 1967-1968

[35] Hoeschele D.F.,

Analog-to-Digital/Digital to Analog conversion Techniques, John Wiley and Sons, New York, 1968

[36] Horowitz, P. and Hill W.,

The Art of Electronics, Cambridge University Press, New York, 1987

[37] Institute of Mechanical Engineers,

Vehicle structures, Papers C166/84 (Petty S.P.F.), C175/84

(Landgraf R.W.), C177/84 (Stockley B.), London, 1984

[38] Institute of Mechanical Engineers,

The Design, Construction and Operation of public service vehicles, Papers C137/77 (Peel R.J.), C 138/77 (Pitcher R.H.),

London 1977

[39] Jacobs, P.,

(Private communication), Head of pavement design and maintenance, Transport and Road Research Laboratories, England

[40] Jacoby G.,

Mechanical testing in the Automobile Industry, Schenk (Germany), Pamphlet

[41] Jenkins G.M., Watts D.G.,

Spectral analysis and its applications, Holden-Day, San Francisco, 1969

[42] Levy S., Wilkinson J.P.D.,

The Component Element method In Dynamics, McGraw Hill, N.Y., 1976

[43] Marley, R.G.,

Fundamentals of vibration study, Chapman & Hall ltd., London, 1982

[44] McConnel W.A.,

Fords 4-step test program simulates driver performance, SAE Journal, pp 78-86, New York, April 1960

[45] Mieke B.,

Prozessautomatisierung eines servohydraulischen Prueffeldes, Automobiltechnische Zeitschrift, 85 (1983) 10

[46] Neilson, I.D.,

The motion and stability of a vehicle moving over surfaces which are bumpy, sloping or cambered, Vol 183 Pt 3A, Proc IMechE, pp 145-153, London, 1968-69

[47] Newland, D.E.,

An Introduction to Random Vibration and Spectral Analysis, 2nd edition, Longman, New York, 1984

[48] Nolan S.A., Linden N.A.,

Simulation for endurance testing, Automotive Engineering, June 1988, Volume 96 Number 6, pp 55-59, New York

[49] Nordeen D.L., Rasmussen R.E.,

When a vehicle gets the shakes the tyres may be the culprits, SAE Journal, May 1966, Volume 74 Number 5 pp 60-66, New York

[50] Overton J.A., Mills B., Ashley C.,

The vertical response characteristics of the non-rolling tyre, Proc IMechE Vol 184 Pt 2A No 2, pp 25-40, London, 1969-1970,

[51] Ray R.W., Gibson P.D.,

Vehicle Handling: data acquisition and analysis methods, (C126/83) Proc IMechE, pp 165-174, London, 1983

[52] Robson, J.D.,

An introduction to random vibrations, Edinburgh, the University Press, 1963

[53] Robson, J.D.,

Deductions from the spectra of vehicle response due to road profile excitation, pp 156-158, J. Sound and Vibration (1968) Vol 7(2),

[54] Robson, J.D.,

Deductions from profile excited random vibration response, Proc. 12th Int. Cong. of Applied Mechanics, Stanford University, August 1968

[55] Robson, J.D.,

Response of dynamical system to surface imposed random excitation, Dept. of Mech. Eng., University of Glasgow (no date)

[56] Robson, J.D., Virchis, V.J.,

Response of an accelerating vehicle to random road undulation, J. Sound and Vibration (1971), Vol 18(3), 423-427

[57] Rocard, Y.,

Dynamic Instability, Crosby Lockwood & Son, Ltd., 1957

[58] Ruether, Prof.

(Private Communication), October 1989, Department of Surveying, UCT

[59] Schefter J.,

Sonar suspension, Popular Science, New York, pp 62,104, December 1987



[60] Schenk (Germany),

Dynamic Testing of Automobiles (Pamphlet)

[61] Serridge, M., Licht, T.R.,

Piezoelectric Accelerometer and Vibration Preamplifier Handbook,

Brueel and Kjaer, 1986

[62] Shear D.,

The Influence of road surface properties on vehicle fuel consumption, (M.Sc. Thesis) University of Stellenbosch, 1987

[63] Shinkle,

Accelerated Vibration Testing. a practical approach, Automotive Engineering, June, 1985 pp 60-64, New York

[64] Shinozuka, M.,

Digital simulation of random processes and its applications, Journal of Sound and Vibration (1972), Vol 25(1), pp 111-128

[65] Singh B.,

Laboratory methods for evaluating car body structure dynamics and durability performance, C161/84, Proc IMechE, pp 115-120, London, 1984

[66] Smith K.V., Stornant R.F.,

Cumulative approach to durability route design, Society of Automobile Engineers, SAE 791033, Warrendale, Pa., 1979

[67] Stockley, B., Devlukia, J., Wood, K.,

Durability route correlation, C177/84, Vehicle Studies, Proc IMechE, pp 131-138, London, 1984

[68] Thompson A.G.,

Optimum damping in a randomly excited non-linear suspension, Proc IMechE Vol 184 Pt 2A No 8, pp 169-178, London, 1969-1970,

[69] Timms G., O'Brien J.,

Noise, Vibration and Harshness: Instrumentation and test techniques, C107/71, from Vibration and Noise in Motor Vehicles, Proc IMechE, pp 122-132, London, 1971

[70] VW Technisches Bericht (HD4004),

Synthetische Strasse

[71] Vogel W., Bosch R.

Die Verteilung der Wellenlaengen und -hoehen verschiedener Strassenoberflächen, Automobiltechnische Zeitschrift, Vol 67(1), pp 7-11

[72] Wenstrup, L., Pickornick, W. Agarwal, A.,

Testing for product validation, C108/85 from Prediction and Simulation of Service Conditions, IMechE, pp 119-130, London, 1985

[73] White, K.J.,

The road simulator- a practical laboratory approach, c110/85,  
from Prediction and Simulation of in Service Conditions,  
IMechE, pp 69-80, London, 1985

[74] Whitehead G.D.,

The application of statistics to the vehicle ride comfort  
problem, from Advances in Automobile Engineering (Part III),  
pp 147-180, Ed. G.H.Tidbury, Pergamon Press, Oxford, 1964

[75] Wong J.Y.,

Theory of Ground Vehicles, John Wiley and Sons, New York, 1978

## APPENDIX A: REVIEW OF THE STATISTICS OF RANDOM PROCESSES

The profile of the road surface is random. In order to analyse it, it is necessary to describe its characteristics. This can be done by assuming a Gaussian distribution and analysing it statistically. In this way, based on previous samples, the behavior of other similar road surfaces can be predicted. The following is a brief review of the statistical terms and mathematical treatments employed.

### A RANDOM PROCESS

A random process is one in which the value of the dependent variable ( say  $x(t)$  ) cannot be predicted for a given value of the independent variable ( in this case  $t$  ). Such a process is shown below.

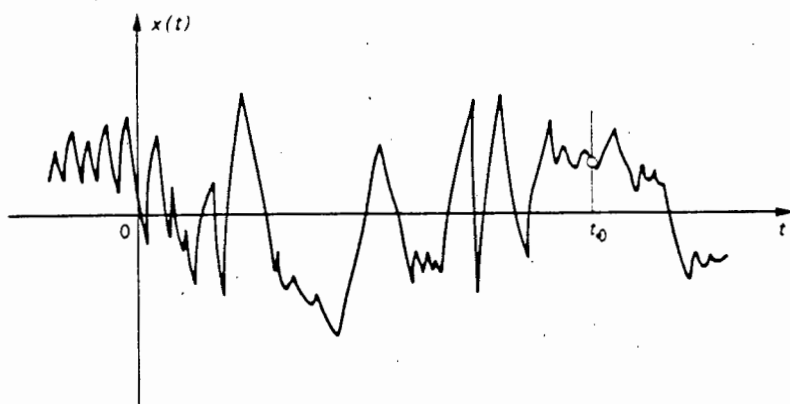


Figure A.1 A random process

By observation of the past history of the signal, it is possible to determine the typical distribution (if it exists) of the signal. It is then possible to calculate the statistical properties of the signal, and to predict the probability of the future distribution of the random signal.

A measure of the signal's behaviour is the proportion of the total record of  $t$  that the signal spends between the levels  $x$  and  $x + dx$  on the  $x(t)$  axis.

By measuring these events, and the proportion of the total record spent in each band, it is possible to predict the future probability of the signal's having a value within a certain bandwidth.

Plots may be made of the probability of  $x(t)$  having a certain value (  $p(x)$  ) against various values of  $x(t)$ .

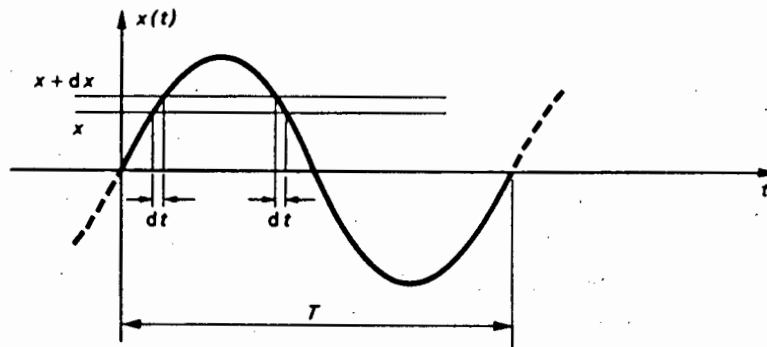


Figure A.2 Drawing of sine wave with band levels shown

For the sine wave shown, (which is a deterministic and not a random process), the amount of time  $t$  spent in the band  $x$  to  $x + dx$  is the sum of the  $dt$ 's shown. The probability function describing the distribution is some function of  $\sum dt/T$ , where  $T$  is the total sampling time or period. In the case of the sine wave the probability density function is

$$p(x) = \frac{dx}{\pi \sqrt{(x_0^2 - x^2)}} \quad \text{for } -x_0 \leq x \leq x_0$$

The probability that  $x$  has lies within a certain band is given by the equivalent area under the curve. The probability that  $x$  has any value is the area under the curve.

$$\begin{aligned} \text{Probability } (-x_0 \leq x \leq x_0) &= \int_{-x_0}^{x_0} \frac{dx}{\pi \sqrt{(x_0^2 - x^2)}} \\ &= 1 \quad \text{for } -x_0 \leq x \leq x_0 \end{aligned}$$

The graph of this function is shown on the next page. It shows the area of the strip equivalent to the probability that  $x$  lies in the band  $x$  to  $x + dx$ .

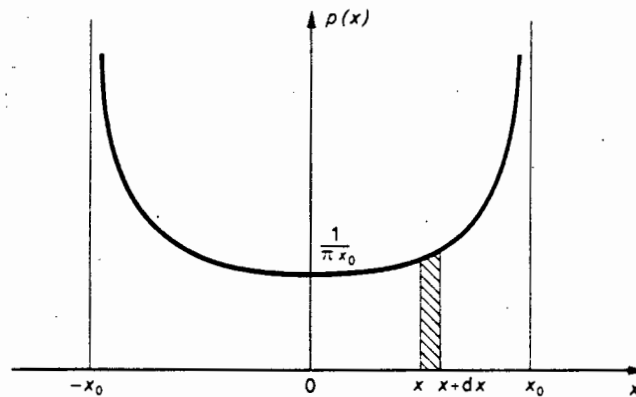


Figure A.3 The probability density function  $p(x)$  vs  $x$  for the sine wave

#### The Gaussian Distribution

Many naturally occurring processes have the bell-shaped or Gaussian probability distribution shown below.

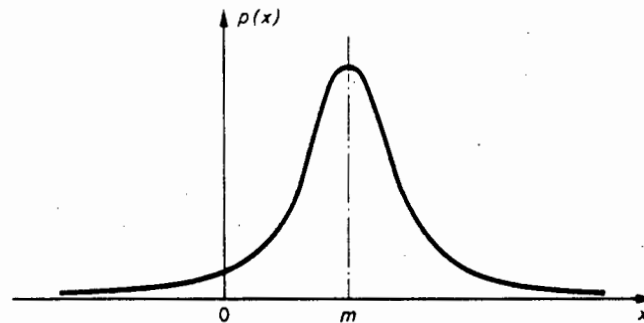


Figure A.4 First order probability density for a Gaussian process

This is a plot of the probability density function against different values of the variable. The area under the curve between the two points gives the probability of  $x$  lying within that range. The equation for the curve is given by

$$p(x) = \frac{1}{\sigma\sqrt{2\pi}} e^{-(x-m)^2/2\sigma^2}$$

$m$  is the mean or average value of the distribution of  $x$

$$m = \frac{\sum x}{\text{no. of samples}}$$

and  $\sigma$  is the standard deviation, which is an indication of the scatter of the measurements about their mean.

$$\sigma = \sqrt{\frac{\sum (x-m)^2}{\text{no. of samples}}}$$

### Ensemble Averaging

If a collection of readings over multiple occurrences of an event is made, then an ensemble of functions is obtained. By taking the average value of the data at the same value of the independent variable for all the samples, an ensemble average is made.

Depending on the number of measurements taken, the order of the probability distribution is increased. Two sets of measurements would thus produce a second order probability distribution. For a Gaussian random process, the ensemble probability distributions must all be Gaussian.

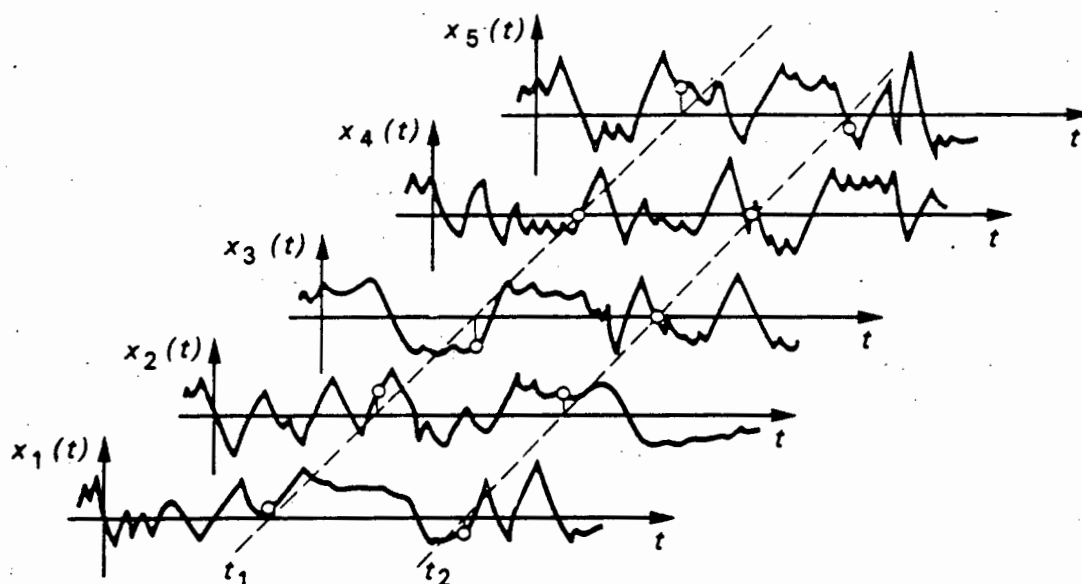


Figure A.5 The concept of ensemble averaging

### Stationarity

The random process is said to be stationary if the ensemble averages are not dependent on the value of the independent variable at the time of sampling. The average over one section is the same as that over any other. For second order functions and higher, the ensemble averages are then dependent on the interval between measuring points. This implies that the mean, the mean square, variance and standard deviation are independent of time.

### Ergodicity

The signal is described as ergodic if in addition to the ensemble averages being stationary, the averages along any one sample are the same as the ensemble averages. This implies that each sample is representative of the random process. If a function is stationary and ergodic, then averages across the samples are equivalent to the averages along any one sample.

### Correlation

This describes the degree of association between two or more variables. If the degree is high, the correlation coefficient  $\rho_{xy}$  is close to unity. If it is low, the correlation is close to zero.

$$\rho_{xy} \text{ is defined by } \frac{E[(x - m_x)(y - m_y)]}{\sigma_x \sigma_y}$$

where  $E[ ]$  denotes the ensemble averaged value of the quantity in brackets

### Autocorrelation

The autocorrelation function  $R_x(\tau)$  for a random process  $x(t)$  is defined as the average value of  $x(t) \cdot x(t + \tau)$  across the ensemble.  $\tau$  is a fixed interval and  $t$  is allowed to vary over the sample. The autocorrelation function is a measure of fluctuations in the data.



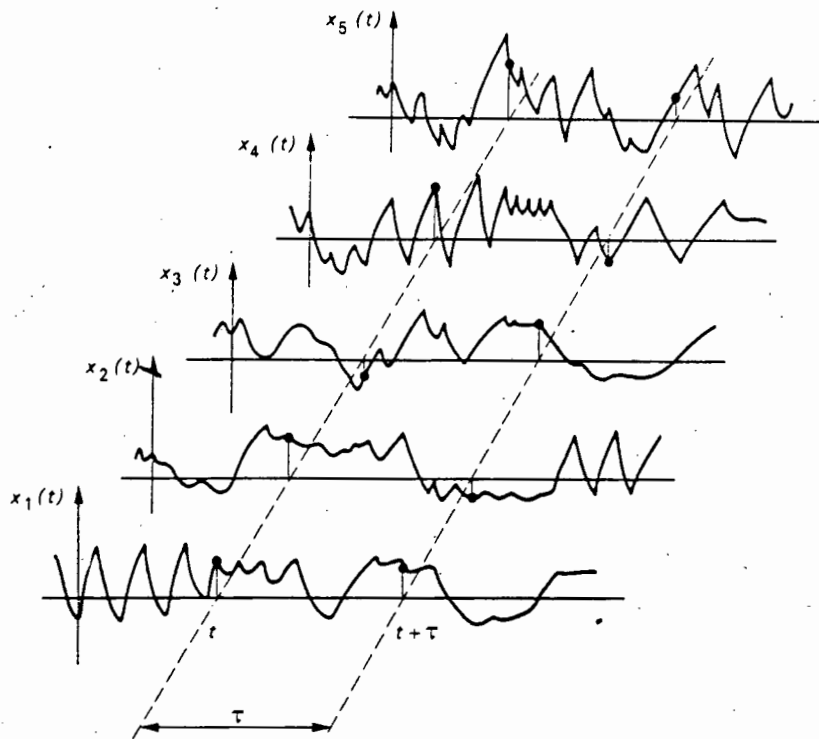


Figure A.6 Calculation of autocorrelation for parallel processes

The average of  $x(t) \cdot x(t + \tau) = E[x(t) \cdot (x(t + \tau))] = R_x(\tau)$ .  $R_x(\tau)$  is called the autocorrelation function for  $x(t)$ . If  $x(t)$  is stationary, then  $m$  and  $\sigma$  are independent of  $t$ , and  $E[x(t)] = E[(x(t + \tau))] = m$ . The function then has perfect autocorrelation. The correlation coefficient for  $x(t)$  and  $x(t + \tau)$  is given by

$$\rho = \frac{R_x(\tau) - m^2}{\sigma^2}$$

It can also be shown that  $R_x(\tau) = R_x(-\tau)$ , i.e.  $R_x(\tau)$  is an even function of  $\tau$ .

A plot of the autocorrelation function for various values of  $\tau$  can be made. As  $|\tau|$  becomes increasingly large,  $R_x(\tau)$  will tend to the mean value of  $x(t)$ . The distance from the vertical axis at which it does this is an index of the suddenness of fluctuations in the function.

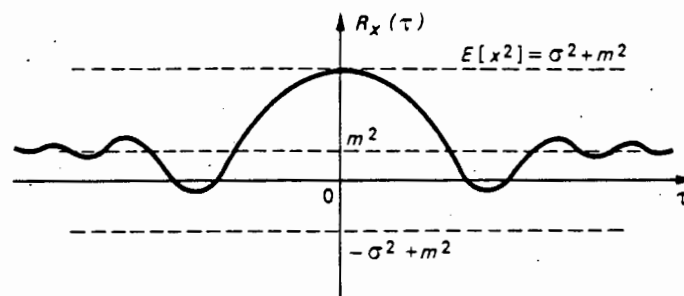


Figure A.7 The autocorrelation function of a stationary random process

### Cross-Correlation

The degree of correlation between two different stationary random functions.

$$R_{xy}(\tau) = E [x(t).y(t + \tau)]$$

$$R_{yx}(\tau) = E [y(t).x(t + \tau)]$$

These can be expressed in terms of the normalised covariance.

$$R_{xy}(\tau) = \sigma_x \sigma_y \rho_{xy}(\tau) + m_x m_y$$

$$R_{yx}(\tau) = \sigma_y \sigma_x \rho_{yx}(\tau) + m_y m_x$$

APPENDIX B: FOURIER ANALYSIS

If a function  $f(t)$  of the variable  $t$  is periodic with a period  $\tau$ , so that  $f(t) = f(t + k\tau)$ , where  $k$  is any integer, then the function can be expressed as a Fourier series.

Other ways of defining this are that the autocorrelation function is equal to the mean value of the series, or that the function is perfectly correlated.

Its statistical characteristics do not vary with time, it is stationary and ergodic. Any one sample has the same statistical properties as any other sample of the same function.

The Fourier series for the function is expressed as follows

$$f(t) = a_0 + \sum_{k=1}^{\infty} a_k \cos \frac{2\pi kt}{T} + \sum_{k=1}^{\infty} b_k \sin \frac{2\pi kt}{T}$$

where  $T$  is the period.

$$a_0 = \frac{1}{T} \int_{-T/2}^{T/2} x(t) dt \quad - \text{the constant term}$$

$$a_k = \frac{2}{T} \int_{-T/2}^{T/2} x(t) \cos \frac{2\pi kt}{T} dt$$

$$b_k = \frac{2}{T} \int_{-T/2}^{T/2} x(t) \sin \frac{2\pi kt}{T} dt$$

Or in complex form,

$$\text{using } e^{-j(2\pi k/T)t} = \cos \frac{2\pi kt}{T} - j \sin \frac{2\pi kt}{T}$$

$$\text{and letting } X_k = a_k - j b_k$$

$$\text{we can write } X_k = \frac{1}{T} \int_0^T x(t) \left[ \cos \frac{2\pi kt}{T} - j \sin \frac{2\pi kt}{T} \right] dt$$

$$= \frac{1}{T} \int_0^T x(t) e^{-i(2\pi kt/T)} dt$$

For discrete series  $\{x_r\}$ ,  $r = 0, 1, 2, \dots (N-1)$

$r$  = the number of the sample

$\Delta$  = the space between samples

$t = r\Delta$

$= T/N$

$= \text{Period/ Number of samples}$

$\omega_k = 2\pi k/T$  and  $k \equiv r$

$= 2\pi k/N\Delta$

$$\begin{aligned} \text{then } X_k &= \frac{1}{T} \sum_{r=0}^{N-1} x_r e^{-i(2\pi k/T)(r\Delta)} \Delta \\ &= \frac{1}{T} \sum_{r=0}^{N-1} x_r e^{-i(2\pi kr/N)} \end{aligned}$$

Alternatively, putting  $f = 1/T$  the real series may be expressed as

$$f(t) = a_0 + 2 \sum_{n=1}^{\infty} a_n \cos n(2\pi f)t + \sum_{n=1}^{\infty} b_n \sin n(2\pi f)t$$

with  $n$  integer. The equivalent complex expansion is

$$f(t) = a_0 + \sum_{n=1}^{\infty} C_n \sin n(\omega_0 t + \phi_n)$$

where  $C_n^2 = a_n^2 + b_n^2$  and  $\tan(n\phi_n) = a_n/b_n$

$\omega_0$  is the fundamental frequency of the function

$a_0$  is the constant or average term

The term in the series with  $n = 1$  is the fundamental component. Terms of higher order ( $n \geq 2$ ) are harmonics of the fundamental. The higher the number of harmonics considered in the series, the better the approximation to the original waveform will be.

The illustrations on the following pages (Figure B.2) show how a square wave can be constructed from a series of sine waves. The harmonics of smaller amplitudes are added to the fundamental. The approximation becomes better as more are added. The very high frequencies sharpen the corners of the wave.

The discrete coefficients can be shown graphically as follows, assuming that the average value  $a_0$ , is zero.

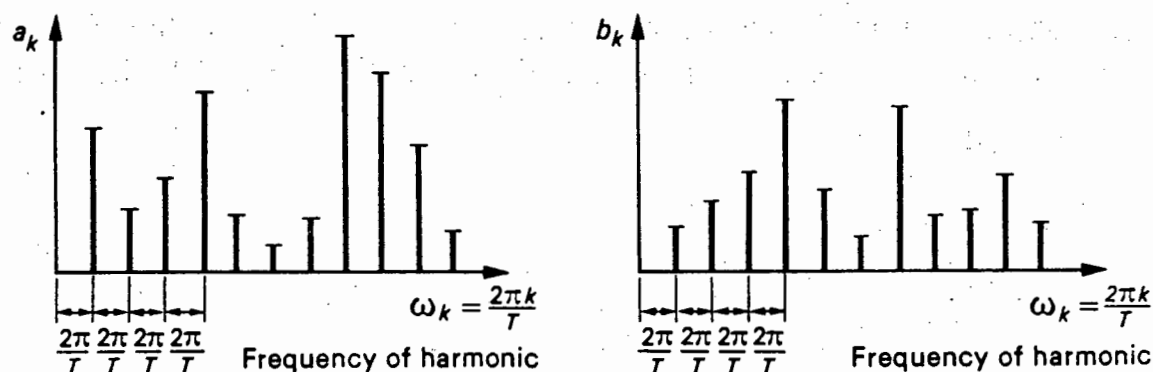


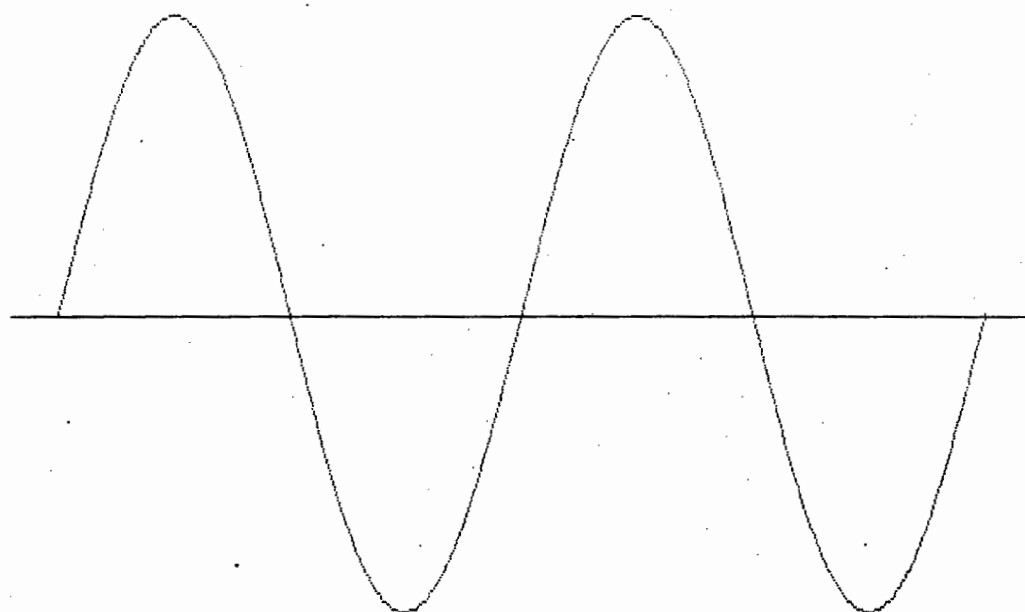
Figure B.1 Graphical representation of the Fourier coefficients

The location of the  $k$ 'th coefficient is at  $\omega_k = 2\pi k/T$ . The spacing between adjacent harmonics is  $\Delta\omega_k = 2\pi/T$ . As  $T \rightarrow \infty$ ,  $\Delta\omega \rightarrow 0$  and the harmonics merge to form a continuous spectrum. The Fourier series turns into a Fourier integral, and the coefficients turn into continuous functions of frequency called Fourier transforms.

### Fourier Integrals

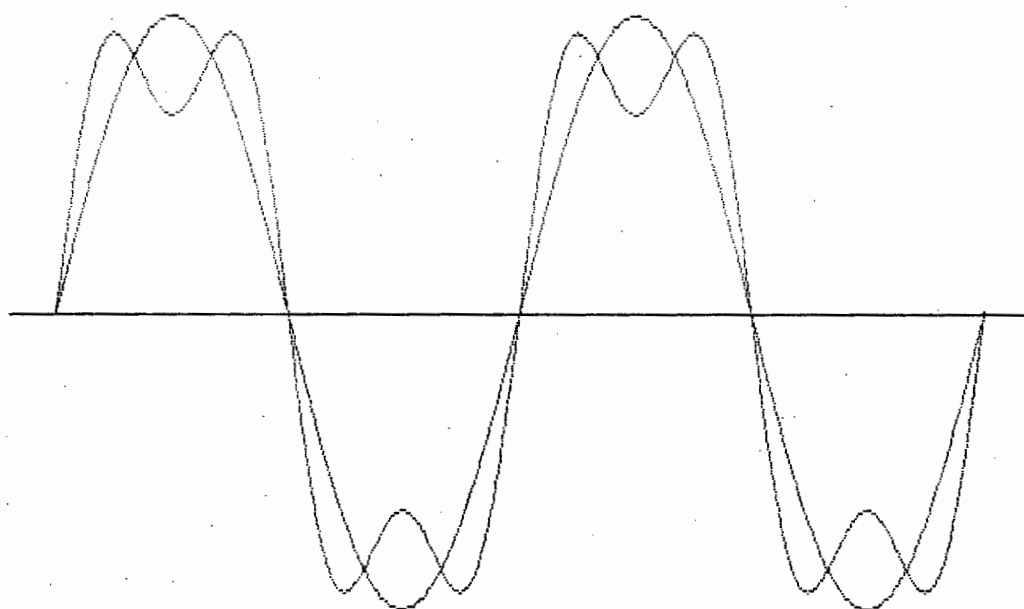
A non-periodic function (sampled over a finite time) can only be treated as a Fourier series if we consider it to be periodic with infinite period. The wave has its original value over the sample period, and is zero elsewhere. The fundamental frequency becomes infinitesimal.

The differences between the discrete terms of the Fourier series disappear and they give a continuous curve. The series becomes an integral.



Number of harmonics ? 0

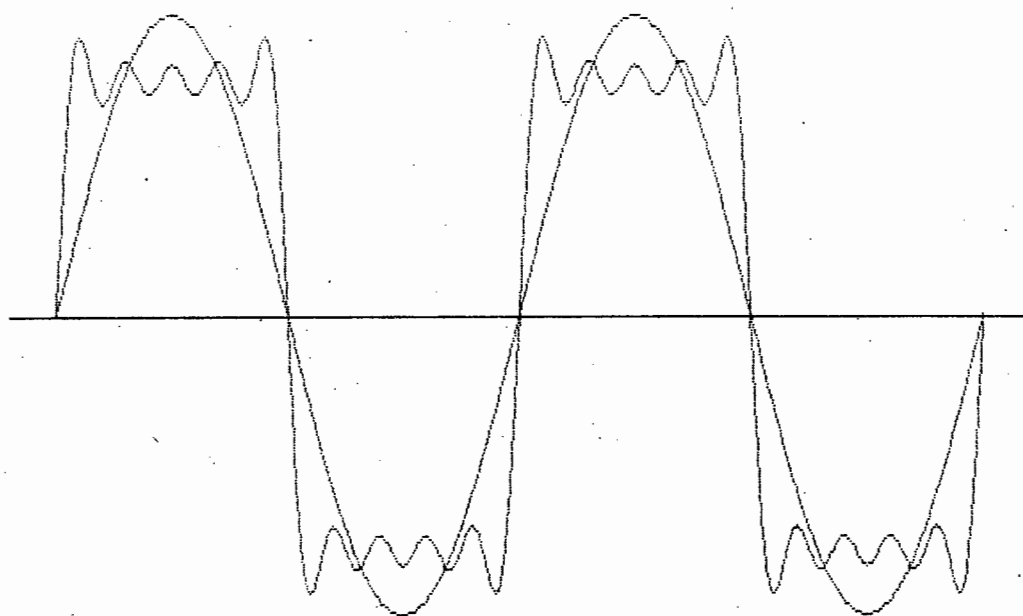
Figure B.2 a)



Number of harmonics ? 1

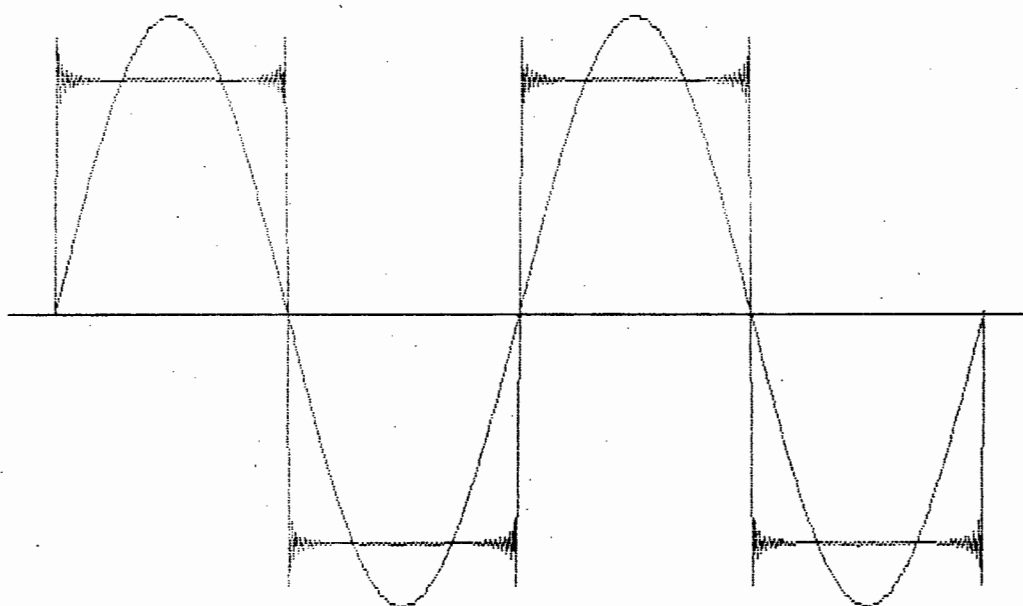
Figure B.2 b)

Fourier Approximation to a Square Wave



Number of harmonics ? 4

Figure B.2 c)



Number of harmonics ? 50

Figure B.2 d)

Fourier Approximation to a Square Wave

With  $a_0 = 0$ , i.e. no average value, manipulation of the series, with substitution of the integrals for the coefficients, gives

$$x(t) = \int_{\omega=0}^{\infty} \frac{d\omega}{\pi} \left\{ \int_{-\infty}^{\infty} x(t) \cos(\omega t) dt \right\} \cos(\omega t) + \\ + \int_{\omega=0}^{\infty} \frac{d\omega}{\pi} \left\{ \int_{-\infty}^{\infty} x(t) \sin(\omega t) dt \right\} \sin(\omega t)$$

Writing

$$A(\omega) = \frac{1}{2\pi} \int_{-\infty}^{\infty} x(t) \cos(\omega t) dt$$

$$B(\omega) = \frac{1}{2\pi} \int_{-\infty}^{\infty} x(t) \sin(\omega t) dt$$

Gives

$$x(t) = 2 \int_0^{\infty} A(\omega) \cos(\omega t) d\omega + 2 \int_0^{\infty} B(\omega) \sin(\omega t) d\omega$$

The equation is a representation of  $x(t)$  by a Fourier integral or inverse Fourier transform. The terms  $A(\omega)$  and  $B(\omega)$  are the components of the Fourier transform of  $x(t)$ . They are equivalent to the coefficients of the discrete series. The values of  $A(\omega)$  and  $B(\omega)$  may be calculated by the substitution of the expansion for the function and performing the integration.



To write in complex notation, we follow the same procedure as before, using the result that

$$e^{i\theta} = \cos(\theta) + i\sin(\theta)$$

We define  $X(\omega) = A(\omega) - iB(\omega)$ , and using the expressions derived for  $A(\omega)$  and  $B(\omega)$

$$\begin{aligned} &= \frac{1}{2\pi} \int_{-\infty}^{\infty} x(t)(\cos\omega t - i \sin\omega t) dt \\ &= \frac{1}{2\pi} \int_{-\infty}^{\infty} x(t)e^{-i\omega t} dt \end{aligned}$$

$X(\omega)$  is called the Fourier transform of  $x(t)$

The inverse transform is given by

$$x(t) = \int_{-\infty}^{\infty} X(\omega)e^{i\omega t} d\omega$$

### Spectral Density

If a process is random and stationary, it is assumed to have commenced at  $t = -\infty$  and to continue to  $t = +\infty$ . Its Fourier transform  $X(\omega)$  cannot be defined.

One can define the Fourier transform  $X_T(\omega)$  of a signal  $x_T(t)$  that is identical with  $x(t)$  over the interval  $-T/2 < t < T/2$  and is zero at all other times.

The mean square value of  $x_T(t)$  or the power can be expressed in terms of  $X_T(\omega)$ . This relationship is called Parseval's theorem.

$$\langle x_T^2 \rangle = \frac{1}{T} \int_{-T/2}^{T/2} x_T^2(t) dt$$

$$= \frac{1}{T} \int_{-\infty}^{\infty} x_T^2(t) dt$$

$$= \frac{2}{T} \int_0^{\infty} |X_T(\omega)|^2 d\omega$$

$|X_T(\omega)|^2$  is an even function of  $\omega$

If we let  $T \rightarrow \infty$ , the expression becomes

$$\begin{aligned}\langle x^2(t) \rangle &= \int_0^{\infty} \lim_{T \rightarrow \infty} \left[ \frac{2}{T} |X_T(\omega)|^2 \right] d\omega \\ &= \int_0^{\infty} S_x(\omega) d\omega\end{aligned}$$

where

$$S_x(\omega) = \lim_{T \rightarrow \infty} \left[ \frac{2}{T} |X_T(\omega)|^2 \right]$$

$S_x(\omega)$  is the mean square spectral density of  $x(t)$ . It indicates the distribution of the harmonic power content of  $x(t)$  in the frequency domain.

Also, for a zero mean signal

$$\sigma^2 = \langle x^2(t) \rangle = \int_0^{\infty} S_x(\omega) d\omega$$

The spectral density can be shown to have as its Fourier inverse the Autocorrelation function

$$S_x(\omega) = \frac{1}{2\pi} \int_{-\infty}^{\infty} R_x(\tau) e^{-i\omega\tau} d\tau$$

$$R_x(\tau) = \int_{-\infty}^{\infty} S_x(\omega) e^{i\omega\tau} d\omega$$

$S_x(\omega)$  is the mean square power spectral density of the process.

$R_x(\tau)$  is the autocorrelation function, previously described in the section on statistical analysis.

## APPENDIX C: DIGITAL SAMPLING AND FILTERING

### C.1 Digital Sampling

Digital sampling is a method of storing a signal as a series of numbers which represents the waveform in discretised form. An example is shown below.

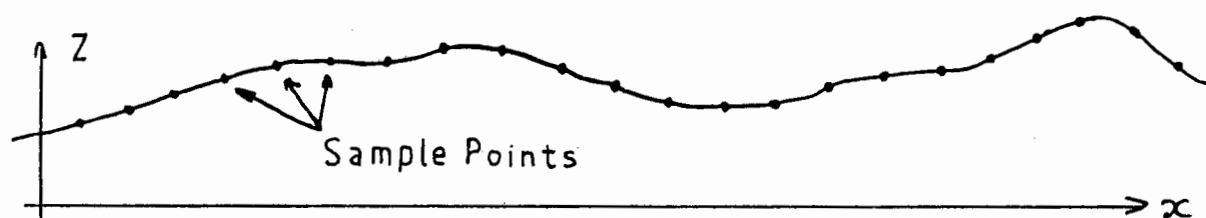


Figure C.1.1 Sampling of data. Each point represents a sample.

#### The purpose of digital sampling

The object of digitising the signal (or converting it into a series of numbers) is to have it in a form in which it can be stored, manipulated and analysed in a computer.

#### How the data is sampled digitally

The analogue data must be converted into an analogue voltage waveform by a transducer. By means of an analogue to digital converter between the voltage waveform and the storage device, the value of the voltage is read at discrete intervals.

These intervals are generally of time, but may also be related to some other parameter. Each voltage reading is converted into a number, and this value is stored. The storage medium might be a digital tape recorder, but is often computer memory or floppy disk.

#### The theory of sampling

The number of samples taken per second is called the sampling frequency. It has been shown (Newland [47], Hamming [30]) that the highest frequency ( $f_{\max}$ ) that can be accurately detected is less than half the sampling frequency.

This can also be stated as follows: the sampling frequency,  $f_{\text{samp}}$ , must be greater than twice the highest frequency,  $f_{\text{max}}$ , in the signal, that is to be measured. This sampling frequency is called the Nyquist frequency or folding frequency.

Alias error occurs when frequencies higher than  $f_0$  are present in the signal to be sampled. They can distort the true shape of the sampled wave.

The difference between the two applications of the sampling theorem should be understood. The one application tells us that aliasing will occur if frequencies higher than half the sampling frequency are present. The other tells us that we can only detect frequencies up to half the sampling frequency. Sampling may be done at frequencies much less than  $1/2 f_{\text{max}}$  of the sampled waveform. The anti-alias filter will filter out all the higher frequencies, since it starts to filter at  $1/2 f_{\text{samp}}$ . However, no frequencies above  $1/2 f_{\text{samp}}$  can be detected.

Bias error occurs as a result of too low a sampling rate, ( $f_{\text{samp}} < 2 f_{\text{max}}$ ) and the amplitude and shape of the waveform are not attained. It can also lead to errors in the apparent frequency of the wave. The phenomenon of beating occurs between the sampling frequency and the sampled frequency.

It is thus necessary to ensure that the sampling rate is high enough to capture all frequencies of interest. It may also be necessary to filter the analogue data with a low-pass time domain filter in order to eliminate the spurious effects of the higher frequencies before sampling the signal.

Although the Nyquist frequency is more than twice the highest frequency ( $f_{\text{samp}} > 2 f_{\text{max}}$ ), in practice a sampling frequency of at least six times  $f_{\text{max}}$  is required to regain the wave if linear interpolation between points is used. A sampling frequency of at least ten times  $f_{\text{max}}$  gives good results.

The illustrations on the following pages show the effects of varying the sampling frequency in reproducing a sine wave.

(Figures C.1.2 to C.1.7 )

WAVE FREQUENCY (Hz) = 2

SAMPLING FREQUENCY = 4

SAMPLED OVER ONE SECOND

SAMPLING AT 2.00 TIMES THE WAVE FREQUENCY

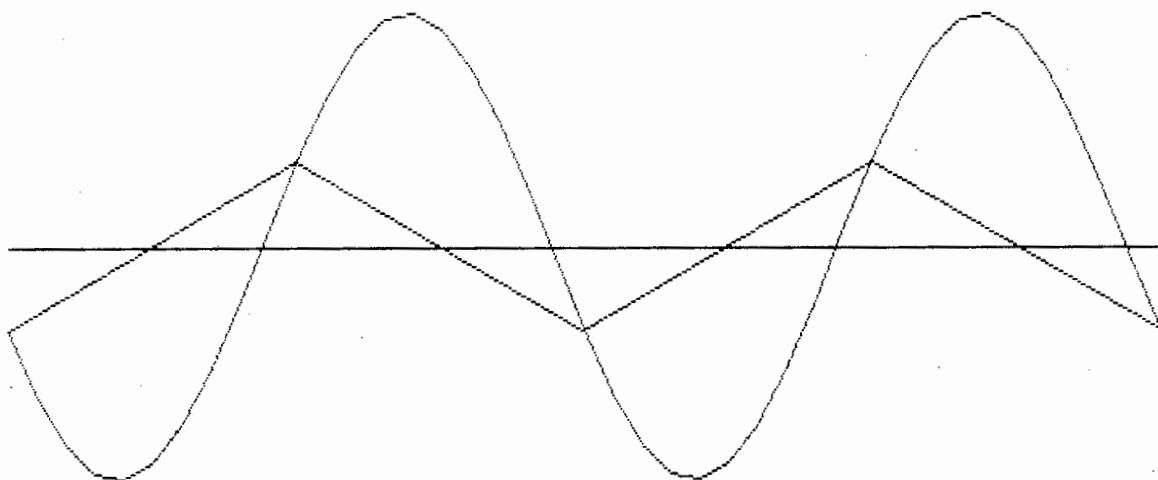


Figure C.1.2

WAVE FREQUENCY (Hz) = 2

SAMPLING FREQUENCY = 10

SAMPLED OVER ONE SECOND

SAMPLING AT 5.00 TIMES THE WAVE FREQUENCY

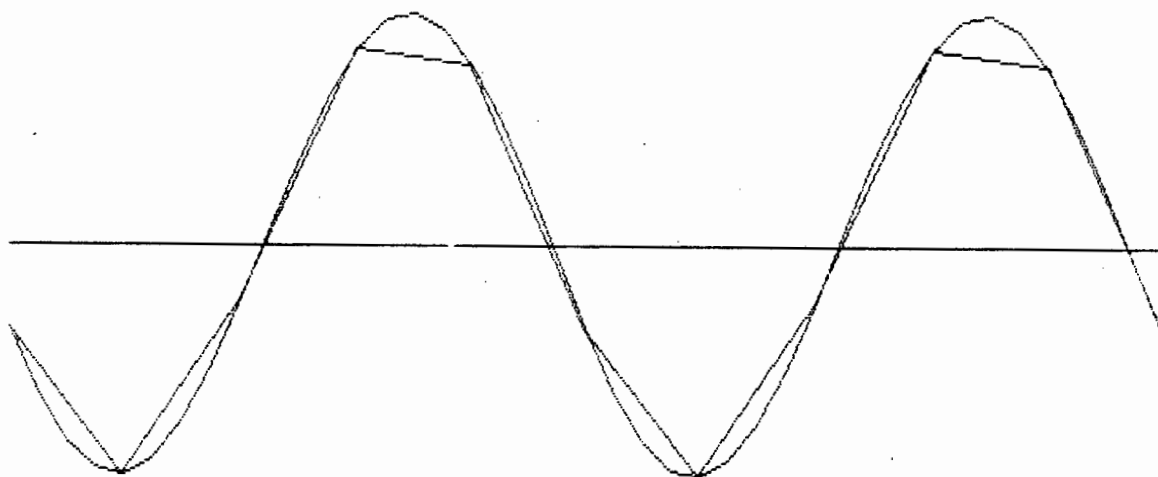


Figure C.1.3

WAVE FREQUENCY (Hz) = 2  
SAMPLING FREQUENCY = 20  
SAMPLED OVER ONE SECOND

SAMPLING AT 10.00 TIMES THE WAVE FREQUENCY

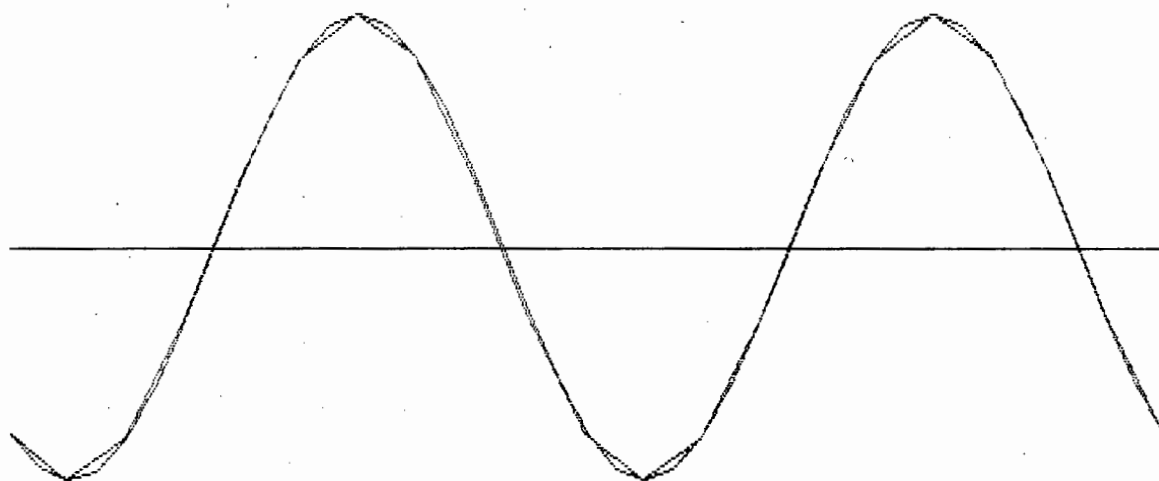


Figure C.1.4

WAVE FREQUENCY (Hz) = 50  
SAMPLING FREQUENCY = 144  
SAMPLED OVER ONE SECOND

SAMPLING AT 2.88 TIMES THE WAVE FREQUENCY

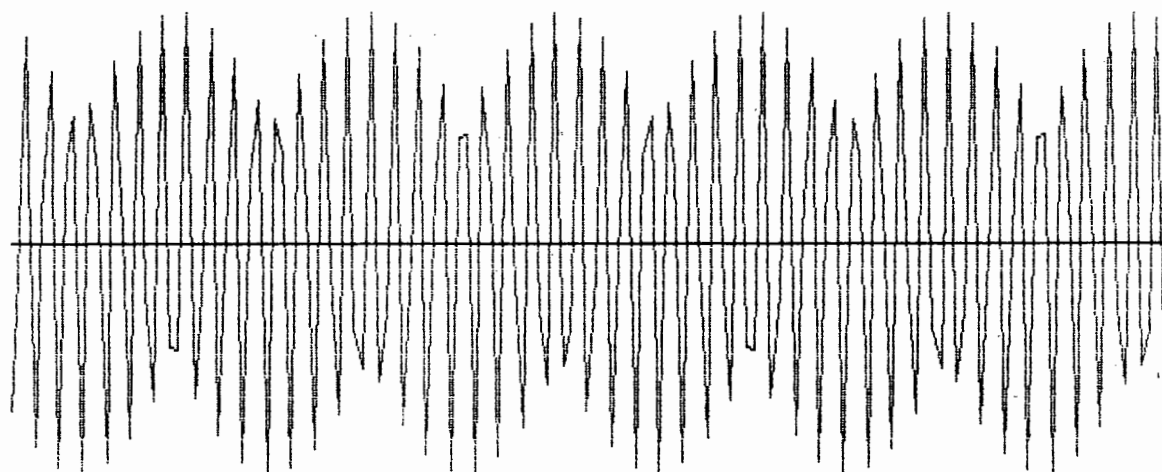


Figure C.1.5

Bias error is strongly apparent  
in the reproduction of the sine wave

WAVE FREQUENCY (Hz) - 100  
SAMPLING FREQUENCY = 210  
SAMPLED OVER ONE SECOND

SAMPLING AT 2.10 TIMES THE WAVE FREQUENCY

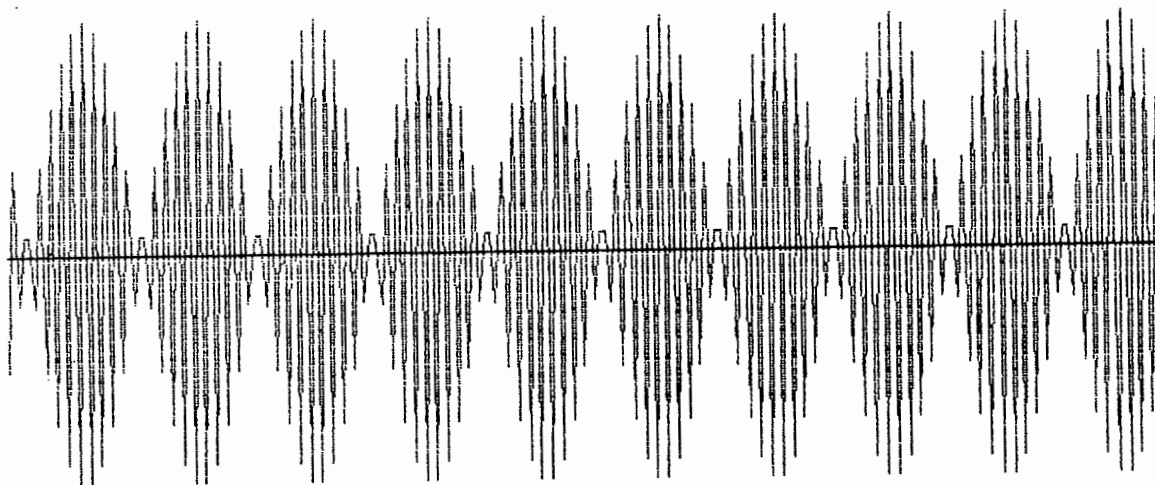


Figure C.1.6

WAVE FREQUENCY (Hz) = 100  
SAMPLING FREQUENCY = 500  
SAMPLED OVER ONE SECOND

SAMPLING AT 5.00 TIMES THE WAVE FREQUENCY

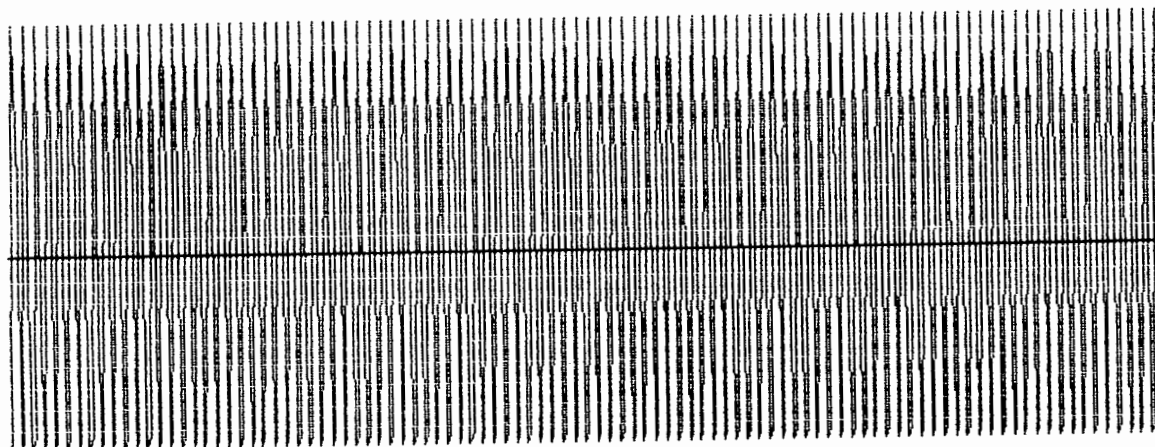


Figure C.1.7

The true peak to peak amplitude of the sine wave is not attained, due to biasing.

Triggering for sampling

Triggering for digital sampling is usually done off a clock pulse. The stored information is thus related to a time base. For the purposes of this project it was more convenient to have the data related to wavelength, which is a way of describing the distance covered.

This can be done by triggering a sampling after each traversal of a specified distance. The length of this sampling distance corresponds to the sampling frequency in the time domain, and must satisfy at minimum the Nyquist relation with regard to the shortest wavelength (highest frequency) that can be measured.

In this case the shortest wavelength or highest frequency of 0.3m was sampled 13 times over its length. This is much greater than the Nyquist frequency, and captures the true shape of the wave.



## C2: ELECTRICAL FILTERS

This section of the appendix describes the circuits and calculations used for high-pass and low-pass filter design. It also describes the similar circuits used for integration and differentiation. The triggering circuit for the A/D sampling card, using the wheel generated pulse which was not sufficiently strong is described as well.

### C.2.1 Low Pass Filters

#### C.2.1.1 The passive filter

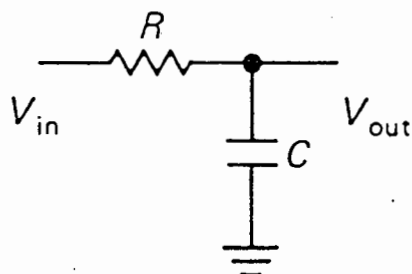


Fig C.2.1 Circuit of a passive low-pass filter

$$\left( \frac{V_{in}}{V_{out}} \right)^2 - 1 = (2\pi f)^2 R^2 C^2$$

$$f_{3dB} = \frac{1}{2\pi RC} \quad \text{This is the frequency at which } V_{out} = 0.707V_{in}$$

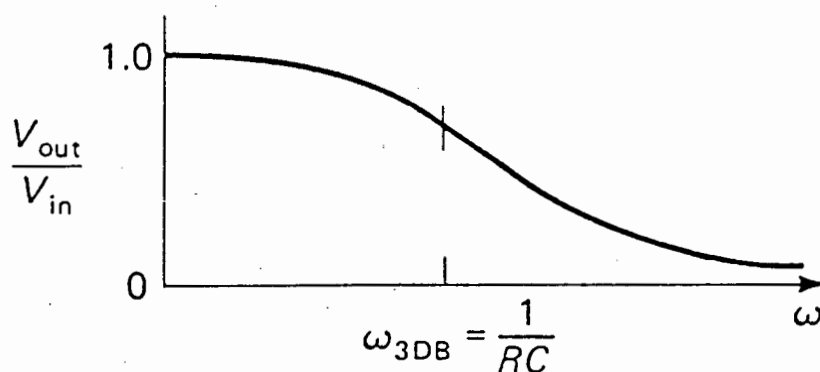


Fig C.2.2 Frequency response of a low-pass filter

### C.2.1.2 The active filter

The new unit in the active filter is the operational amplifier or Op-Amp. The type used is an 8-pin Integrated Circuit. It is used to amplify the signal. The connections are as shown below.

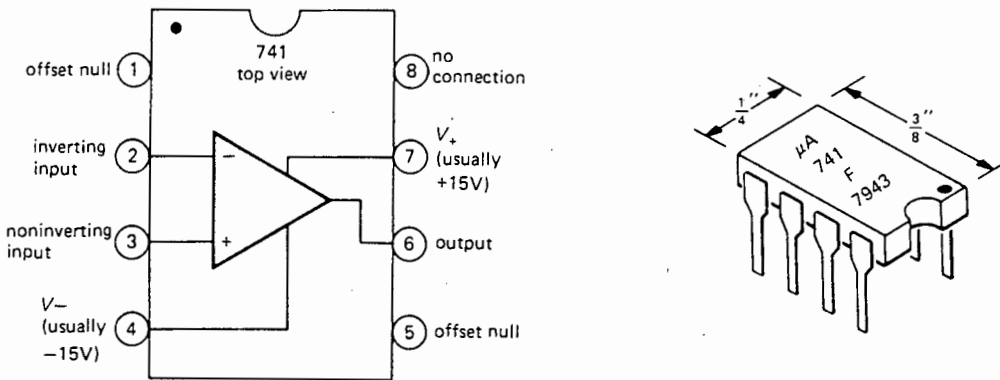


Fig C.2.3 The pin connections of an op-amp.

The gain of the amplifier is the ratio of the output voltage to the input voltage. The feedback voltage is the voltage that is taken from the output and reapplied to one of the inputs. It is used to control the output, since the amplifier will attempt to balance the difference between the two inputs.

$$\begin{aligned} \text{Amplifier gain} \quad G &= -V_2/V_1 \\ \text{Feedback factor} \quad H &= V_f/V_2 \\ \text{Gain with feedback } G_f &= G/(1 + G.H) \\ V_2 &= G/(1 + G.H) \times V_1 \end{aligned}$$

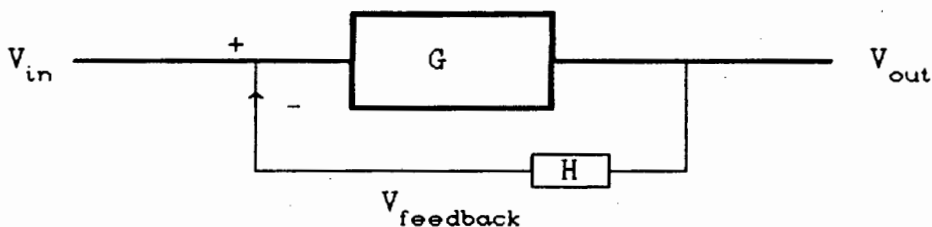


Fig. C.2.4 A feedback circuit

### C.2.1.3 The Active Low-pass Butterworth Filter

This is the type of filter used in this project for anti-aliasing. Only one stage was used for each channel of data, since it was considered that the roll-off was sufficient. 6th order switched-capacitor filters are available on a single chip. These were tried, but problems in using them made the simpler circuit the choice. However if they can be used they would provide a far steeper roll-off which would be important in critical applications.

To find the 3dB point the equation of  $RC = \frac{1}{2\pi f_{3dB}}$  is again used.

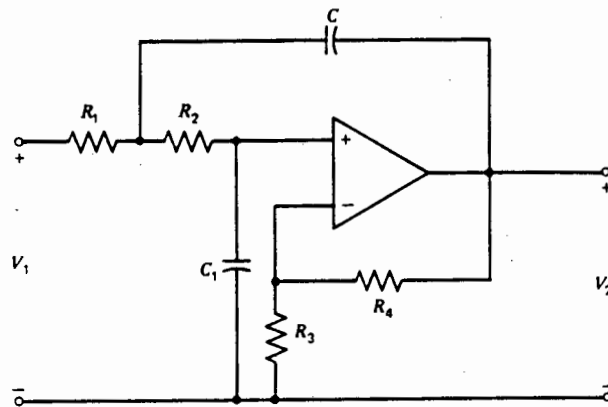


Fig. C.2.5 Circuit of the active Butterworth low-pass filter.

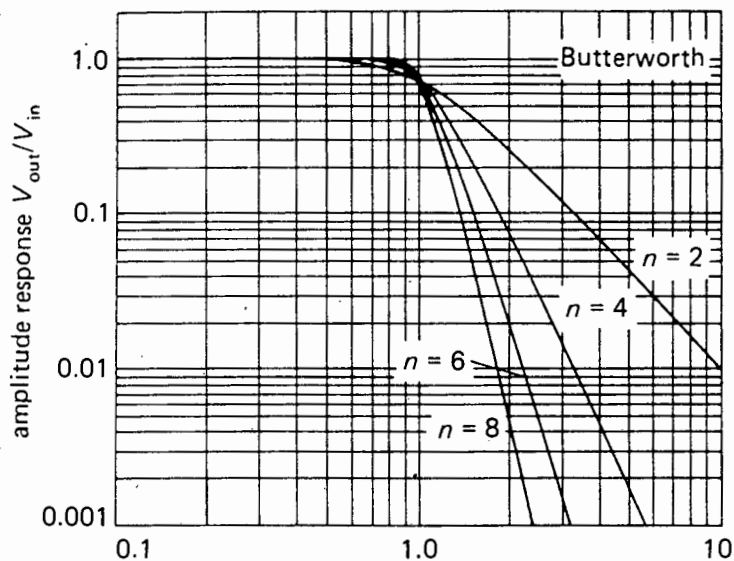


Fig. C.2.6 Normalized frequency response of the Butterworth filter of order  $n$

## C.2.2 High-Pass Filters

### C.2.2.1 The passive filter

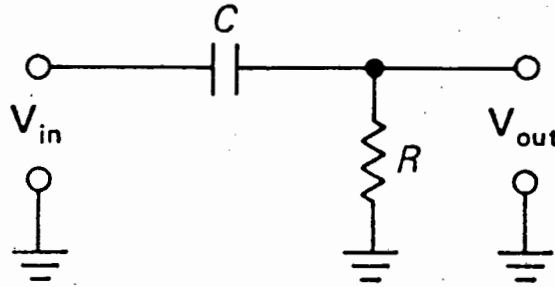


Fig. C.2.7 Circuit of passive high-pass filter

$$\left( \frac{V_{out}}{V_{in}} \right)^2 = \frac{(2\pi f) RC}{[1 + (2\pi f RC)^2]^{1/2}}$$

$$f_{3dB} = \frac{1}{2\pi RC}$$

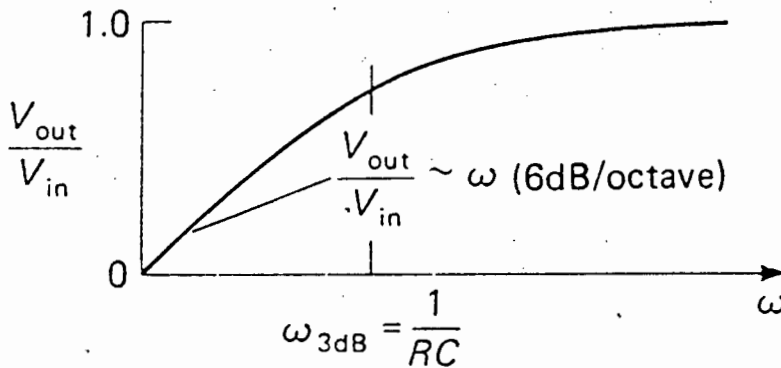


Fig. C.2.8 Frequency response of the high-pass filter

### C.2.2.2 The active filter

Passive filters cause a drop in the signal amplitude of 3db/octave, or 3db for every doubling of frequency after the 3db point. They also cause a fixed drop in the voltage in the pass band. Cascading filters increases the rate of attenuation, but also increases the voltage drop in the pass-band.

Using active filters allows unity gain in the pass-band. The basic configuration of these filters usually gives 6db/octave attenuation for a single stage, as opposed to 3dB for a passive filter.

As an aside, it should be noted that it is better to use high values of R rather than C in constructing circuits. Large capacitors tend to drift, and can load the stages they are connected to.

### C.2.3 Integrating circuits

The layout for passive integrators and differentiators is the same as that for high and low pass filters. The configuration for active circuits is not the same as for the active filters. It was attempted to use electrical integrators to integrate the accelerometer signal to give displacement. Both passive and active circuits were tried, with little success.

The passives suffered from too high a voltage drop and a small dynamic range. The active integrators were used at the bottom of their frequency range. Part of the signal was greatly amplified, and the other part which fell below the 3db point was too severely attenuated. Although this is the way an integrator should work, namely to filter out the high frequencies, it was not doing so in the correct ranges. It was not possible to design one that did.

Later reading (Horowitz and Hill) revealed that the passive integrator should be used at frequencies higher than the 3db point. This is perhaps something that should be tried with the active integrator.

Further consideration of the integration process shows that it is difficult to have a wide frequency response.

If the input is  $A \cos \omega t$

$$\text{then the output} = \iint A \cos \omega t \cdot dt dt$$

$$= -A/\omega^2 \cos \omega t$$

For low  $f$ ,  $\omega$  is small, and the gain is high.

for larger  $f$ ,  $\omega$  increases and the gain decreases.

So if integration took place over the range 0.1 to 50 Hz:

$$f = 0.1\text{Hz}, 1/\omega^2 = 100$$

$$f = 50\text{ Hz}, 1/\omega^2 = 0.0004$$

This gives a dynamic ratio of 250 000

The usual dynamic range of the op-amp is about 100. Thus one or other end of the frequency range would be distorted. For the integrator it would be better to distort the higher frequencies which will be strongly attenuated in any case.

### C.2.3.1 The Active Integration Circuit

$$\text{As before, } f_{3\text{dB}} = \frac{1}{2\pi R_1 C}$$

$$\text{Also given } f_{\text{unity gain}} = \frac{1}{2\pi R_1 C}$$

$$f_{\text{constant gain}} = f_{\text{unity gain}} / (R_2/R_1)$$

$$= \frac{1}{2\pi R_2 C}$$

$$\text{The Gain ratio} = (R_2 + X_C)/R_1$$

$$= (R_2 + 1/\omega C)/R_1$$

$R_2/R_1$  = gain in constant gain portion of the response  
(within the amplifier's limits)

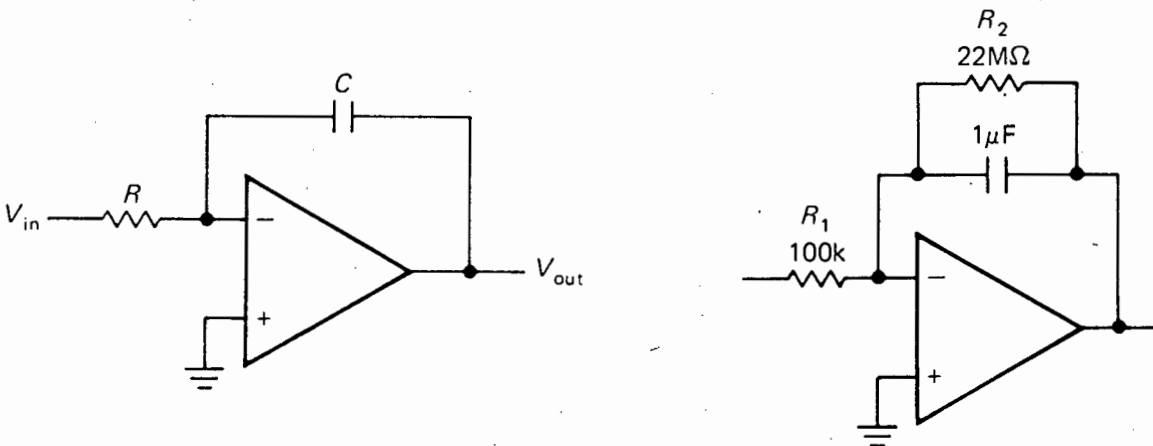


Fig C.2.10 The circuit of an integrator

The basic active integrator design does not have  $R_2$ .  $R_2$  should have a large value, say 22 M ohms. Parallel to  $C$  it provides DC feedback for stable biasing. It rolls the integrator performance off for  $f < 1/(R_2 \times C)$ .

For the Integrator,  $V_{out} = \frac{1}{RC} \int V_{in} dt + \text{constant}$ .

The integrator has similar frequency response to the low-pass filter.

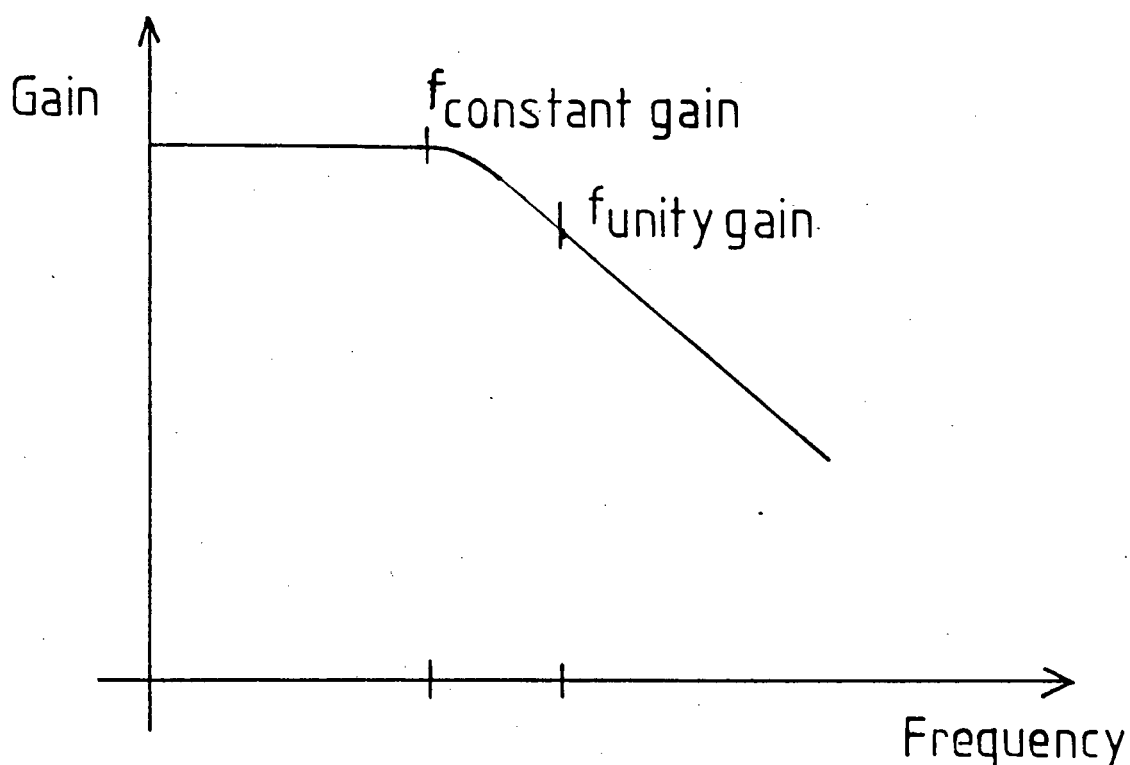


Fig. C.2.11 Frequency response of the Integrator

The differentiating circuit is included for completeness.  
The equation describing the ideal differentiator performance is

$$V_{out} = -RC \frac{d(V_{in})}{dt}$$

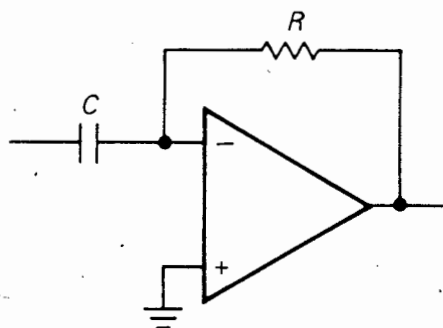


Fig. C.2.12 The Active Differentiator Circuit



### C.3 The Trigger Circuit for A/D Conversion

This circuit was designed because the output voltage of the chain pulse was not always sufficient to trigger the sampling. It amplifies the signal to TTL logic level ( $>3V$ ) to ensure its amplitude is sufficient for triggering. The circuit runs off the +5V output voltage of the A/D card.

A capacitor at the input decouples the circuit, so that it is not affected by DC offset. An input pulse produces a square wave out. The chip (CA 3130E) is static sensitive and must be carefully handled. No input voltage may be applied if the power supply is not connected first.

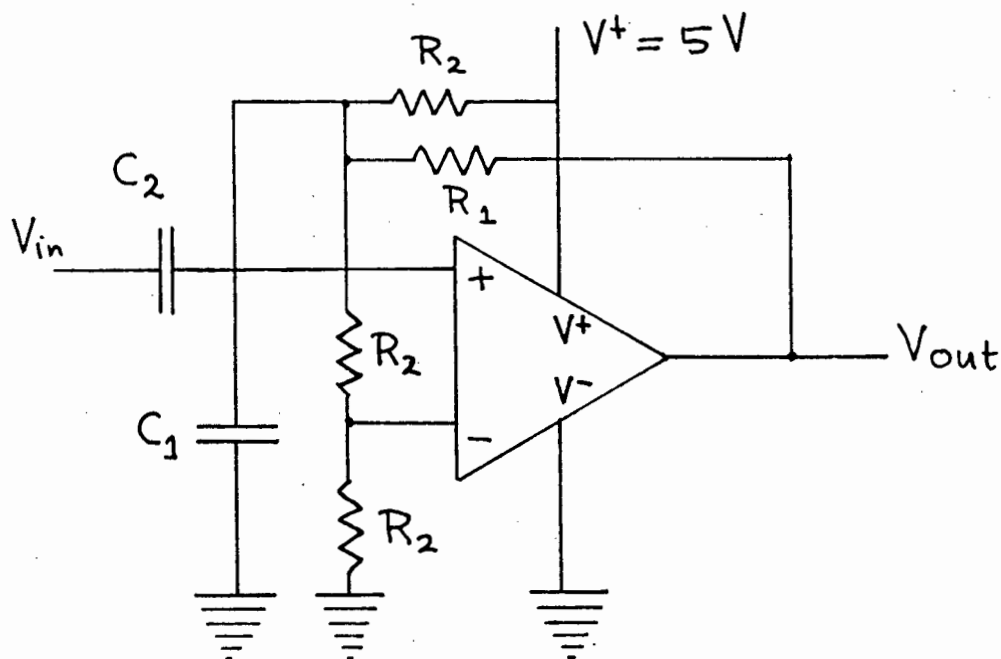


Figure C.2.13 Circuit diagram of the pulse generator

$$R_1 = 10 \text{ k}\Omega \quad C_1 = 0.22 \text{ }\mu\text{F}$$

$$R_2 = 8.2 \text{ M}\Omega \quad C_2 = 1.5 \text{ }\mu\text{F}$$

In the photograph below two low-pass filters on the breadboard are shown connected in series to two of the inputs to the A/D card. The circuit below holds the pulse generating circuit. The connections are from left to right; output to trigger port A0, pulse input,  $V^0 = \text{ground}$ ,  $V^+ = 5V$ .

The box on the left has 10 BNC female sockets for connection to the PC-30 card. The first six are connected to the input channels of the card.

The seventh is connected to port A0. The ninth is connected to the output of timer 2. Provision is thus made to connect the output of Timer 2 to port A0, if it is desired to use the internal clock rather than an external trigger. The last socket is connected to the 5V output of the card. All the sockets have a common earth.

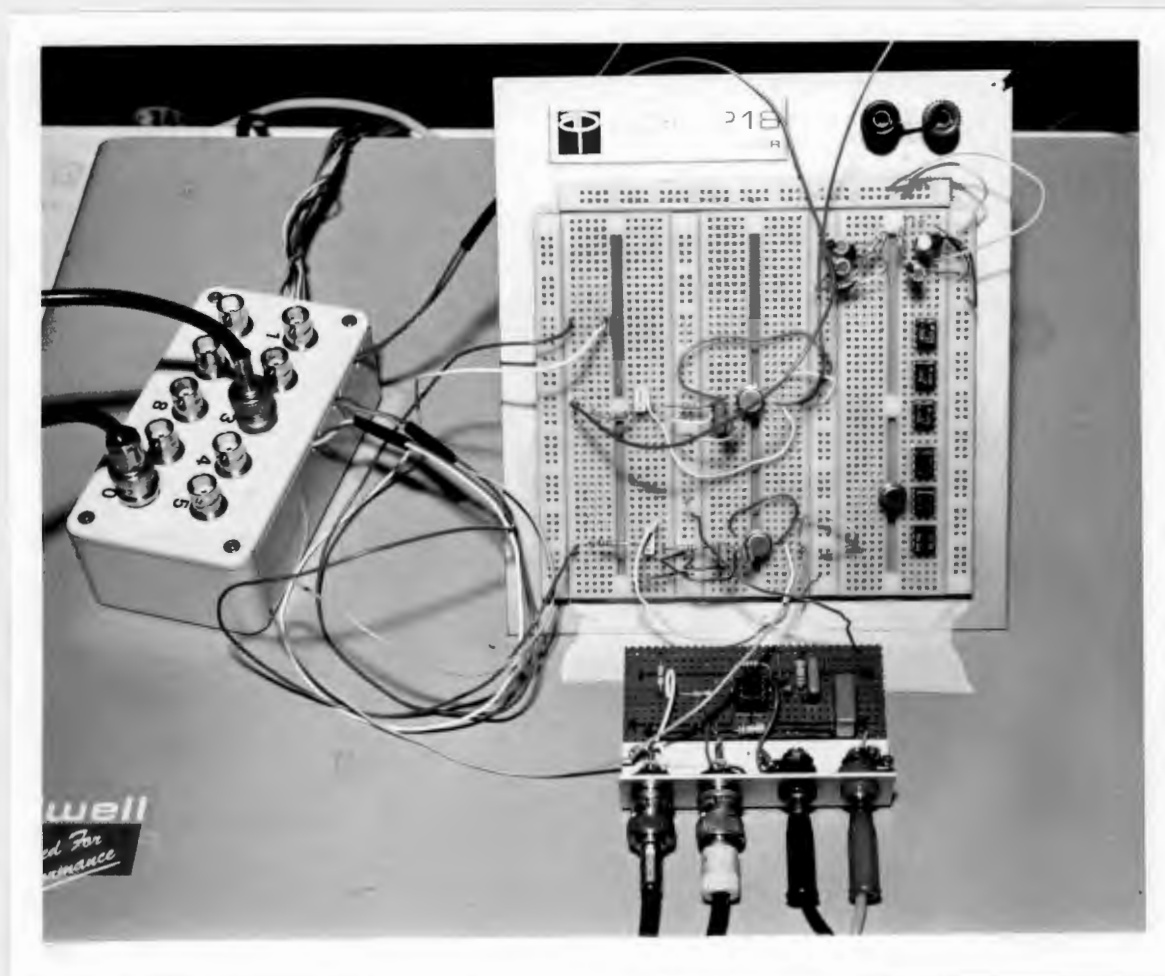


Fig C.2.13 Photograph of anti-alias filters on breadboard  
The trigger circuit is below , and the A/D card  
inputs and outputs at the left.

## APPENDIX D: DEVELOPMENT OF THE MEASURING EQUIPMENT

This appendix describes the choice and calibration of the equipment used.

The equipment can be divided into four parts:

- 1) the transducers
- 2) the recording and playback system
- 3) the digitisation and analysis section
- 4) that used for calibration

### Transducing Equipment

Endevco Piezoresistive accelerometer type 2262-25

Endevco Signal conditioning amplifier.

Hewlett-Packard Linearly Variable Differential Transducer

Invertek DC to AC Inverter

Fifth wheel

### Recording Equipment

TEAC 4-Channel Digital Tape Deck,

Frequency range 0-10 000 Hz

### Digitisation

Eagle Electric PC-30 A/D conversion card

Bondwell PC

### Calibration

King instruments electronics co. signal generator

LOS amplifier

Electromagnetic shaker

Steel Drum with Electric DC Motor and Ward-Leonard drive.

Tektronix 4-channel analogue Storage Oscilloscope

### The Method used to measure the road

The fifth wheel is mounted on the back of the car which runs over the road surface and moves according to the undulations thereof. The movement of the fifth wheel relative to its supporting frame is measured by the LVDT, mounted by its body to the frame. The moving core of the LVDT rests on and moves with the swing-arm of the wheel suspension.

The acceleration of the LVDT body and the frame relative to an absolute datum is measured by a piezoresistive accelerometer mounted next to it. These give measurements in the vertical axis.

A signal is provided to measure the distance covered on the horizontal axis. This is provided by a metal disc with teeth cut into its perimeter. The teeth break the beam of a photosensitive device. Every time that the beam is broken, a square wave voltage pulse output is generated.

These pulses are directly related to the distance travelled. Counting the number of pulses generated per second determines the speed of rotation.

The three signals are stored on a Digital tape recorder. The power supply for the tape recorder, as well as for the accelerometers voltage amplifier and the LVDT voltage supply is an inverter run off the test car's electrical system.

Once the test has been completed, the signals stored on the tape are downloaded into a microcomputer. Between the tape recorder and the computer they are passed through low-pass anti-aliasing filters.

The input connections to the A/D card have been modified in such a way that the card can either run off the computer clock, or be triggered by an external TTL Clock pulse. This is done by connecting the input to the trigger bit of the A/D converter to either the external source or to the clock output.

In this case the trigger bit used is the Least Significant Bit of port A0 of the A/D card. The software written (Appendix G) is designed to trigger on the changing of this bit. In this case the pulse generated by the chain is used for triggering. The data is thus in distance related rather than time related form.

Calibration of the equipment

The LVDT and the accelerometer were calibrated together using a large shaker and an oscilloscope.

D.1 Individual calibration

The LVDT was first calibrated on its own. The sensitivity in volts/inch was specified on the instruction sheet. This was checked by moving the core through measured distances and comparing the change in voltage output. The output was found to be 0.26 V/mm or 1 V/ 3.85 mm.

The piezoresistive accelerometer was calibrated statically at first. The accelerometer sensitivity in mV/g was set on the rotary switch. The stepped switch controlling the percentage of full scale output was rotated from 20% to 100% with steps of 20%.

At each step the accelerometer was held vertical, and then inverted. This gave a static change of 2g acceleration force. By reading the voltage change on the oscilloscope, it was possible to determine the output in V/g for each position of the switch.

The values determined from the independant calibrations.

- LVDT Output = 3.85 mm/V or 0.259 V/mm
- 50 Hz Ripple on output = 0.008 V

- Endevco piezoresistive accelerometer.
- Sensitivity setting on amplifier = 1.75 mV/g
- 50 Hz ripple on output = 0.004 Volts

Scale setting	g/V	FSD (±) g's
100 %	4.0	10.0
80 %	3.2	8.0
60 %	2.4	6.0
40 %	1.66	4.2
20 %	0.8	3.2

Figure D.1 Table of Accelerometer output for various settings of output Full Scale Deflection.

The slight roughness in the shaker movement, as well as its deviations from true sinusoidal behaviour at low frequencies are cause for this. The accelerometer might also behave differently under dynamic and static loadings, perhaps overshooting slightly in the dynamic case.

Tests run at 100% output of accm. amplifier

This test also measured the low frequency and low acceleration level response of the accelerometer. The test was limited by the shaker's stroke of  $\pm 4$  mm.

The minimum acceleration level that could be measured was 0.1 m/s. By comparison, the minimum acceleration level the piezoresistive accelerometer could measure was 0.7 m/s.

The lowest frequency that this was measured at was 1.0 Hz. The shaker could not provide sufficient stroke at lower frequencies to provide the minimum acceleration level. It started clipping, with resultant high shock. At low frequencies the shaker movement was not truly sinusoidal, and the accelerometer and LVDT signals reflected this.

The outputs of the accelerometer and the LVDT were then entered into the computer and analysed in the way the signal from the road would be, to check on the validity of the proposed method. The calculated displacement signals were subtracted from each other, to see if the result came to zero as it should.

It was found that down to frequencies of 2 Hz there was good agreement between the signals. At lower frequencies and at the low amplitudes of the shaker stroke, the accelerometer did not measure the amplitude of the motion accurately. It did detect the correct shape of a 1/2 Hz, 6mm peak to peak sine wave.

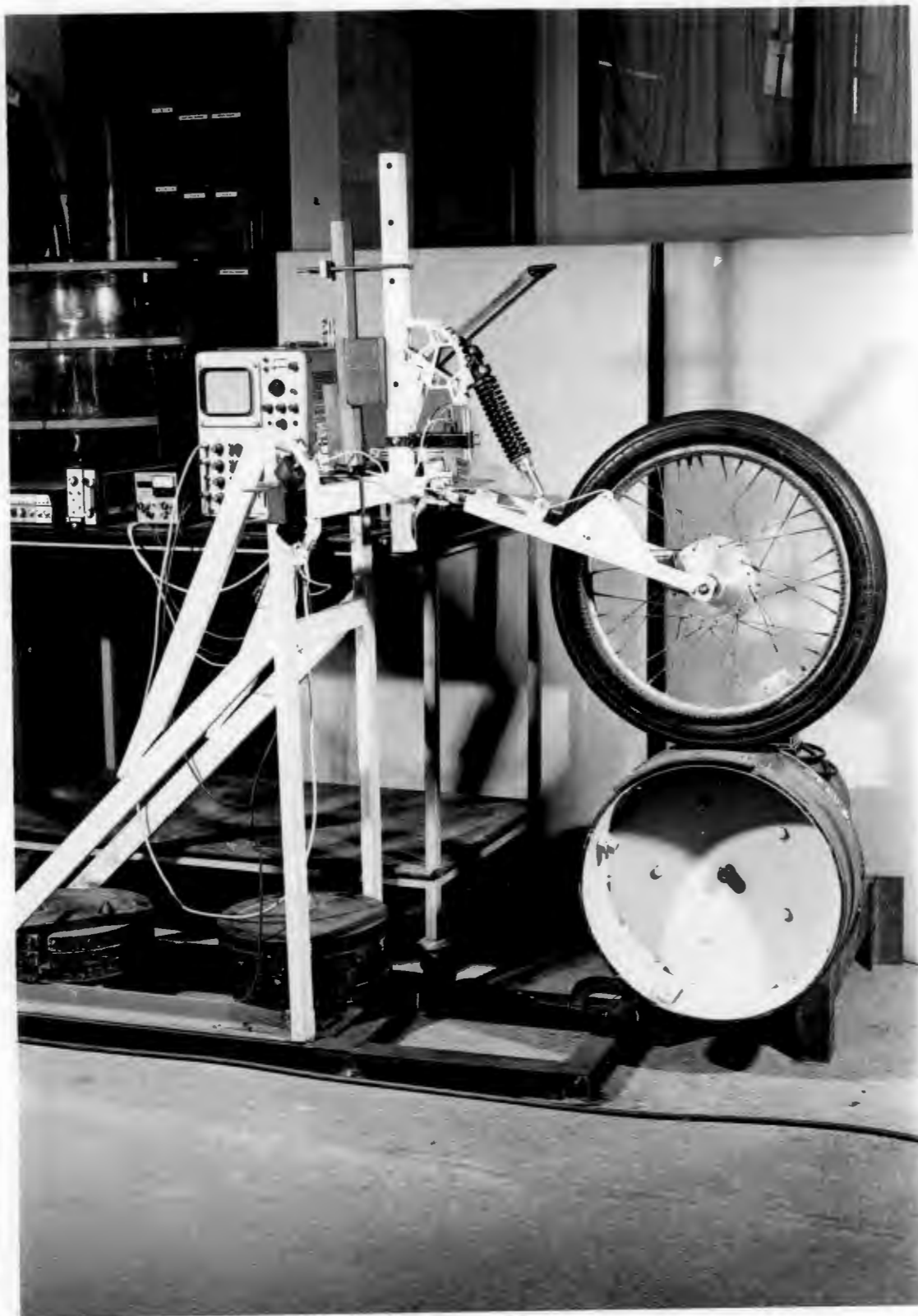


Figure E.1 Fifth wheel using motorcycle wheel on test rig. The accelerometer and LVDT are shown in position. The wheel is on top of the 0.3m long bump, which is the shortest wavelength of interest.

### D.3 Tests on the Rotating Drum

After testing on the shaker, the accelerometer and LVDT were mounted on the fifth wheel, which ran on a drum of 1.5m circumference with a bump of 0.3m length and 0.011m height on it. The bump length corresponded to the minimum wave-length to be measured. The transducer signals were subtracted from each other, but the result was now compared to that of the known drum profile.

### D.4 Testing on the Road

The device was now ready to use on the road. It was mounted on a car and towed over surfaces whose properties were known, to see how it measured them.

Once the results were acceptable, the assembly was ready for use to measure the test tracks at the VW plant.



## APPENDIX E: DEVELOPMENT OF THE FIFTH WHEEL

The object of this design within the project was to create a moving surface to simulate driving over a road surface with the fifth wheel. From the literature it seemed that a rotating drum was an acceptable method of providing a translating surface.

The main difference between the drum and the road surface is that the drum is periodic, especially if the surface is not smooth but rough. It also curves away from both sides of the point of contact which is not very often typical of the road surface. A drum of several metres diameter would have been most suitable, since its large perimeter would reduce the effect of the above mentioned errors.

The design was constrained by:

- the road speeds which it was wished to simulate.
- the height of the centreline of the electric motor drive-shaft above the floor, thus limiting the radius.
- the speed range of the electric motor used.

When the wheel was tested on the drum it was found that above speeds of rotation corresponding to 6 kph  $\rightarrow$  10 kph, the wheel was not held onto the drum surface, but bounced uncontrollably, seriously distorting the output. It no longer corresponded to the drum profile, but to the uncontrolled motion of the wheel. After a simple analysis of the wheel's spring/damper system (given below), it was decided that the damping was ineffective. The damper therefore should have been replaced by a firmer one. Unfortunately it was not possible to obtain a unit with significantly higher damping.

However an assembly with a much stiffer spring was found, and this was used. In fact both units only had damping on the rebound stroke. The new spring had twice the stiffness of the old one, and allowed a greater preload to be applied. The wheel was still limited to low road speeds for accurate measurement, but followed the profile more closely.

Data for the new spring:

Spring constant = 22 kN/m Free length = 177 mm

Initial compression of spring = 9 mm

Compressed further to hold wheel to road.

The last step was to replace the motorcycle wheel with a bicycle wheel. Because of the lighter mass of the wheel, it was much easier to hold it onto the road surface. The natural frequency was also raised. The natural frequency using the motorcycle wheel was only slightly above the frequencies to be measured, and had some masking effect on them. The raised natural frequency reduced this effect.

The bicycle wheel tyre also had much less resilience than the motorcycle wheel. It therefore did not distort the profile of the road as much through being compressed. This was especially noticeable on the rebound after having struck the bump.

Some data for the Fifth Wheel

Mass of Swing Arm = 2 kg

Mass of Motorcycle Wheel = 6.4 kg

Mass of Bicycle wheel = 1.75 kg

Mass of disk to generate pulses = 0.5 kg

#### Comparison of the Bicycle and Motorcycle wheel response.

Figures E.2 and E.3 shows acceleration and LVDT traces for the motorcycle and bicycle tyres. They were obtained by placing the accelerometer at the axle of the wheel and letting it pass over the bump on the drum.

The accelerometer trace indicates the forces acting at the wheel, which the spring and damper must control. It also indicates the dynamic response of the assembly to the bump. The LVDT trace indicates the displacement of the wheel passing over the bump.

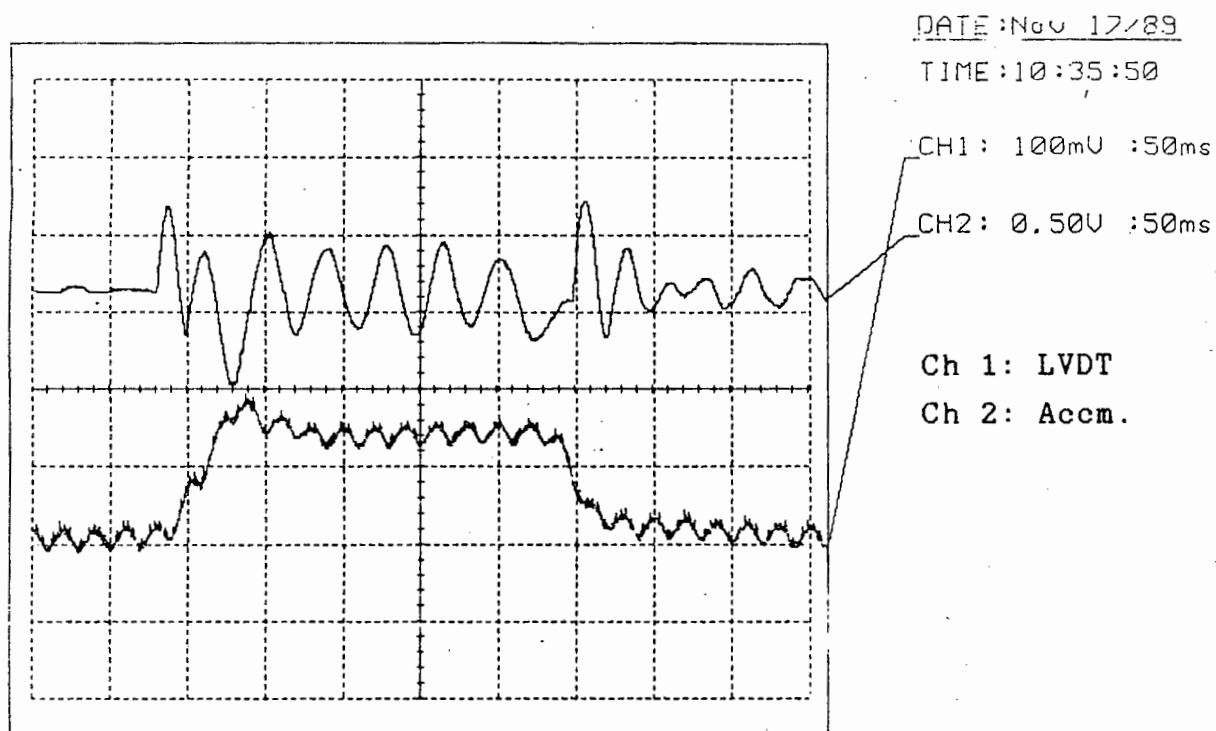
In the first pair of traces, the drum is rotating slowly at 2 m/s. The LVDT indicates that they both follow the profile of the bump accurately. The motorcycle wheel acceleration level is four times that of the bicycle wheel. It shows a decaying frequency response to the bump.

In the second pair of traces, the drum is rotating at 7 m/s. The LVDT shows that neither wheel follows the bump accurately.

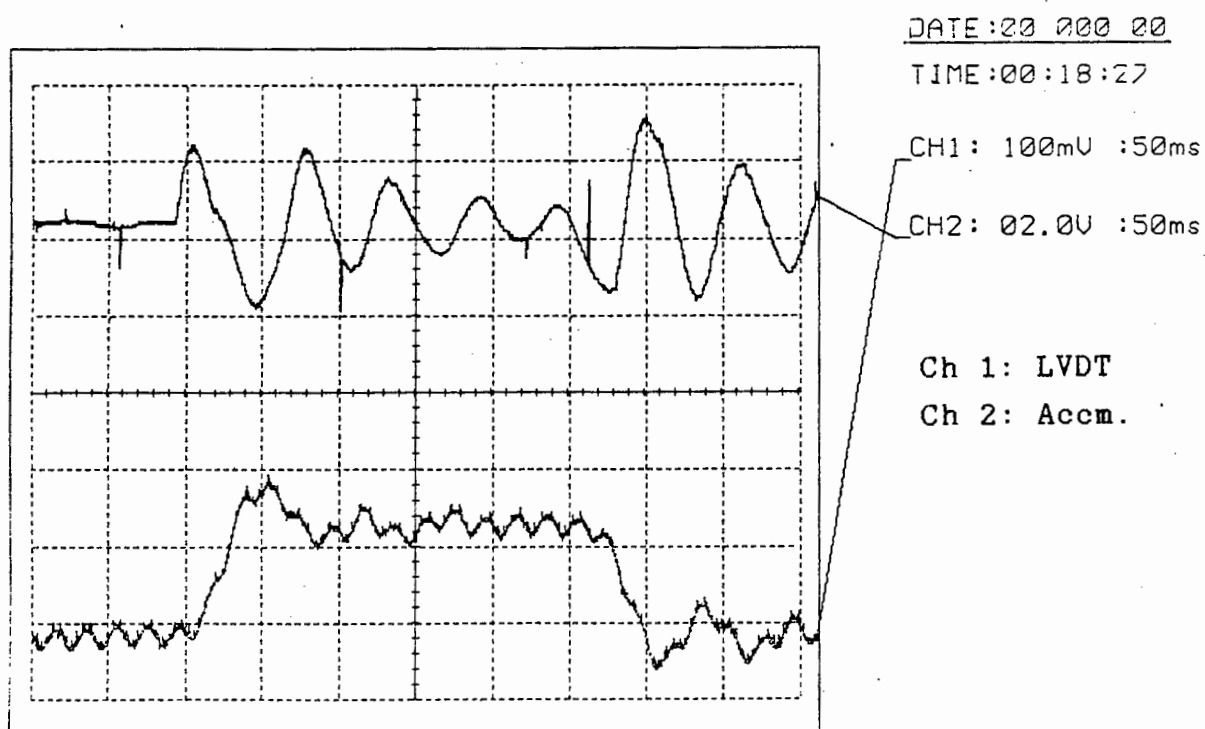
The bicycle wheel indicates the presence of the bump distinctly from its bouncing response to the bump. The amplitude of the bump is indicated as being slightly larger than before. The wheel also shows very little compression (negative displacement) after passing over the bump. The peak acceleration has been raised by a factor of 6.

The motorcycle wheel also detects the bump at this speed, but with far less accuracy. Its greater storage of energy is also evident in the way it bounces after striking the bump. The tyre is compressed after striking the smooth surface again, and indicates a non-existent depression. It is difficult to tell what the amplitude of the bump is from this signal. The acceleration force has been raised 3 times, and is still much larger than the bicycle wheel's.

Figure E.2 Response of the Bicycle and Motorcycle wheels at 2 m/s

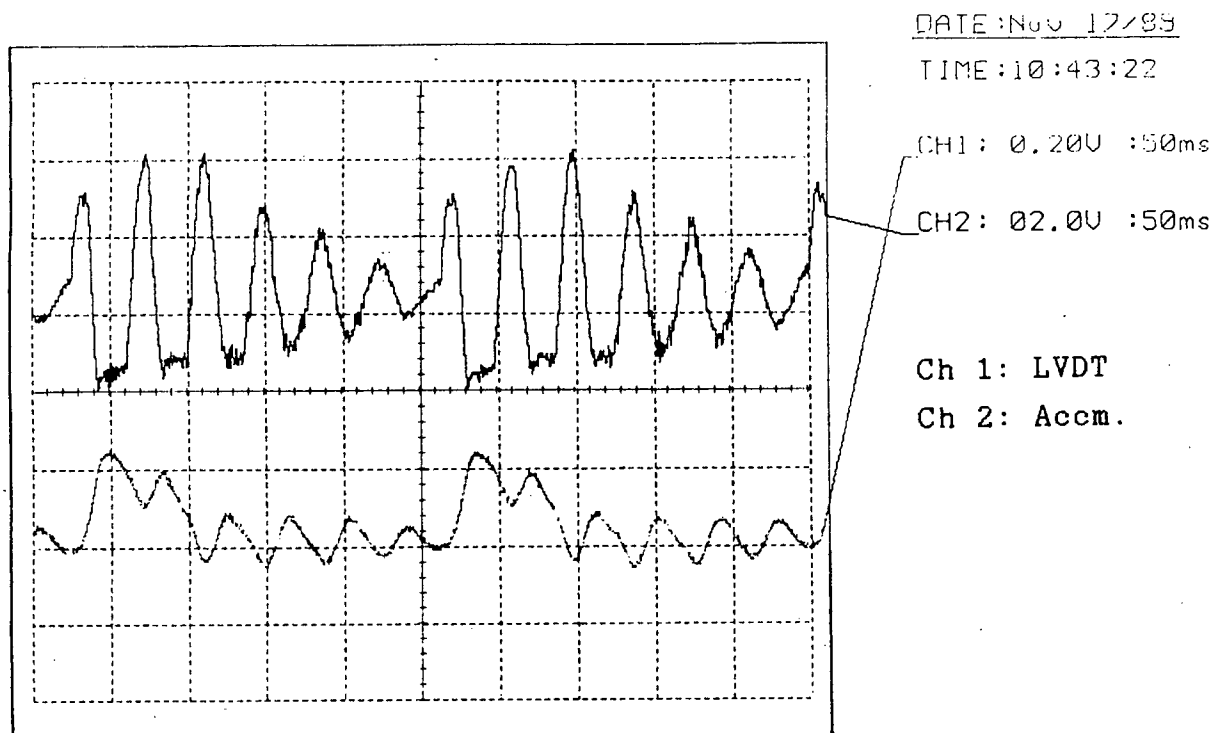


a) the bicycle wheel response

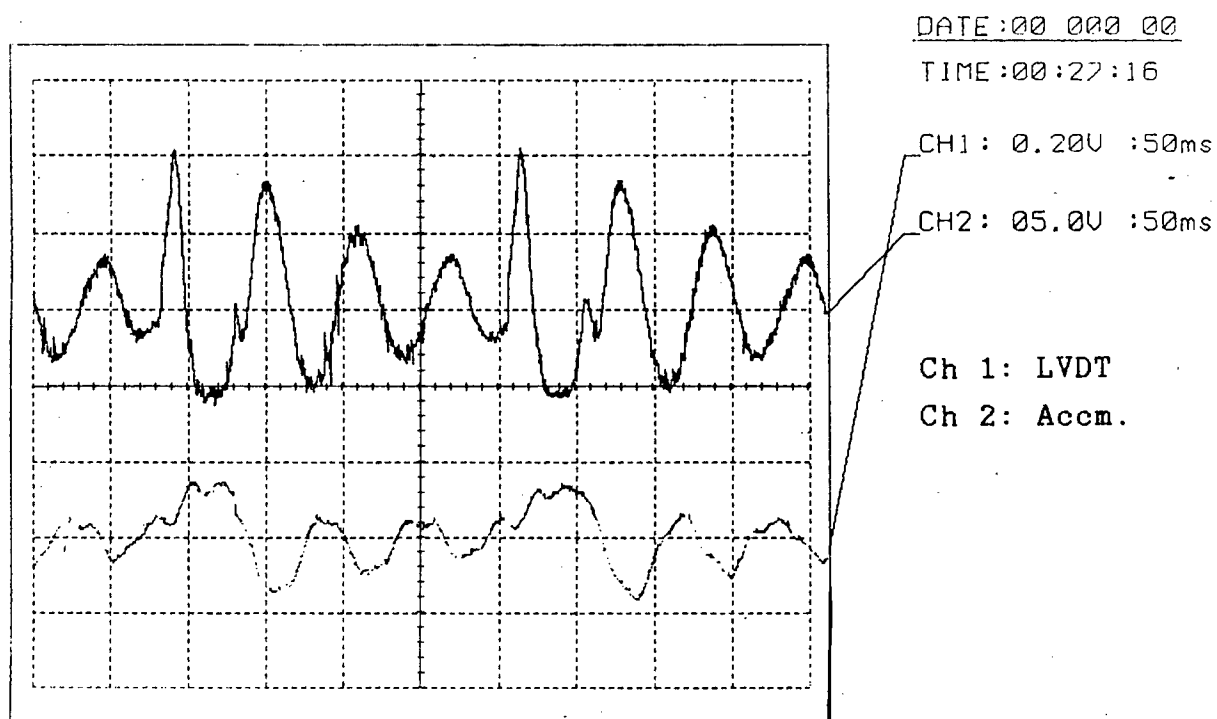


b) the motorcycle wheel response

Figure E.3 Response of the Bicycle and Motorcycle wheels at 7 m/s



a) the bicycle wheel response



b) the motorcycle wheel response

### Dynamic Analysis of the System

The dynamic behaviour of the fifth wheel is modelled using differential equations. The energy method is used. The layout of the wheel is as shown below.

A dynamical system has the following properties or characteristics.

- a) A (differential) equation of motion
- b) A natural frequency
- c) Initial conditions
- d) A transient (impulse) response
- e) A steady state (continuous input) response
- f) A transfer function relating the output to the input.

Force is divided through the system, i.e. the sum of the forces over the system is zero.

Velocity is divided across the system.

Forces at a node are zero. For each force there is a reaction force.

Velocities at a node are equal. There are no discontinuities in the system.

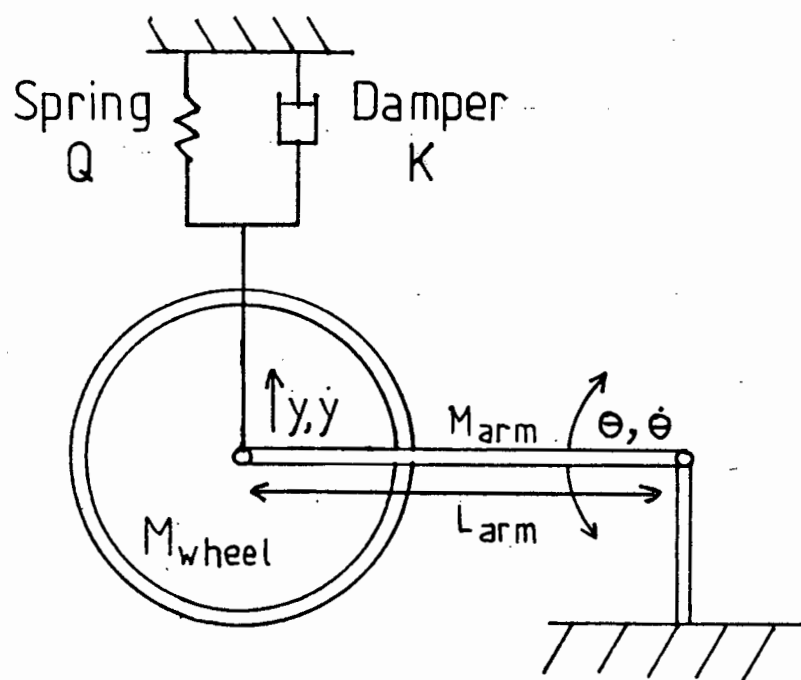


Figure E.4 The layout of the dynamic components of the 5th wheel

Assume small angular displacement of the arm, i.e. small  $\theta$ .

For  $M_1$ : (The mass of the wheel)

$$\begin{aligned} KE &= \frac{1}{2} M_1 \dot{y}^2 \\ PE &= M_1 g y \end{aligned} \quad -(1)$$

For  $M_2$ : (The mass of the swing arm, assumed uniform)

$$PE = M_2 g (y/2) \quad -(2) \text{ about its C.G.}$$

$$\begin{aligned} L_2 \dot{\theta} &= \dot{y} \Leftrightarrow \dot{\theta} = \dot{y}/L_2 \\ KE &= \frac{1}{2} I_A \dot{\theta}^2 = \frac{1}{2} I_A (\dot{y}/L_2)^2 \end{aligned} \quad -(3)$$

For the Spring:

$$\begin{aligned} P.E. &= M_s g (y/2) \\ K.E. &= \frac{1}{2} M_s (\dot{y}/2)^2 \\ \text{Stored energy} &= F \times \frac{1}{2} y = yQ \times \frac{1}{2} y = \frac{1}{2} Qy^2 \\ E &= \frac{1}{2} Qy^2 + \frac{1}{2} M_s (\dot{y}/2)^2 + M_s g (y/2) \end{aligned} \quad -(4)$$

For the Dashpot:

$$\begin{aligned} E &= \int_0^t (\text{Force} \times \text{velocity}) dt = \int_0^t \text{Power} dt \\ &= \int_0^t K\dot{y} \times \dot{y} dt \\ &= K \int_0^t (\dot{y})^2 dt \end{aligned} \quad -(5)$$

$$P.E. = M_d g \left( \frac{y}{2} \right)$$

The mass of the damper is lumped with that of the spring in the analysis.

The Total Energy E:

The total energy is the sum of all the energies. Gathering terms gives the following.

$$\begin{aligned}
 E_{\text{total}} = & \frac{1}{2} M_1 \dot{y}^2 + M_1 g y \\
 & + \frac{1}{2} I_A / (L_z)^2 \dot{y}^2 + \frac{1}{2} (M_2 g) \times y \\
 & + \frac{1}{8} M_s \dot{y}^2 + \frac{1}{2} (M g)_s \times y + \frac{1}{2} Q y^2 \\
 & + K \int_0^t (\dot{y})^2 dt \quad \quad \quad -(6)
 \end{aligned}$$

The Energy Relationship may now be written

$$E_{\text{Total}} - E_{\text{dissipated}} = E_{\text{stored}}$$

$$\text{or } E_{\text{stored}} + E_{\text{dissipated}} = \text{constant} = E_{\text{Total}}$$

Energy Equation

Lumping together the coefficients of the various terms lets the energy equation be written as

$$\frac{1}{2} A \dot{y}^2 + B y + \frac{1}{2} Q y^2 + K \int_0^t (\dot{y})^2 dt = C \quad \quad \quad -(7)$$

Differentiating with respect to time to remove the integral

$$A \ddot{y} + B \dot{y} + Q y \dot{y} + K \dot{y} = 0$$

Dividing by  $\dot{y}$

$$A \ddot{y} + B + K \dot{y} + Q y = 0$$

$$A \ddot{y} + K \dot{y} + Q y = -B \quad \quad \quad -(8)$$

$$\text{Let } -B = f(t)$$

Then

$$A \ddot{y} + K \dot{y} + Q y = f(t) \quad \quad \quad -(9)$$

Using the D- operator in the DE (8)

$$(D^2 A + D K + Q)y(t) = f(t)$$

Then the characteristic equation is  $AD^2 + KD + Q = 0$



The roots of this quadratic equation are given by

$$\begin{aligned}
 D &= \frac{-K \pm \sqrt{K^2 - 4AQ}}{2A} \\
 &= \frac{-K}{2A} \pm \frac{\sqrt{K^2 - 4AQ}}{2A} \\
 &= -\sigma \pm j\omega
 \end{aligned}$$

Thus

$$y(t) = e^{-\sigma t} \left[ a \cos \omega t + b \sin \omega t \right]$$

with initial conditions

$y(0) = 0$  which gives  $a = 0 \Leftrightarrow$  the function starts at 0

$\dot{y}(0) = v$ , the initial velocity

then

$$y(t) = e^{-\sigma t} \left[ b \sin \omega t \right] \quad \text{This is the natural mode.}$$

$$\dot{y}(t) = -\sigma e^{-\sigma t} (b \sin \omega t) + e^{-\sigma t} (\omega b \cos \omega t) \quad \text{where } \omega b = v$$

$$\text{so } y(t) = e^{-\sigma t} \frac{v}{\omega} \sin \omega t$$

$$\begin{aligned}
 \dot{y}(t) &= -\sigma e^{-\sigma t} \left( \frac{v}{\omega} \sin \omega t \right) + e^{-\sigma t} (v \cos \omega t) \\
 &= v e^{-\sigma t} \left[ \sigma \cos \omega t - \frac{\sigma}{\omega} \sin \omega t \right]
 \end{aligned}$$

$$\begin{aligned}
 \ddot{y}(t) &= -\sigma v e^{-\sigma t} \left[ \cos \omega t - \frac{\sigma}{\omega} \sin \omega t \right] + \\
 &\quad + v e^{-\sigma t} \left[ -\omega \sin \omega t - \sigma \cos \omega t \right] + \\
 &= v e^{-\sigma t} \left[ -2\sigma \cos \omega t + \left( \frac{\sigma^2}{\omega} - \omega \right) \sin \omega t \right]
 \end{aligned}$$

$$\ddot{y}(t) = v e^{-\sigma t} \cdot B \sin(\omega t + \theta_0) \quad , B \text{ is the coefficient of the combined sin and cos terms}$$

The Energy Equation can now be rewritten

$$\begin{aligned}
 &A \left[ v e^{-\sigma t} \cdot B \sin(\omega t + \theta_0) \right] + K \left[ v e^{-\sigma t} \left[ \sigma \cos \omega t - \frac{\sigma}{\omega} \sin \omega t \right] \right] + \\
 &+ Q \left[ e^{-\sigma t} \left[ b \sin \omega t \right] \right] = f(t)
 \end{aligned}$$

The term multiplied by the damping coefficient is the only one with a cosine term in it.

This is the equation for an underdamped cosinusoid starting at  $t = 0$ . If the damping is insufficient, then this term will not die out as quickly as the others, and the system will be underdamped. In practice this means that the wheel will not follow the road accurately, which was the case.

The springing and damping of the tyre has been neglected in the above analysis. Further testing by means of removing the tyre from the wheel rim removed the decaying oscillation seen on the oscilloscope trace. This indicated that the tyre had significant properties of its own.

Although the tyre helped to damp out some of the high frequency shocks, it also added its own natural springiness. This was in the same frequency region that was to be measured.

The motorcycle tyre was therefore replaced by a bicycle tyre. This raised the natural frequency of the wheel springiness, since the assembly was much stiffer. Further, the bicycle tyre ( $m = 1.75$  kg) was very much lighter than the motorcycle tyre. This made it easier for the spring to hold it to the road surface. The natural frequency of the whole assembly was raised.

#### Influence on measuring speed

The new assembly allowed a much higher measuring speed. This was good, since the accelerometer did not work well enough at the very low speeds previously used.

By using higher speeds the same distances as before are covered at a much higher speed. They then have a higher frequency. This improves the accuracy of the measurement. The accelerometer is used in a higher frequency range and is more reliable.

## APPENDIX F: DESIGN OF MECHANICAL ACCELEROMETER

The first type of accelerometer used was piezo-electric. The piezo-electric crystal is placed in shear or compression by the acceleration forces. Deformation of the crystal produces an electrical charge proportional to the deforming force. This charge is converted to a voltage by a charge amplifier. The piezo-electric does not have adequate low-frequency performance ( $< 4\text{Hz}$ ), since the charge leaks away at low frequencies. (Piezo-resistive accelerometers offer better low frequency response, ( $< 2\text{Hz}$ ) but were not initially available, although one was finally obtained and used.)

The design of a seismic mass as an absolute displacement meter was then tried. The principle of the seismic mass is that it is a large mass mounted on a soft spring. It has an extremely low natural frequency, and operates well above it. The inertia of the mass holds it in place when the base on which the spring rests moves. The change in distance between the base and the mass is approximately the same as the displacement of the base.

The natural frequency is used to design the mass and spring as follows.

$$\omega_n = 2\pi f_n [\text{rad.s}^{-1}] \text{ --- (a)}$$

$$\omega_n^2 = k/m \text{ --- (b)}$$

$k$  = the spring stiffness  $[\text{N/m}]$

$m$  = the mass of the mass  $[\text{N}]$

combining (a) and (b),

$$(2\pi f_n)^2 = k/m$$

$$f_n = 0.05 \text{ gives}$$

$$k/m = 0.098 \quad \text{or } k \cong 0.1 m$$

If  $m$  has a mass of  $1\text{kg}$ , it weighs  $9.8\text{N}$ . The spring coefficient is  $0.98$ . The initial static deflection of the spring  $= m/k = 10\text{m}$ . This is clearly an impractical length.

Since the spring stiffness and the mass are in direct relation, the static deflection will be the same no matter what mass is used. If the resonant frequency is made to be 0.5 Hz,  $k = 96 \text{ N/m}$  and the initial static deflection is reduced to 0.1m, which is better.

The seismic mass has been designed without damping. It is likely that after undergoing several inputs at the base of the spring, the mass would eventually start to oscillate, and no longer give a true measurement. Damping would raise the natural frequency of the system. Difficulty would be experienced in measuring the mass' displacement without affecting its behaviour. It was therefore decided to build a mechanical accelerometer.

The accelerometer operates well below its natural frequency. To design an accelerometer, it is necessary to know the range over which it must operate. This is done by calculating the minimum and maximum accelerations that it must measure.

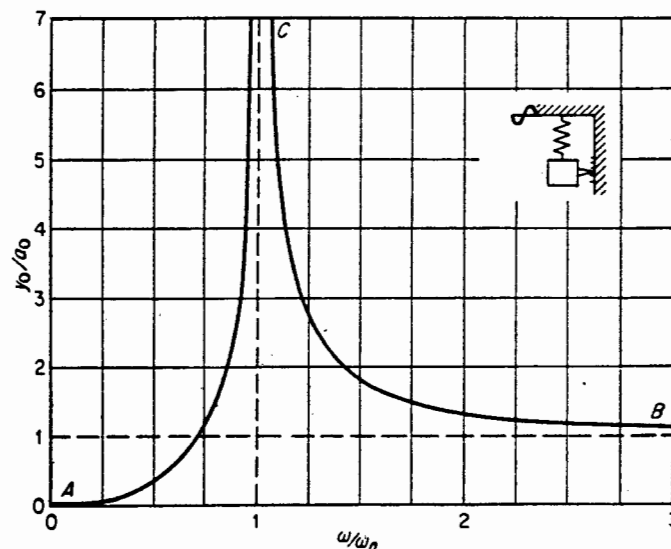


Figure F.1 Graph of the operating regions of the seismic mass and the accelerometer.

a = the movement of the base  
y = the relative movement of the mass and the base  
 $\omega$  = the frequency of vibration

The accelerometer operates in the spring stiffness-dominated region, and the seismic mass in the mass-dominated region, as shown above.

Calculation of the accelerations is conveniently done by considering the input to be sinusoidal. The value of the acceleration can then easily be calculated, as follows.

$$\text{If } Y = A \sin(\omega t)$$

$$D(Y) = \omega A \cos(\omega t)$$

$$D^2(Y) = -\omega^2 A \sin(\omega t)$$

Now for  $v = 1.66 \text{ m/s} = 6 \text{ kph}$

and using the data for the synthetic road used by VW

$$\lambda_{\max} = 12.6 \text{ m} \Leftrightarrow f_{\min} = 0.08 \text{ Hz}$$

$$\lambda_{\min} = 0.3 \text{ m} \Leftrightarrow f_{\max} = 3.33 \text{ Hz}$$

$$A_{\max} = 0.020 \text{ m}$$

$$A_{\min} = 0.001 \text{ m}$$

$$\begin{aligned} \text{then } D^2(Y)_{\max} &= |(2\pi 3.3)^2 \times 20 \times 10^{-3}| & (\sin(\omega t) \leq 1) \\ &= 8.75 \text{ m.s}^{-2} \\ &= 0.89 \text{ g} \end{aligned}$$

$$\begin{aligned} D^2(Y)_{\min} &= |(2\pi 0.08)^2 \times 1 \times 10^{-3}| \\ &= 0.00025 \text{ m.s}^{-2} \\ &= 0.00003 \text{ g} \end{aligned}$$

These acceleration values occur at points where the sine wave has its maximum or minimum values, that is at  $\lambda/4$  and  $3\lambda/4$ .

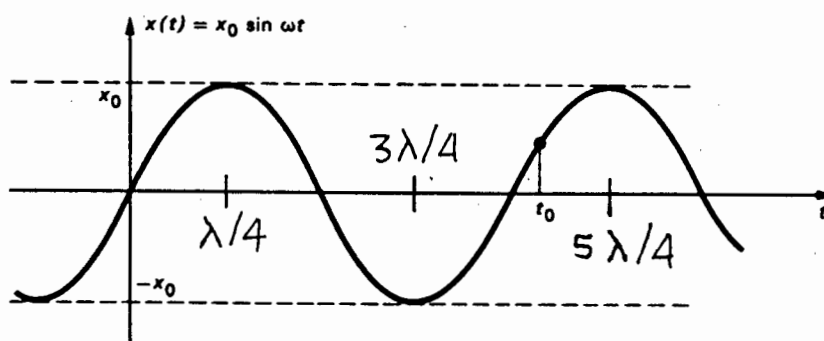


Figure F.2 Graph of sine wave showing points of peak acceleration

### The Accelerometer design

The design of accelerometer considered was the following. A cantilever beam with a mass at the free end is used. The mass is acted on by gravity. If the fixed end of the beam is moved, the mass will resist a change in its position. This produces deflections in the beam, which can be measured by strain gauges mounted on its top and bottom surfaces.

The equations and variables used to model the beam employed in the accelerometer are the following:

$\epsilon$  = strain [m/m] commonly measured in micro-strains

$\theta$  = the angle (in radians) of the slope of the beam at any point

$V$  = distance from the neutral axis to the point of interest in the beam [m]

$r$  = the radius of curvature of the neutral axis of the beam [m]

$m$  = the applied or resultant moment [Nm] due to loading

$W$  = the loading force [N]

= mass x acceleration [kg.m/s<sup>2</sup>]

$E$  = Young's Modulus  $\cong 210 \times 10^9$  N/m<sup>2</sup> for steel

$l$  = the distance from the fixed end of the beam to the free end [m]

$x$  = distance from the fixed end to the point of interest [m]

$$y = \frac{Fx^2}{6EI}(x - 3l) \text{ --- (1) the deflection at any point}$$

$$= \frac{Wl^3}{3EI} \text{ the deflection of the beam at its end}$$

$$k = \frac{3EI}{l^3} \text{ --- (2) the stiffness of the beam}$$

$$= \frac{W}{y}$$

$$\epsilon = v \left[ \frac{W(l-x)}{EI} \right] \quad \text{--- (3) the strain in a plane parallel to the surface at a point}$$

$$= \frac{v}{r}$$

$$= \frac{\sigma}{E}$$

$$= \frac{My}{EI}$$

$$\omega_n = \sqrt{\frac{k}{m}} \quad \text{--- (4) The natural frequency of the beam}$$

$$f_n = \frac{\omega_n}{2\pi}$$

$$I = \frac{1}{12}bh^3 \quad \text{--- (5) The moment of inertia}$$

$$\theta = \frac{Wl^2}{2EI} \quad \text{--- (6) The angular deflection at a point}$$

$$\frac{1}{r} = \frac{M}{EI} \quad \text{--- (7) The radius of curvature at a point}$$

$$= \frac{W(l-x)}{EI}$$

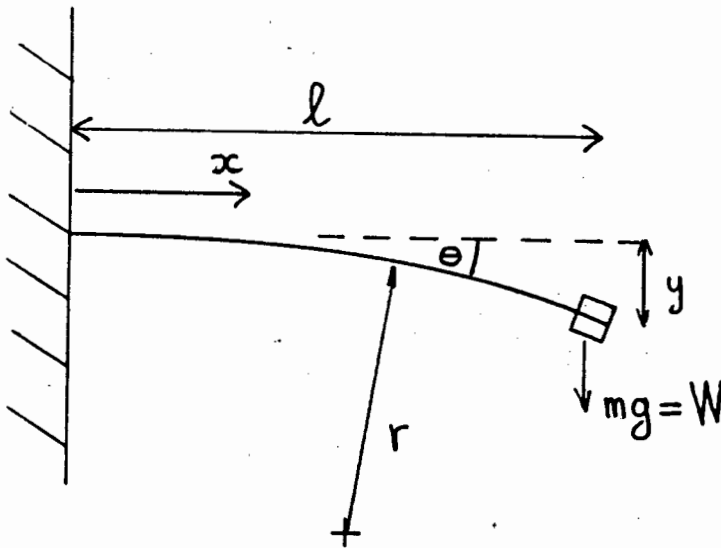


Figure F.3 Sketch of the beam showing the dimensions

According to den Hartog [33], with a mechanical accelerometer one may measure up to  $0.4\omega_n$  without damping, and up to approximately  $0.7\omega_n$  with damping. Damping will also eliminate harmonics which would cause an error in the undamped instrument.

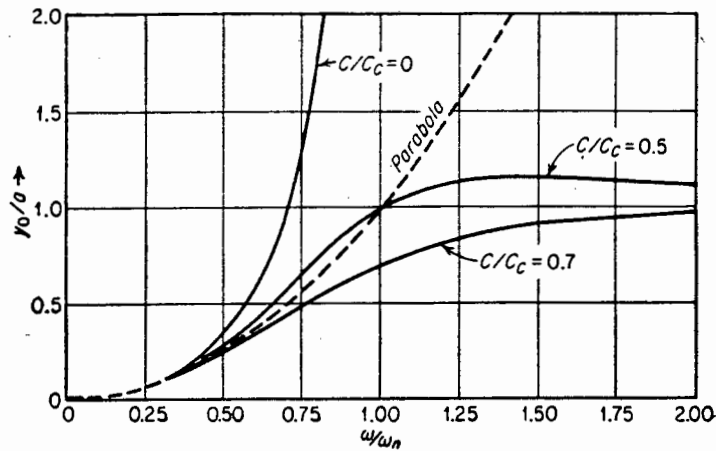


Figure F.4 Resonance curves with various amounts of damping compared with the parabolic curve of an ideal accm.

The maximum strain that can be measured with ordinary strain gauges is 2.8 % . The maximum strain in the working range is taken to be 0.5% ( = 0.005 strains). This would occur at maximum deflection of the beam.

For a certain natural frequency (fixed), the stiffness and mass are always in the same ratio. Therefore for the same acceleration the beam will undergo the same deflection at the same point.

As the natural frequency is raised by reducing the mass or stiffening the beam, the sensitivity at lower frequencies is reduced. Conversely, increasing the low-frequency sensitivity leads to large displacements for high accelerations.

#### Sample calculation for the accelerometer

For the beam of the accelerometer it was proposed to use a steel hacksaw blade, with dimensions of 12mm by 0.5mm.

$$\begin{aligned}
 I &= \frac{1}{12} b h^3 \\
 &= \frac{1}{12} (12 \times 0.5^3) \times 10^{-12} \text{ m}^4 \\
 &= 1.25 \times 10^{-13} \text{ m}^4
 \end{aligned}$$



The maximum frequency to measure = 4 Hz. The accelerometers' natural frequency should be at least twice this. It is made three times as great here.

$$f_n \geq 4 \times 3$$

$$= 12 \text{ Hz}$$

$$\omega_n = 75.4 \text{ rad.s}^{-1}$$

$$\omega_n^2 = 5685 = \frac{k}{m}$$

$$\text{or } k = 5685 \times m \quad (i)$$

Combining (3) and (4) gives

$$5685 \times m = \frac{3EI}{l^3}$$

$$\begin{aligned} ml^3 &= \frac{3 \times 210 \times 10^9 \times 12 \times bh^3}{5685} \\ &= 1.11 \times 10^8 \times 1.25 \times 10^{-13} \\ &= 0.000014 \end{aligned}$$

Choosing a value of 0.1 m for the length of the beam gives a mass of 0.014 kg. Substituting this into (i) above gives a spring stiffness of  $5685 \times 0.014 = 78.89 \text{ N/m}$ .

Calculation of the displacements and strains at the maximum and minimum accelerations

$$\begin{aligned} y_{\max} &= \frac{Wl^3}{3EI} \\ &= \frac{(0.014 \times 8.75) \times 0.1^3}{3 \times 210 \times 10^9 \times 1.25 \times 10^{-13}} \\ &= 0.00156 \text{ m} \end{aligned}$$

$$\begin{aligned} \varepsilon_{\max} &= v \left[ \frac{W(l-x)}{EI} \right] \\ &= 0.00156 \left[ \frac{(0.014 \times 8.75)(0.1/2)}{0.02625} \right] \end{aligned}$$

$$\varepsilon_{\max} = 0.00036 \text{ strains} \quad > 5 \mu \text{ strains}$$

By iterating this procedure it is possible to design the accelerometer to give a high enough output at the maximum acceleration. As the mass, length of the beam and amplitude of motion are decreased,  $\omega_n$  is raised. If the maximum acceleration gives a strain of 0.005, and the minimum acceleration that can be reliably measured has a strain of 0.000 01, then the dynamic range over which it can measure is 27 dB. If the minimum strain is taken as being 0.000 005 strains, the range is extended to 30 dB.

Thus if the maximum acceleration to be measured is  $8.75 \text{ m.s}^{-2}$ , the minimum acceleration that can be measured is  $0.008 75 \text{ m.s}^{-2}$ . This is still 15 dB more than the smallest acceleration it is desired to measure, viz.  $0.000 25 \text{ m.s}^{-2}$ . The mechanical accelerometer therefore does not have a satisfactory dynamic range for this application.

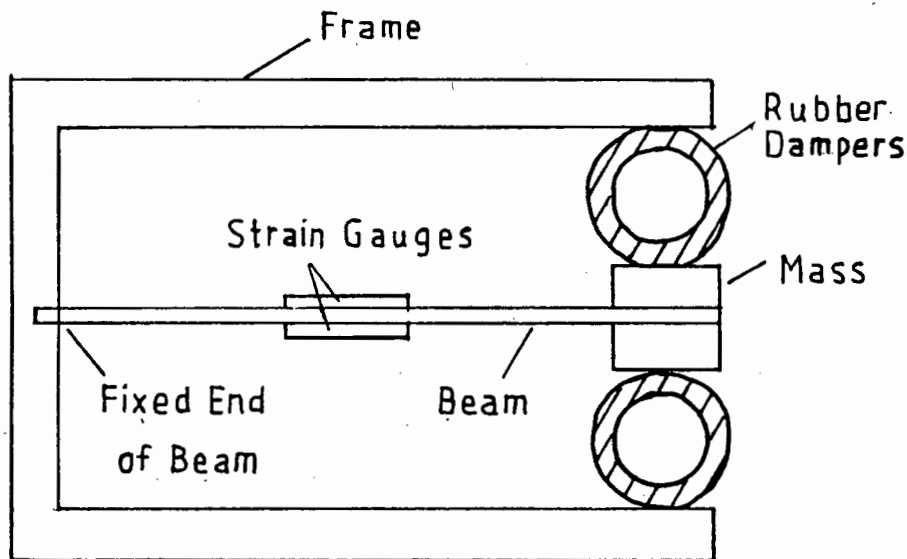


Figure F.5 Sketch of proposed design for strain-gauge accelerometer

## APPENDIX G: DATA SAMPLING PROGRAM

This program is used to control the sampling procedure of the Eagle Electric PC-30 A to D/ D to A conversion card. It samples the first two input channels every time that the Least Significant Bit of port A0 changes sign. This is caused by applying a voltage to the LSB port.

The voltage change is caused by the pulse generator of the fifth wheel. The data from the two inputs is read into two arrays, and then stored to disc for later analysis.

The program is compiled to run as an executable file.

The section labelled Initial Statements (line 100) sets up all arrays, functions and constants, and the addresses for the A/D card.

The Main Program (line 500) gives the choice of writing the data to file or disk.

The following subroutines read two channels of data and display them on the screen (line 1000), or give the choice of reading two or three channels of data and saving them to disk (line 2000).

```

*****
      NETRIGSA.BAS FROM SAMPLE.BAS
      PROGRAM TO READ A to D
      FROM 2 OR 3 CHANNELS AND SHOW OR STORE
      DATE 18/x/89
      BY : J. KOHLER
*****
      -----INITIAL STATEMENTS-----
100
ON ERROR GOTO 30000

KEY OFF
DIM CHAN.0%(7000),CHAN.1%(7000),CHAN.2%(7000)

DEF FNF(WW$) = 40-LEN(WW$)/2
DEF FNPOSX(S,E,XS,X,XE) = S+(X-XS)*(E-S)/(XE-XS)
DEF FNPOSY(T,B,YT,Y,YB) = T+(B-T)*(YT-Y)/(YT-YB)

YTOP% = 1:      YBOT% = 285
XLEFT% = 0:     XRIGHT% = 700
PI =22/7 : PAGE% = 1 : BA% = &H700
HR% = 0 : MINT% = 0 : SEC% = 0 : FRAC% = 0 : DIGIT% = 1
D.OUTB% = 0 : D.OUTC% = 0
CHOICE% = 1

LOCATE , ,0
OUT BA%+3,&H92      'AD754 CONTROL WORD
CW% = 128+16        :OUT BA%+11,CW%  '8255 PPI A INPUT,B C OUTPUT
CW% = 128+32+16+4+2 :OUT BA%+7,CW%  '8253 TIMER COUNTER 2,MODE 3

*****
      -----MAIN PROGRAM-----
500
CLS
PRINT
INPUT "NUMBER OF READINGS (MAX 6500) :";NO.LOOPS%
INPUT "FILE NAME FOR DATA :";FILE.NAME$
INPUT "DATA TO SCREEN (1) OR DISK (2) ?";CHOICE%
PRINT "ANY KEY TO CONTINUE"
WHILE LEN(INKEY$) = 0:WEND

IF CHOICE% = 1 THEN GOSUB 1000 ELSE GOSUB 2000

PRINT:PRINT
INPUT " DO YOU WANT TO GO AGAIN (1) OR QUIT " ;CARON
IF CARON = 1 THEN GOTO 500

END

*****
      -----DATA CAPTURE (AND INTERROGATION)-----
1000      Enter subroutine with NO.LOOPS% defined.

PRINT:PRINT "PRESS ANY KEY TO START THE DATA CAPTURE"
WHILE LEN(INKEY$) = 0:WEND

OUT BA%+6,LO% : OUT BA%+6,HI%

```

PRINT:PRINT " IF ON *g* TEN VOLT JUMPER SETTING, THEN MULTIPLY  
VOLTS BY TWO"

PRINT

PRINT " CHANNEL 1

CHANNEL 2

N"

FOR N% = 1 TO NO.LOOPS%

CHAN% = 0 : CALL ATOD (CHAN%,DIGIT%) : CHAN.0%(N%) = DIGIT%

PRINT USING "££££";DIGIT%,:PRINT USING "£££.£££";((digit% -  
2047)/409.4);:PRINT " V ",

CHAN% = 1 : CALL ATOD (CHAN%,DIGIT%) : CHAN.1%(N%) = DIGIT%

PRINT USING "££££";DIGIT%,:PRINT USING "£££.£££";((digit% -  
2047)/409.4);:PRINT " V ",

WHILE INP(&H708)=0:WEND :WHILE INP(&H708) = 1 :WEND

PRINT N%

NEXT N%

PRINT:PRINT " CHANNEL 1

CHANNEL 2

N"

RETURN

\*\*\*\*\*  
2000

INPUT "DATA : TWO CHANNELS (2) OR THREE (3) ?";CHOICE2%

IF CHOICE2% = 3 THEN GOSUB 3000 ELSE GOSUB 2100

RETURN

\*\*\*\*\*  
2100

PRINT:PRINT " DATA STORED ON FILE AS NUMBERS FROM CARD "

PRINT:PRINT " LVDT ON FIRST CHANNEL, ACCM. ON SECOND "

PRINT:PRINT " PRESS ANY KEY TO START THE DATA CAPTURE"

WHILE LEN(INKEY\$) = 0:WEND

OUT BA%+6,LO% : OUT BA%+6,HI%

A\$ = "CHAN1" :B\$ = "CHAN2"

CHAN.0%(0)=A\$ : CHAN.1%(0)=B\$

FOR N% = 1 TO NO.LOOPS%

CHAN% = 0 : CALL ATOD (CHAN%,DIGIT%) : CHAN.0%(N%) = DIGIT%

CHAN% = 1 : CALL ATOD (CHAN%,DIGIT%) : CHAN.1%(N%) = DIGIT%

WHILE INP(&H708)=0:WEND :WHILE INP(&H708) = 1 :WEND

NEXT

PRINT "DATA CAPTURED - SAVING TO DISK..."

OPEN FILE.NAME\$ FOR OUTPUT AS £1

FOR N% = 1 TO NO.LOOPS%

PRINT £1,(CHAN.0%(N%)) ,(CHAN.1%(N%)), N%

NEXT

CLOSE £1

PRINT:PRINT "DATA SAVED TO DISK ... THANKS AND GOODBYE"

PRINT:PRINT "ARE YOU GOING TO BE DOING ANYTHING LATER TONIGHT  
?"

RETURN

```
*****
```

```
3000
```

```
PRINT:PRINT "PRESS ANY KEY TO START THE DATA CAPTURE"
```

```
WHILE LEN(INKEY$) = 0:WEND
```

```
OUT BA%+6,LO% : OUT BA%+6,HI%
```

```
FOR N% = 1 TO NO.LOOPS%
```

```
  CHAN% = 0 : CALL ATOD (CHAN%,DIGIT%) : CHAN.0%(N%) = DIGIT%
```

```
  CHAN% = 1 : CALL ATOD (CHAN%,DIGIT%) : CHAN.1%(N%) = DIGIT%
```

```
  CHAN% = 2 : CALL ATOD (CHAN%,DIGIT%) : CHAN.2%(N%) = DIGIT%
```

```
    WHILE INP(&H708)=0:WEND :WHILE INP(&H708) = 1 :WEND
```

```
NEXT
```

```
PRINT:PRINT "DATA CAPTURED - SAVING TO DISK..."
```

```
OPEN FILE.NAME$ FOR OUTPUT AS £1
```

```
FOR N% = 1 TO NO.LOOPS%
```

```
  PRINT £1,(CHAN.0%(N%)) ,(CHAN.1%(N%)),(CHAN.2%(N%)), N%
```

```
NEXT
```

```
CLOSE £1
```

```
PRINT "DATA SAVED TO DISK ... THANKS AND GOODBYE"
```

```
RETURN
```

```
*****
```

```
-----ERROR TRAP-----
```

```
30000
```

```
CALL TMODE
```

```
ON ERROR GOTO 0
```

```
STOP
```

```
END
```

```
*****
```

APPENDIX H: SPECTRAL ANALYSIS PROGRAM

This program, written in Tru Basic is used to process the signals from the LVDT and accelerometer, mounted on the fifth wheel during measurement. The FFT routine is the one described in the book by Newland [46]. The program reads and operates on the LVDT and accelerometer signals stored in a file by the A/D program NETRIGSA.BAS.

Line 100. The initial statements are made here.

Line 200. The data array is set up. The constants relating to the data are entered. From these values information on the sampling rate is calculated and displayed.

Line 500. The program reads data from the files created in BASIC. The numbers created by the A/D card are converted into the equivalent displacement and acceleration values from the sensors.

Line 1000. The signals are processed. The LVDT signal is first operated on. The data are averaged and a cosine taper window is applied to the first and last tenths before the FFT is run. The spectrum is calculated and displayed. High and low frequencies outside the regions of interest are filtered, and the wave reconstituted and redisplayed.

Line 2000. The accelerometer signal is similarly operated on. Before the signal is reconstituted, double integration of the frequency components is done. The result is the accelerometer displacement.

Line 3000. The two profiles are then summed together, giving the profile of the road.

Line 4000. The spectrum of the road profile is calculated and displayed. No spectral components longer than 12 m are calculated, since the accelerometer cannot accurately measure the equivalent low frequencies. The spectral components may be printed out or saved to disk.

Subroutine Doubint: Performs double integration of the accelerometer signal to give its displacement.

Subroutine Offoff: Removes any offset from the data.

Subroutine Offon: Adds the offset back to the data.

Subroutine Freq\_remove: Filters high and low wavelengths from the spectra.

Subroutine Arrayval: Sends the spectral values to the screen, printer or disk.

Subroutine FFT/Spectrum/IFFT: Calculates the Fourier components of the data, then calculates the spectral components, and reconstitutes the data from the spectral values.

Subroutine Grphc: Dimensions the graph according to the data values, and draws the axes and the graticules.



### A comment on the integration of the frequency spectrum

The FFT transform routine produces a spectrum containing  $N_b$  spectral components (including the DC component) for a series of  $N_b$  data points. The spectral components shown in the spectral plots are the sums of the squares of the real and imaginary (sine and cosine) coefficients for each term. It is symmetrical about its middle point at the  $(N_b/2 + 1)$ 'th coefficient.

As a consequence of the sampling theorem which says that the highest frequency which can be detected is half the sampling frequency, the spectrum can only be read up to the centre. The coefficient at the centre is that of the frequency equivalent to two successive data points, or half the sampling frequency.

Double integration in the time domain becomes a convolution in the frequency domain, and is done by multiplying the coefficients of each frequency component by  $(1/(2\pi n f_0))^2$ .  $f_0$  is the frequency of the fundamental, and  $n$  is the order of the harmonic. This has the effect of reducing the size of the frequency components. It reduces the higher frequencies more strongly than the lower ones, since it is inversely proportional to the square of the frequency.

In order to maintain the symmetry of the spectrum, the operation is reflected about the middle of the spectrum. This does not include the steady state component.

Except for the purpose of illustration, the spectrum is only shown up to the centre frequency.

```

=====
!                                     OPERATE ON AND ADD TWO ARRAYS
!      PROGRAM TO CALCULATE Fft USING NEWLANDS METHOD
!
!      NAME: FFT2LVAC                      by J.Koehler
!      PREVIOUS NAME: FFT_LVAC              original date: 25/09/89
!      *****
!      DATE      :8/i/90 :last revision :16/xi/89
!      COMMENTS: GRAPH ROUTINE, DFFT ROUTINE COMPILED
!                  READS BASIC TEXT FILES AND CONVERTS TO NUMBERS
!                  FILES GENERATED BY TRIGSAM FAMILY
!                  WINDOW APPLIED TO FIRST AND LAST TENTHS OF DATA
!                  ALLOW DELETION OF "SPURIOUS" LOW FREQUENCIES
!                  ALLOW FOR SETTINGS OF DIG. TAPE INPUT/OUTPUT
!      *****
! 100      INITIAL STATEMENTS

LIBRARY "GRPHC2.TRC"
LIBRARY "DFFT_2.TRC"
SET MODE "80"
OPTION ANGLE radians

DIM value(5000)      ! DATA POINTS FOR ANALYSIS
DIM Ar(5000)         ! THE ACCELEROMETER SIGNAL
DIM Ai(5000)         ! IMAGINARY COMPONENT
DIM LV (5000)        ! LVDT SIGNAL
DIM AC (5000)        ! ACCELEROMETER SIGNAL
DIM prof1(5000)      ! FINAL PROFILE SIGNAL

=====
! 200      SET UP DATA ARRAY

! INPUT PROMPT " MAXIMUM AMPLITUDE CARD CAN READ (V) ? ":VAMP
! INPUT PROMPT " SETTING OF LVDT CHANNEL ON TAPE DECK ? (MAX OUT
= 2V) ":LVT
! INPUT PROMPT " SETTING OF ACCM. CHANNEL ON TAPE DECK ? (MAX
OUT = 2V) ":ACT
! INPUT PROMPT " SENSITIVITY OF ACCELEROMETER AMPLIFIER ?
":AMPSENS
! INPUT PROMPT " WHEEL CIRCUMFERENCE ? ": WRCUM
! INPUT PROMPT " NUMBER OF PULSES PER REVOLUTION ? ":PUPREV
INPUT PROMPT " NUMBER OF PULSES PER SECOND ? ":PUPSEC

LET VAMP = 5          ! max +- voltage of card
LET LVT = 1 ! LVT/2
LET ACT = 1 ! ACT/2
LET AMPSENS = 100
! LET WRCUM = 2*PI*WHEELRAD
LET WRCUM = 2.095      ! METERS
LET PUPREV = 120
LET STEP = WRCUM/PUPREV ! DISTANCE BETWEEN SAMPLES
IN METERS

LET SPEED = PUPSEC*STEP
LET BB = 1/SPEED      ! M/S

```

```

PRINT
PRINT USING "    STEP SIZE = £.£££":STEP;
PRINT " m"
PRINT USING "    AVERAGE SPEED  = ££.££":SPEED;
PRINT " m/s";
PRINT USING "    OR ££.££":SPEED*3.6;
PRINT " km/h"
PRINT USING "    FACTOR BB = £.£££":BB
PRINT USING "    TIME PER PULSE = £.£££":BB*STEP;
PRINT " s"
PRINT
! 500 READ DATA HERE *****
DO
  WHEN ERROR IN
    LET flag1 = 0                !checks for error condition
    INPUT PROMPT " NAME OF FILE TO READ ? ":FILENAM$
    OPEN £1:NAME FILENAM$, ACCESS INPUT, CREATE OLD
  USE
    PRINT " ERROR ";EXTTEXT$
    PRINT " PLEASE TRY AGAIN "
    LET FLAG1 = 1
  END WHEN
LOOP UNTIL FLAG1 = 0

INPUT prompt" NUMBER OF DATA POINTS Nb = ": Nb
LET noe = Nb

WHEN ERROR IN
  FOR I = 1 TO NOE
    INPUT £1: a$                ! ALL THIS TO READ BASIC ASCII FILES
                                ! READS EACH LINE OF DATA AS 1 STRING
    LET B$ = A$[1:6]            ! divide the string into substrings
    LET C$ = A$[14:20]
    LET lv(i) = val(B$)         ! THANKS TO PRETTY LASS AT HOT SEAT
    LET AC(i) = val(C$)         ! CONVERT STRINGS TO NUMBERS
  NEXT I
USE
  PRINT " ERROR :";EXTTEXT$
  LET NOE = I - 1                ! must pad with zeroes, if
                                ! difference not too great
  PRINT " NUMBER OF DATA POINTS = ";I-1
  ! LET Nb = NOE                ! MUST ROUND TO 2^N
  ! IF NOE >2 THEN EXIT

  IF NOE <=2 THEN
    PRINT
    PRINT " NOT ENOUGH DATA - PROGRAM ABORTED"
    STOP
  END IF

  DO
    GET KEY NM
    LOOP UNTIL NM > 0
    CLEAR
  END WHEN

! SET SENSITIVITY OF ACCM.
LET SEN = AMPSENS / 25 * 9.81*1000 ! (MM/S/S) g/volt to mm/s^2

```

```

FOR I = 2 TO NOE          ! TO REMOVE SPURIOUS MAX/MIN EXCURSIONS
  IF LV(I) <= 1 AND (LV(I-1) <> 0 OR LV(I+1) <> 0) THEN LET
    LV(I) = (LV(I-1) + LV(I+1))/2
  IF LV(I) >= 4095 AND (LV(I-1) < 4095 OR LV(I+1) < 4095) THEN
    LET LV(I) = (LV(I-1) + LV(I+1))/2
  IF AC(I) <= 0 AND (AC(I-1) <> 0 OR AC(I+1) <> 0) THEN LET
    AC(I) = (AC(I-1) + AC(I+1))/2
  IF AC(I) >= 4095 AND (AC(I-1) < 4095 OR AC(I+1) < 4095) THEN
    LET AC(I) = (AC(I-1) + AC(I+1))/2      !VAMP,AMPSSENS
  LET LV(I) = (LV(I) - 2047)/(2047/VAMP)*3.85*LVT
  LET AC(I) = (AC(I) - 2047)/(2047/VAMP)*SEN*ACT
  ! REMOVE CARD OFFSET AND SCALE VOLTAGES IN ORDER TO MAKE DISPL.
  AGREE
NEXT I

```

```

FOR I = 1 TO Nb          ! TO SMOOTH EXCESSIVE
  EXCURSIONS
    WHEN ERROR IN
      IF LV(I+1)/LV(I) < 1/9 THEN LET LV(I) = LV(I+1)
    USE
      LET LV(I) = 0          ! must be zero anyway
    END WHEN
    WHEN ERROR IN
      IF AC(I+1)/AC(I) < 1/9 THEN LET AC(I) = AC(I+1)
    USE
      LET AC(I) = 0
    END WHEN
NEXT I

```

```

LET TO = Nb*STEP*BB
PRINT
PRINT USING "    FUNDAMENTAL WAVELENGTH = ##.###":Nb*STEP;
PRINT " m"
PRINT
PRINT USING "    FUNDAMENTAL PERIOD = ##.###":TO;
PRINT " SECONDS"
PRINT
PRINT USING "    FUNDAMENTAL FREQUENCY = ##.###":1/TO;
PRINT " Hz"
PRINT
PRINT USING "    WAVELENGTH OF 0.3 m HAS A FREQUENCY
##.###":Nb*STEP/.3;
PRINT " TIMES "
PRINT "    THE FUNDAMENTAL FREQUENCY "
PRINT
PRINT " PRESS A KEY TO CONTINUE "
DO
LOOP UNTIL KEY INPUT
CLEAR

```

```

! *****
! 1000 START OPERATION ON DATA HERE

```

```

CALL OFFOFF (aver, Nb, LV())      ! Removes offset of lvdt signal

FOR I = 1 to noe/10+1            ! window on first tenth of data
  LET PHETA = (i-1)*pi*10/noe
  LET LV(i) = LV(i) * 0.5*(1 + cos(PHETA-pi) )
NEXT i

```

```

FOR I = 9/10*noe to noe                ! window on last tenth of data
  LET pheta = (i-(9/10*noe))*10/NOE*pi
  LET LV(i) = LV(i) * 0.5*(1 + cos(PHETA))
NEXT I
LET lv(Nb) = 0
LET lv(Nb+1) = 0

FOR I = 1 TO NOE
  LET LV(I) = LV(I)*550/45    ! RATIO OF LVDT POSN. TO WHEEL POSN.
  LET VALUE(I) = LV(I)
NEXT I

LET title$ = "Input data with window, from " & FILENAM$
LET ytitle$ = "MEASURED WHEEL DISPLACEMENT (mm)"
LET STEP$ = STR$(truncate(STEP,4))
LET TO$ = STR$(truncate(TO,3))
LET XTITLE$ = "Distance in metres. Step size =" & using$
  ("%%.%%%",step$)&"m."& "(Sample time "& using$("%%.%%%",TO$)
  & "s)"
!LET xtitle$ = "(" & USING$("%%.%%%",STEP$) & " m between
samples) Record Period = " & using$("%%.%%%",TO$) & "
seconds"
! CALL grphdim(title$, ytitle$, xtitle$, noe, value(),vmax,step)

FOR I = 1 TO Nb
  LET AR(I) = LV(I)    PUTS LVDT VALUES INTO SPECTRAL ARRAY
NEXT I

LET type = 1
CALL FFT(AR(), AI(), N, Nb, VALUE(), STEP,BB,type)
! TO CALCULATE SPECTRUM OF LVDT
CALL FREQ_REMOVE (AR(), AI(), Nb, STEP)

CALL IFFT(AR(), AI(),N,Nb,VALUE(), STEP, BB)
FOR I = 1 TO Nb
  let lv(i) = ar(i)
  LET value(I) = LV(I)    ! TO CALCULATE SPECTRUM OF
LVDT SIGNAL
NEXT I
LET ytitle$ = "FILTERED MEASURED WHEEL DISPLACEMENT (mm)"
CALL grphdim(title$, ytitle$, xtitle$, noe, value(),vmax,step)

! *****
! 2000 SHOW ACCELERATION INPUT DATA
LET noe = Nb    ! CF. DATA INPUT
FOR i = 1 to noe
  LET value(i) = AC(i)
  LET AR(I) = AC(I)
  LET AI(i) = 0
NEXT i

CALL OFFOFF(aver, Nb, ar() )

FOR i = 1 to noe/10+1    ! window on first tenth of data
  LET pheta = (i-1)*pi*10/noe
  LET AR(i) = ar(i) * 0.5*(1 + cos(PHETA-pi) )
NEXT i

```

```

FOR i = 9/10*noe to noe          ! window on last tenth of data
  LET pheta = (i-(9/10*noe))*10/NOE*pi
  LET ar(i) = ar(i) * 0.5*(1 + cos(PHETA))
NEXT i

LET Ar(Nb) = 0
LET Ar(Nb+1) = 0

FOR I = 1 TO NOE
  LET VALUE(I) = Ar(I)
NEXT I

!=====
!          SHOW RAW DATA
  LET title$ = "Input data with window"
  LET ytitle$ = "Acceleration (mm/s/s)"
! CALL grphdim(title$, ytitle$, xtitle$, noe, value(),vmax,step)
!=====

!          PERFORM THE FFT

CLEAR
PRINT "          FAST FOURIER TRANSFORM CALCULATIONS"
PRINT

LET type = 2
CALL FFT(AR(), AI(), N, Nb, VALUE(), STEP, BB,type)

CALL FREQ_REMOVE (AR(), AI(), Nb, STEP)

FOR I = 1 TO Nb
  LET VALUE(I) = 0
NEXT I

LET type = 1
CALL doubint(AR(), AI(), Nb, value(), step, bb, type)
! DOUBLE INTEG.
CALL IFFT(AR(), AI(),N,Nb,VALUE(), STEP, BB)
LET title$ = "Re-Synthesized data"
LET title$ = "Double integrated data"
LET ytitle$ = " Displacement (mm) "
CALL grphdim(title$, ytitle$, xtitle$, noe, value(),vmax,step)
! DISPLAY IFFT
! 3000 SUMMATION OF DATA *****
FOR I = 1 TO NOE
  LET PROFLI = LV(I) + VALUE(I)
  LET VALUE(I) = PROFLI
NEXT I

LET title$ = " THE PROFILE "
LET ytitle$ = "Displacement (mm)"
CALL grphdim(title$, ytitle$, xtitle$, noe, value(),vmax,step)
! DISPLAYS SUMMED PROFILE

FOR i = 1 to Nb
  LET ar(I) = value(I)
NEXT I

```

```

! 4000 *** FINAL PROFILE LOOP ***

DO UNTIL FG$ = "y" OR FG$ = "Y"
  INPUT PROMPT " ARE YOU HAPPY WITH THE PROFILE ? ":FG$
  PRINT
  IF FG$ = "y" OR FG$ = "Y" THEN EXIT DO
  CALL FFT(AR(), AI(), N, Nb, VALUE(), STEP, BB, type)
DO
INPUT PROMPT " DO YOU WANT TO DELETE ANY LOW FREQUENCIES ? ":FD$
  PRINT
  IF FD$ = "Y" OR FD$ = "y" THEN
    INPUT PROMPT " UP TO WHICH NUMBER DO YOU WISH TO DELETE ? ":ND
    FOR I = 1 TO ND + 1      ! SINCE FO = AR(2) ; DC = AR(1)
      LET AR(I) = 0
      LET AI(I) = 0
      LET AR(Nb+2-I) = 0
      LET AI(Nb+2-I) = 0
    NEXT I
  END IF
  CALL SPECTRUM (AR(), AI(), N, Nb, VALUE(), STEP, BB, type)
  INPUT PROMPT " ARE YOU HAPPY WITH THE SPECTRUM ? ":FU$
LOOP UNTIL FU$ = "y" OR FU$ = "Y"
  PRINT

CALL IFFT(AR(), AI(), N, Nb, VALUE(), STEP, BB)
FOR I = 1 TO Nb
  LET VALUE(I) = AR(I)
NEXT I
CALL grphdim(title$, ytitle$, xtitle$, noe, value(),
              vmax, step)      ! DISPLAYS SUMMED PROFILE

LOOP

INPUT PROMPT " DO YOU WANT A SPECTRUM FOR THE DATA ? ":DATSPEC$
IF DATSPEC$ = "Y" OR DATSPEC$ = "y" THEN CALL FFT(AR(), AI(), N,
Nb, VALUE(), STEP, BB, type)
IF DATSPEC$ = "Y" OR DATSPEC$ = "y" THEN CALL ARAYVAL(AR(),
AI(), Nb, STEP)
PRINT
PRINT " THAT'S ALL, FOLKS "
! *****

END

! *****
! SUBROUTINES START HERE
! *****

```

```
SUB DOUBINT( Ar(), Ai(), Nb ,value(),step,bb,type)
```

```
!   AR(t) = a*(- SIN(bb*tt))
LET TO = Nb*STEP*BB
```

```
PRINT
PRINT
PRINT "    DOUBLE INTEGRATION BEING PERFORMED "
PRINT
PRINT "    FUNDAMENTAL PERIOD = ";TO;"SECONDS"
PRINT
PRINT "    FUNDAMENTAL FREQUENCY = ";1/TO;"Hz"
PRINT
```

```
LET AR(1) = 0           ! SETS ANY STRAY DC COMPONENT TO ZERO
LET AI(1) = 0
```

```
! TO = Nb*STEP*BB
! PERIOD = No. OF POINTS*STEP SIZE*TIME/POINT
```

```
FOR I = 2 TO Nb/2 + 1
  LET FACTOR = ( (TO) / (2*Pi*(I-1)) )^2
  LET AR(I) = AR(I)*(-FACTOR)
  LET AI(I) = AI(I)*(-FACTOR)
  LET AR(Nb+2-I) = AR(Nb+2-I)*(-FACTOR)
  ! REFLECTION ABOUT Nb/2 + 1
  LET AI(Nb+2-I) = AI(Nb+2-I)*(-FACTOR)
NEXT I
```

```
FOR i = Nb + 1 to Nb + 4
  LET ar(i) = 0
  LET ai(i) = 0
NEXT i
```

```
CALL SPECTRUM (AR(), AI(),N,Nb,VALUE(),STEP, BB,type)
```

```
END SUB
```

```
! *****
```

```
SUB OFFOFF (aver, Nb, ar())
```

```
  FOR i = 1 to Nb
    LET aver = aver + ar(i)
  NEXT i
  LET aver = aver / (Nb-1)
  FOR i = 1 to Nb
    LET ar(i) = ar(i) - aver
  NEXT i
```

```
END SUB
```

```
! *****
```

```
SUB OFFON (aver, Nb, ar() )
```

```
  FOR i = 1 to Nb
    LET ar(i) = ar(i) + aver
  NEXT i
```

```
END SUB
```

```
! *****
```



```

SUB FREQ_REMOVE (AR(), AI(), Nb, STEP)
  FOR I = 2 TO ROUND(Nb*STEP/15) + 1 ! ALL COMPONENTS BELOW 15
  M
    LET AR(I) = 0
    LET AI(I) = 0
    LET AR(Nb+2-I) = 0
    LET AI(Nb+2-I) = 0
  NEXT I

  FOR I = (Nb*STEP/.25) TO Nb/2+1 ! ALL COMPONENTS OVER 0.25 M
    LET AR(I) = 0
    LET AI(I) = 0
    LET AR(Nb+2-I) = 0
    LET AI(Nb+2-I) = 0
  NEXT I

END SUB

! *****

SUB ARRAYVAL(AR(), AI(), Nb, STEP)

INPUT PROMPT " OUTPUT VALUES TO SCREEN (1) or PRINTER (2) or FILE
(3) ? ":NUM

IF NUM = 3 THEN
  PRINT " THE NAME OF THIS FILE IS "
  PRINT " " & FILENAM$
  PRINT "WE RECOMMEND THAT YOU CALL THE FILE BY THE SAME NAME,
WITH THE EXTENSION OF SPC"
  input prompt " NAME OF FILE TO WRITE TO ? ": SPCNAM$
  OPEN %2:NAME SPCNAM$, ACCESS OUTIN, CREATE NEW
  FOR I = 1 TO 250 ! ROUND(Nb*STEP/0.3) + 1
    WRITE %2: AR(I), AI(I), 1 ! WILL DISPLAY SPECTRUM
  NEXT I ! NO NEED TO CORRECT I + 1
  CLOSE %2

ELSE IF NUM = 2 THEN
  OPEN %1:PRINTER
  PRINT %1:" AR(I), AI(I), SPECTRAL VALUE,
WAVELENGTH, ORDER "
  PRINT %1:
  FOR I = 1 TO NB*STEP/.3 + 1
    PRINT %1: AR(I+1), AI(I+1), AR(I+1)^2 + AI(I+1)^2,
Nb*STEP/I, I
  NEXT I
ELSE
  CLEAR
  PRINT " AR(I), AI(I), SPECTRAL VALUE,
WAVELENGTH, ORDER "
  PRINT
  FOR I = 1 TO 20
    PRINT AR(I+1), AI(I+1), AR(I+1)^2 + AI(I+1)^2, Nb*STEP/I, I
  NEXT I
END IF

END SUB

```

```

! *****
! DATE      :14/xii/89
! COMMENTS: FFT / IFFT ROUTINE
! DATE OF LAST REVISION:
! NATURE OF REVISION:
! " " " " :
! DFFT ROUTINE
! NAME; DFFT_2   FOR USE WITH FFT_LVAC AND FFT_ACC
! *****

! ROUTINE TO CALCULATE DFT
EXTERNAL

SUB FFT (Ar(), Ai(), N, Nb, VALUE(), STEP, BB,type)

    LET N = LOG2(Nb)
    PRINT
    PRINT "Number of Elements = ";Nb
    PRINT "Number of Passes = ";N
    PRINT

    FOR J = 1 TO Nb                ! DIVIDE ALL ELEMENTS BY Nb
        LET Ar(J) = Ar(J)/Nb
        LET Ai(J) = Ai(J)/Nb
    NEXT J

                                ! REORDER SEQUENCE
    LET Nbd2 = Nb/2
    LET Nbm1 = Nb - 1
    LET J = 1                    ! REFLECT BITS ABOUT RHS
    FOR L = 1 TO Nbm1
        IF (L<J) THEN
            LET Tr = Ar(J)
            LET Ti = Ai(J)
            LET Ar(J) = Ar(L)
            LET Ai(J) = Ai(L)
            LET Ar(L) = Tr
            LET Ai(L) = Ti
        END IF
        LET K = Nbd2
        DO WHILE (K < J)
            LET J = J - K
            LET K = K/2
        LOOP
        LET J = J + K
    NEXT L

! CALCULATE FFT ***** !!!!!!!!!!!!!!!
PRINT
PRINT " * FFT IN PROGRESS *"
PRINT
PRINT " NUMBER OF PASSES "
PRINT
FOR M = 1 TO N
    LET UR = 1
    LET UI = 0
    LET ME = 2^M
    LET K = ME/2
    LET WR = COS(PI/K)
    LET WI = -SIN(PI/K)

```

```

FOR J = 1 TO K
  FOR L = J TO Nb STEP Me
    LET LPK = L + K
    LET TR = AR(LPK)*UR - AI(LPK)*UI
    LET TI = AI(LPK)*UR + AR(LPK)*UI
    LET AR(LPK) = AR(L) - TR
    LET AI(LPK) = AI(L) - TI
    LET AR(L) = AR(L) + TR
    LET AI(L) = AI(L) + TI
  NEXT L
  LET SR = UR
  LET UR = UR*WR - UI*WI
  LET UI = UI*WR + SR*WI
NEXT J
PRINT M,
NEXT M
PRINT
PRINT
PRINT " FFT COMPLETED"
PRINT
DO
  GET KEY n
  LOOP until n <> 0
  CLEAR

  CALL SPECTRUM (Ar(), Ai(), N, Nb, VALUE(), STEP, BB, type)
END SUB

! *****
SUB SPECTRUM (Ar(), Ai(), N, Nb, VALUE(), STEP, BB, type)
DO
  PRINT
  INPUT PROMPT "  SELECT GRAPH SCALING: 1=LOG, 2=LINEAR
              3=EXIT: ":GAIN
  IF GAIN = 3 THEN EXIT SUB
! Display data
  DIM HA(6800)
  LET FMIN = 999999
  LET FMAX = -999999
  FOR I=1 TO Nb*STEP/0.25 + 2      !nof = 1/2 NUMBER DATA POINTS
    LET HA(I) = AR(I)^2 + AI(I)^2
    WHEN error in
      IF GAIN = 1 THEN LET HA(I) = LOG10(HA(I))
    USE
      LET ha(i) = LOG10(0.000001)
    END WHEN
    IF HA(I)>FMAX THEN LET FMAX=HA(I)
    IF HA(I)<FMIN THEN LET FMIN=HA(I)
  NEXT I
! Display data
  LET TITLE$ = "FREQUENCY SPECTRUM"
  IF gain = 1 and type = 1 THEN LET YTITLE$ = "mm^2/m
(Logarithmic)"
  IF gain = 1 and type = 2 THEN LET yttitle$ = "(mm/s/s)^2/m
(Logarithmic)"
  IF gain <> 1 and type = 1 THEN LET YTITLE$ = "mm^2/m
(Linear)"
  IF gain <> 1 and type = 2 THEN LET yttitle$ =
"(mm/s/s)^2/m (Linear)"

```

```

    LET afo = 1/(Nb*step*bb)
    LET bfo = Truncate(afo,4)
    LET cfo$ = str$(bfo)
    LET dfo = (Nb*step)
    LET XTITLE$ = "Spectrum of the Wave: Components in
Metres per Cycle"
    !      LET XTITLE$ = "Frequency x Fundamental of "&
using$("%%.%%%",cfo$)&" Hz"

    LET YMIN = FMIN-(.05*(FMAX-FMIN))
    LET YMAX = FMAX+(.05*(FMAX-FMIN))
    LET YTIC = (YMAX-YMIN)/10
    LET XMIN = 0
    LET XMAX = round(Nb*STEP/.3) + 1      !(Nb/2)
    IF XMAX < 1 THEN LET XMAX = Nb
    LET XTIC = ROUND(XMAX/10)
    FOR I = Nb + 1 TO Nb + 5
        IF GAIN = 1 THEN LET ha(i) = FMIN
    NEXT I
    ASK MAX CURSOR r,c
    IF r = 25 THEN SET MODE "HIRES" ELSE SET MODE "hercules"
    CALL AXES2(GL,GR,GB,GT,XMIN,XMAX,XTIC,YMIN,YMAX,YTIC,
        TITLE$,XTITLE$,YTITLE$,STEP,DFO)
    OPEN £1: screen gl,gr,gb,gt
    SET WINDOW xmin,xmax,ymin,ymax
    CALL tic2(xtic,ytic,step)
    PLOT XMIN,YMIN;
    FOR n = 1 TO round(Nb*STEP/.3) + 1 !(Nb/2) !NOF
        PLOT n-1.5,HA(n);
        PLOT n-0.5,HA(n);
    NEXT n
    PLOT ROUND(Nb*STEP/.3)+1-1.5,HA(n);
    PLOT ROUND(Nb*STEP/.3)+1-0.5,HA(n);
    PLOT ROUND(Nb*STEP/.3)+1-0.5,YMIN;
    SET CURSOR "OFF"
    DO
        GET KEY N
        LOOP UNTIL N > 0
    CLOSE £1
    SET MODE "80"
    CLEAR
LOOP

END SUB

! *****
! ROUTINE TO CALCULATE INVERSE DFT (IFFT)

SUB IFFT (Ar(), Ai(), N, Nb, VALUE(), STEP, BB)
    LET N = LOG2(Nb)
    CLEAR
    PRINT
    PRINT " * IFFT IN PROGRESS * "
    PRINT

```

```

! REORDER SEQUENCE
LET Nbd2 = Nb/2
LET Nbm1 = Nb - 1

```

```

LET J = 1

```

```

FOR L = 1 TO Nbm1
  IF (L<J) THEN
    LET Tr = Ar(J)
    LET Ti = Ai(J)
    LET Ar(J) = Ar(L)
    LET Ai(J) = Ai(L)
    LET Ar(L) = Tr
    LET Ai(L) = Ti
  END IF
  LET K = Nbd2
  DO WHILE (K < J)
    LET J = J - K
    LET K = K/2
  LOOP
  LET J = J + K
NEXT L

```

```

! CALCULATE FFT ***** !!!!!!!!!!!!!!!
PRINT " NUMBER OF PASSES "
PRINT
PRINT " Number of Elements = ";Nb
PRINT " Number of passes = ";N
PRINT
FOR M = 1 TO N
  PRINT M,
  LET UR = 1
  LET UI = 0
  LET ME = 2^M
  LET K = ME/2
  LET WR = COS(PI/K)
  LET WI = SIN(PI/K)
  FOR J = 1 TO K
    FOR L = J TO Nb STEP Me
      LET LPK = L + K
      LET TR = AR(LPK)*UR - AI(LPK)*UI
      LET TI = AI(LPK)*UR + AR(LPK)*UI
      LET AR(LPK) = AR(L) - TR
      LET AI(LPK) = AI(L) - TI
      LET AR(L) = AR(L) + TR
      LET AI(L) = AI(L) + TI
    NEXT L
    LET SR = UR
    LET UR = UR*WR - UI*WI
    LET UI = UI*WR + SR*WI
  NEXT J
NEXT M
FOR I = 1 TO Nb
  LET VALUE(I) = AR(I)
NEXT i
PRINT
PRINT " IFFT COMPLETE "

```

```

DO
  GET KEY N
  LOOP UNTIL N <> 0
  CLEAR
END SUB
! *****

! *****
! compiled subroutine grphc.TRC
! dimensions graph, draws axes, graticules
! date: 4/x/89
! *****

EXTERNAL

SUB grphdim (title$, ytitle$, xtitle$, noe, value(),vmax,step)
  LET VMIN = 999999
  LET VMAX = -999999
  FOR I = 1 TO NOE
    IF VALUE(I) > VMAX THEN LET VMAX = VALUE(I)
    IF VALUE(I) < VMIN THEN LET VMIN = VALUE(I)
  NEXT I

  LET YMIN = VMIN-(.05*(VMAX-VMIN))
  LET YMAX = VMAX+(.05*(VMAX-VMIN))
  LET YTIC = (YMAX-YMIN)/10
  LET XMIN = 0
  LET XMAX = NOE+1
  LET XTIC = ROUND(XMAX/10)

  ASK MAX CURSOR r,c
  IF r = 25 THEN SET MODE "HIRES" ELSE SET MODE "HERCULES"
  CALL AXES(GL,GR,GB,GT,XMIN,XMAX,XTIC,YMIN,YMAX,YTIC,
    TITLE$,XTITLE$,YTITLE$,STEP)

  OPEN &1: SCREEN gl,gr,gb,gt
  SET WINDOW xmin,xmax,ymin,ymax
  CALL tic(xtic,ytic)

  SET WINDOW 0,noe,ymin,ymax
  FOR n = 1 to noe
    PLOT n,value(n);
  NEXT n

  SET CURSOR "off"

  DO
    GET KEY N
    LOOP UNTIL N <> 0
  CLOSE &1
  SET MODE "80"
  CLEAR

end sub

```

! Graph Subroutine

SUB

axes(gl,gr,gb,gt,xmin,xmax,xtic,ymin,ymax,ytic,title\$,xtitle\$,yt  
itle\$,step)

LET gl = 8.5/80  
LET gr = 78.5/80  
LET gb = 3.5/25  
LET gt = 22.5/25

SET WINDOW 0,80,0,25

FOR n = ymin to ymax step ytic  
LET nn = round(100\*n)/100  
LET q\$ = str\$(nn)(0:6)  
IF len(q\$) < 6 then LET q\$ = repeat\$(" ",6-len(q\$)) & q\$  
PLOT TEXT,AT 1,24:q\$  
BOX KEEP 1,7,24,25 in q\$  
BOX CLEAR 1,7,24,25  
LET y = 3+19\*(n-ymin)/(ymax-ymin)  
BOX SHOW q\$ at 1,y  
NEXT n

IF XMIN = XMAX THEN PRINT ERROR  
IF XMAX = XMIN THEN EXIT SUB

FOR n = xmin to xmax step xtic  
LET nn = round(100\*n\*step)/100  
LET q\$ = str\$(nn)(0:6)  
LET x = 8.5+70\*(n-xmin)/(xmax-xmin)-len(q\$)/2  
PLOT TEXT,AT 1,24:q\$  
BOX KEEP 1,7,24,25 in q\$  
BOX CLEAR 1,7,24,25  
BOX SHOW q\$ at x,2  
NEXT n

LET x = (85-len(title\$))/2  
PLOT TEXT, AT x,24: title\$  
LET Yytitle\$ = "Vertical units : " & ytitle\$  
LET x = (85-len(Yytitle\$))/2  
PLOT TEXT, AT x,23: Yytitle\$  
LET x = (85-len(xtitle\$))/2  
PLOT TEXT, AT x,1: xtitle\$

END SUB

```
! *****
```

```
SUB tic(xtic,ytic)
```

```
ASK WINDOW xmin,xmax,ymin,ymax
BOX LINES xmin,xmax,ymin,ymax
```

```
FOR n = xmin to xmax step xtic
  IF round(100*n)/100 = 0 then
    PLOT LINES: n,ymin;n,ymax
  ELSE
    FOR nn = ymin to ymax step ytic/10 !5
      PLOT n,nn
    NEXT nn
  END IF
NEXT n
```

```
!           PLOT LINES (XMIN,0);(XMAX,0)
!   FOR n = ymin to ymax step ytic
!     IF round(100*n)/100 = 0 then
!       PLOT LINES: xmin,n;xmax,n
!     ELSE
!       FOR nn = xmin to xmax step xtic/5
!         PLOT nn,n
!       NEXT nn
!     END IF
!   NEXT n
```

```
FOR nn = xmin to xmax step xtic/5
  PLOT nn,0
NEXT nn
```

```
END SUB
```



## APPENDIX I: TEST RESULTS

This appendix contains the results of the different tests made during the course of the project. These results are described in Section 5.

### I-1) Waveforms used to test the integration routine

The following pages describe the wave forms used to test the integration routine in the frequency domain. After the description they show:

a) the input wave, b) its spectrum, c) the result of the double integration and d) its spectrum. Each example is referred to by number, and its different graphs by letter.

#### 1) A sine wave : Figure I-1

When a sine wave is integrated twice, it becomes a -sine wave. If the period is greater than  $2\pi$ , its amplitude is increased. If the period is less than  $2\pi$ , its amplitude is decreased.

The program is tested for different amplitudes and frequencies. The example shows a sine wave of period  $\pi$  integrated over an interval of  $2\pi$ . Its amplitude is decreased by  $-(\pi/(2\pi \times 1))^2$ , which is equal to  $1/4$ . The correct result is obtained.

The complete spectrum generated by the FFT routine is shown. The line in the centre shows how far the spectrum has meaning. It corresponds to half the sampling frequency, and also to half the number of data points. The peak at the fundamental frequency is prominent. Nothing is to be seen over the rest of the spectrum.

## 2) A sine wave with noise : Figure I-2

A sine wave has high frequency random oscillations added to it. It has frequency components over its entire spectrum. As can be seen, there are frequencies present below the frequency of the sine wave. These are introduced by the presence of the high frequencies, which distort the sine wave.

Although the frequency of the original wave can still be seen after integration and reconstitution, a strong low frequency component is superimposed on it. This can be removed by deleting the lowest components of the spectrum.

The high frequencies are not present in the double integrated signal, which illustrates that integration in the frequency domain also acts as a low pass filter, just as the electrical integrator does.

## 3) A square wave : Figure I-3

The calculated spectrum of the square wave shows the correct shape, with the first peak at the frequency of the wave, and the others at twice the distance of the first peak from the y-axis, from each other.

The double integral has a sinusoidal shape as expected. It has one prominent peak in its spectrum at the waves frequency, and a few insignificant ones at higher frequencies.

The amplitude of the resultant sine wave was checked by hand. This was done by calculating the area under the square wave, and then its integral. The first integral of the square wave is a triangular wave. Depending on whether integration starts on the positive or negative half of the cycle, the triangular wave will be offset to the positive or negative side of the axis. If its offset is calculated and removed, and it is then integrated again, the resulting wave is sinusoidal in shape, and has the same amplitude as that calculated from the spectrum.

#### 4) An ideal acceleration : Figure I-4

The acceleration is determined by constructing a mathematically simple displacement from the functions  $x^2$ ,  $x$  and constants. Differentiating it twice gives the corresponding acceleration. This is the curve described in Section 4.

Integration of the displacement via its spectrum gives the correct shape. By calculating the areas under the two successive curves numerically, the amplitude is proved to be correct.

The spectrum of the displacement curve shows the low frequencies to be predominant. This is not surprising, since the period of the bump is close to that of the sample.

## I-2) Comparison of the LVDT and the accelerometer displacement measurements

The program for combination of the integrated accelerometer trace and the LVDT signal is tested after the integration has been shown to work.

First the accelerometer and LVDT are kept stationary and their outputs recorded for a sample time of 10 seconds and processed. The average value due to the 1g static acceleration force is filtered from the accelerometer signal. The object is to see what error their noise levels cause.

The LVDT indicates a displacement of 0.08mm peak to peak. The accelerometer noise indicates acceleration of 500mm/s/s peak to peak. Integration of the accelerometer signal gives a displacement of about 20mm peak to peak. As the accelerometer was stationary, this indicates an error due to the noise.

## Measurement on the shaker

The signals shown are from measurement of the sinusoidal motion of an electromagnetic shaker by the LVDT and accelerometer. The displacement signal calculated from the acceleration is subtracted from the LVDT signal. For perfect agreement of the measurement, the signals should cancel each other out.

The spectra are now only shown as far as they are valid, up to the folding frequency, or the  $(N_b/2 + 1)$ 'th spectral value.

Complete cancellation of the signals does not occur. At frequencies above 2Hz, the amplitude of the combined signals is reduced by a factor of ten over the original, from 6mm to 0.6mm after the exaggerated low frequencies have been removed.

At frequencies lower than 2Hz, the accelerometer performance is not as accurate. At 0.5Hz and 6mm peak to peak excursion, the correct shape of the accelerometer displacement is calculated, but the amplitude is  $5/3$  too large.

The measurement can only be expected to give accurate results for small amplitude displacements from 2Hz. (Larger amplitudes generating higher acceleration forces can be measured at lower frequencies.) The accelerometer can only measure millimetric displacements above 2Hz.

#### 5) Figure I-5

This shows the measurement of a 10Hz oscillation of the shaker. The peak to peak amplitude is three millimetres. The first two plots show the LVDT signal and its spectrum. The effects of the cosine taper window applied to the first and the last tenths of the data can be seen. As described in Appendix H, it is used to smooth the record at its start and finish. This is done because the FFT process assumes that the actual signal is infinitely long, and is periodic over the period shown. Applying a window to the data removes discontinuities between one period and the next.

The plot of the acceleration (c) shows a sinusoidal wave of the same period and in anti-phase to the displacement trace.

The spectrum of the acceleration (d) is similar to the displacement curve around the peak. The strong harmonics occur at different points for each spectrum.

The spectrum of the double integral (e) of the acceleration still demonstrates strong peaks around the frequency of the wave. Although all values have been much reduced, the very low frequencies are proportionally much larger than before. They overshadow the peak at the signal frequency.

(This is because the input is not perfectly sinusoidal, or only of one frequency. Furthermore, there is some noise on the signal. This is especially noticeable in the region close to either side of the zero axis on the displacement curve.)

As shown in the integration of ideal sine waves, a pure sine wave is easily transformed. A sine wave with noise superimposed effectively has frequencies present lower than its own. The effect of the low frequencies is shown in the reconstituted wave, which now represents the accelerometer displacement (f).

When the two signals are added (g), the frequencies including and above 10Hz largely cancel each other out. The low frequencies are strongly evident (h). By setting to zero that part of the spectrum which was below the spectral peak of the original 10Hz wave, a new wave is obtained (i).

This shows (apart from the first and the last tenths), that once the extremely high frequency spikes have been removed, the resulting wave has a peak to peak amplitude of 0.3mm. This is a ten-fold reduction of the original amplitude.

6) Figure I-6

The measurement of the shaker movement takes place at a frequency of 2Hz, and a peak to peak amplitude of approximately 3mm. The period of the shaker motion is twice that of the record period. The LVDT (a) shows the motion to be sinusoidal, but not perfectly smooth.

The accelerometer (b) trace is correctly in anti-phase to the LVDT trace. It shows substantial noise. This is due to the roughness of the shaker movement. Once again, on integration and reconstruction of the accelerometer trace (c), the very lowest frequency is enlarged proportional to the others.

On addition of the signals the high frequencies cancel (d). The fundamental frequency distorts the result completely. When frequencies so close to the fundamental (e) are already present before integration, it is not acceptable to delete them. A longer record should be taken to ensure that the lowest frequency to measure is well above the fundamental frequency.

## 7) Figure I-7

This is a 1/2Hz sine wave. The sample length has been doubled to capture the full cycle. This is shown on the LVDT plot (a).

The acceleration trace (b) is heavily masked by high frequencies. The data can be seen to be offset about its mean value in anti-phase to the displacement. On integration (c) the high frequencies are removed, and only the fundamental is effectively present.

Reconstitution of the accelerometer signal gives a displacement trace similar to that measured by the LVDT. The final displacement (d) calculated is twice as large as the actual displacement measured. The resulting wave is of opposite phase to the displacement trace. With the accelerometer signal so inaccurate this has no meaning.

The input force is very low, since the amplitude is only a few millimetres. With a larger displacement at the same frequency, the force would be larger and the accelerometer could measure it.



I-3) Signals generated on the drum using the measuring wheel

Wheel circumference = 2.095m

25.2 km/h = 7 m/s = 3.34 rev/s = 400 pulses/sec

At this speed: 23Hz = 0.3m

10Hz = 0.7m

1Hz = 7m

.5Hz = 14m the lower limit of the  
accelerometer performance.

Drum circumference = 1.52m

Runout = 0.001m

Bump length = 0.30m

Bump height = 0.011m

Effective bump length, due to the bridging effect  
of the tyre = 0.37m

Tests are run on the drum, with and without the bump. Only the results from testing with the bump are shown.

The illustrations for measurement on the drum are in the same order as before. The spectrum is limited to wavelengths shorter than 14m (the lower limit of the accelerometers time response) and larger than 0.3m, the shortest wavelength simulated on the simulator. Any obtrusive low frequencies are removed at the end of the process. Since subtraction is a linear operation, this is permissible.

### 8) With Bump : Figure I-8

The signal from the LVDT is shown first (a), after the window has been applied to it. The wheel follows the bump. It overshoots at the start of the bump, but measures the correct length and amplitude of the bump. Some bounce after leaving the bump and striking the drum surface is shown. The spectrum (b) shows peaks at the wavelength of the bump, and at the wavelength of the drum circumference. This is because the wheel measures the bump as occurring repeatedly at a fixed interval, once every revolution of the drum. The LVDT signal is then shown again, after the frequencies outside the measuring range have been removed (c).

The acceleration signal (d), (e) shows the periodic effect of the drum rotation more strongly than the displacement curve. As before, the low frequencies are exaggerated by integration (f), and distort the displacement (g).

The profile, calculated by adding the two displacements (h), is closer to the true displacement after the low frequencies have been removed (i), (j). Because the signal has been averaged, the lowest value, which should indicate zero displacement, has a negative value. This can be changed by adding a positive offset. It does not affect the spectrum.

The presence of a non-zero average value would blur the spectral peaks around it during calculation. If the bridging effect of the tyre is taken into account, the bump has an effective length of about 0.38m, and this peak is strongly emphasized in the final spectrum.

#### I-4 Signals generated driving on the road

The Appendix contains the graphs of the measurements made on the road. The discussion is found in Section 5.

The graphs are given for:

- i) A smooth road. (figure I-9)
- ii) A tarred road with a speed bump. (Figure I-10)
- iii) A dirt track. (Figure I-11)

The graphs show: a) the LVDT signal, b) the accelerometer signal, d) its integral, e) the resultant profile , and f) the profile spectrum.

#### I-5 Measurements made on the test tracks at Uitenhage

Figure I-12 gives the plots for the average, maximum and minimum values of the profile spectrum for the ten different sections of the Steytlerville road measured.

Figure I-13 gives the same spectral plots for the three sections of the Van Staden's pass that were measured.

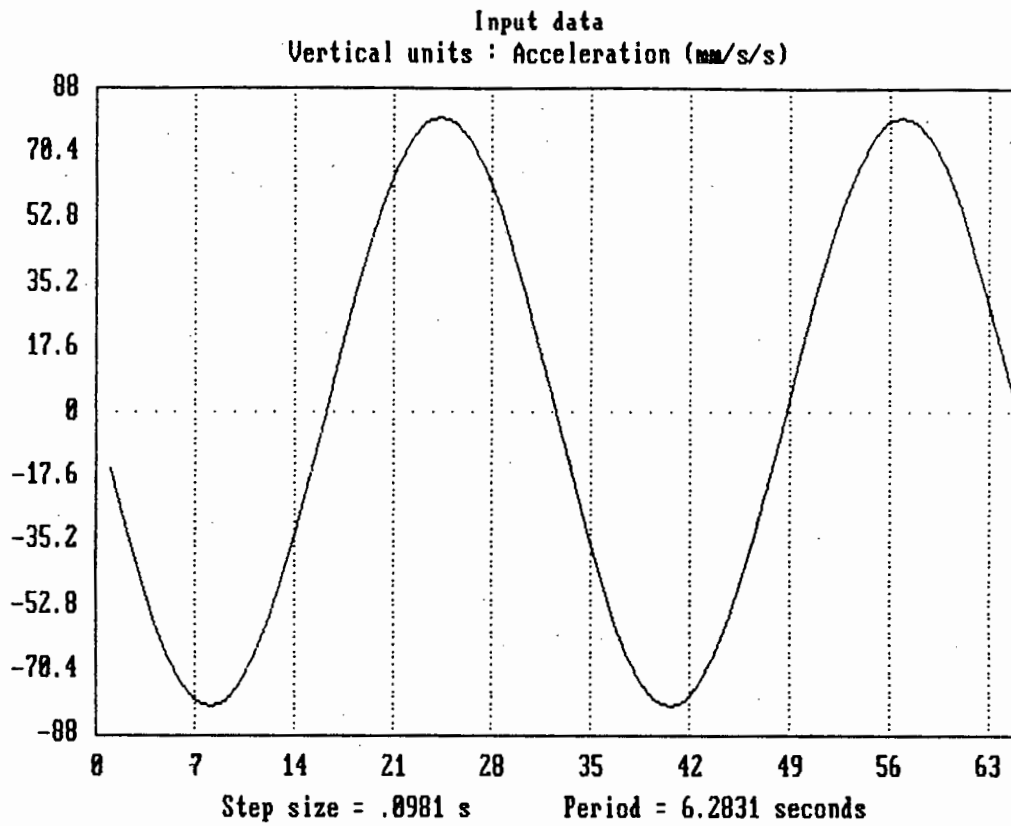


Figure I-1a Sinusoidal Acceleration

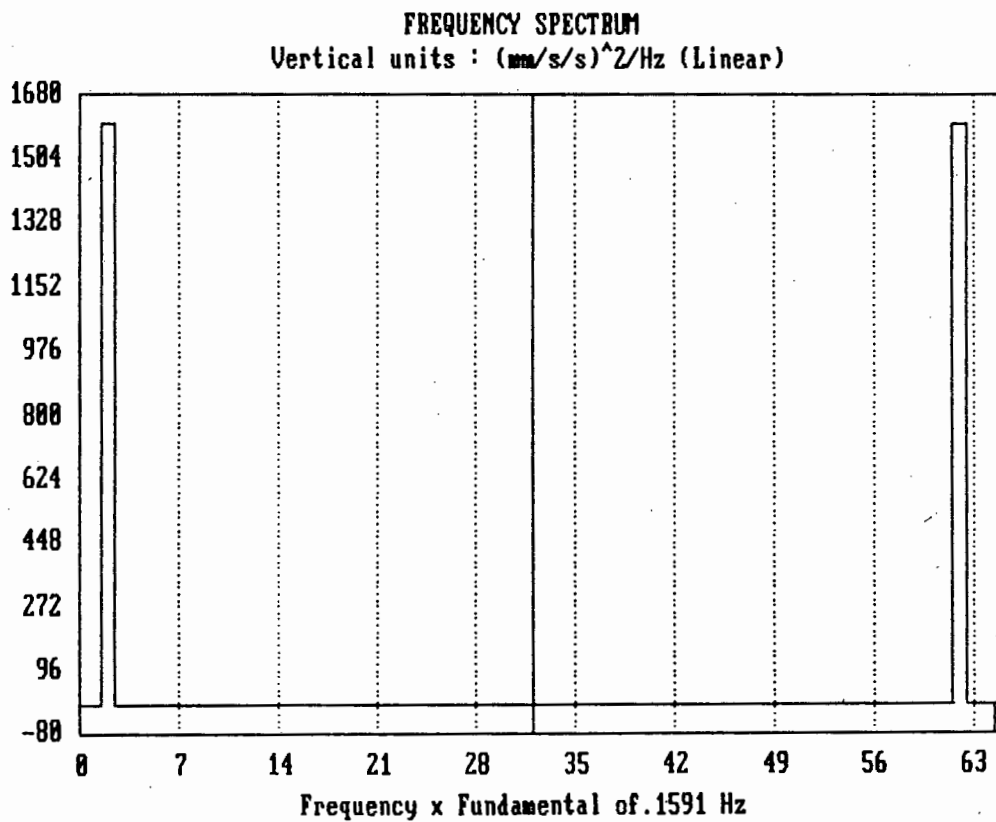


Figure I-1b

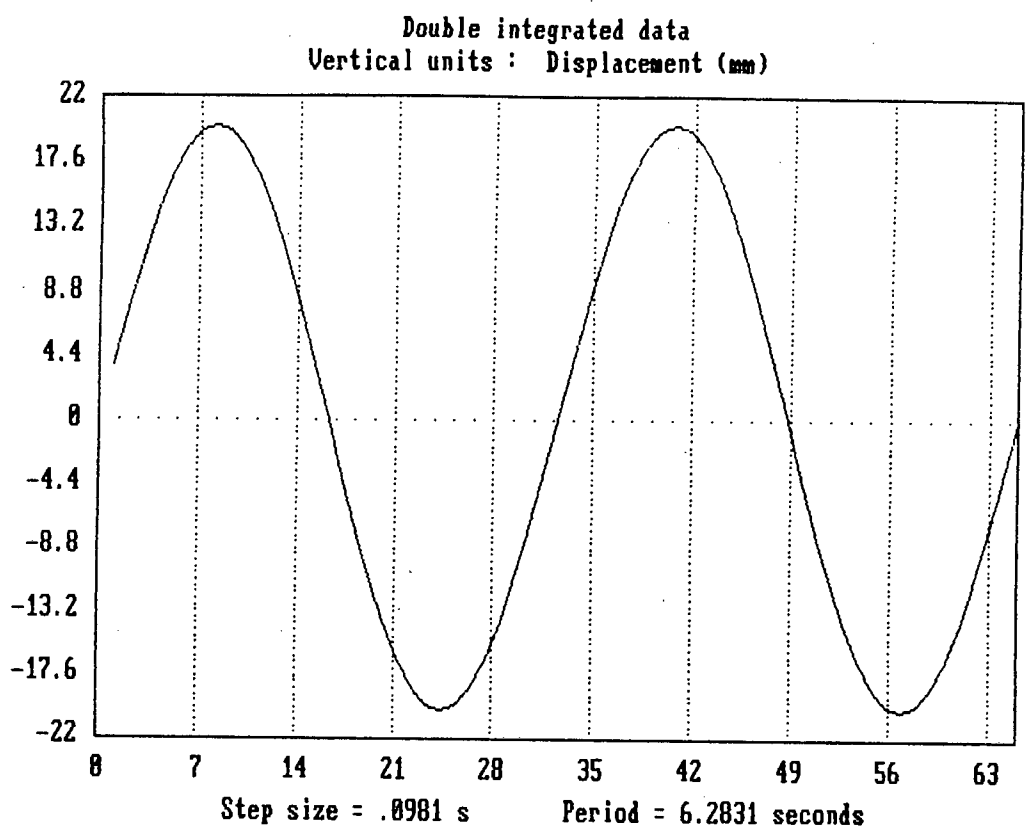


Figure I-1c

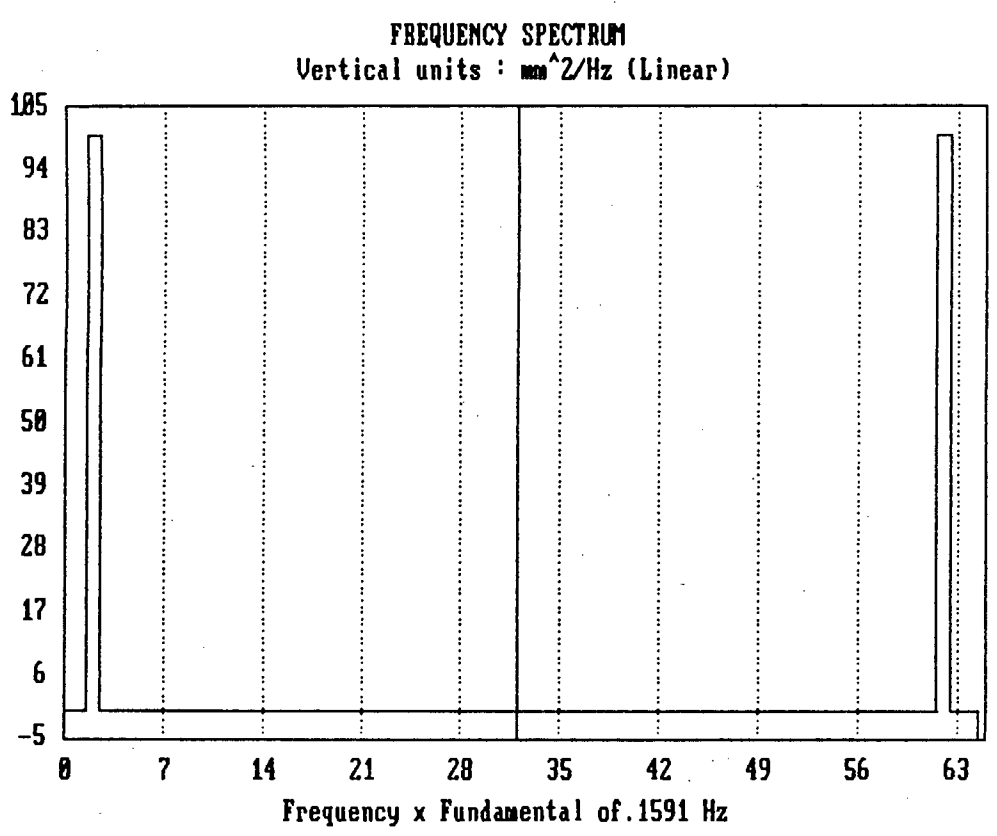


Figure I-1d

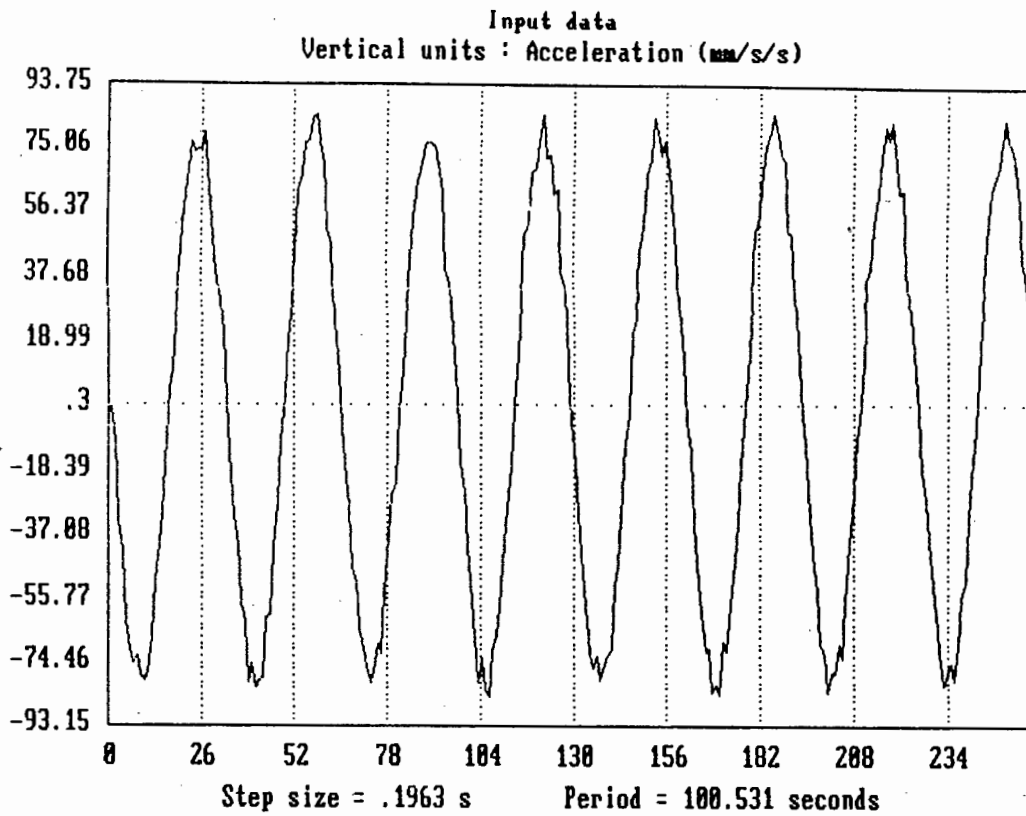


Figure I-2a Sinusoidal Acceleration with Noise

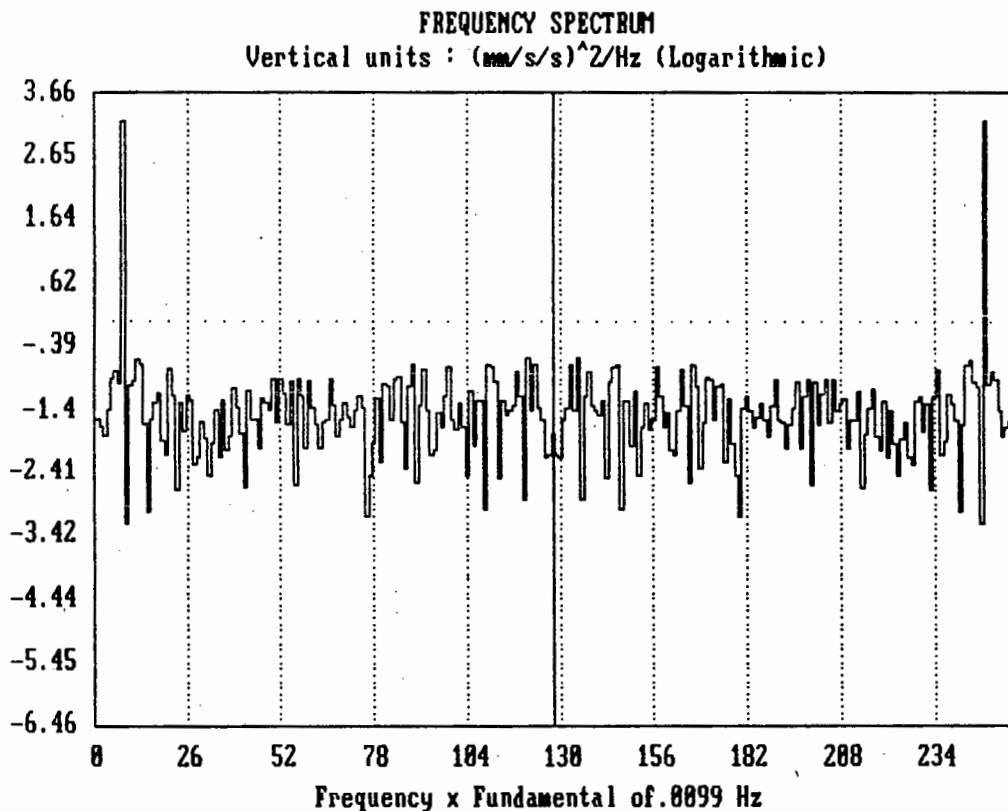


Figure I-2b

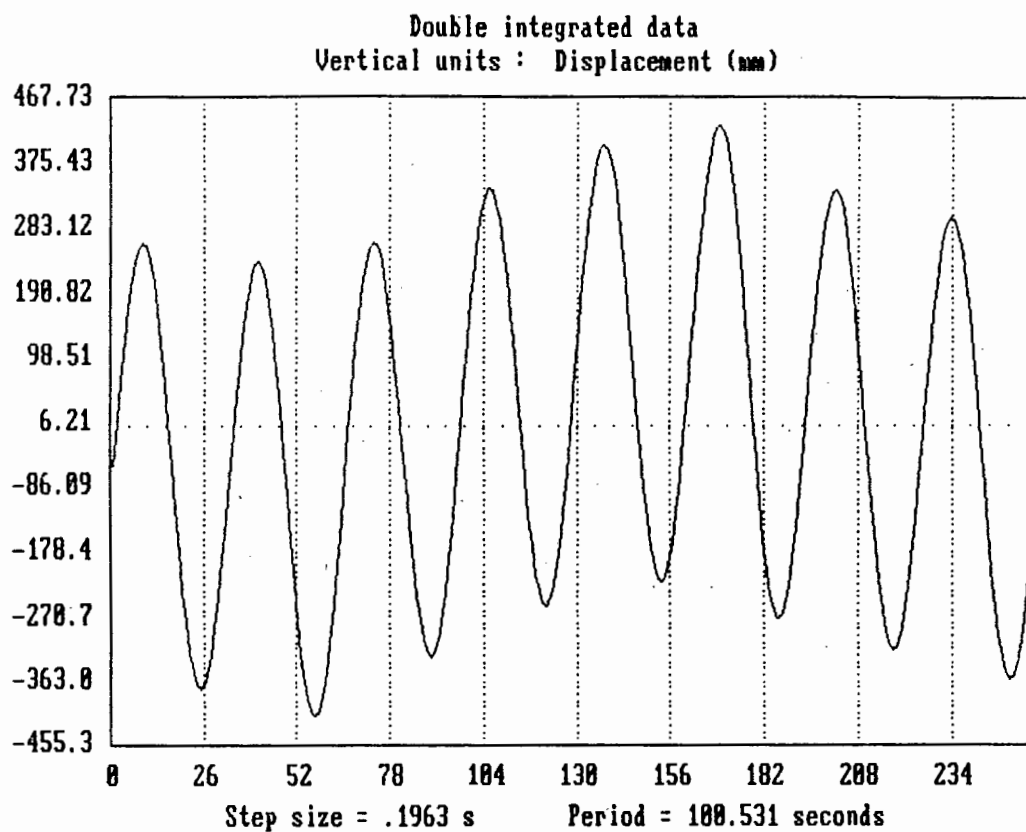


Figure I-2c

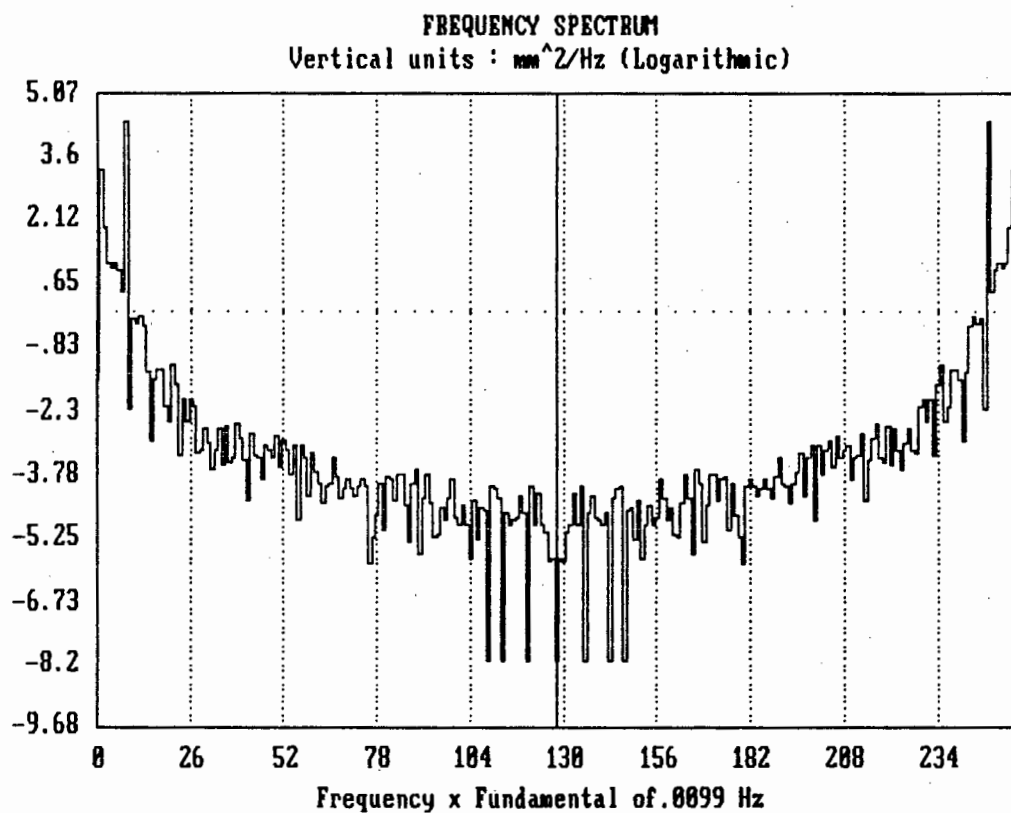


Figure I-2d

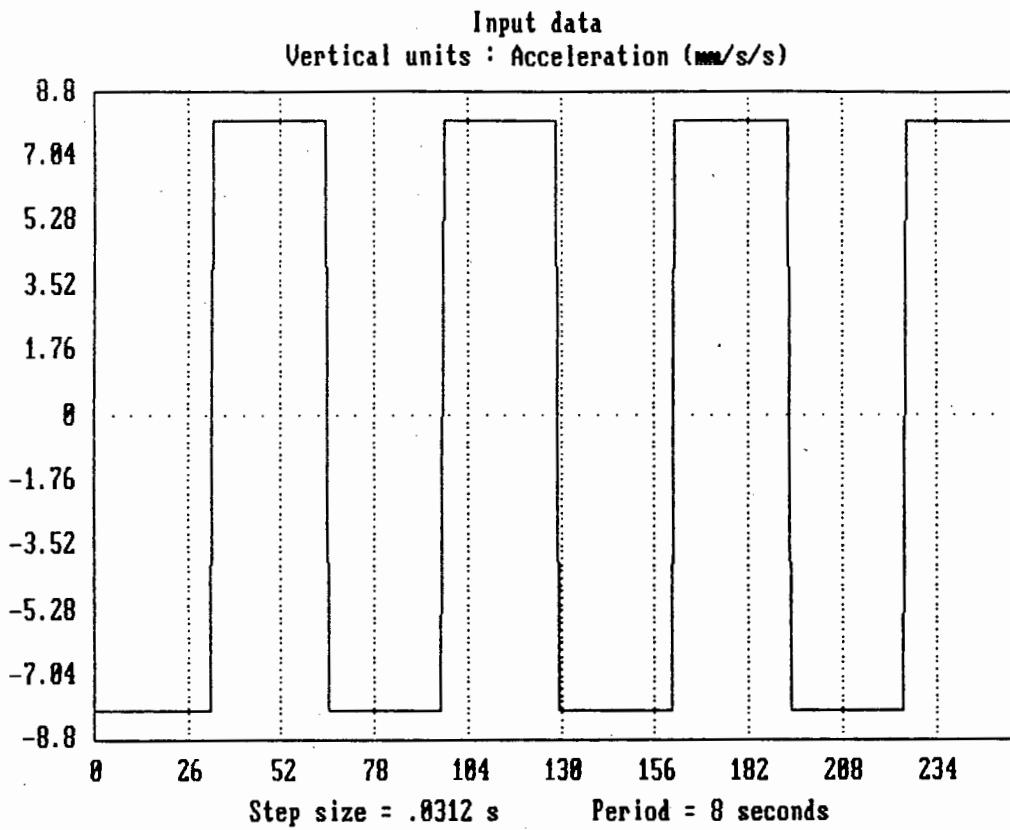


Figure I-3a Square Wave Acceleration

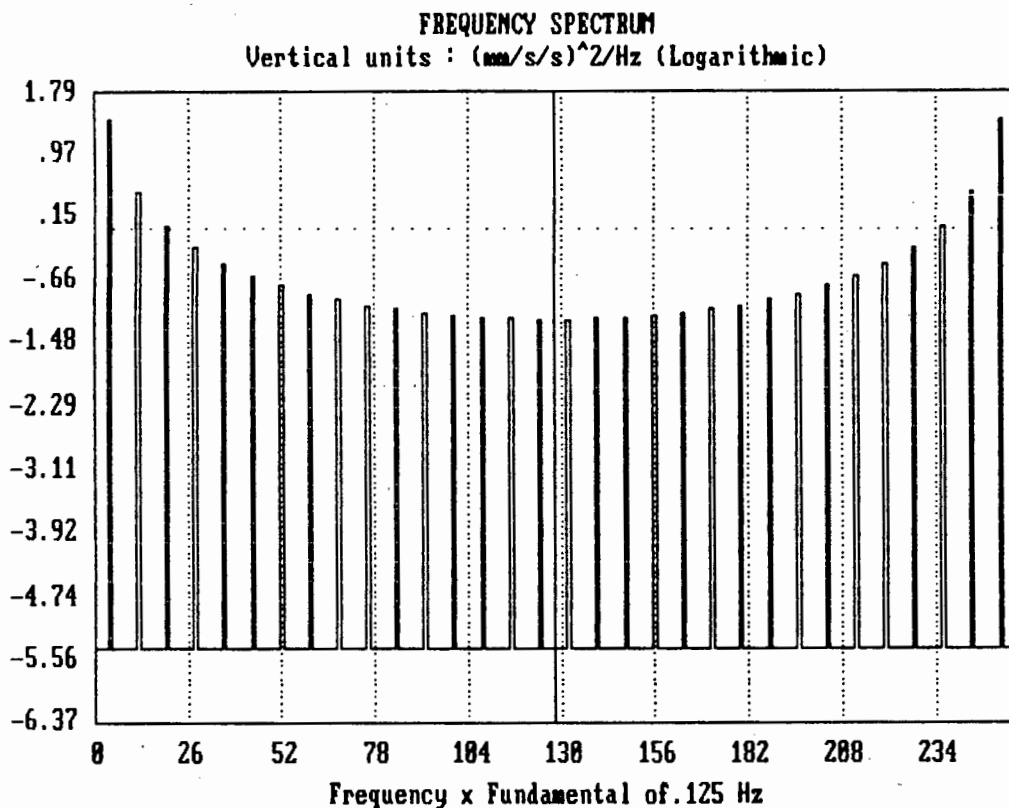


Figure I-3b



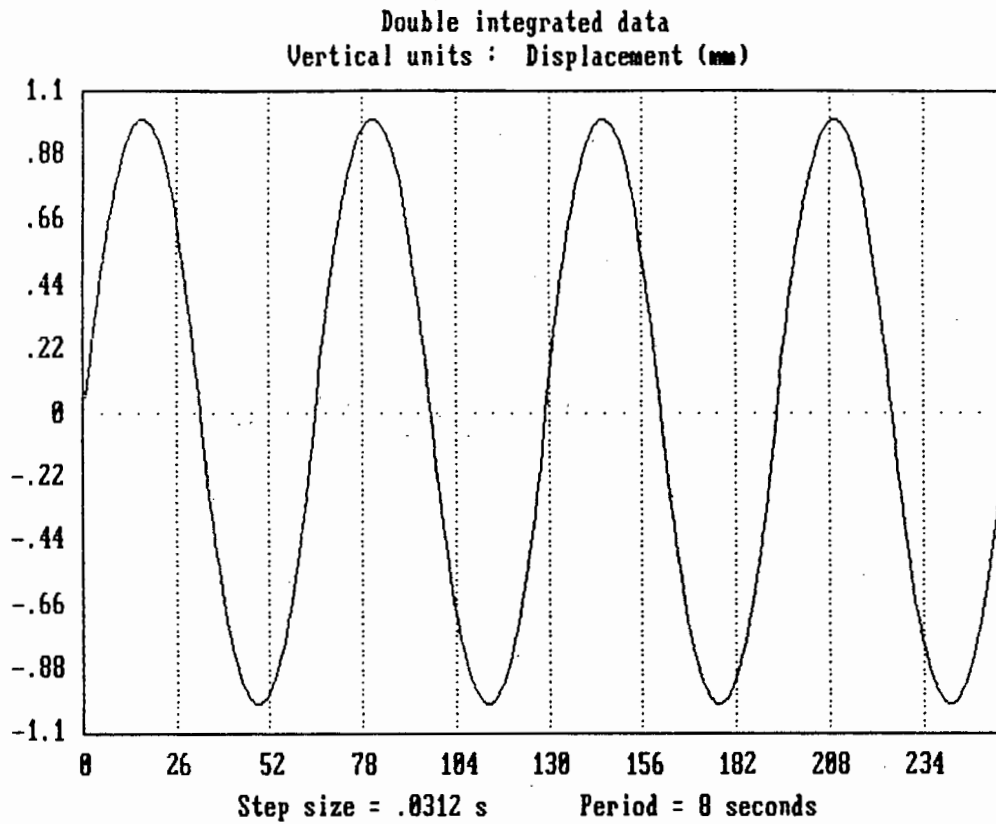


Figure I-3c

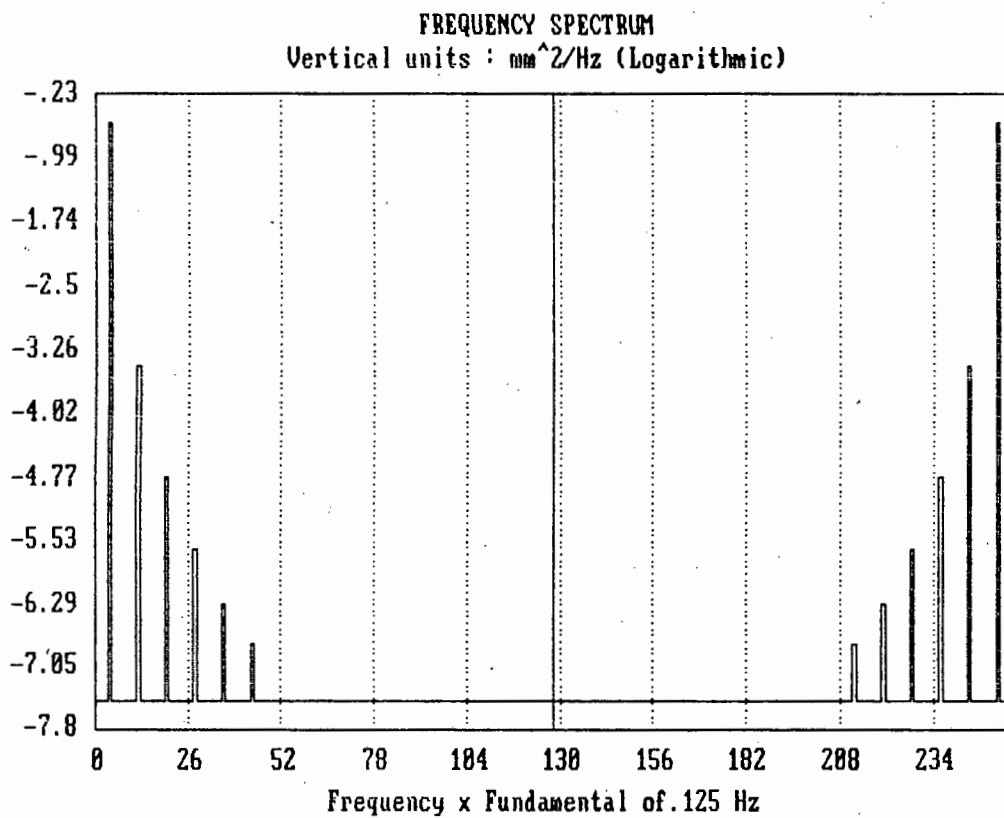


Figure I-3d

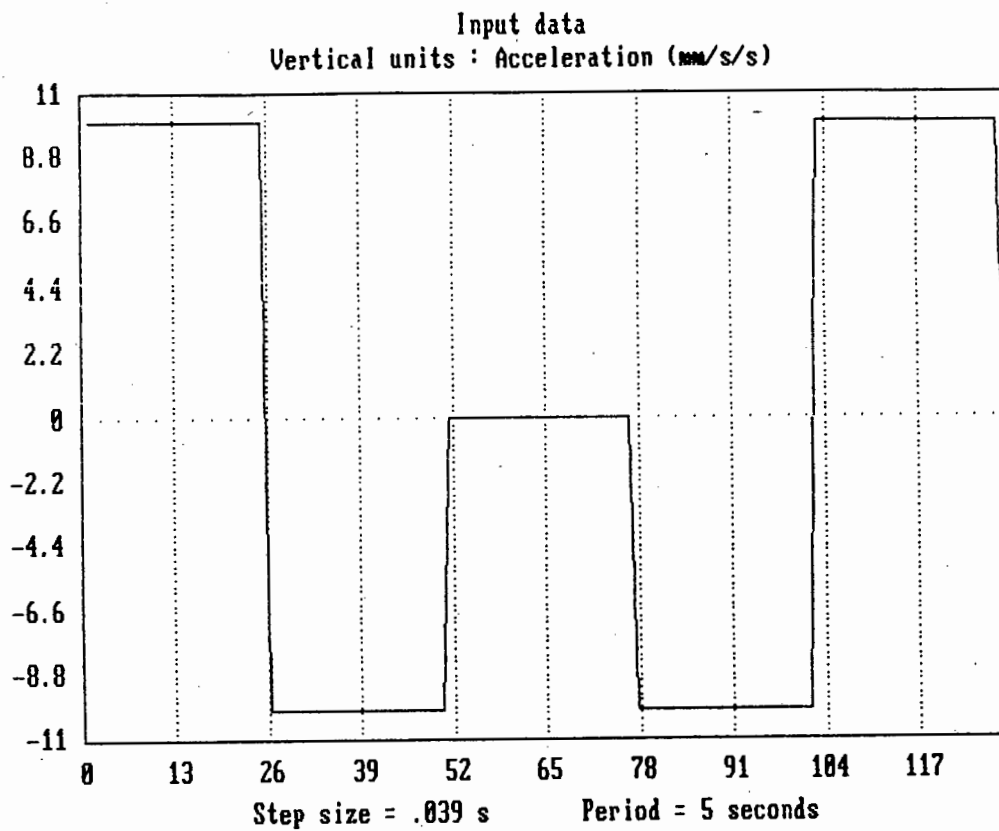


Figure I-4a Ideal Acceleration

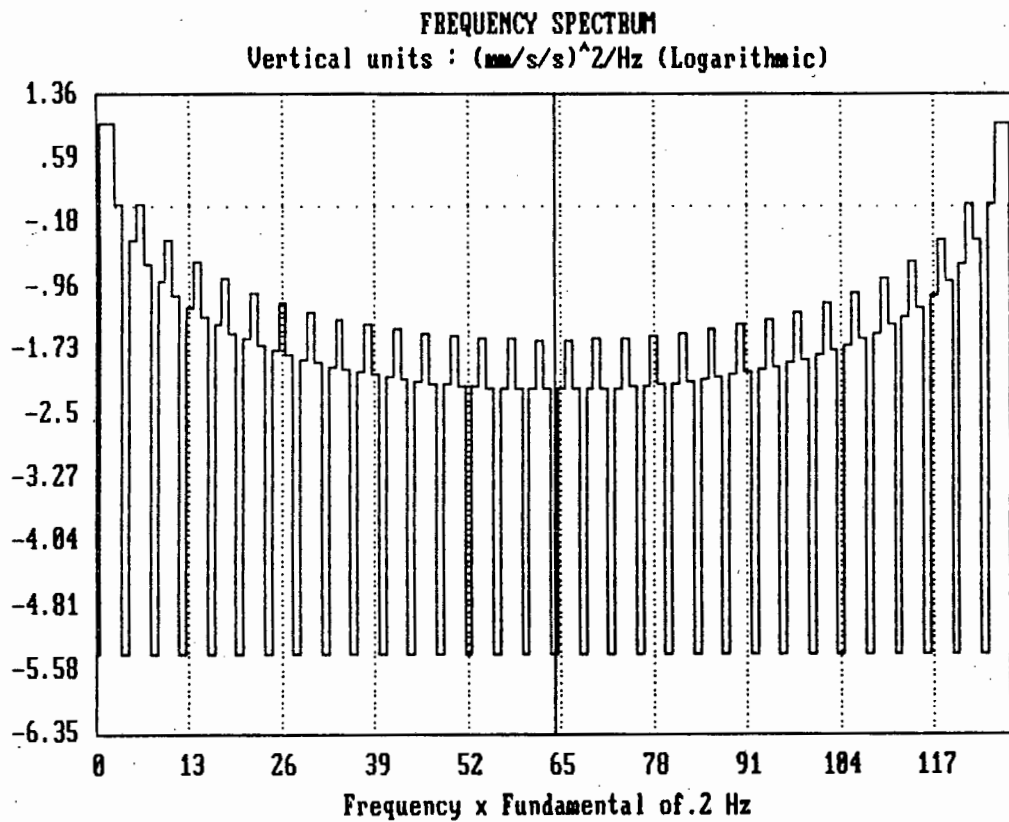


Figure I-4b

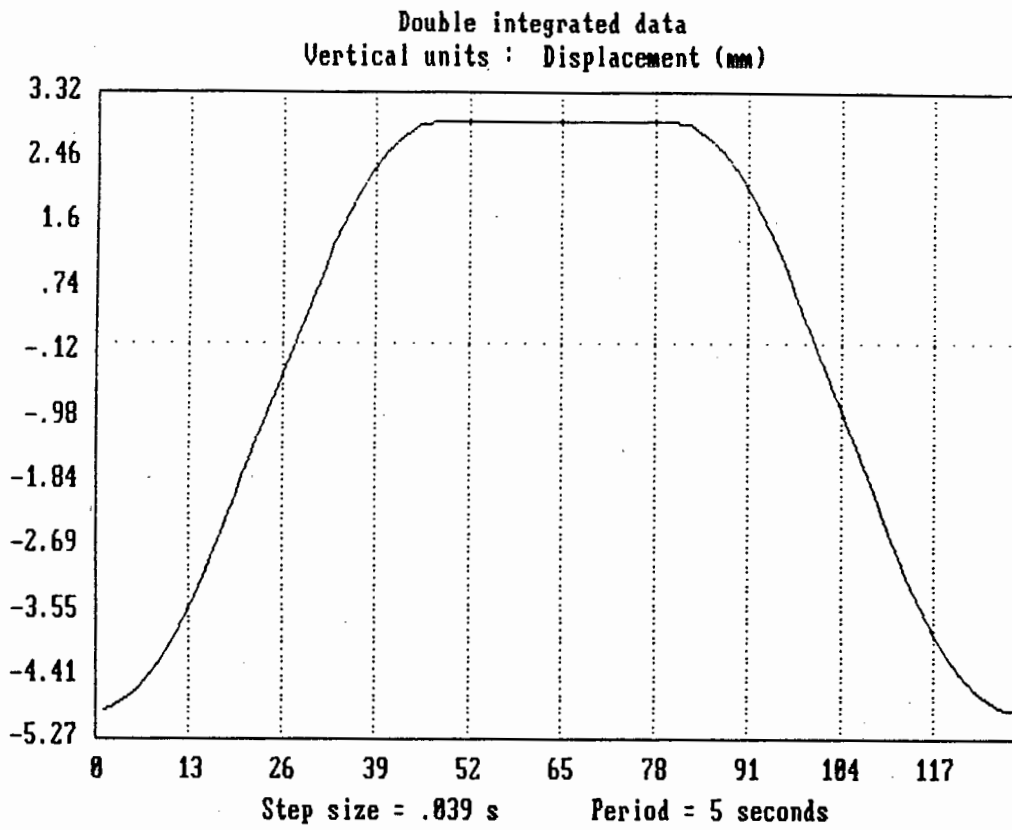


Figure I-4c

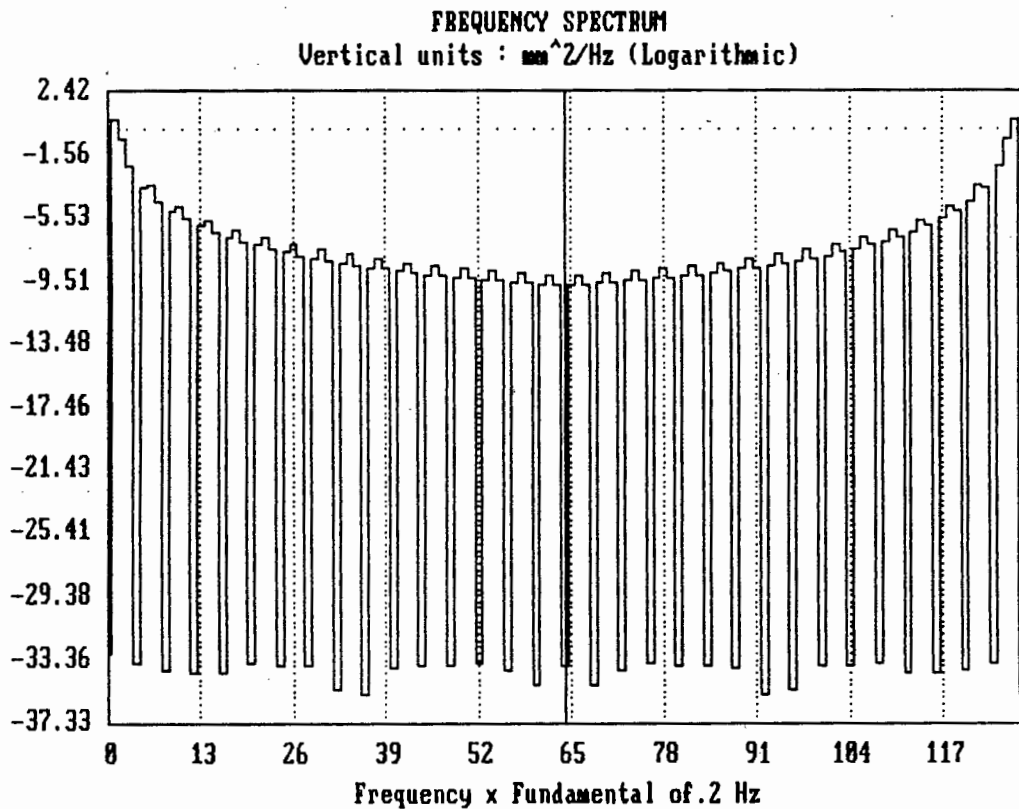


Figure I-4d

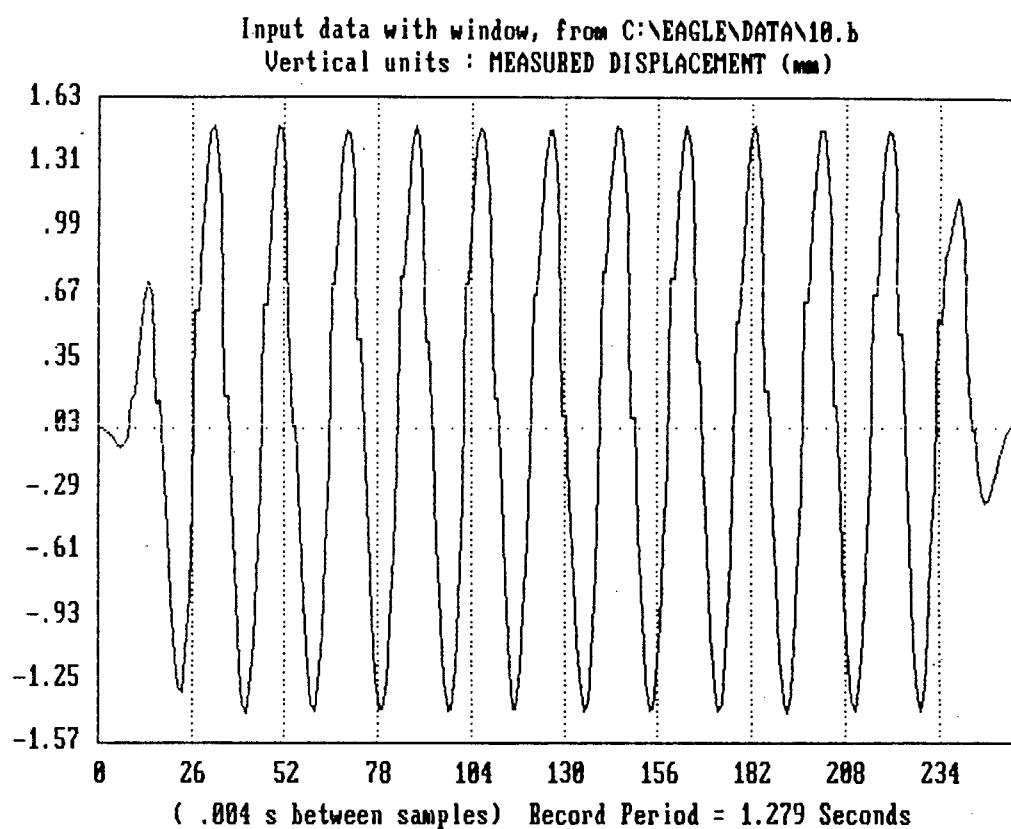


Figure I-5a LVDT Signal measuring Shaker Movement at 10Hz

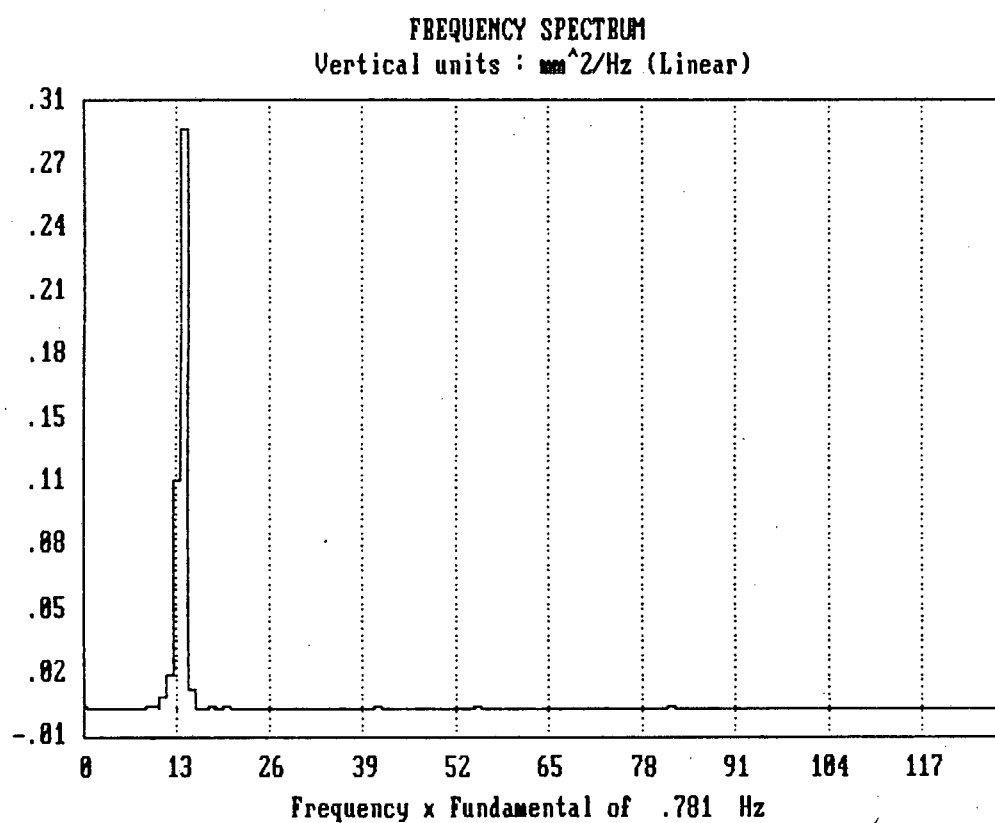


Figure I-5b

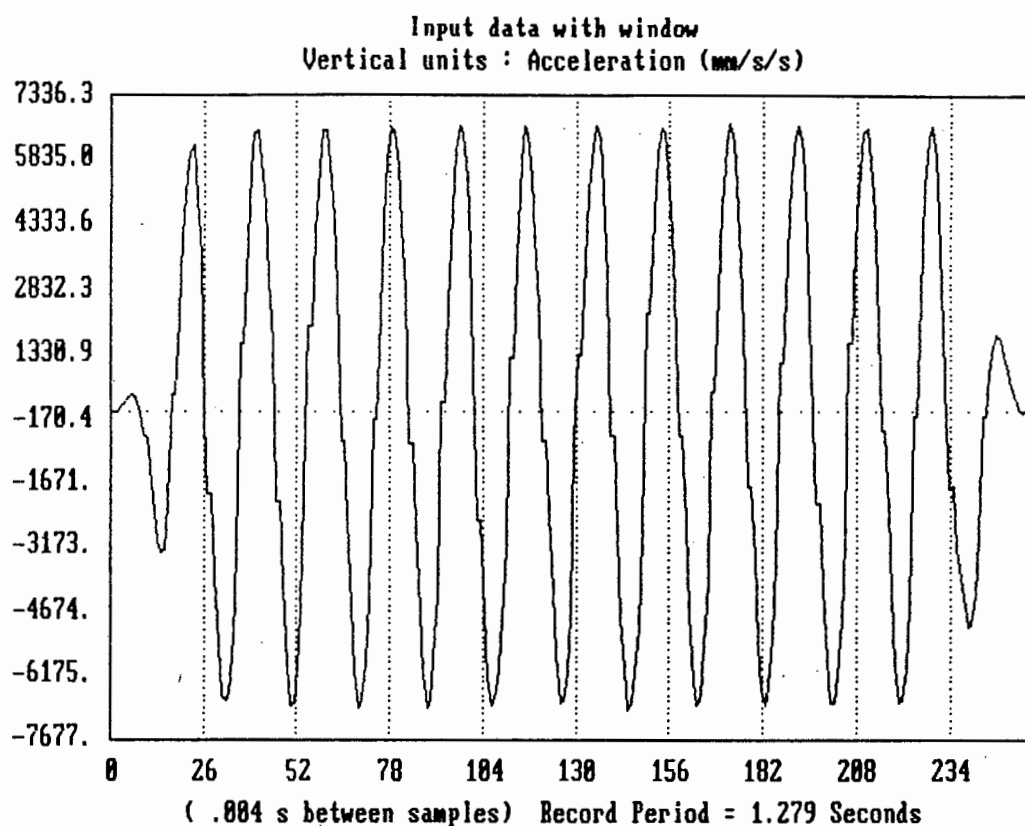


Figure I-5c Accelerometer Signal measuring Shaker Movement

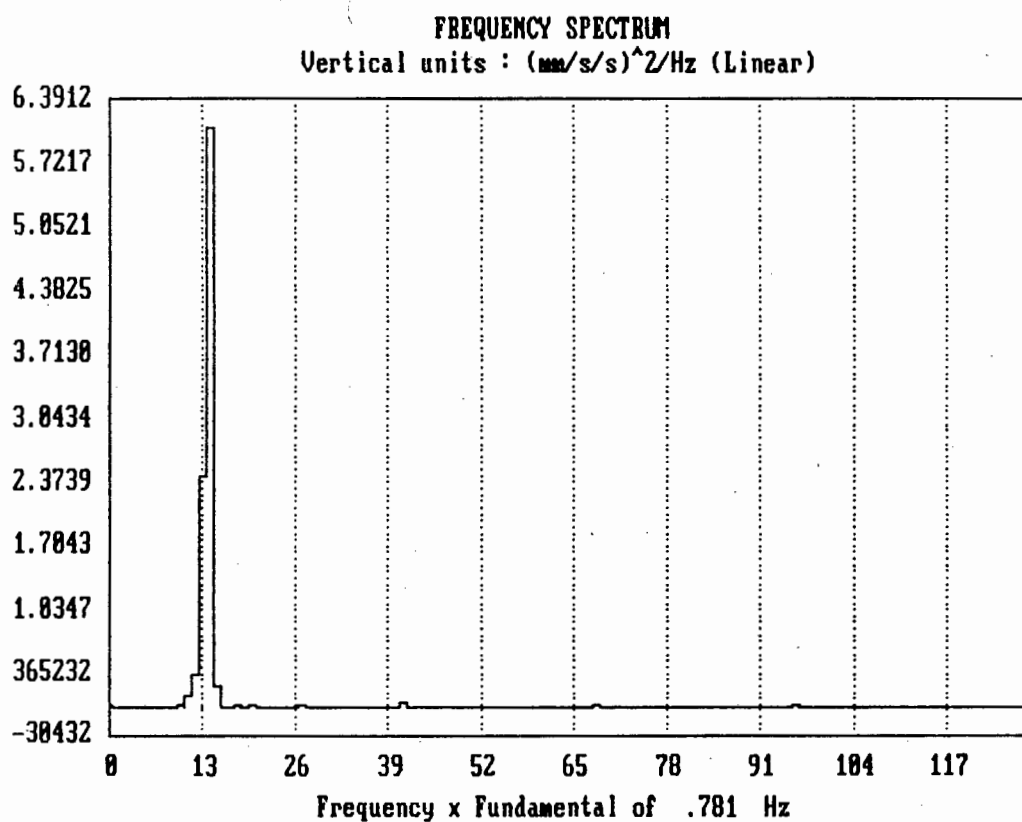


Figure I-5d

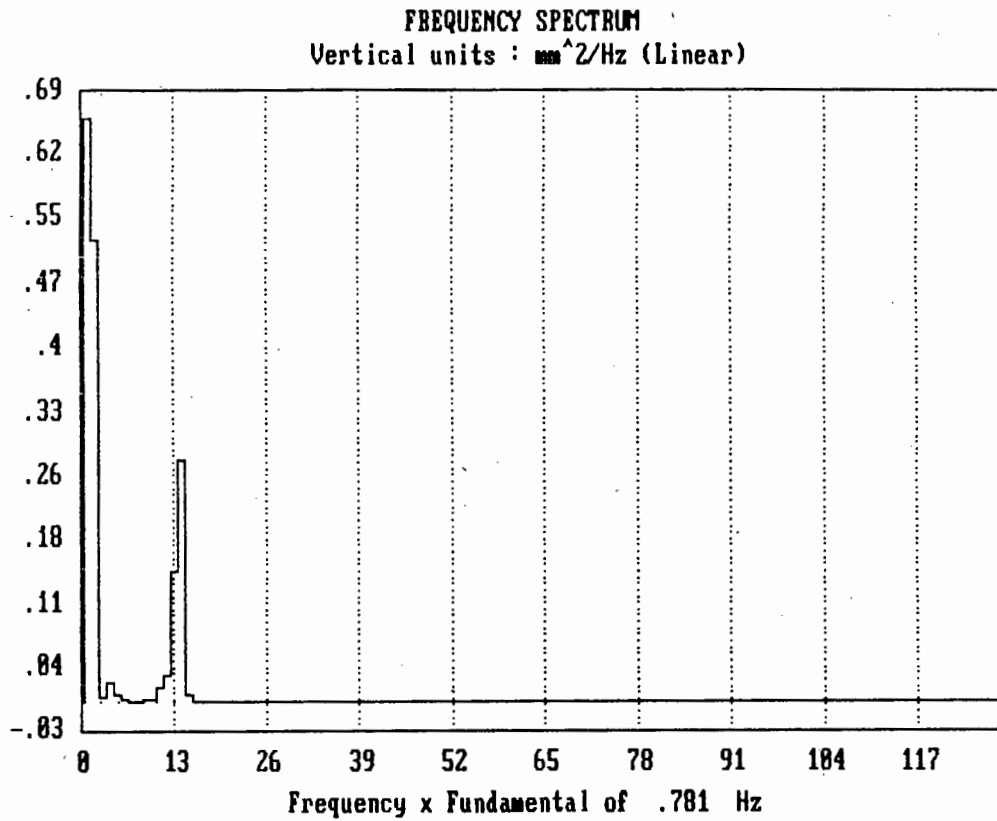


Figure I-5e

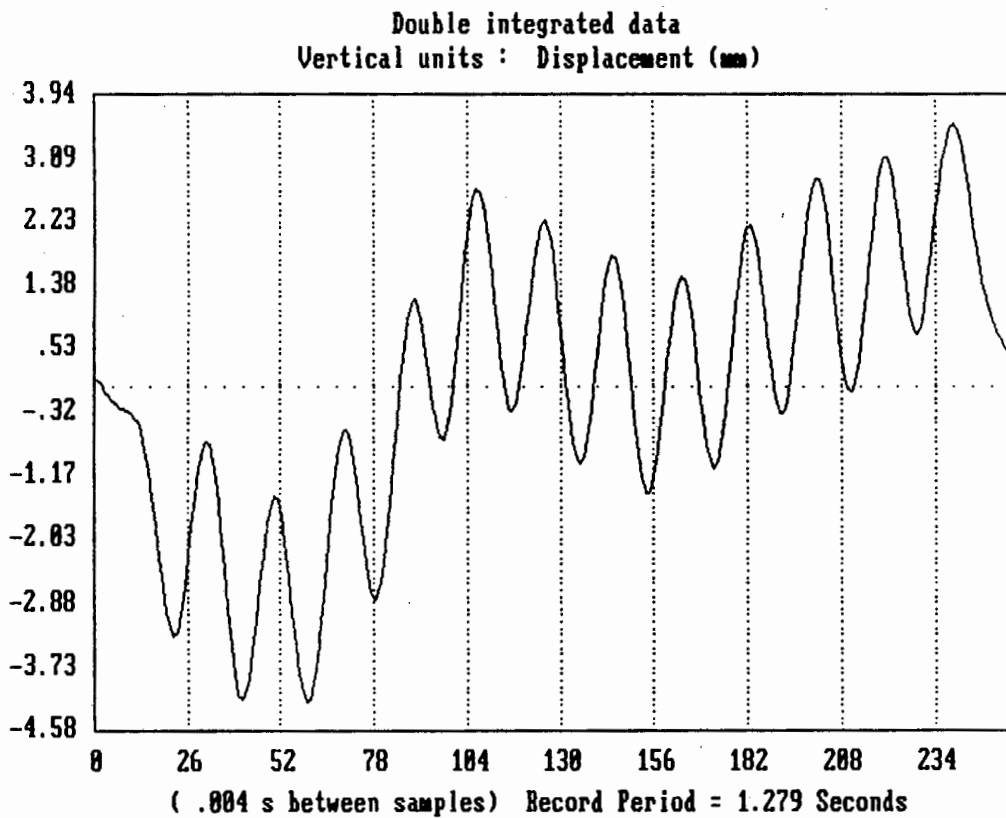


Figure I-5f

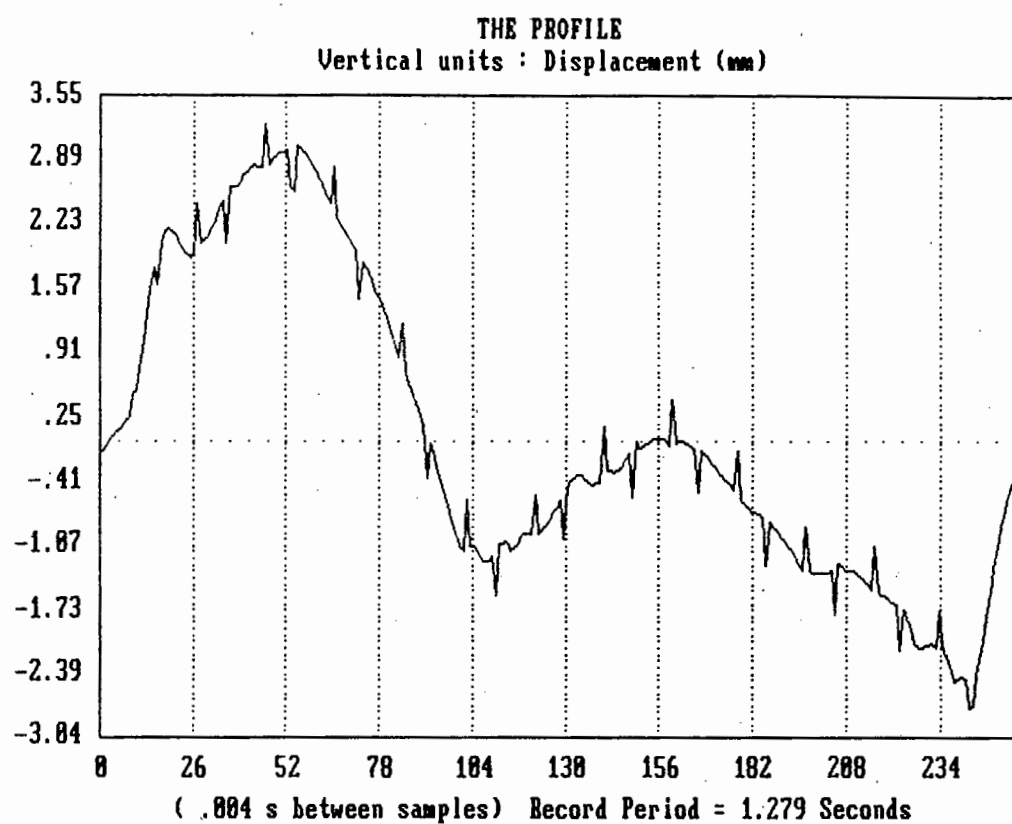


Figure I-5g

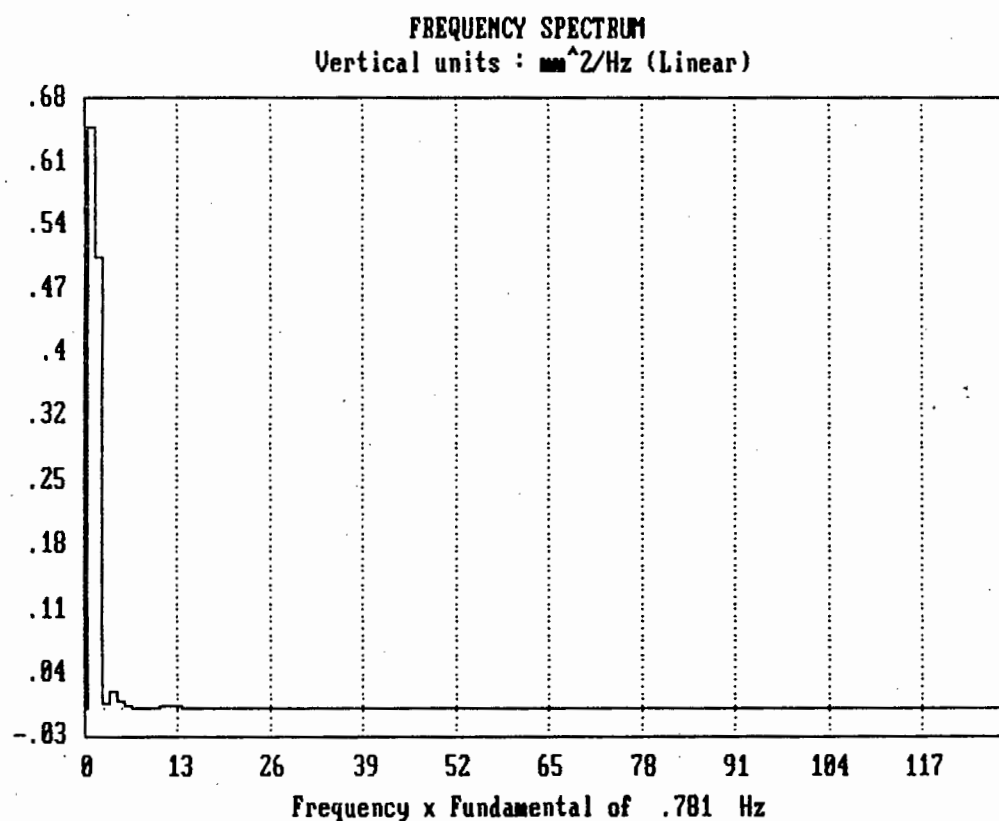


Figure I-5h

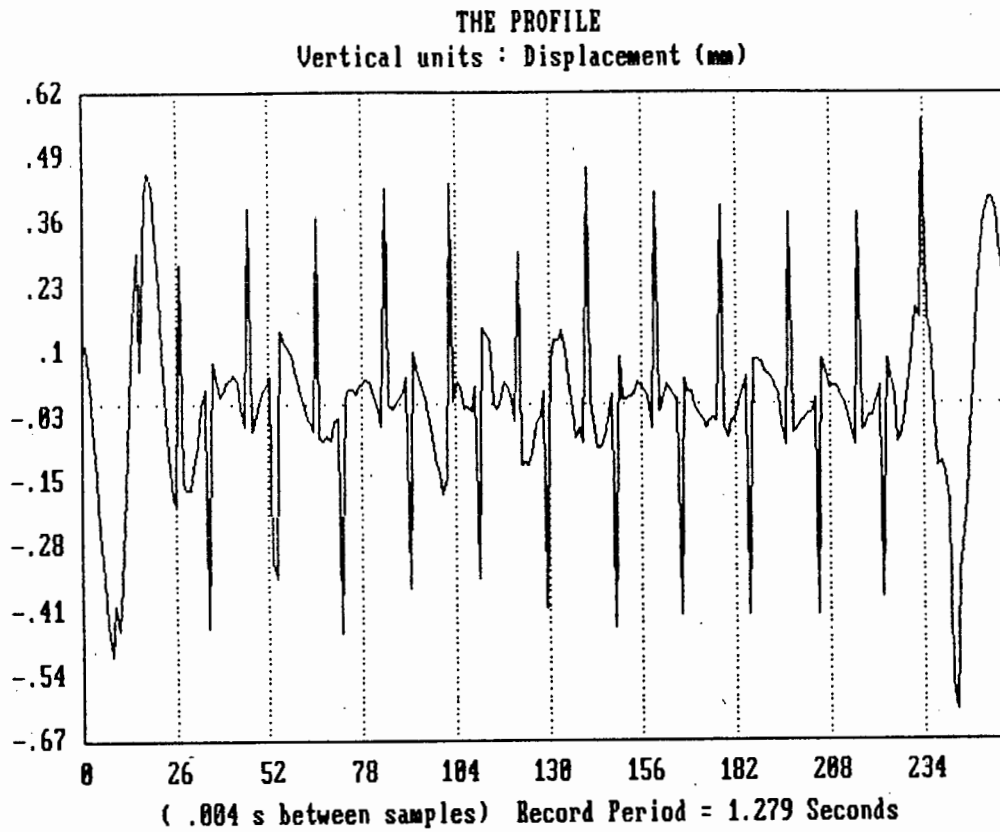


Figure I-5j

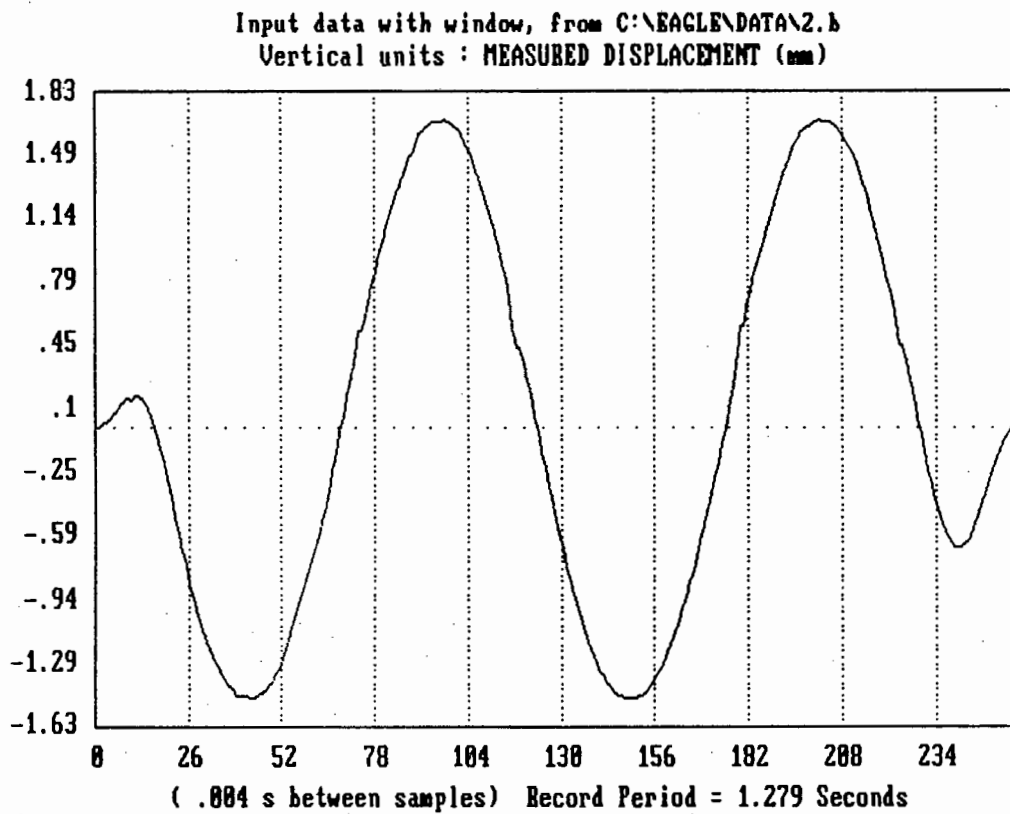


Figure I-6a LVDT Signal measuring Shaker Movement at 2Hz



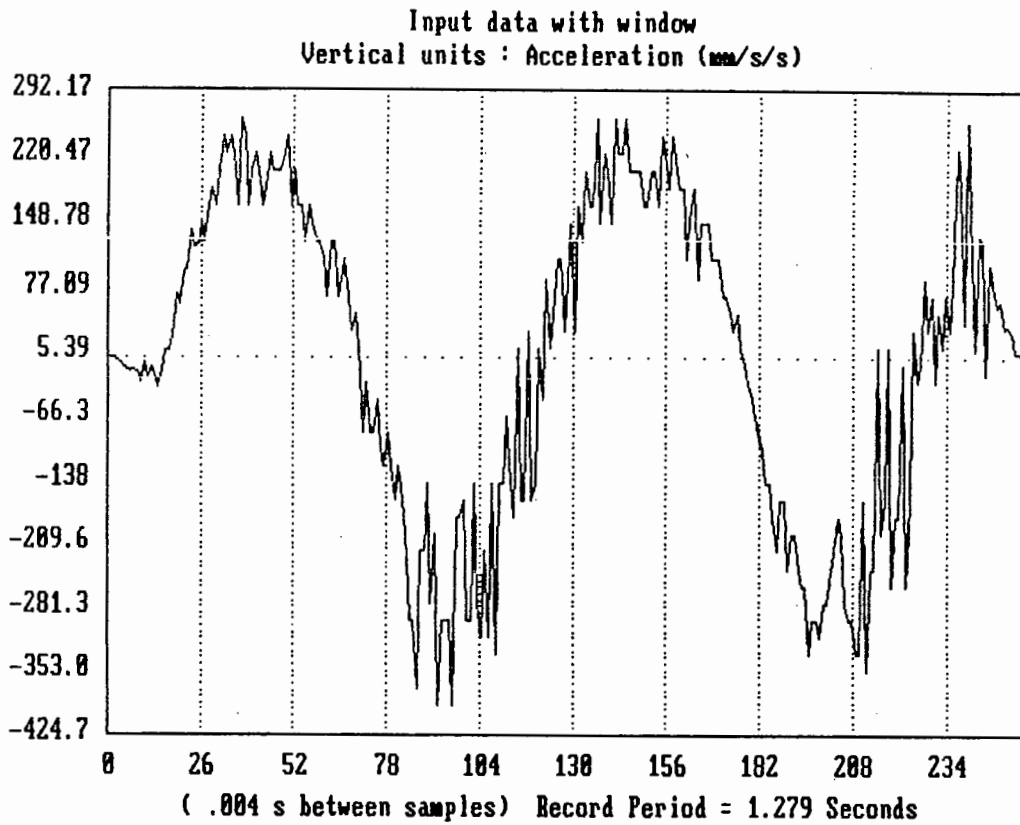


Figure I-6b Accelerometer Signal measuring Shaker Movement

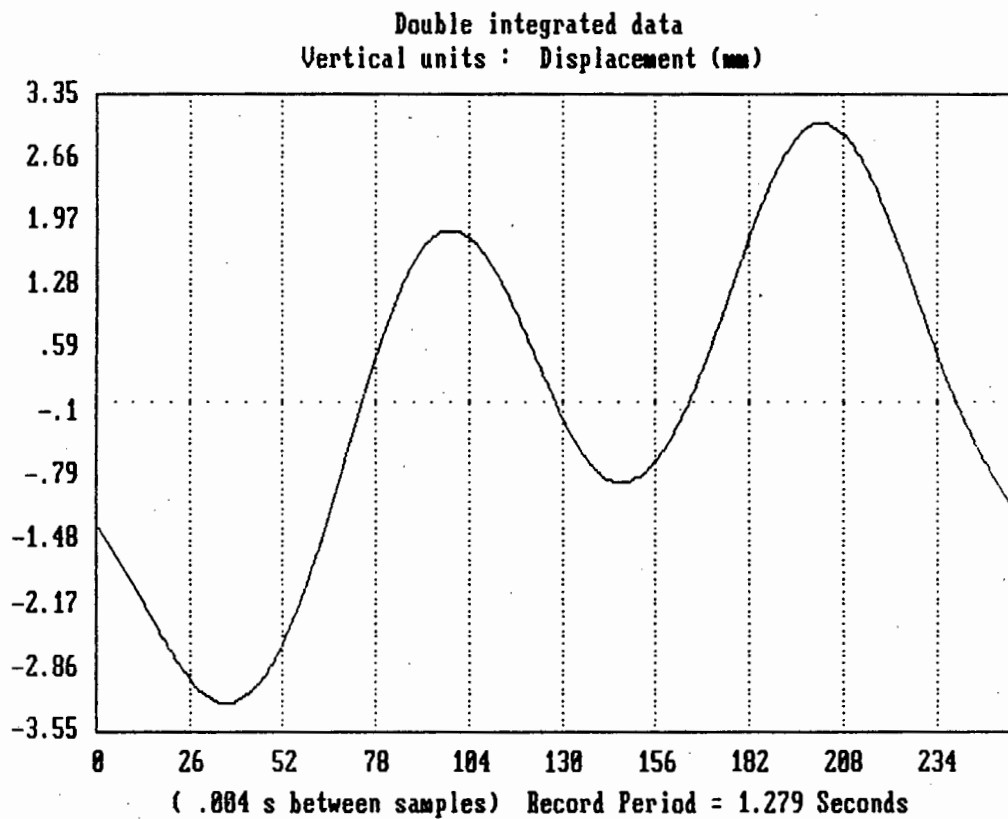


Figure I-6c

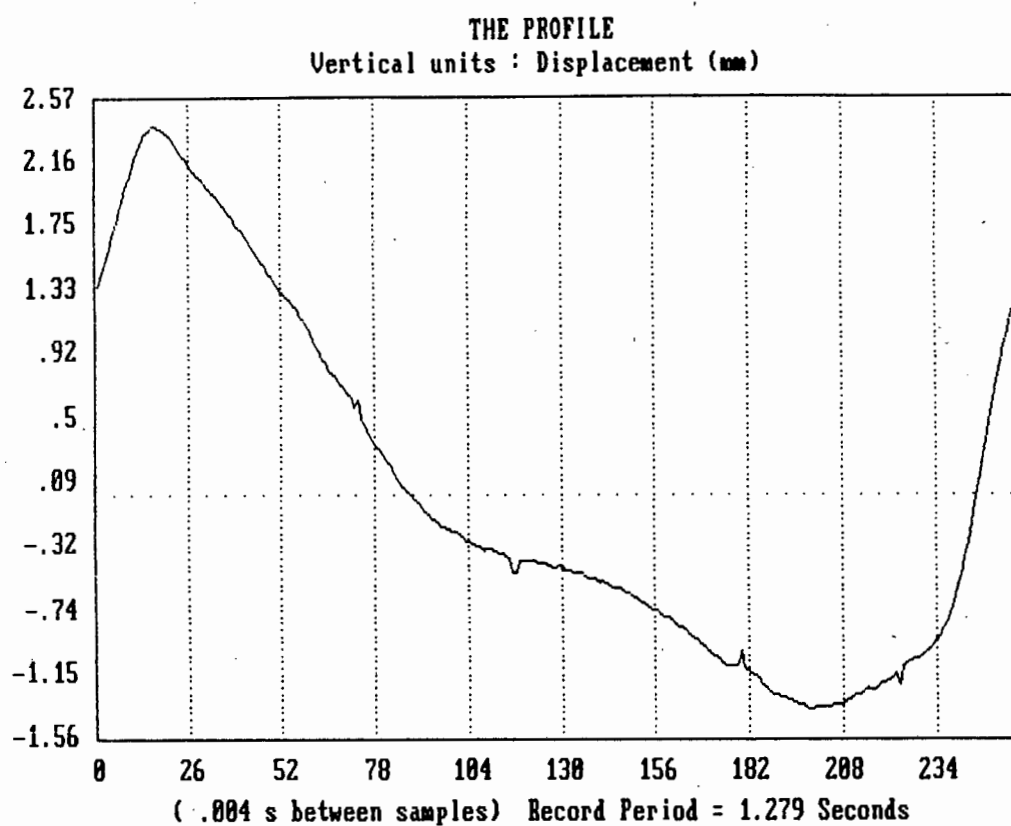


Figure I-6d

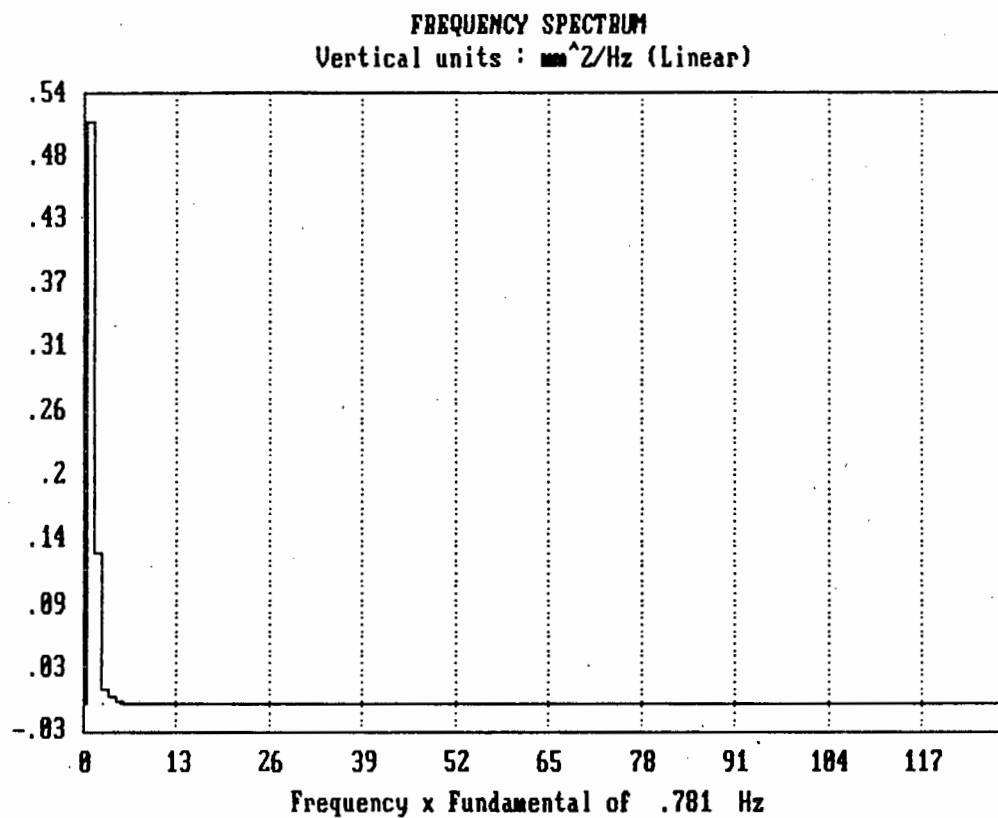


Figure I-6e

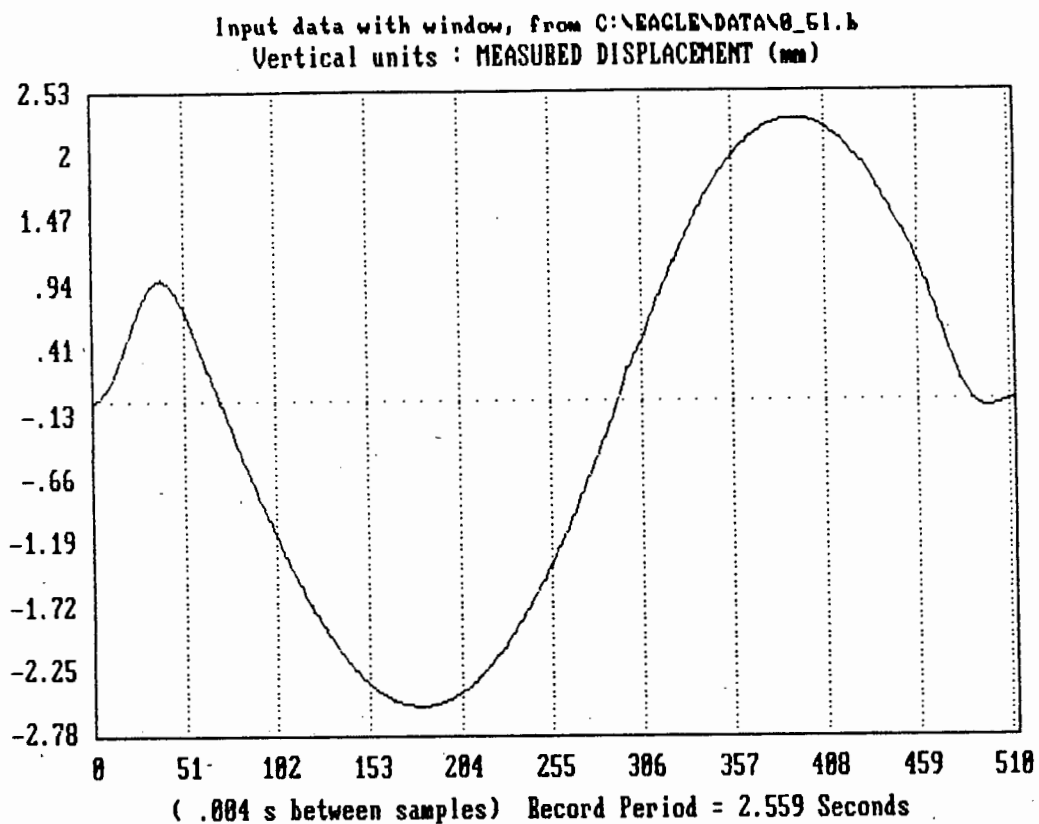


Figure I-7a LVDT measuring Shaker Movement at 0.5Hz

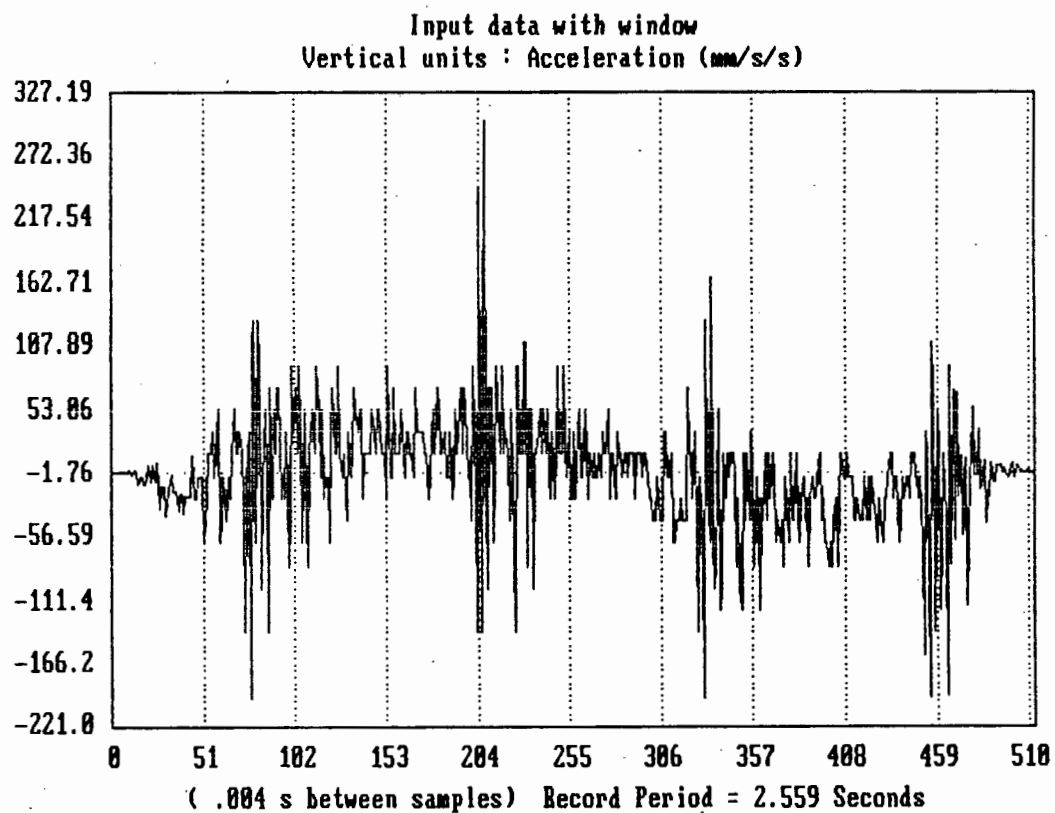


Figure I-7b Accelerometer Signal measuring Shaker Movement

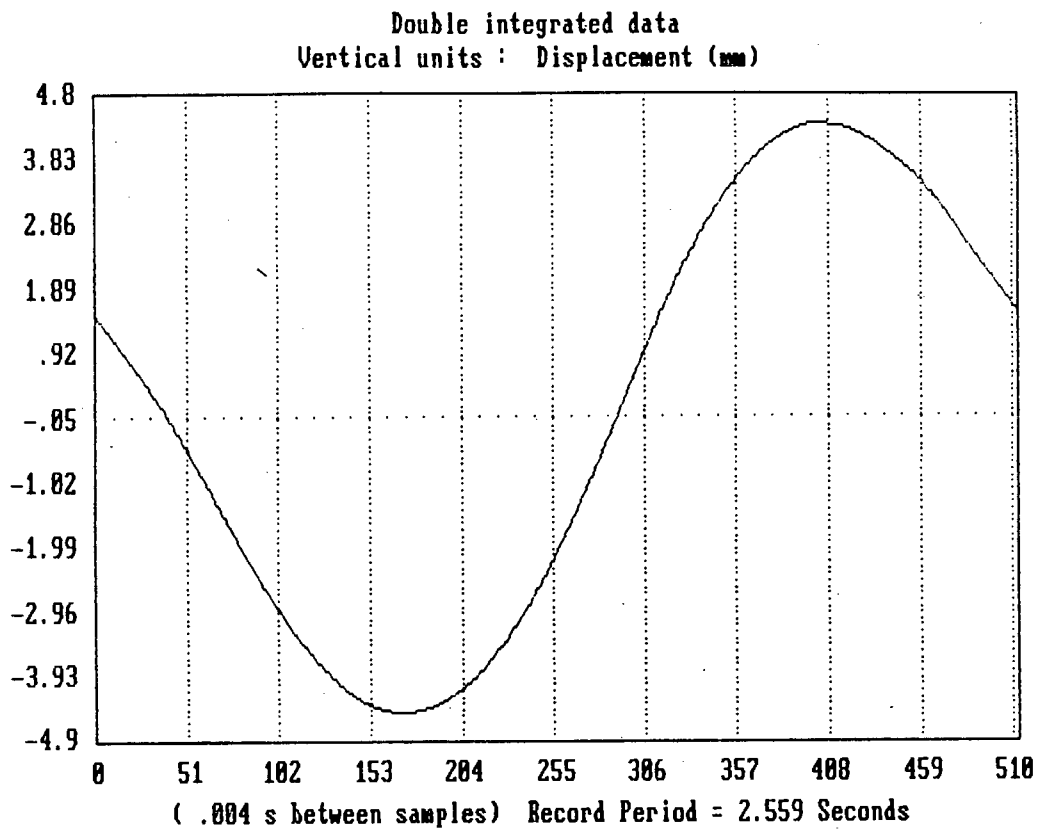


Figure I-7c

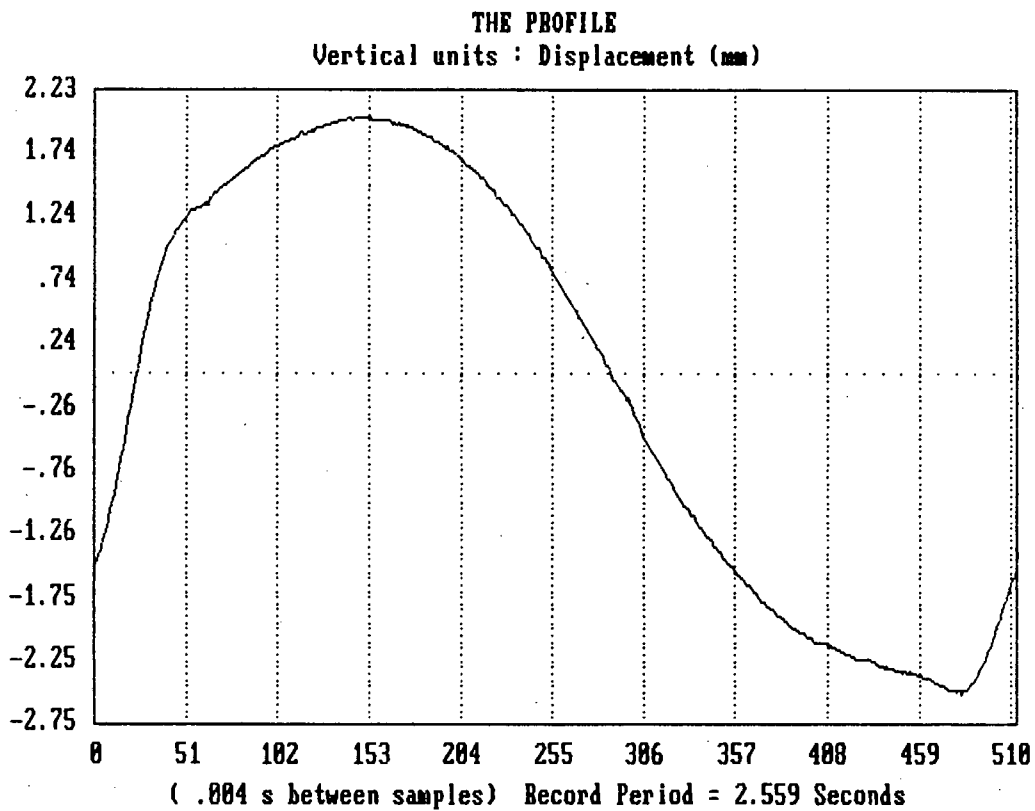


Figure I-7d

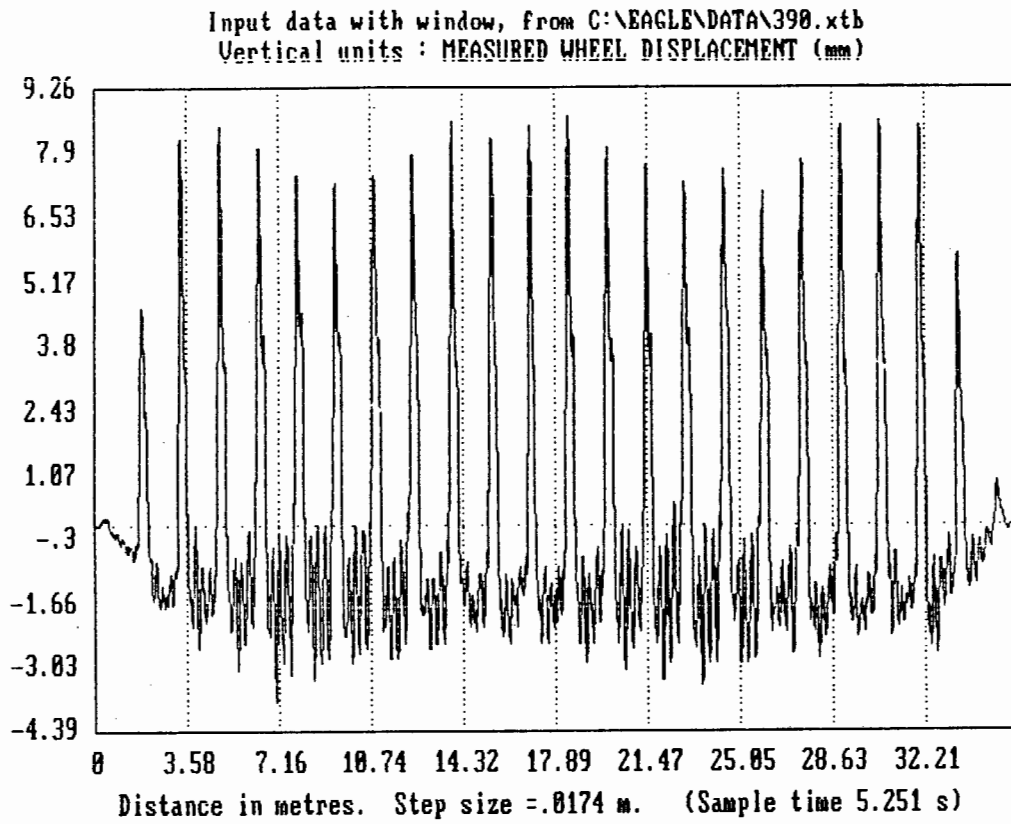


Figure I-8a Measurement on the Drum with an Obstruction on it

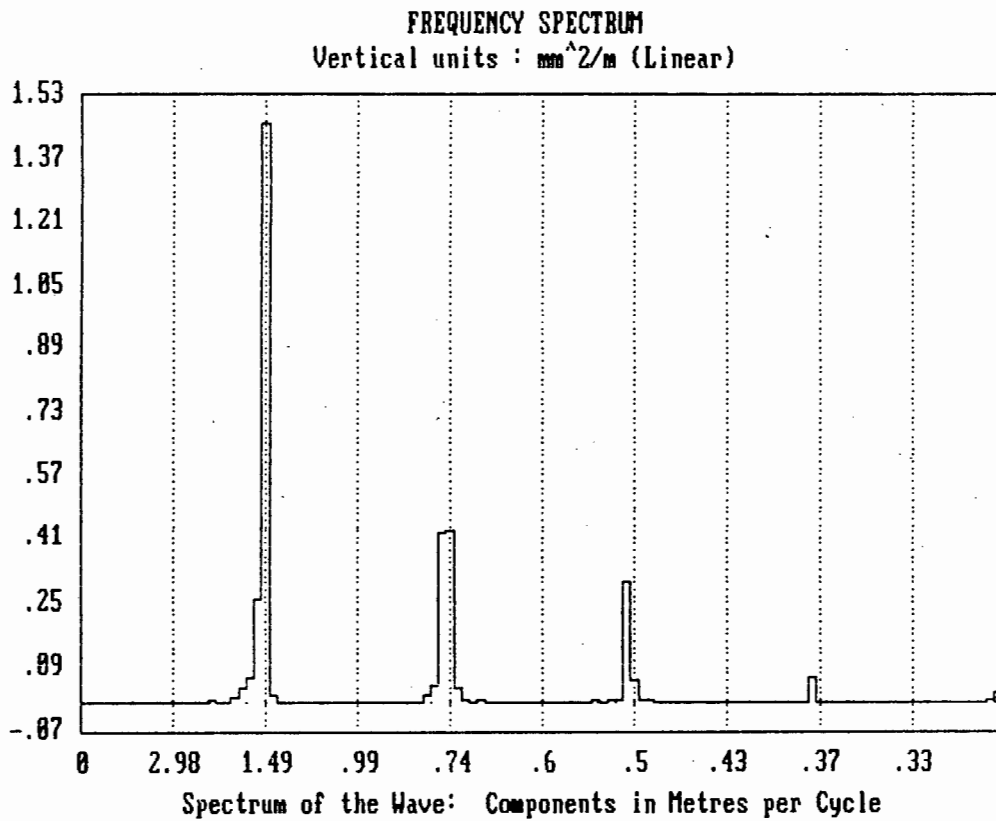


Figure I-8b

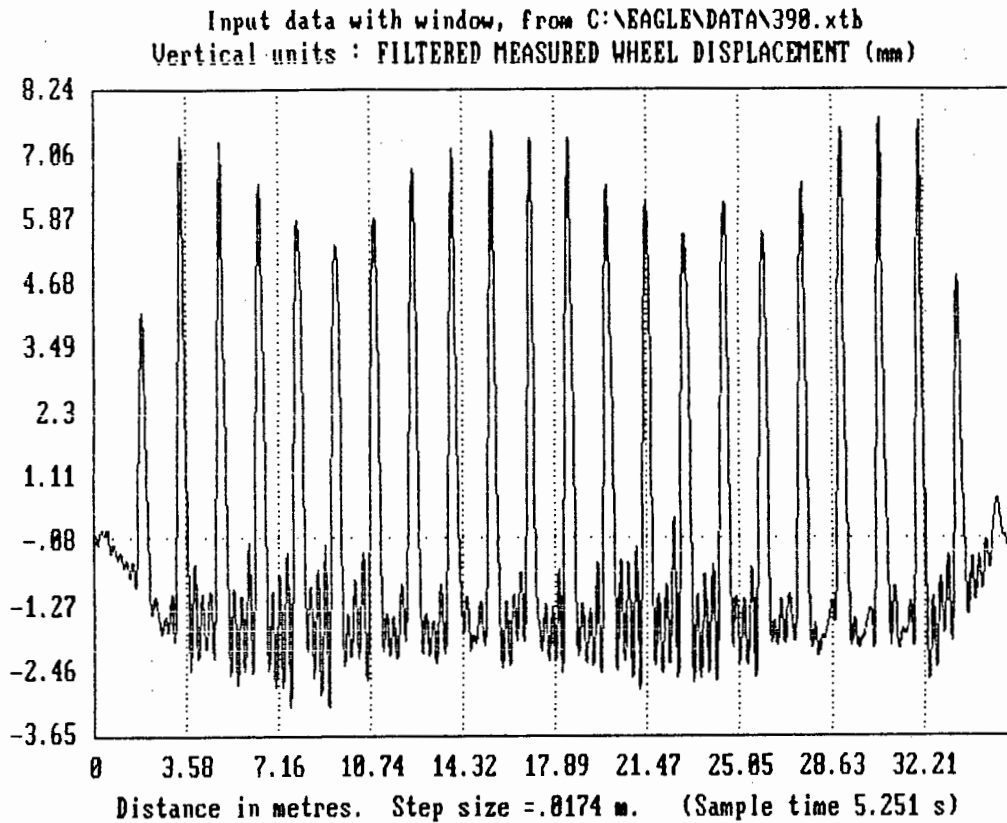


Figure I-8c

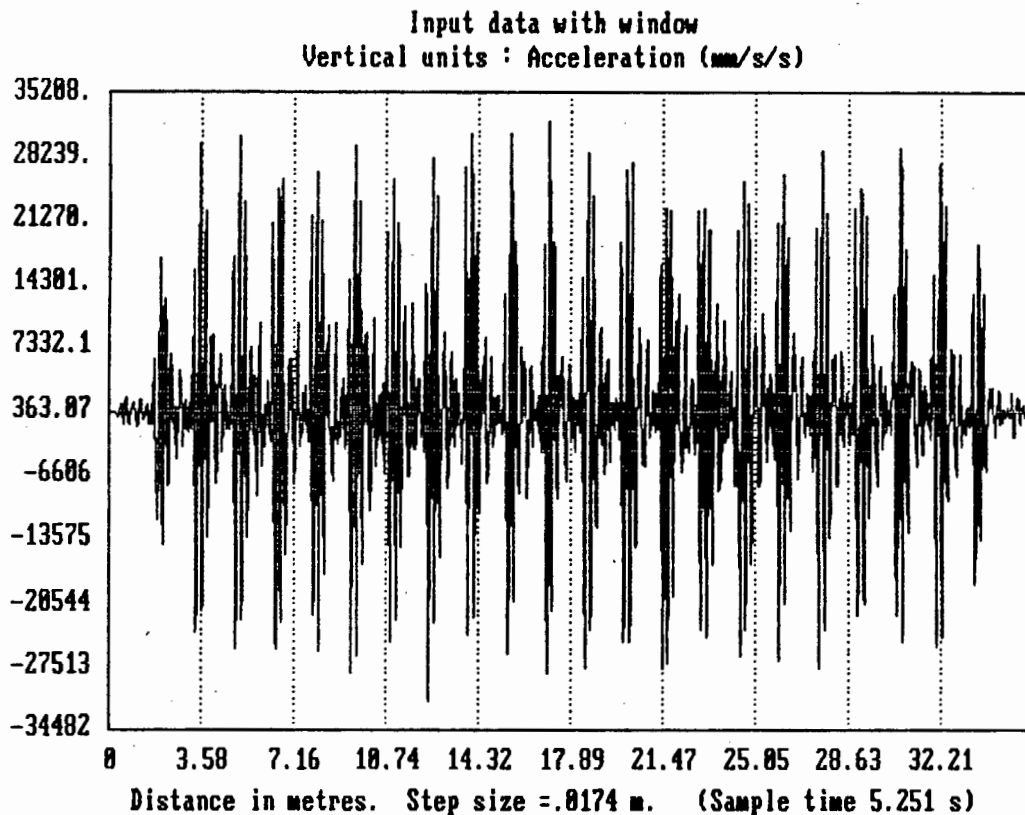


Figure I-8d

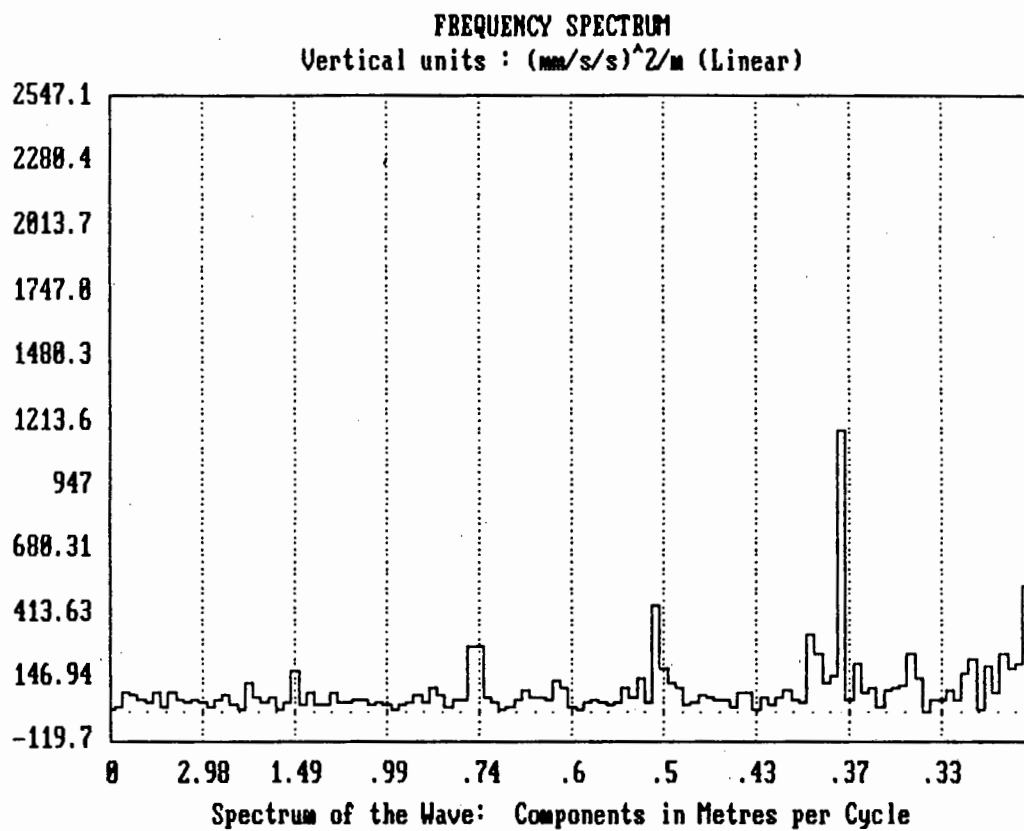


Figure I-8e

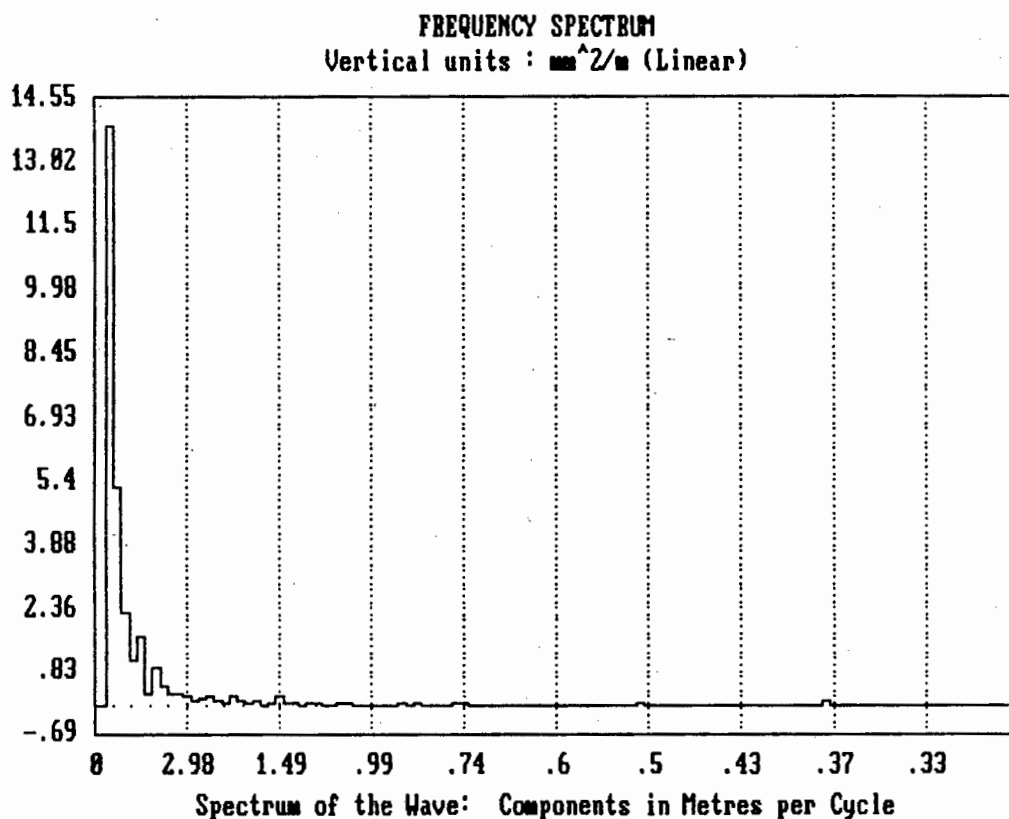


Figure I-8f

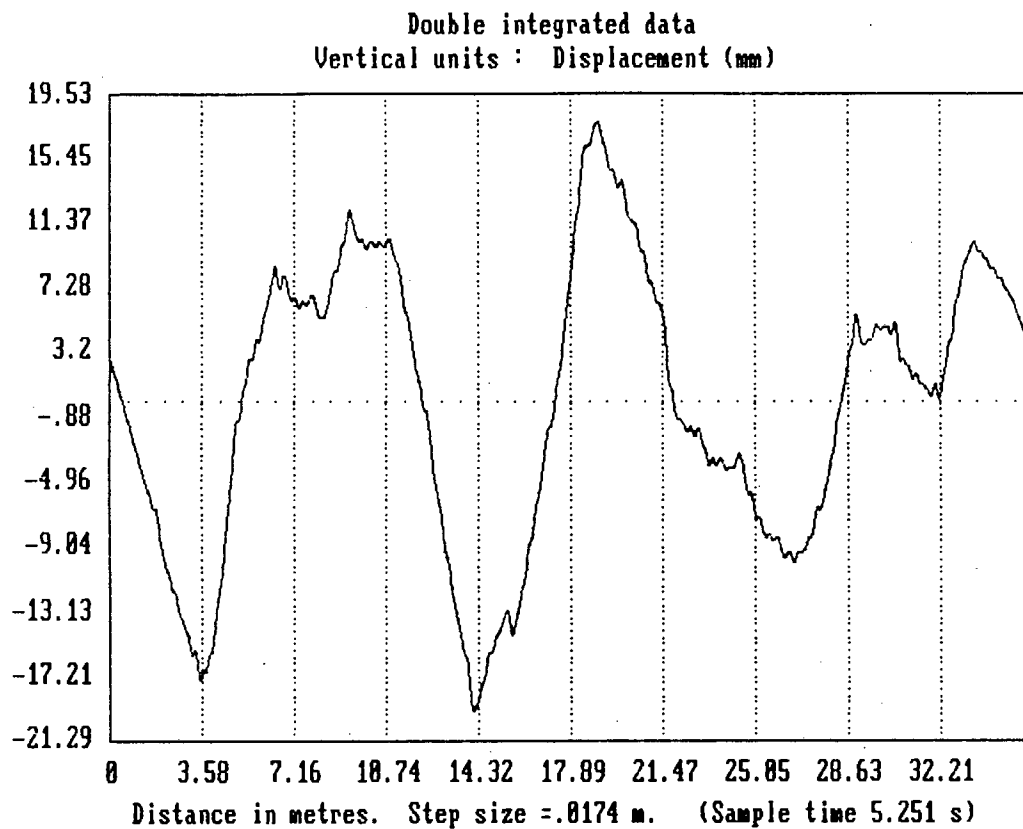


Figure I-8g

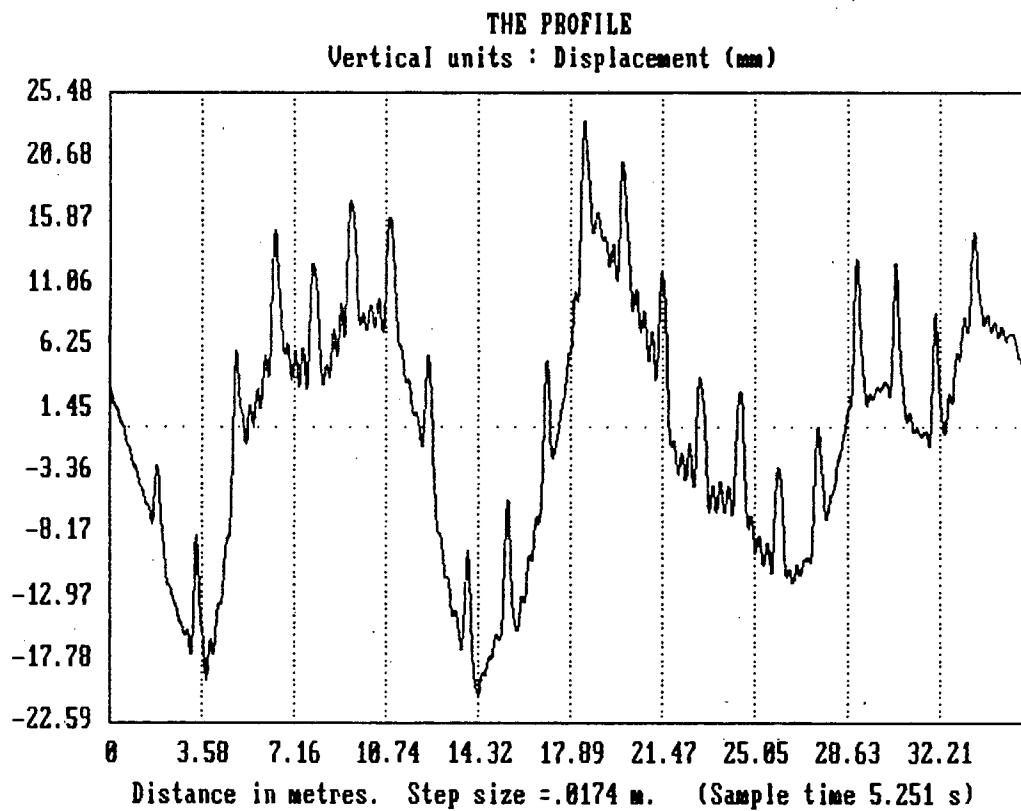


Figure I-8h



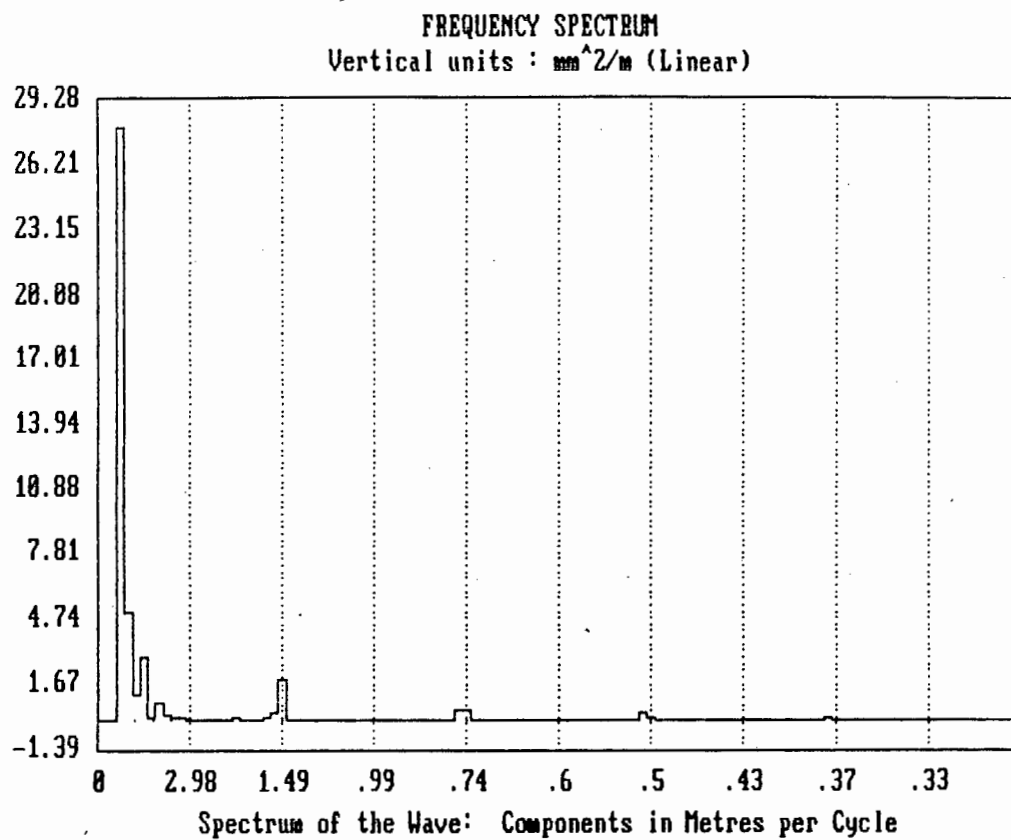


Figure I-8i

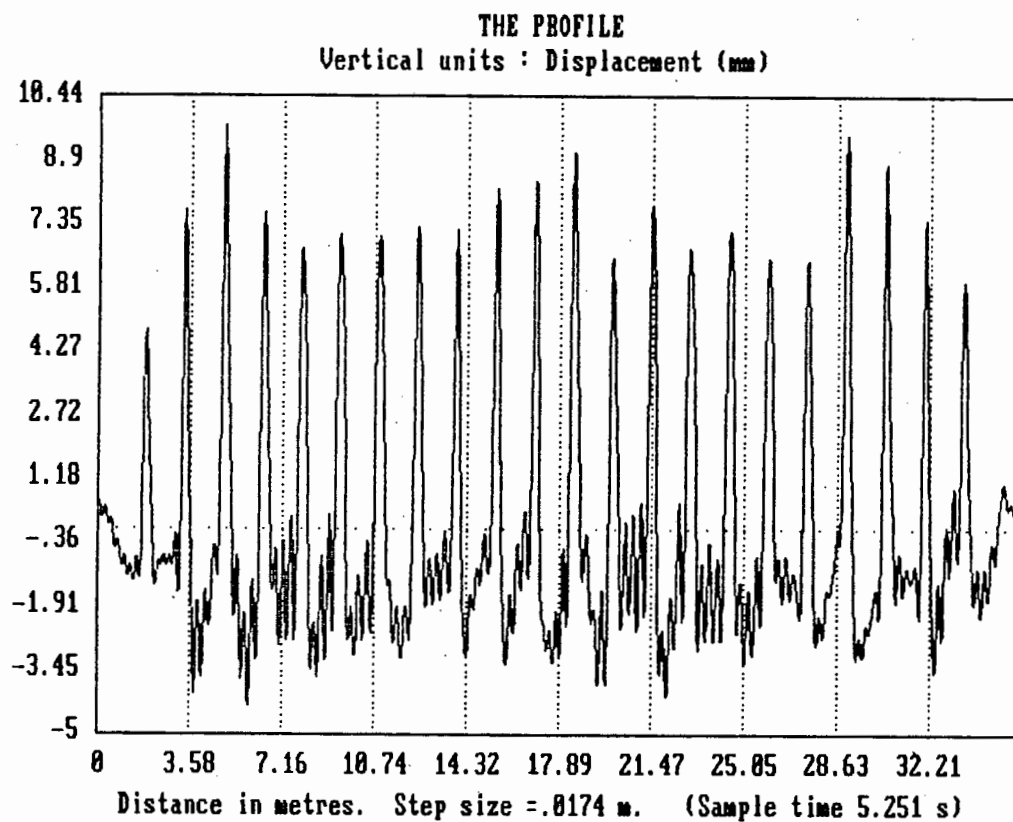


Figure I-8j

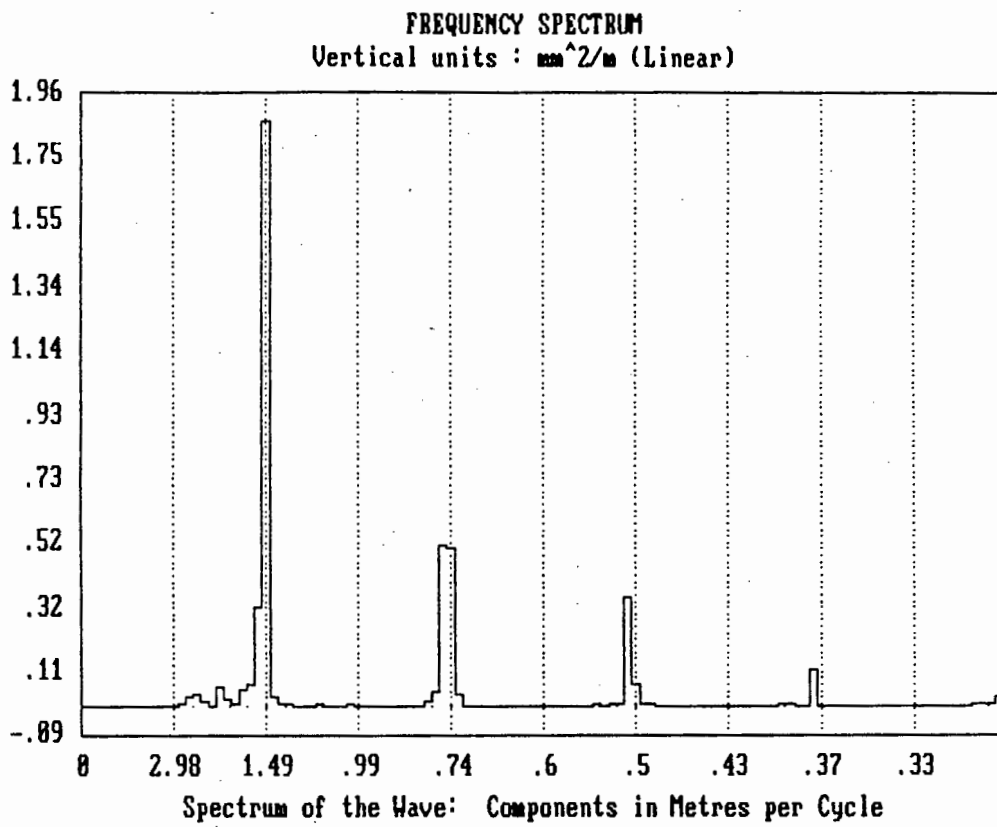


Figure I-9a Measurement of a Speed Bump on the Road

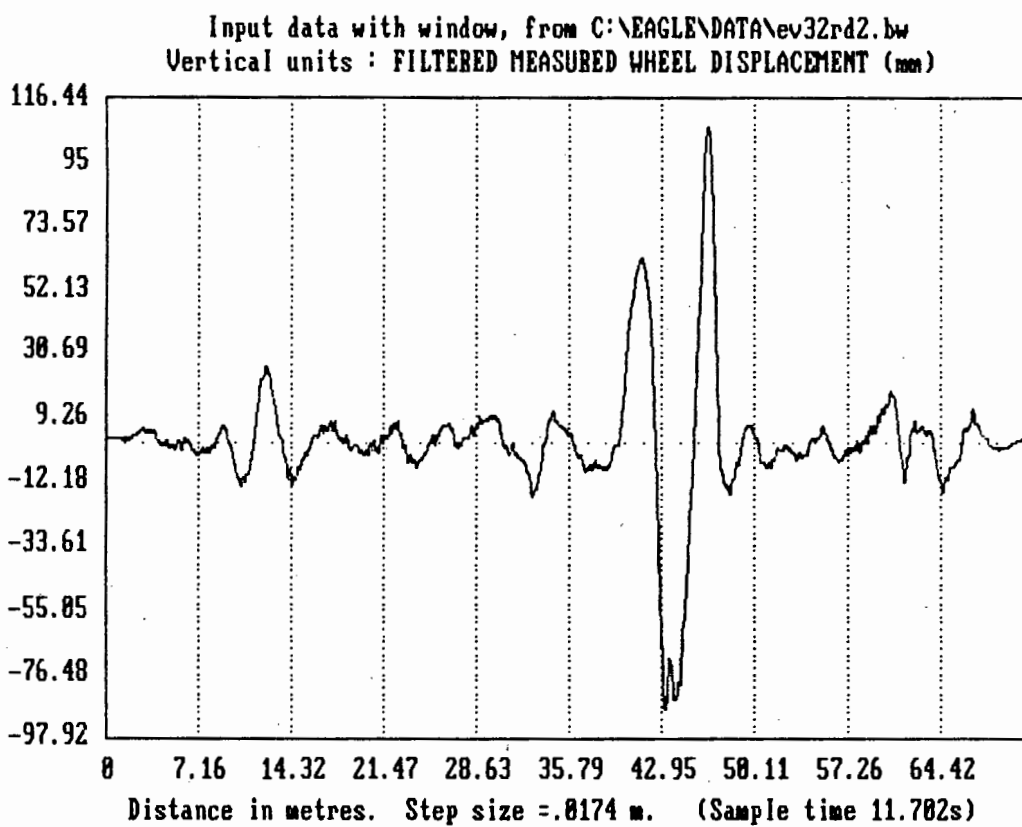


Figure I-9b

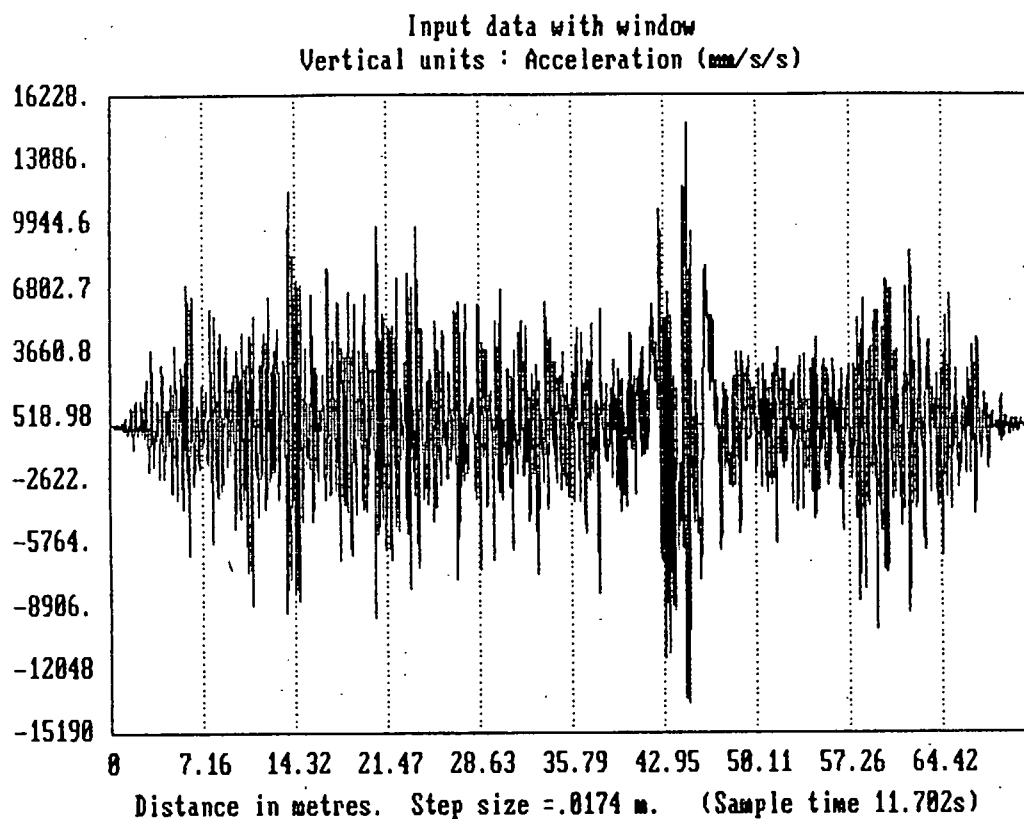


Figure I-9c

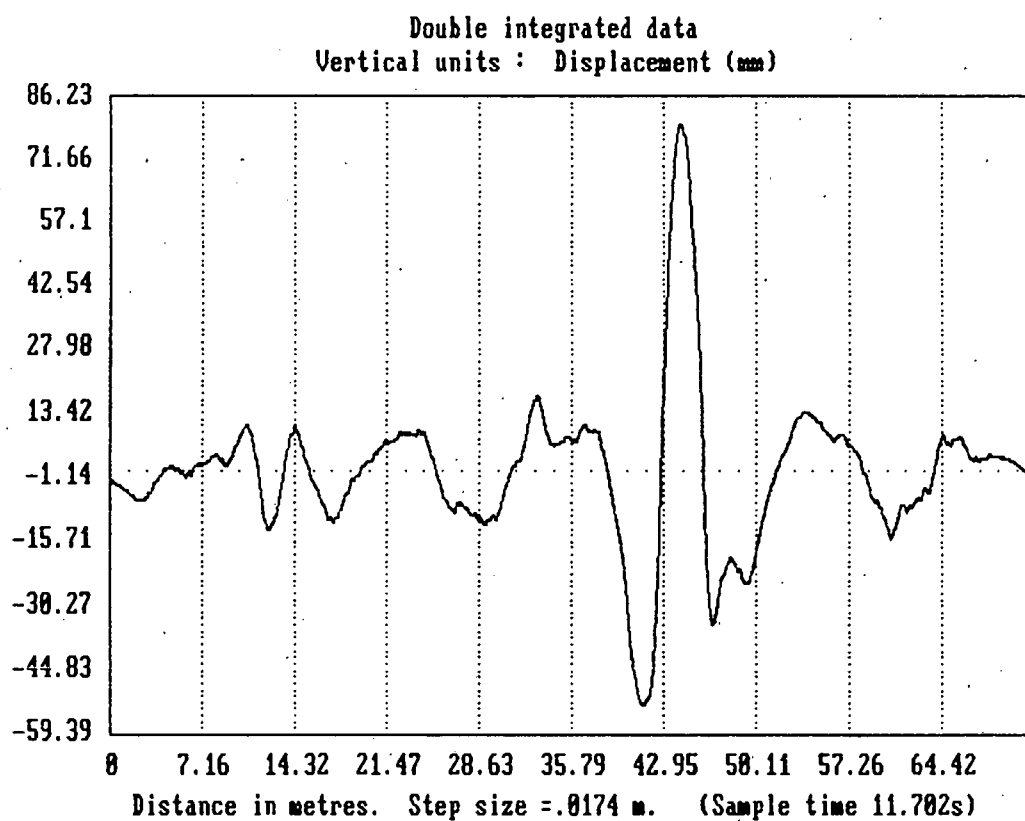


Figure I-9d

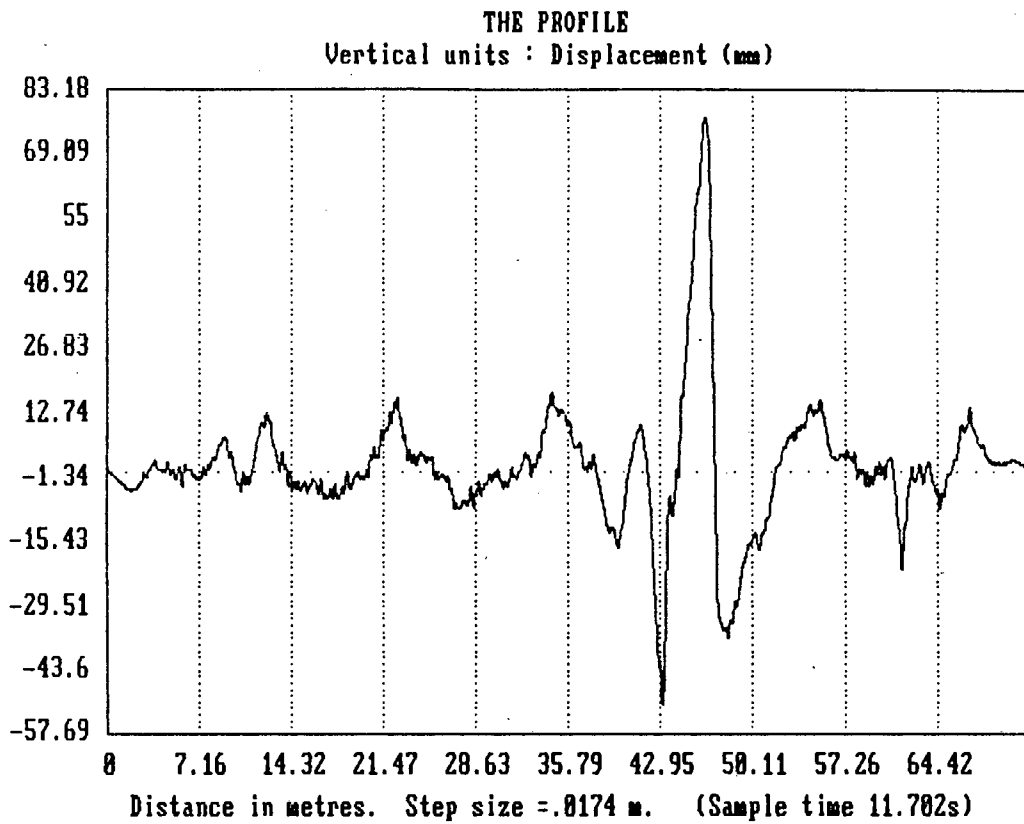


Figure I-9e

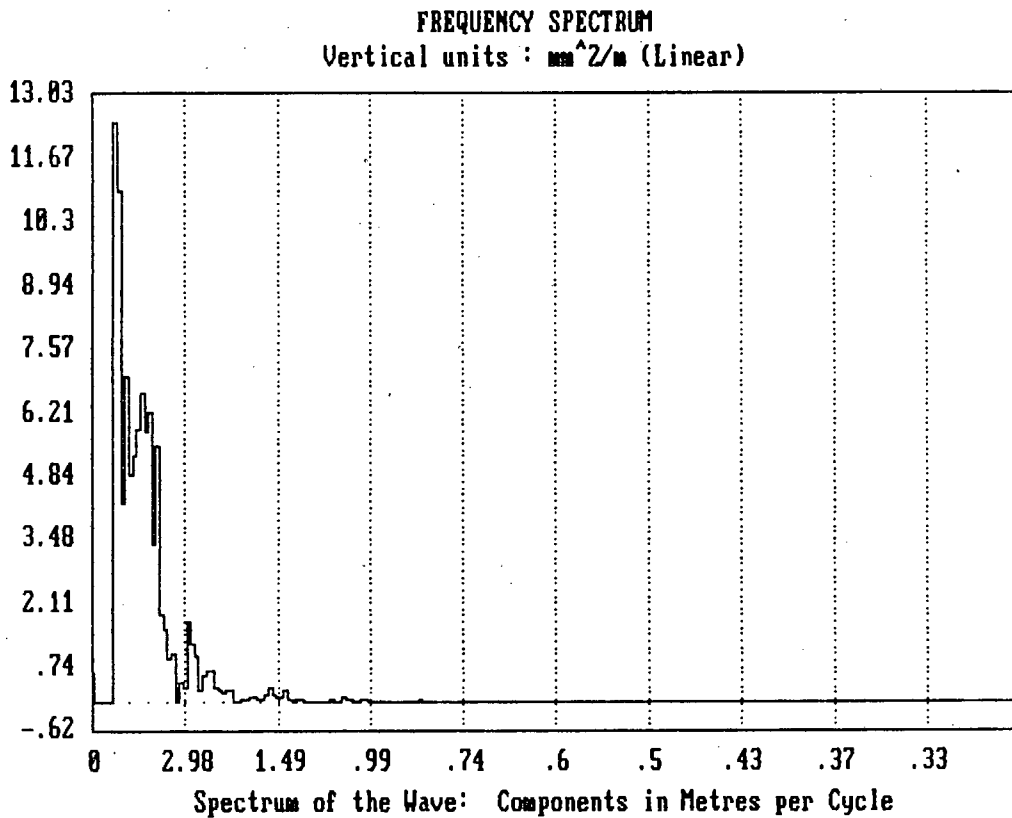


Figure I-10a Measurement of a level, Tarred Road

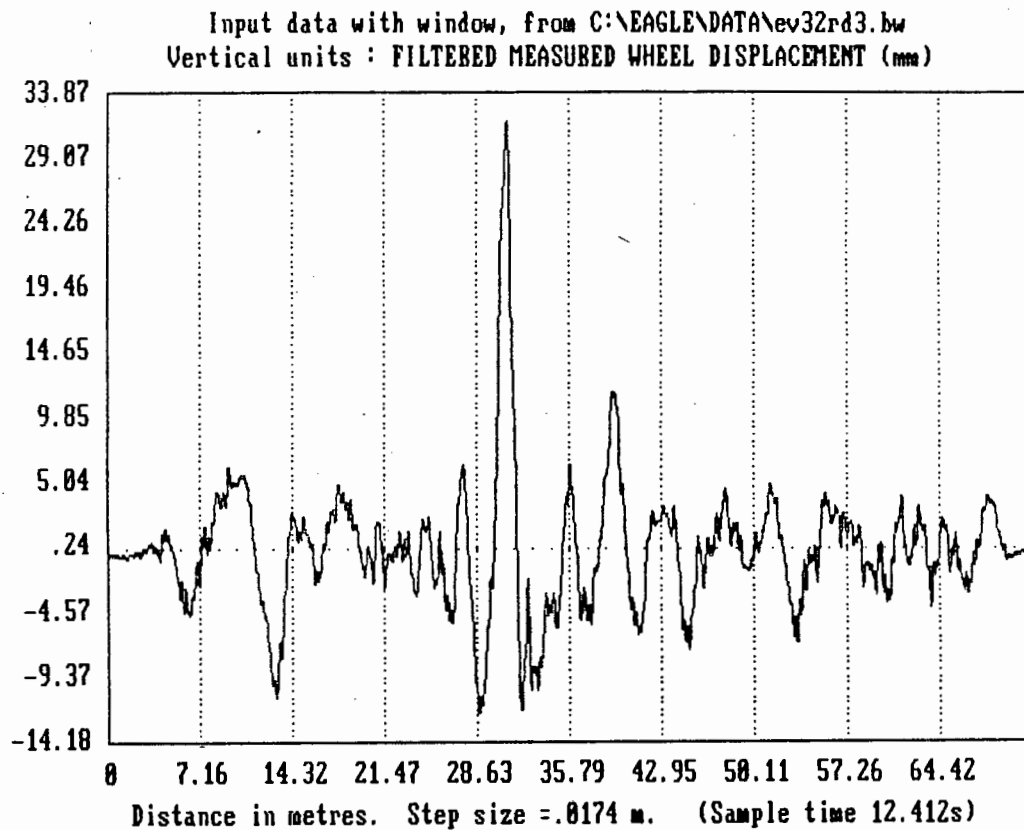


Figure I-10b

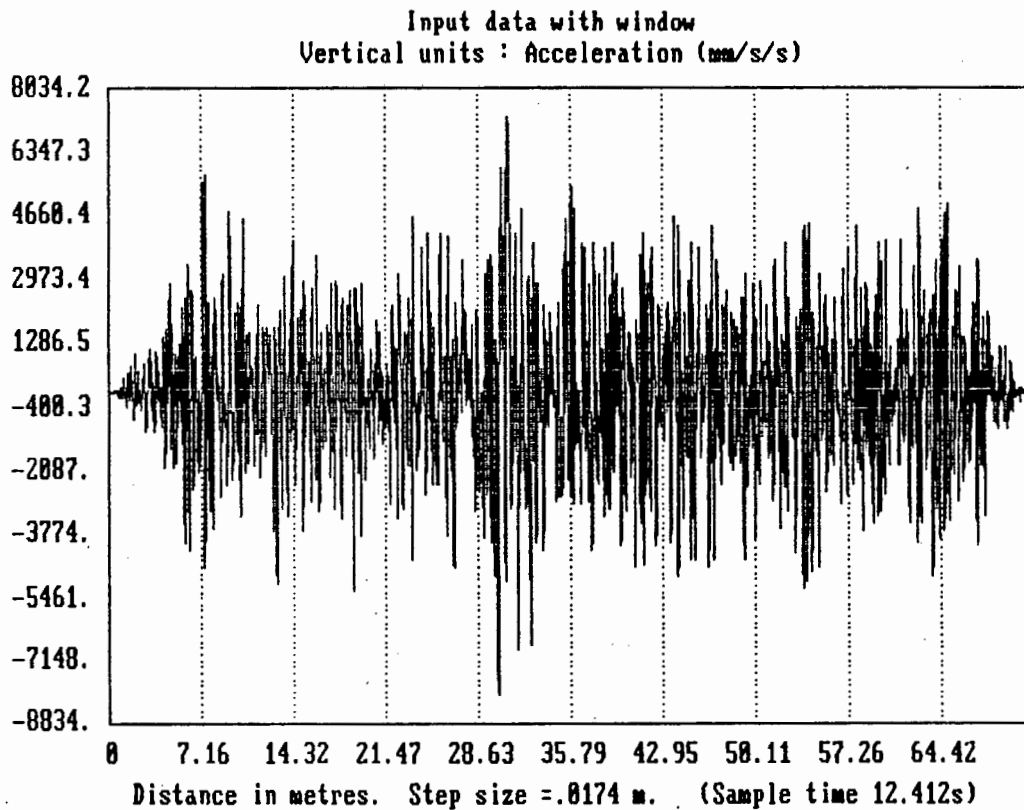


Figure I-10c

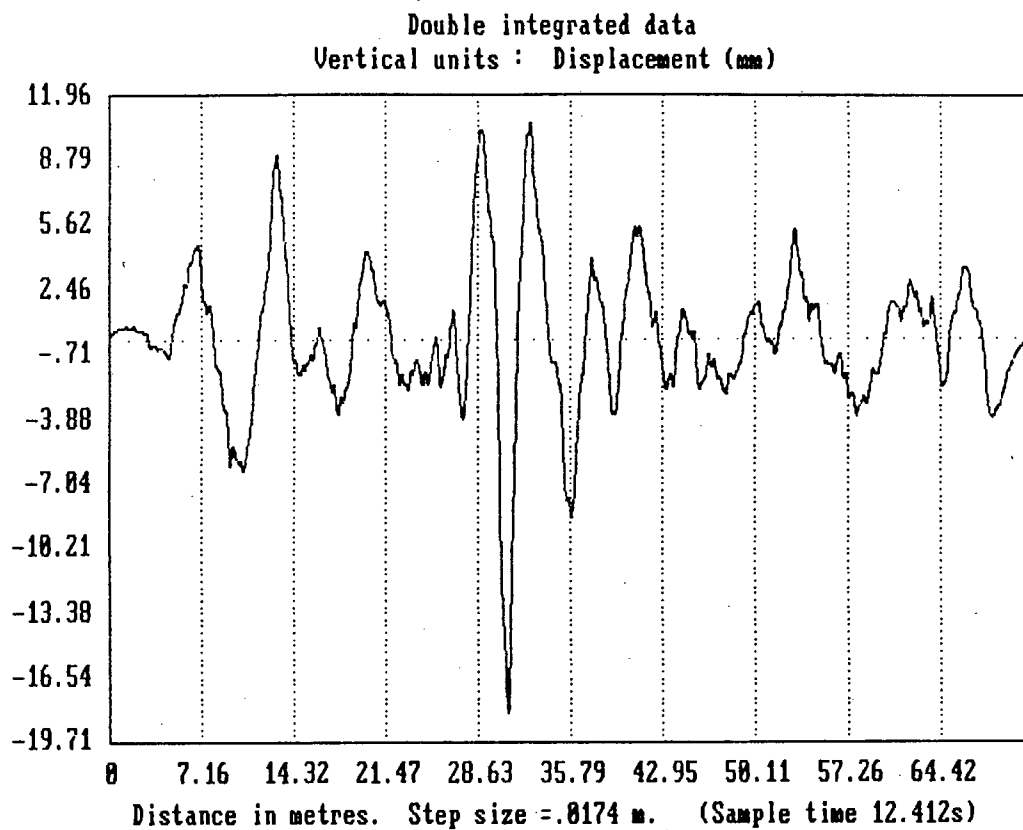


Figure I-10d

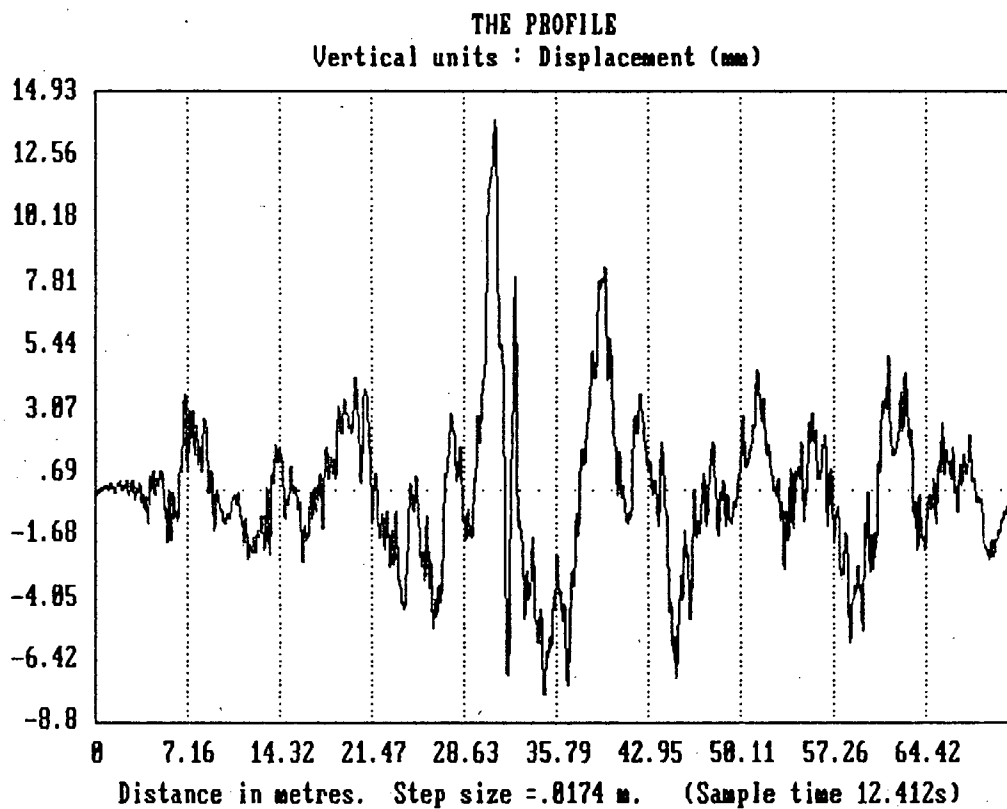


Figure I-10e

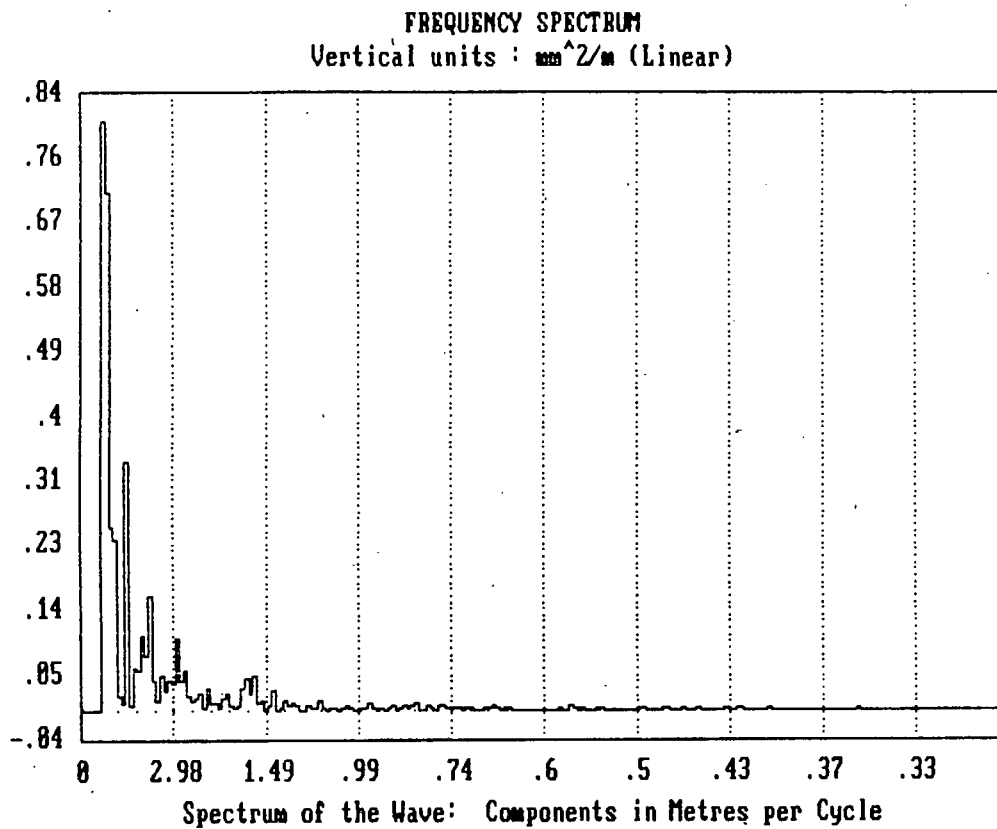


Figure I-11a Measurement of a rough Dirt Road

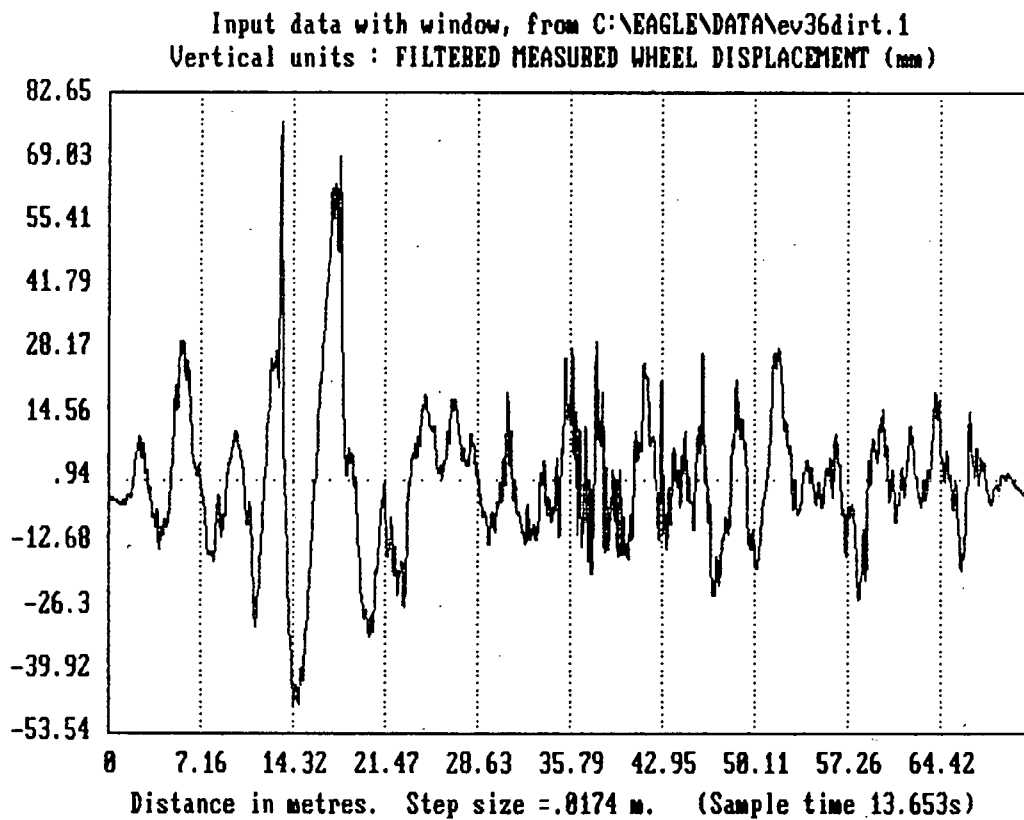


Figure I-11b

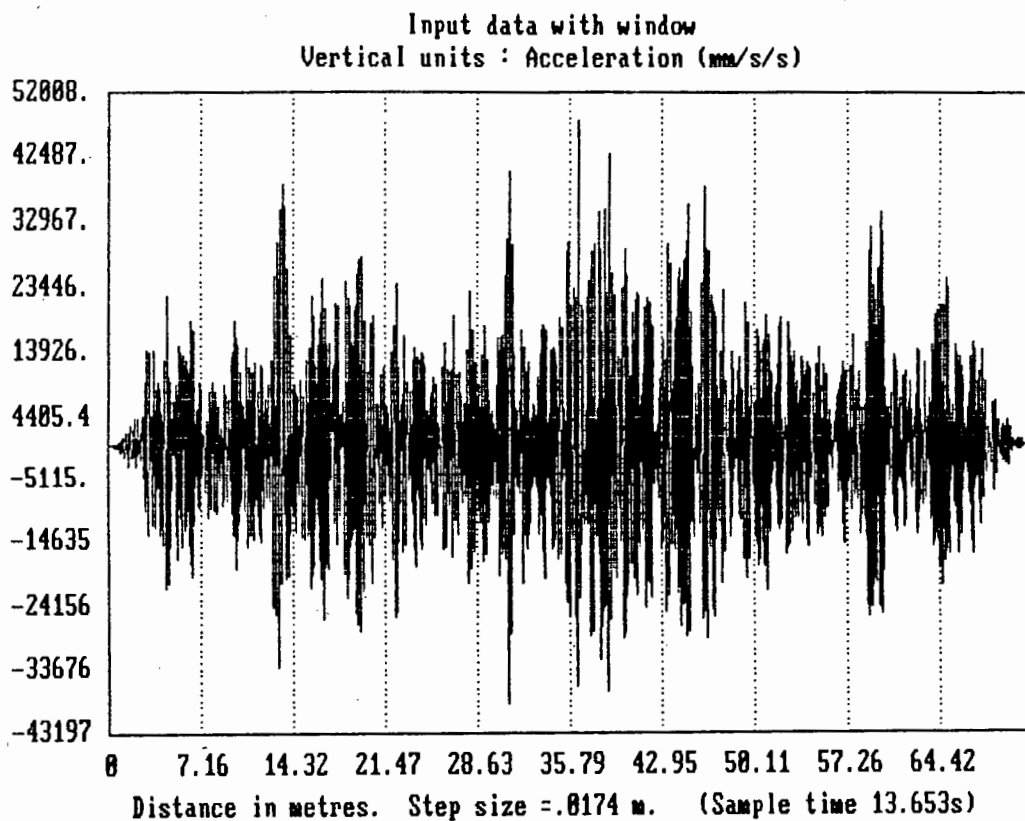


Figure I-11c

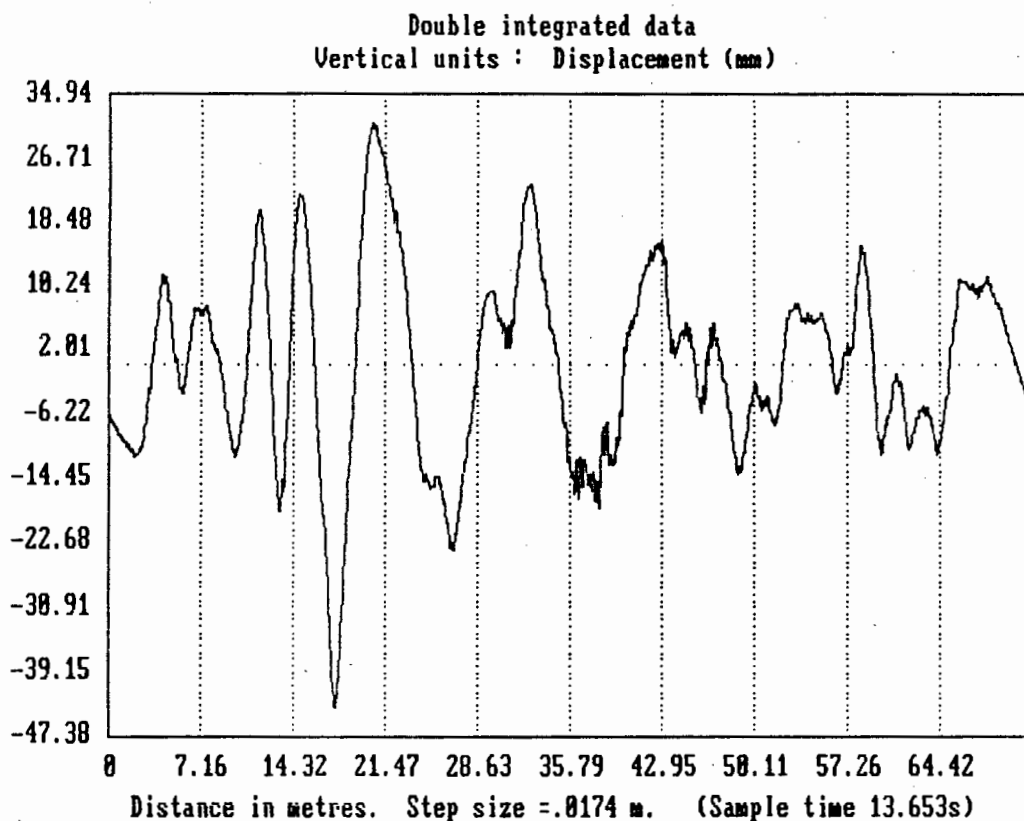


Figure I-11d



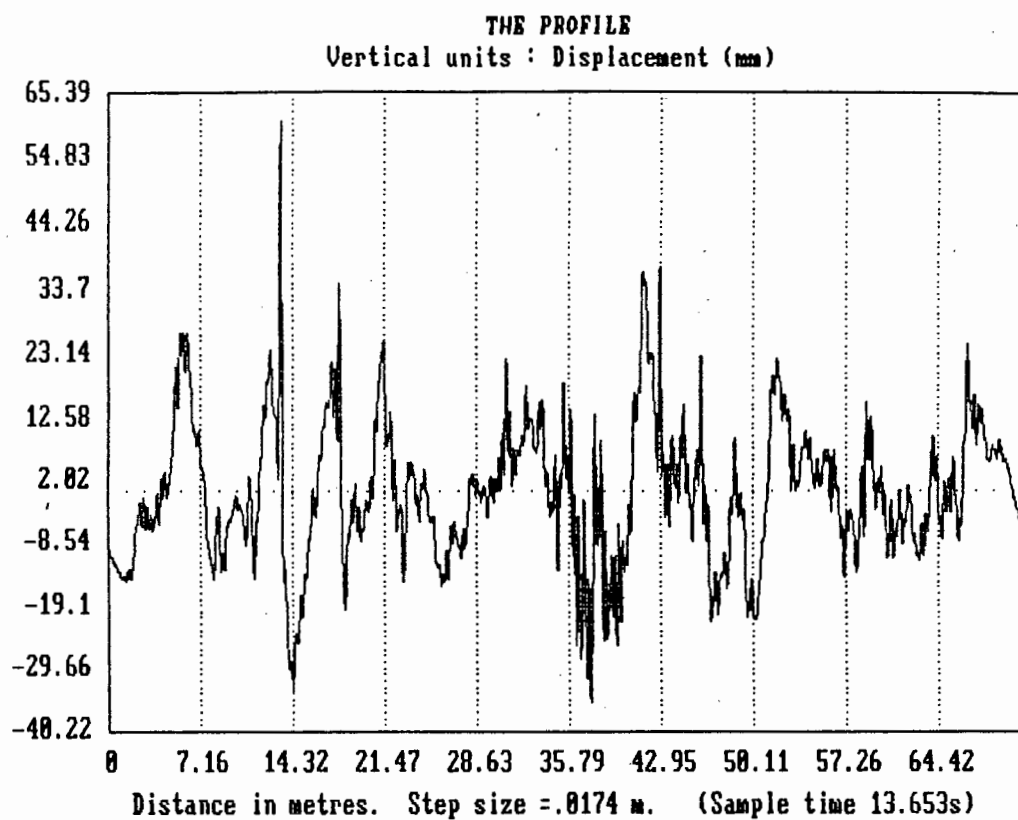


Figure I-11e

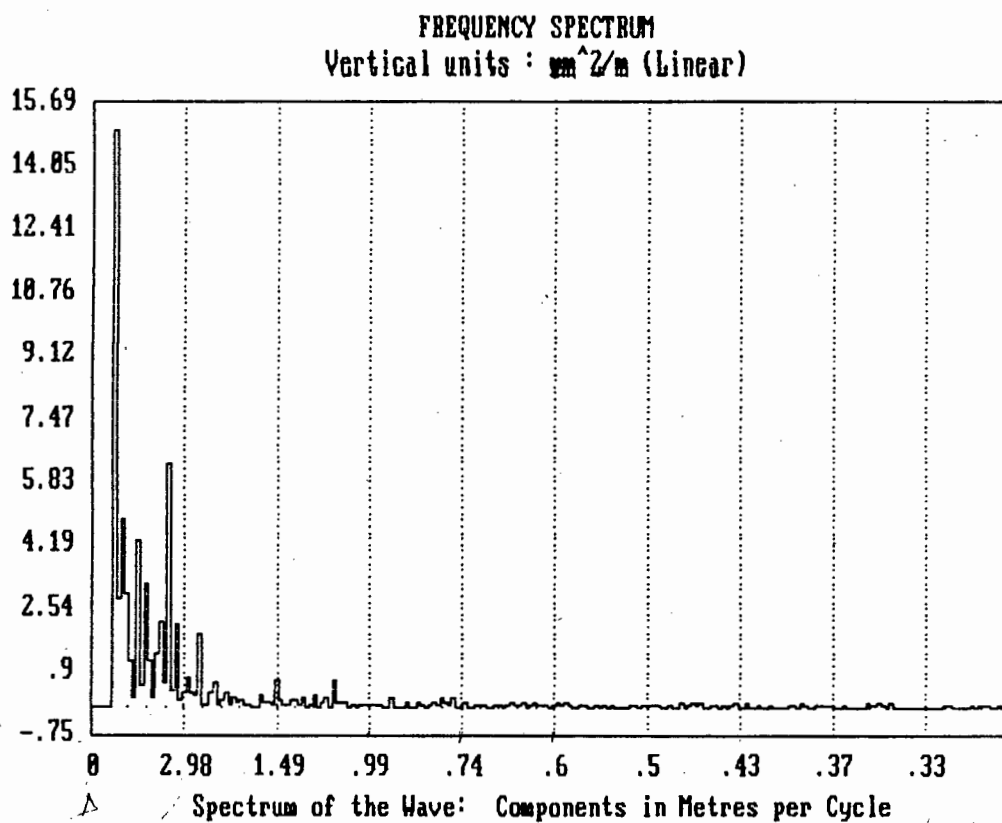


Figure I-11f

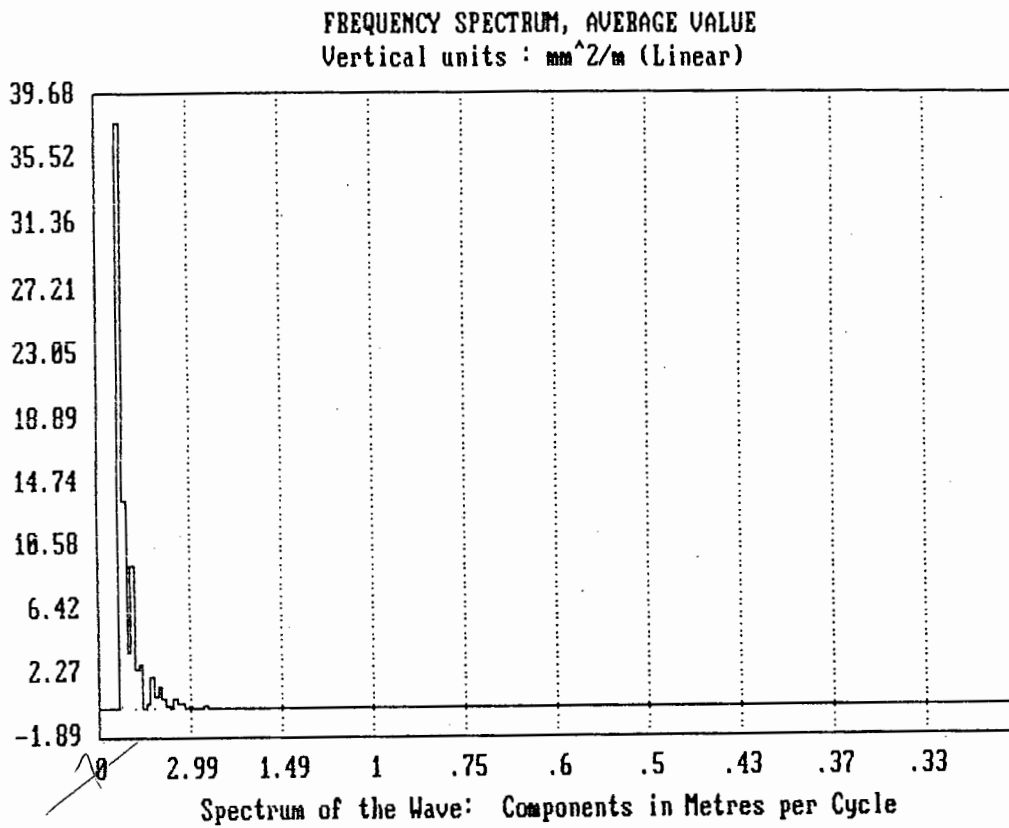


Figure I-12a Spectra for the Steytlerville Road

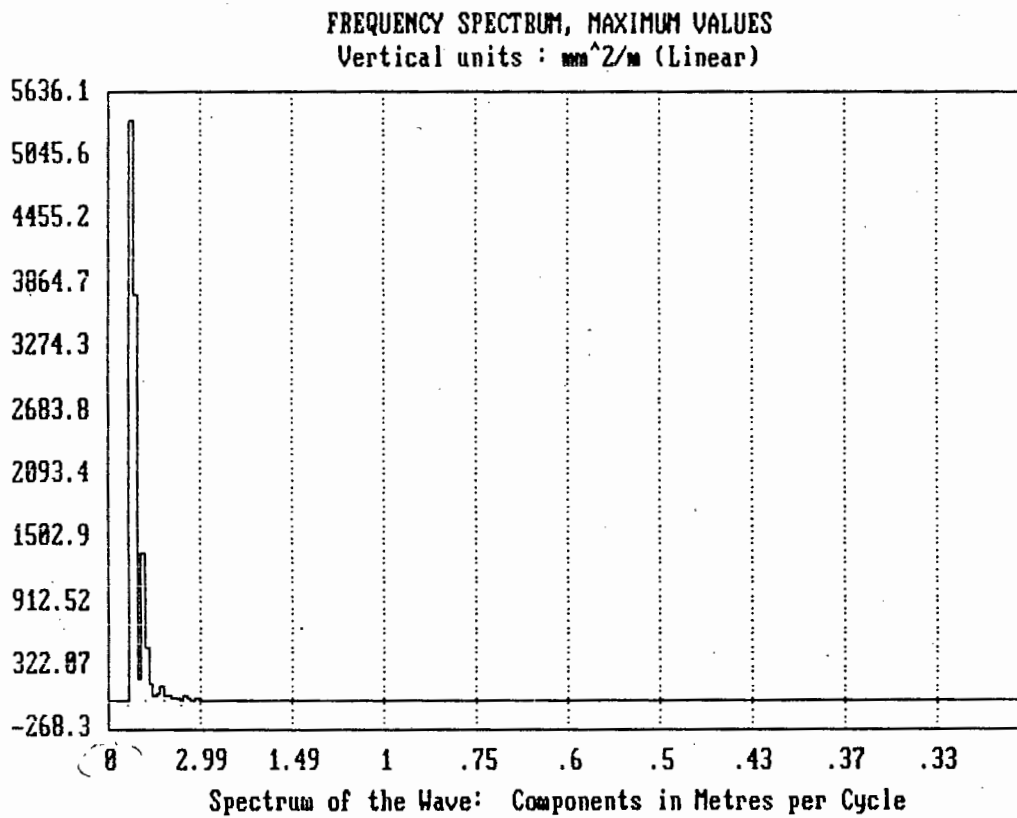


Figure I-12b

FREQUENCY SPECTRUM, MINIMUM VALUES  
Vertical units :  $\text{mm}^2/\text{m}$  (Linear)

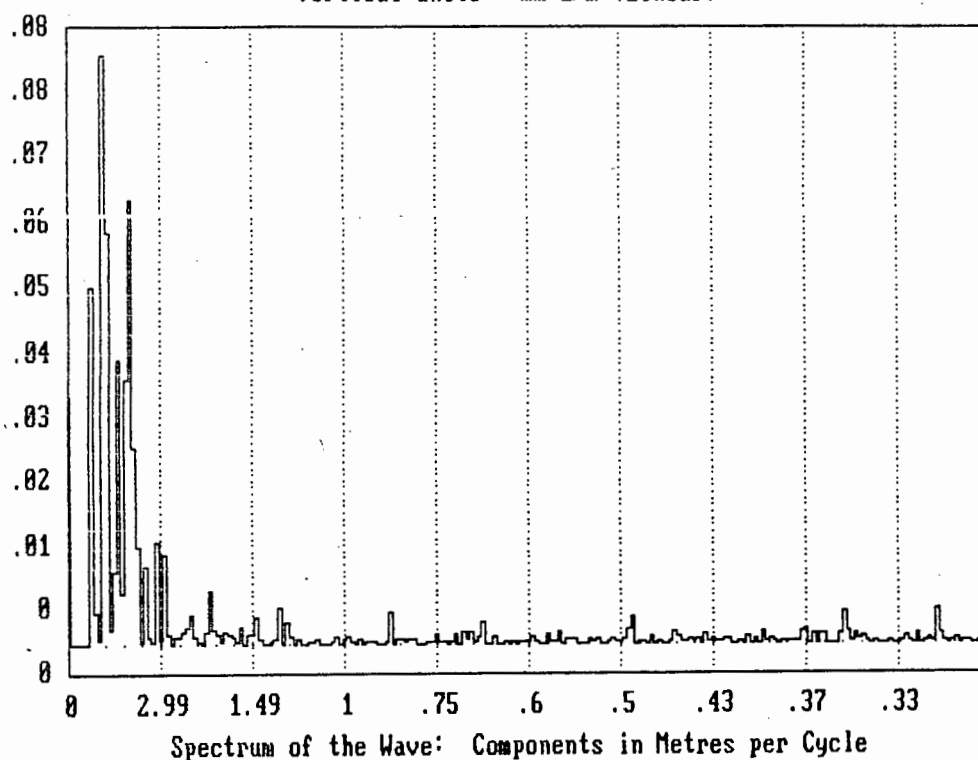


Figure I-12c

FREQUENCY SPECTRUM, AVERAGE VALUE  
Vertical units :  $\text{mm}^2/\text{m}$  (Linear)

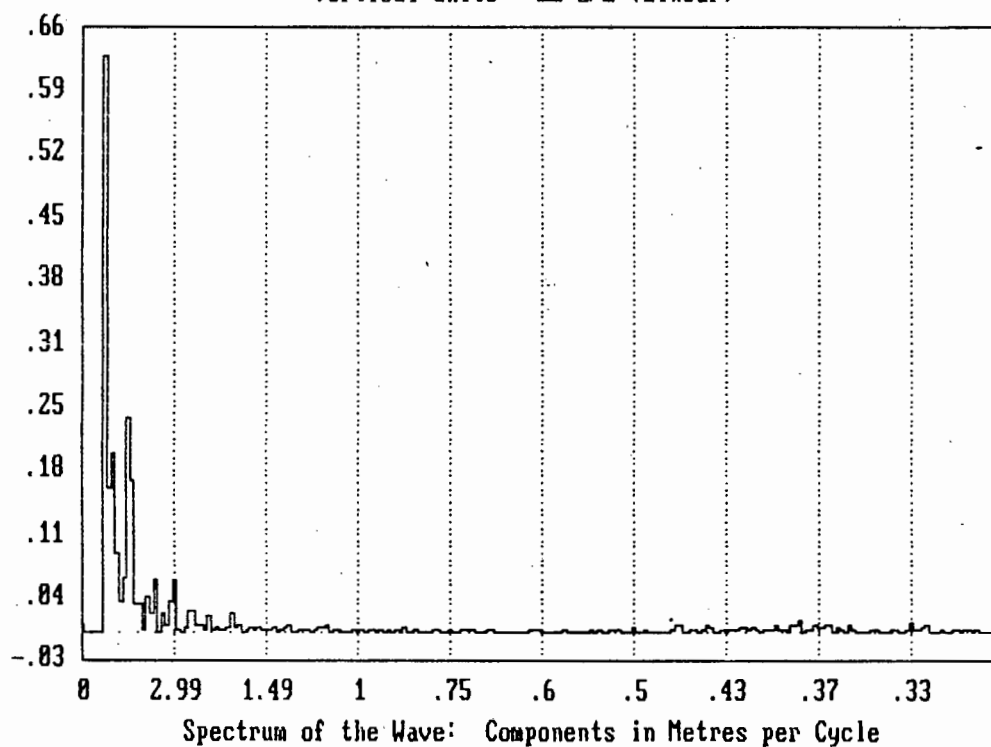


Figure I-13a Spectra for the Van Staden's pass road

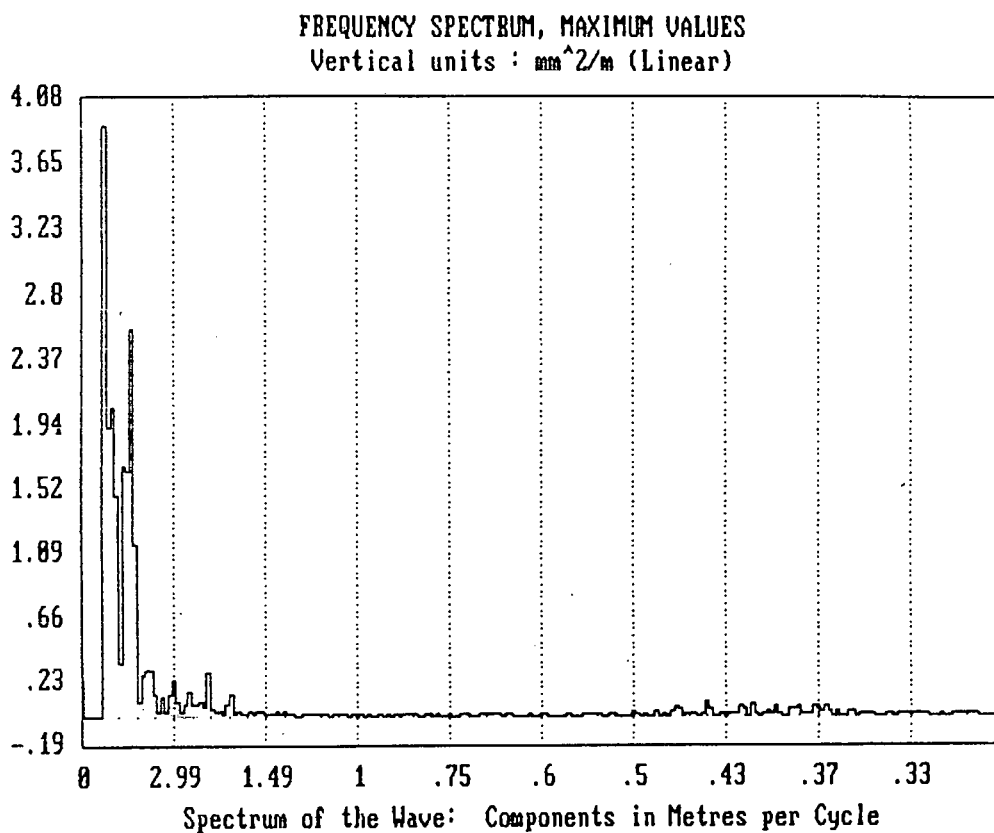


Figure I-13b

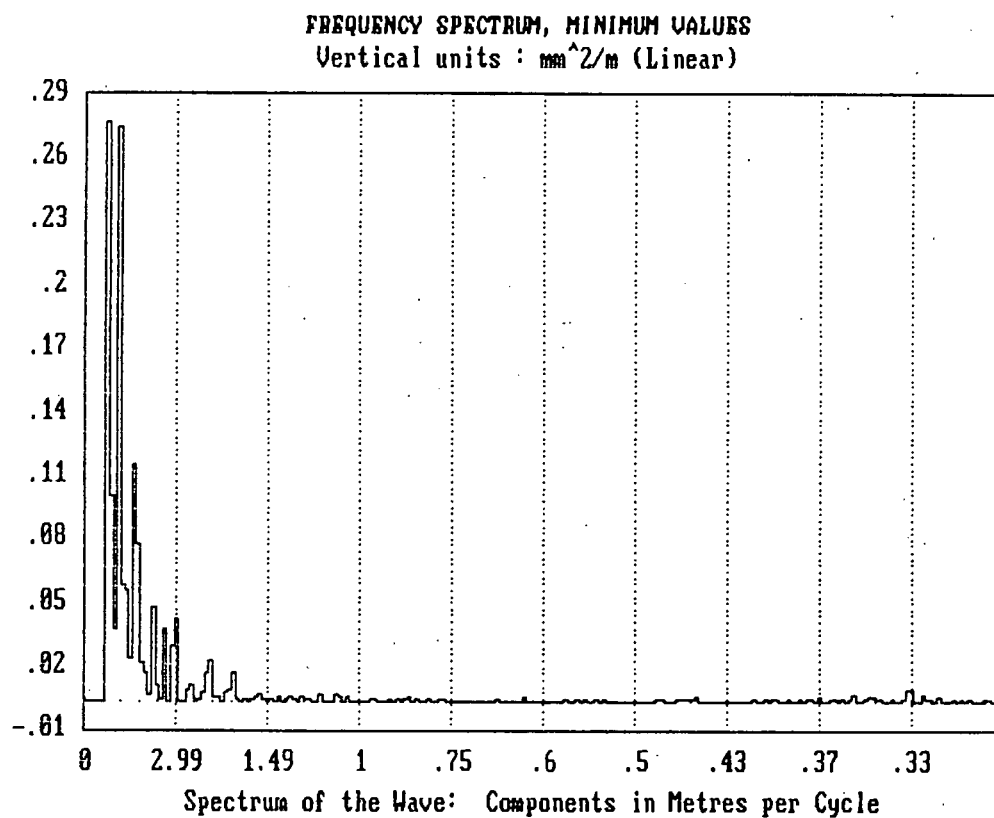


Figure I-13c